Syntheses and Characterization of Steroid Glucuronides for the Preparation of Horseradish Peroxidase Conjugates *via* Hemin Modification

A thesis presented in partial
fulfilment of the requirements
for the degree
of Doctor of Philosophy
in Chemistry at
Massey University

Yinqiu Wu

1996

Acknowledgements

First, and foremost I wish to express my sincere thanks to my supervisor Associate Professor Len Blackwell for providing me with invaluable assistance and guidance during the course of this work, and also for his help in proof reading this thesis. In addition, he has introduced me to an interesting, new area of research which has proved both scientifically and commercially exciting and immensely rewarding and for this I am extremely grateful.

Secondly, I would like to acknowledge Associate Professor Joyce Waters, for helping to solve the crystal structure of one steroid compound; Dr Bryan Anderson, for assisting in the enzyme model building experiments and analysis; Mrs Heather Baker, for her gift of Chelex 100 resin; Mr Dick Poll, for his great help in running HPLC analyses; and Mr David Elgar, for his gift of quaternary ammonium cellulose resins.

It remains for me to thank Associate Professor David R. Harding, Dr David Officer and my co-supervisor Associate Professor John Ayers for their many valuable discussions. I am also especially indebted to my colleagues Ms Delwyn Cooke and Mr Mark Smales for their assistance in my excursion into the world of enzyme chemistry.

The scholarships from The St Michael Research Foundation and The Massey University New Technology Foundation are gratefully acknowledged.

Finally, I would especially like to thank Associate Professor Paul Buckley for his tremendous support, help and encouragement, which have made my life in New Zealand so enjoyable. I also like to thank my family and my parents for their support and patience.

Abstract

Steroid glucuronides including estrone glucuronide **12**, estriol 3-, 16α- and 17β-monoglucuronides **13-15** and pregnanediol glucuronide **16** have been successfully synthesised. In particular, a new scheme for the synthesis of estriol monoglucuronides **13-15** from estriol provides a simple procedure and good yields of pure products based on the protection and deprotection of hydroxyl groups of estriol, glucuronidation, and hydrolysis. The new synthetic route retains the original stereochemical integrity of the estriol, and thus produced the estriol monoglucuronides with the correct stereochemistry. The steroid glucuronides **12-16** were characterised by ^{1}H-^{1}H 2D-COSY, 2D-NOESY and ^{1}H-^{13}C HETCOR spectra and the results unambiguously showed the β-linkage of the glucuronide ring with the steroid moiety in all of the steroid glucuronides. The conjugation positions of the glucuronic acid to estriol, as in estriol 16- or 17-glucuronide **14-15**, were distinguished from their ^{13}C chemical shift values and the proton 2D-NOESY spectra. The crystal structure analysis of one estriol 17-glucuronide derivative **112** also confirmed that the absolute configuration at all stereocentres was maintained during synthesis.

Subsequently some α-amino acids (DL- or L-phenylalanine, L-tryptophan and L-arginine), estrone glucuronide (E1G) **12** and pregnanediol glucuronide (PdG) **16** have been successfully linked to hemin IX **227** (the prosthetic group of horseradish peroxidase) either by selective mono-acylation of protoporphyrin IX **216** followed by insertion of Fe^{2+} or by direct mono-conjugation of hemin IX **227** with α-amino acids or steroids. The mono-coupling reactions provided good yields and simlple reaction conditions, which have established the feasibility of this new methodology. The mono-conjugated structures and the high purities of both hemin-phenylalanine mono-conjugate **230** and the hemin-estrone glucuronide mono-conjugate **232** were confirmed by their ^{1}H NMR and mass spectra. Both purified conjugates (**230**, **232**) showed no contamination by unreacted hemin IX **227** by HPLC analyses.

The reconstitution of hemin-estrone glucuronide mono-conjugate **232** with apo-horseradish peroxidase has been successfully achieved to form a new enzyme. The new enzyme (estrone glucuronide-horseradish peroxidase conjugate) retains good peroxidase activity (76% relative to reconstituted horseradish peroxidase), which is sufficient for exploitation in immunoassays. A suitable molecular linker (L-lysine) between the hemin propionate side chain and the estrone glucuronide moiety is crucial for retaining good peroxidase activity. Without a molecular linker, reconstitution of hemin-phenylalanine monoconjugate **230** with the apo-horseradish peroxidase showed a very poor reconstitution yield and activity. The extra carboxyl group, introduced by L-lysine, probably also made a great contribution in retaining a high activity of the new enzyme. Therefore, this thesis has exploited a new methodology in the preparation of horseradish peroxidase-hapten conjugates *via* hemin-modification. The new methodology is generic and it can be extended to the synthesis of horseradish peroxidase-conjugates with any analytes of interest. It will be very useful, not only as markers of fertility in home assays, but also in many other areas such as food, agriculture, medicine and the environmental monitoring. Hence, wide commercial applications for this new technology are expected in the future.

CONTENTS

Abbreviations

A	alanine
A_{278}	absorbance at 278 nm
A_{403}	absorbance at 403 nm
Arg	arginine
Asn	asparagine
BSA	bovine serum Aabumin
CcP	cytochrome c peroxidase
CLIA	chemiluminescence immunoassay
DCC	dicyclohexylcarbodiimide
2D-COSY	two-dimensional homonuclear correlation spectroscopy
DMAP	4-dimethylaminopyridine
DMF	dimethylformamide
DMSO	dimethylsulfoxide
2D-NOESY	two-dimensional nuclear overhause effect spectroscopy
DtBP	ditertiary butyl peroxide
E (Glu)	glutamic acid
E1G	estrone 3-glucuronide or estrone glucuronide
E1G-hemin	estrone glucuronide-hemin mono-conjugate
E1G-HRP	estrone glucuronide-horseradish peroxidase conjugate
E3-3G	estriol 3-glucuronide
E3-16G	estriol 16α-glucuronide or estriol 16-glucuronide
E3-17G	estriol 17β-glucuronide or estriol 17-glucuronide
EIA	enzyme immunoassay
FAD	flavin adenine dinucleotide
FIA	fluoroimmunoassay
FPLC	fast protein liquid chromatography
Gln	glutamin
H (His)	histidine
HETCOR	heteronuclear correlation spectroscopy
HPLC	high performance liquid chromatography
HRP	horseradish peroxidase
Hz	hertz
Ile	isoleucine
K	lysine
Lip	lignin perosidase

Lit	literature
NMR	nuclear magnetic resonance
P-450scc	cytochrome P-450 enzyme for side chain cleavage
PdG	pregnanediol 3-glucuronide or pregnanediol glucuronide
PGLIA	prosthetic group-labelled immunoassay
ppm	part per million
Pro	proline
ref	reference
RIA	radioimmunoassay
R_F	rate of flow
rt	room temperature
RZ	reinheitszahl
Ser	serine
ΔT	change in transmission
THF	tetrahydrofuran
TLC	thin layer chromatography
Tyr	tyrosine
Val	valine

Chapter 1

Introduction

1.1 Background to the Study

1.1.1   Ovarian function and the menstrual cycle

Every month in the human female one, or sometimes two, follicles grow in the ovaries to a size of about 25 mm before bursting and releasing an oocyte. This process, known as ovulation, is the central event of the menstrual cycle and forms the basis of the regular pattern of events which occurs every month. During this cycle there is a period of time during which the oocyte may be fertilised by a spermatozoon leading to conception, pregnancy and birth. The period of time during which conception can occur is known as the fertile period and is a function of two factors; the sperm survival time and the ovum survival time. The survival time of the ovum is short, being 12-24 hours or less,[1] hence the fertile period is really determined by the sperm survival time.

There is considerable debate regarding the sperm survival time and estimates range from 1-2 days to 6-7 days. According to the World Health Organisation[2] the mean survival time is 3-4 days. The survival of the sperm depends in part on the presence and quality of the cervical mucus and elegant studies by Professor Odeblad in Sweden[3] have shown how the sperm may survive in cervical crypts for long periods of time in the presence of so-called fertile mucus. In studies from Professor Brown's laboratories[4] pregnancies have been documented hormonally which require a sperm survival time of up to 7 days.

Thus fertility is in one sense a male factor problem and the fertile period is seen to be the time when the life time of the sperm overlaps with the life time of the ovum. Clearly, this combined fertile period will have a maximum value of about 7 days. If this fertile period could be recognised accurately in advance then the remainder of the cycle would be infertile and the necessity of taking contraceptive precautions would be avoided. A successful achievement of this aim would change fundamentally family planning behaviour. It would make little sense to take a hormonal preparation for 30 days when only 7 of them were potentially fertile. To understand how the fertile period might be recognised and predicted it is necessary to

have an understanding of the underlying processes of follicle recruitment, selection and dominance.

The recruitment of a cohort of follicles (up to 12 each cycle) is under the control of a pituitary hormone known as follicle stimulating hormone (FSH). At the beginning of each cycle the pituitary begins to slowly increase the levels of FSH in an attempt to cause a follicular response from the ovary. It is essential for the FSH level to hunt slowly upwards to avoid the possibility of superovulation: that is more than one follicle going on to ovulate. The major role of FSH at this stage of the cycle is to bind to the FSH receptors on the granulosa cells of small follicles and stimulate the granulosa cells to divide and grow. As a consequence the follicles grow larger until at about the antral stage when fluid filled spaces occurs and coalesce (see Figure 1) the granulosa cells then acquire the competence to express a cytochrome P450 enzyme known as aromatase. The is an essential event in the life cycle of a follicle and if this does not occur the follicle dies (becomes atretic). Usually only one follicle out of the cohort makes this transition and becomes dominant.
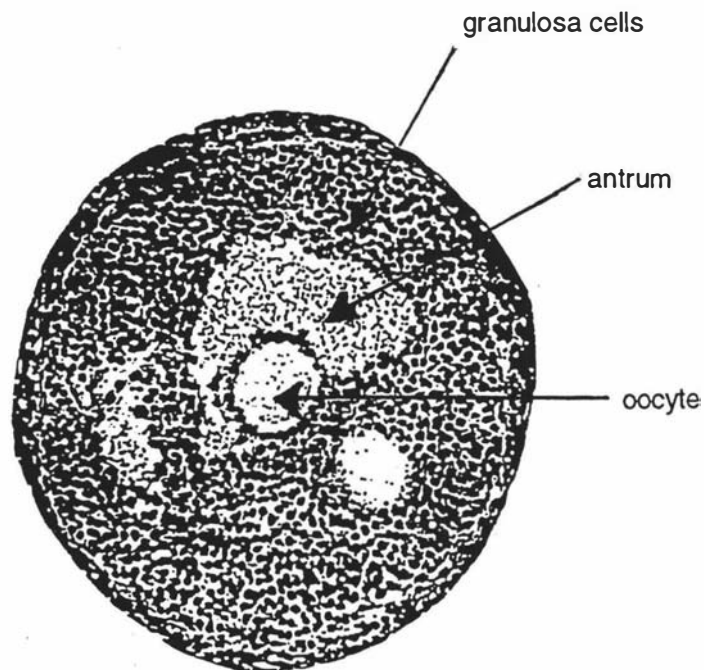
Figure 1. Antral follicles.

The aromatase enzyme in the granulosa cells of the dominant follicle carries out two hydroxylations of the 19-methyl group of adrenal androgens such as

androstenedione (see Scheme I section 1.1.2) and a third in the 2-position of ring A resulting in a spontaneous base-catalysed aromatisation to produce an estrogen (either estrone or estradiol as shown in Scheme 1, Section 1.1.2). The principal ovarian estrogen is estradiol. Since there is always some androgen being produced by the adrenal glands, there is always a baseline production of estrogens by peripheral aromatisation of the adrenal androgens. The presence of a growing healthy follicle is therefore revealed by rising levels of circulating estradiol above this baseline which signals to the hypothalamic/pituitary axis that no further stimulation by FSH is necessary. This is achieved by a negative feedback mechanism which dampens down the output of pituitary FSH. As the dominant healthy follicle (which becomes virtually independent of circulating FSH levels) continues to grow it gets larger and the number of granulosa cells increases. Hence the output of estradiol increases as well.

It is now known from ultrasonography[5] that in normal women there is a linear relationship between the diameter of the dominant follicle and the number of days of its growth. The mean rate of increase is 2.4 mm ± 0.7/day. This is shown in Figure 2 for a hypothetical follicle which can be monitored by ultrasound once its diameter reaches about 4 mm (the early antral stage). Since a normal follicle ovulates when its diameter reaches 20 ~ 25 mm this requires an 8 day span from first emergence of the follicle in ultrasound until its ovulation. McNatty showed in 1981[6] that there was a correlation between follicle diameter and the maximum number of granulosa cells in healthy follicles. Hence Figure 2 can be replotted in terms of the maximum number of granulosa cells (Figure 3).

Figure 2. Daily Increase in Follicle Diameter
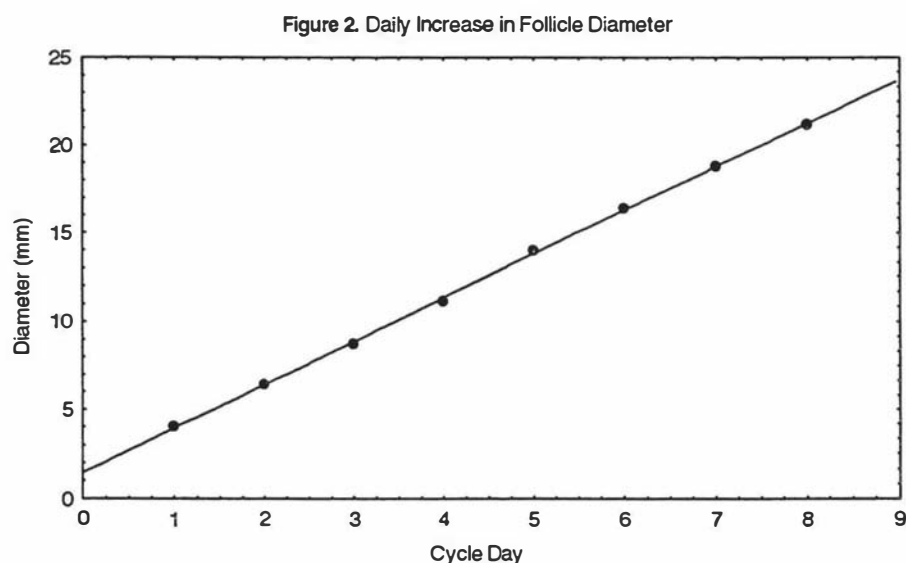
Figure 3. Daily Increase in Number of Granulosa Cells
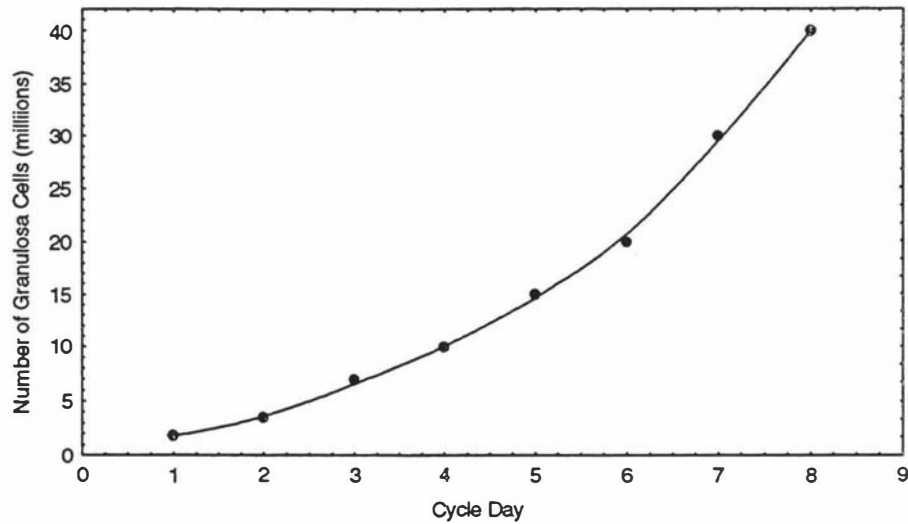
Figures 2 and 3 show that for a linear increase in the diameter of a dominant follicle, which is regarded as indicative of normal follicle development, there is a logarithmic increase in the number of granulosa cells. Hence, if the output of estradiol from each granulosa cell due to its aromatase activity is approximately constant, as seems reasonable, there should also be a logarithmic increase in the rate of excretion of estradiol. This is confirmed experimentally in many situations for estradiol or its metabolites (see for example Figure 4).[7]
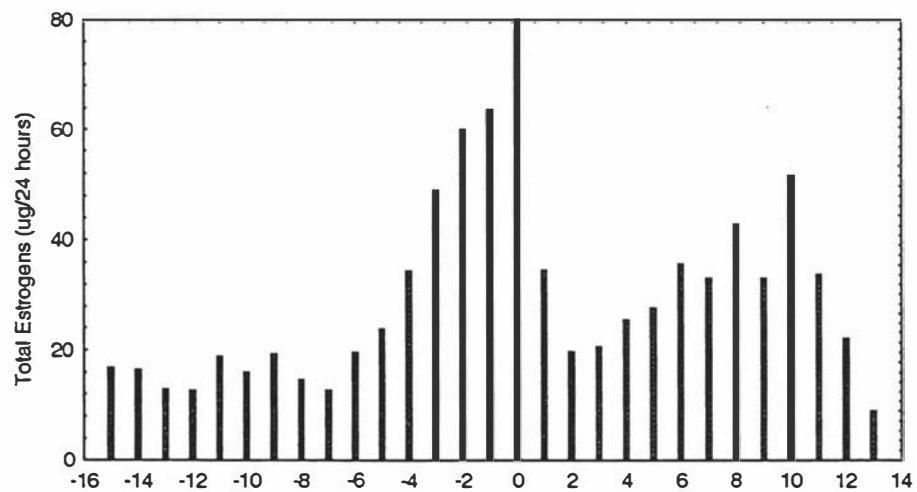
Figure 4. Cycle Day Relative to Total Urinary Estrogens (TE) Peak

The detection of this first rise in urinary estrogen excretion can be used in non-invasive technologies to signal the presence of a growing, healthy follicle. An atretic, or dying follicle, does not release estradiol. Hence in principle the detection of a rise in serum estradiol (or in its urinary metabolites) from a pre-ovulatory baseline level will serve to mark the entry of a dominant follicle into its rapid (logarithmic)

growth phase and thus also the beginning of potential fertility. The rise in urinary total estrogens in Figure 4 is clearly visible on cycle day -4 and this confirms that a dominant follicle is now present and potential fertility has begun.

The end of fertility can also be signalled hormonally by an increase in the production of progesterone after ovulation. The remnants of the follicle after exposure to LH and a process known as luteinisation become a steroid excreting structure called the corpus luteum. Studies by Hoff et al[8] have clearly shown that the rise in progesterone (P_4) levels around the time of ovulation and afterwards from the corpus luteum is biphasic (Figure 5)
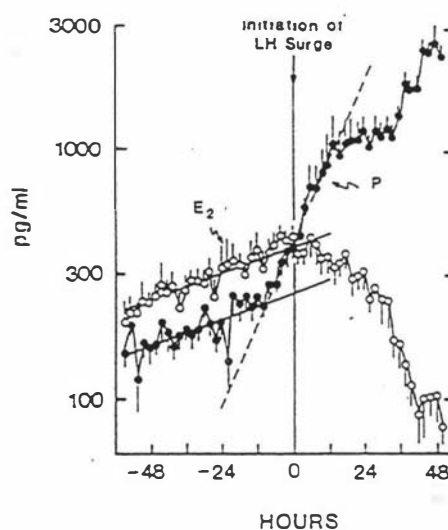
Figure 5. Mean ($\pm$SE) serum E_2 and P_4 concentrations measured every 2 hours for 5 days at midcycle in seven cycles, referenced to the initiation of the LH surge and plotted on a logarithmic scale. Note the multiphasic rise in P_4 before, during, and after the onset of the LH surge.

The increase in progesterone begins 12 hours before the commencement of the surge in luteinising hormone (LH) secretion from the pituitary gland which serves as the zero point in Figure 5. The almost 4-fold linear increase continues until 12 hours afterwards even though LH levels are now rising steeply. Following this initial increase there is a lag phase followed by an enormous increase in progesterone output as the follicle luteinises thus increasing the supply of the precursor cholesterol. This second phase is related to the end of fertility and serves as a marker for the end of the potentially fertile phase of the cycle. Figure 6[7] shows the pregnanediol values for the menstrual cycle pictured in Figure 4. The rise in the urinary metabolite pregnanediol clearly marks the end of fertility, exceeding a threshold value of 1.4 mg/24 hour[7] on

cycle day 3. Thus from a biochemical point of view the fertile period of the menstrual cycle is faithfully reflected in the changes in serum estradiol and progesterone or in their urinary metabolites. An understanding of the hormonal patterns and the ability to measure these changes provides the facility to eavesdrop on the ovary as it exchanges chemical information on its status with the pituitary gland. Ovarian activity can therefore be monitored in this manner in a prospective fashion.
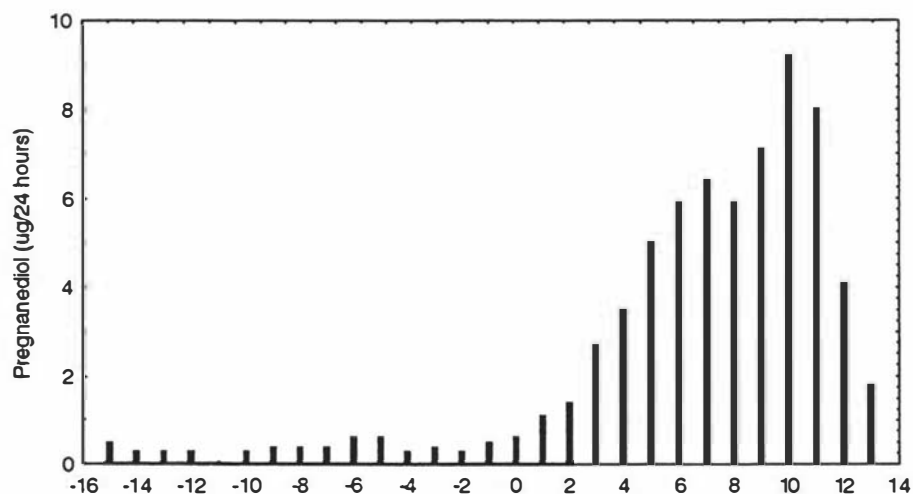
Figure 6. Cycle Day Relative to Urinary Total Estrogens Peak

This thesis is concerned with the development of an enzyme system which can be used in new assays to monitor the ovary by detecting these chemical messages (the ovarian hormones) to the hypothalamic pituitary complex.

1.1.2 Biosynthesis of ovarian steroid hormones

Before making a choice of which hormones to measure in any testing system it is necessary to consider the cyclic hormonal changes in some detail. To understand the physiological significance of the hormonal changes it is necessary in turn to consider the biosynthesis of the ovarian steroids and their relationship to follicle growth and development. Steroid hormones are normally synthesised from cholesterol (Scheme 1).[9] The first stage in the biosynthesis of the steroid hormones from cholesterol is removal of the C_6 unit from the side chain of cholesterol 1 by hydroxylation at C-20 and C-22. This is catalysed by a cytochrome P-450 enzyme (known as P-450scc) which is expressed in the mitochondria of all steroid producing cells. The cytochrome P-450 enzymes are important in controlling the biosynthetic pathway since their tissue dependent expression determines which parts of the steroid nucleus are hydroxylated and hence which steroids are formed. These enzymes all contain a heme group and their mechanisms are discussed in detail in a review by

Hall.[10] For cholesterol, the hydroxylations are followed by cleavage of the bond between C-20 and C-22, presumably by a reverse aldol condensation, to form pregnenolone **3**. The pregnenolone is then transported to the microsomes where the subsequent metabolism takes place. Progesterone **4** is then synthesised from pregnenolone **3** in two steps: the 3-hydroxyl group is oxidised to a 3-keto group and the Δ^5 double bond is isomerized to a Δ^4 double bond by the enzymes 3-β-hydroxy steroid dehydrogenase and ketosteroid isomerase.

The synthesis of the androgens **6** and **7** starts with the obligatory hydroxylation of progesterone **4** at C-17 by the enzyme 17-α-hydroxylase (cytochrome-P-450$_{17\alpha}$) and the side chain consisting of C-20 and C-21 is then cleaved by the enzyme desmolase to yield androstenedione **6**. Testosterone **7** is formed from androstenedione **6** by subsequent reduction of the 17-keto group of androstenedione **6** with a transhydrogenase. This is an equilibrium reaction, the position of which is determined by the ratio of oxidised and reduced co-enzymes and occurs in all steroid producing cells.

Both estrone **8** and estradiol **9** are derived from the related androgens **6** or **7** by aromatisations with the enzyme aromatase (P-450$_{Ar}$). The physiological importance of this transformation of male into female sex hormones has made it the subject of intensive investigation. The aromatisation of androgens **6** or **7** by placental aromatase involves three hydroxylations which take place in sequence (Scheme 2).[11] The first two hydroxylations occur at the C-19-methyl group and yield the C-19 diol, and subsequently the C-19 aldehyde. The third hydroxylation has been identified as being a 2β-hydroxylation, which is the rate-determining step. Hence, the stoichiometry of the androgen to estrogen bioconversion includes the participation of 3 hydroxylations at 2 enzyme sites, involving the loss of the C-19 methyl group and of a hydrogen each from C-1 and C-2.

In the ovary, the equilibrium position is such that estradiol is the major aromatisation product and is the major estrogen of biological importance. Once the estradiol leaves the ovary, the equilibrium shifts in favour of the formation of estrone and as a result the metabolite estrone sulphate is the major circulating steroid in ovulating women. Estradiol **9** is metabolised to the less bioactive estrone **8** by oxidation of the 17α-OH group and also to estriol **10** by hepatic conversion in the peripheral circulation.[12] This is an important control feature of steroid metabolism as the rapid removal of potent estrogens is necessary to ensure the rapid response of the body to changes in the level of estrogen production from the ovaries.[12]

Scheme 1. Biosynthesis of Estrogens and Progesterone
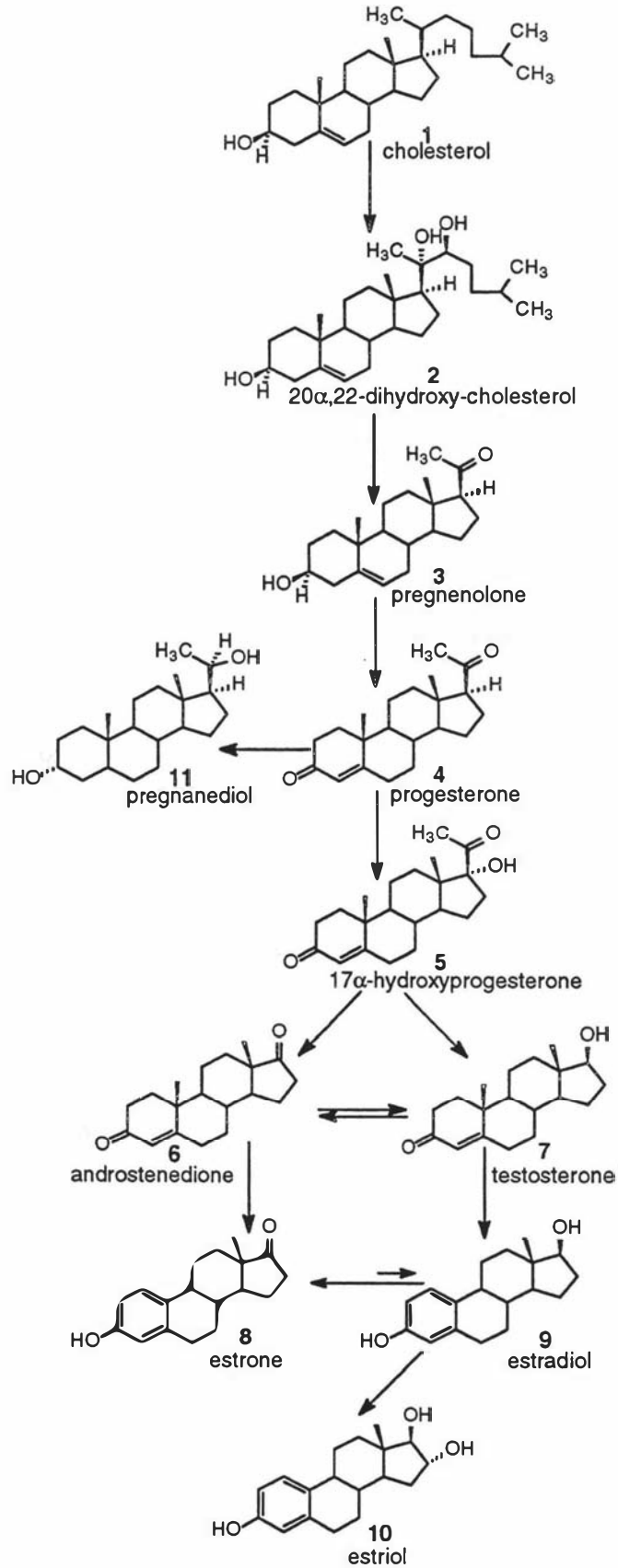
Scheme 2. Estrogen (**8, 9**) biosynthesis sequence and
mechanism for aromatization of androgens (**6, 7**)
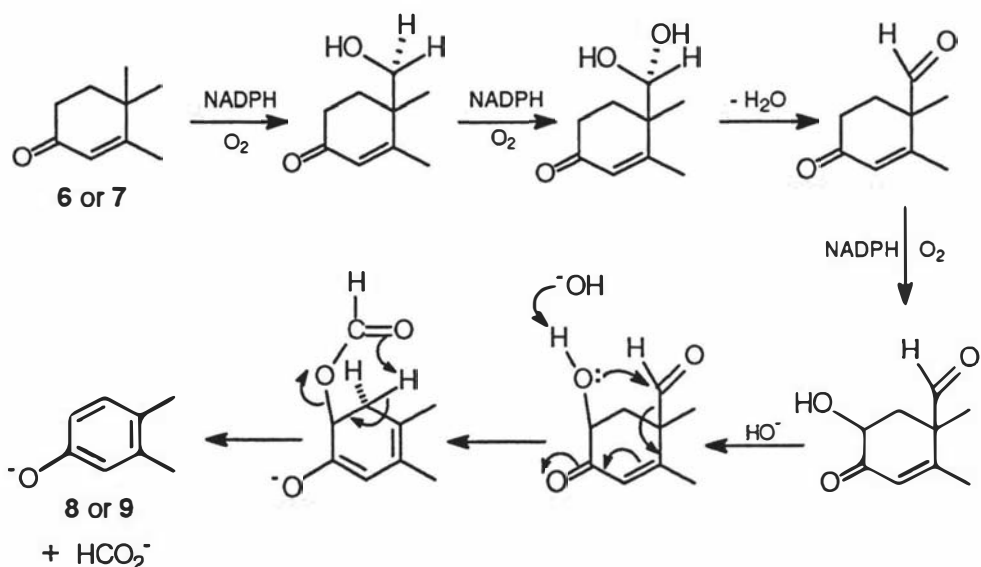
The hydroxylation step requires molecular oxygen and the coenzyme NADPH

1.1.3 Metabolism and excretion of ovarian steroids

Although it is clear that measurement of serum estradiol **9** and progesterone **4** or their metabolites could be used as markers of fertility, the decision which has to be made is whether to assay blood or biological fluids. Since a blood assay is an invasive procedure it is usual to seek metabolites for analysis which are present in biological fluids such as urine or saliva. The preference in these laboratories is to measure urinary metabolites. It is generally recognised that in humans the endogenous ovarian steroid hormones are excreted in urine principally as water-soluble glucuronide, sulphate or mixed glucuronide-sulphate derivatives.[13] The three classic estrogens, estradiol, estrone and estriol (Scheme 1) all appear in the urine as such conjugates. Estradiol and estrone are the principal estrogens produced by the ovary, the former being produced in higher concentrations. Although estradiol-17β-3-glucuronide is the first metabolite to be excreted in urine, it is not a major metabolite of estradiol and is only present in the urine at low concentrations.[14] In contrast, estrone glucuronide (E1G) **12** or the sum of the estriol monoglucuronides (E3-3G) **13** and (E3-16G) **14** are present in relatively large amounts and are excreted in regular cyclical patterns.[15]

Progesterone **4** has more than twenty metabolites, most of which are excreted *via* the bile and the gastrointestinal tract. As the major urinary metabolite of progesterone **4**, pregnanediol (5β-pregnane-3α, 20α-diol) **11** is also excreted in the urine mostly as the glucuronide (PdG) conjugate **16**.[16]

Thus, in summary, urinary estrone glucuronide (E1G) **12** or the sum of urinary estriol 3-glucuronide (E3-3G) **13** and estriol 16β-glucuronide (E3-16G) **14** are suitable metabolites for measurement of circulating estrogen levels and urinary pregnanediol glucuronide (PdG) **16** is a good measure of circulating progesterone levels.

The structures of these steroid glucuronides and the numbering system used in this thesis are shown in Figure 7.

Estrone 3-glucuronide (E1G) **12**

Estriol 3-glucuronide (E3-3G) **13**

Estriol 16α-glucuronide (E3-16G) **14**

Estriol 17β-glucuronide (E3-17G) **15**

Pregnanediol 3-glucuronide (PdG) **16**
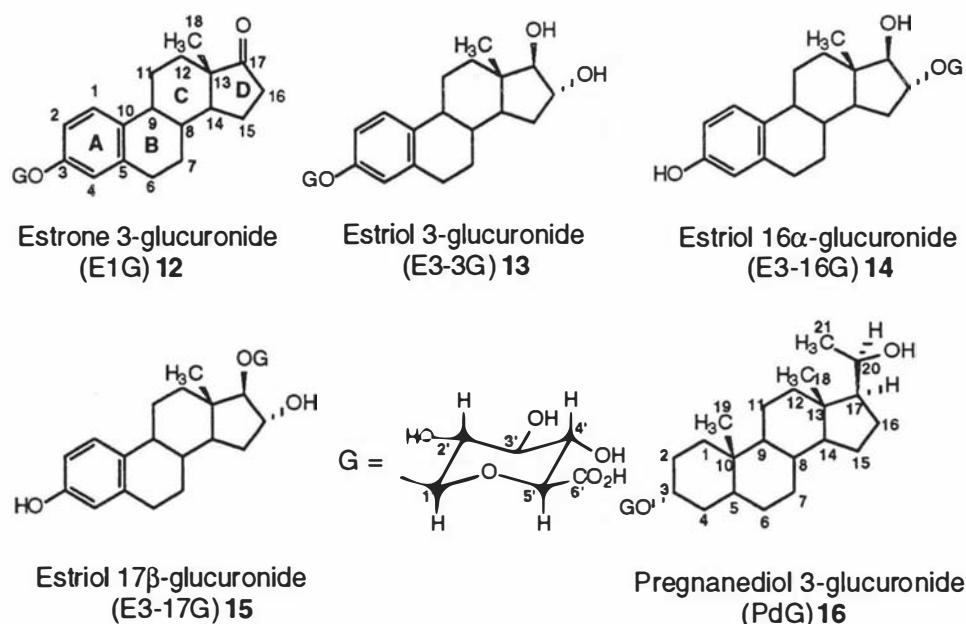
Figure 7. The Structures of Possible Steroid Glucuronide Markers of Fertility

1.1.4 Steroid metabolites as markers of the fertile period

The analysis of steroid glucuronides such as estrone glucuronide **12** and pregnanediol glucuronide **16** in urine as markers of the fertile phase in women has been a goal of the World Health Organisation (WHO) since the 1970's. The first significant increase either in plasma estradiol or its urinary metabolites from baseline values is now accepted as the biochemical marker for the beginning of the potentially

fertile phase of the menstrual cycle.[17] For example, when a reference database of urinary total estrogens (the sum of estrone-, estradiol- and estriol-conjugates in a 24 hour urine sample) was analysed for the first rises as a marker of the beginning of the potentially fertile period,[17] the early estrogen baseline values fluctuated between 3 and 16 µg/24 hours. Once the estrogen values exceeded 20 µg/24 hours, they increased progressively without interruption to the peak value and then decreased rapidly. The peak values ranged from 40 µg/24 hours to 100 µg/24 hours.

When a time series analysis algorithm (Trigg's tracking signal) was applied to these data the first rise in urinary total estrogens from the baseline was unambiguously recognised in all complete cycles. The mean warning of impending ovulation given by the first rises was 6.5±1.4 days.[17] This was sufficient warning for all but the longest sperm survival times. This analysis agrees with the 50th percentile given in Figure 8[18] for the data from 61 ovulatory menstrual cycles which gives a value for the first rise day of about 4 days before the total estrogen peak. Since this is day one of the fertile period and the total estrogen peak day occurs on average 36 hours before ovulation, this also corresponds to a mean warning of ovulation of 6-6.5 days. Thus, the first rise in total urinary estrogens serves as a good marker for the beginning of potential fertility with a high degree of certainty and gives sufficient warning for all but the longest sperm survival times.

The amount of pregnanediol **11** (detected in the form of its glucuronide) in a woman's urine rises rapidly (note the second peak in Figure 8) just after the time of ovulation, indicating the end of fertility, and declines rapidly at the time of menstruation (Figure 8).[17,18] It can be seen from Figure 8 that a pregnanediol excretion rate of 1.4 mg/24 hours signals the end of fertility from 1 to 4 days after the total estrogen peak. This threshold level has been used successfully in the Ovarian Monitor test for PdG (set at 6.3 µmole/24 hours, which is the equivalent of 1.4 mg Pd/24 hours).[18] If conception has occurred, the pregnanediol **11** level remains high thus constituting an early pregnancy test.

Therefore, measurement of E1G (or E3-16G and E3-3G) and PdG levels in urine is very useful for achieving, preventing or diagnosing of pregnancy. The measurement of urinary ovarian steroids is thus very helpful for people to gain a knowledge of their natural periods of fertility and infertility, and in particular as an aid to natural family planning.

Figure 8. Daily urinary estrogen and pregnanediol values throughout 61 ovulatory cycles from 40 women aged 20-40 years. The 10th, 50th and 90th percentile lines are shown. Days are numbered from the day of the pre-ovulatory estrogen peak (day 0).

1.2 Measurement of Steroid Hormones in Urine

1.2.1 Historical notes on the measurement of steroid glucuronides in urine

Measurement of steroid glucuronides in urine has been a continuing challenge since the 1930's when estrogens were first discovered by Marrian *et al.*[19] Despite the many difficulties encountered by previous workers, a number of useful experimental methods have been developed for the measurement of estrogens.

A biological assay for estrogens was described by Astwood[20] in early days, in which the procedure was dependent on the increase in uterine weight of immature rats. Since the method is only semi-quantitative, not specific and a large number of animals are needed to obtain significant results, this biological method is now considered to be too lengthy to enjoy general acceptance, and to lack sensitivity, reproducibility and specificity.

Chemical methods for the measurement of estrogens were carried out by heating with concentrated sulphuric acid and ethanol after hydrolysis of the glucuronides and extraction into organic solvents resulting in the formation of characteristic orange-yellow coloured derivatives (the Kober reaction).[21] These derivatives exhibited an intense green fluorescence, which could be utilised in the development of highly specific colorimetric or fluorimetric methods. Another chemical method, which was originally developed by Professor J. B. Brown,[22] employed initial hydrolysis of the glucuronide conjugates, extraction of the free estrogens with ether and methylation with dimethyl sulphate, purification by alumina column chromatography and final measurement by the Kober colour reaction. Chemical assay is sensitive since 100 ml or more of urine sample may be extracted but this method is obviously impractical for a home test. Although chemical methods are accurate, reliable and provided the background information for the clinical application of the test, they are time-consuming and their use was restricted to only a few centres. Nevertheless, the data in figure 8 forms the reference for all development of alternative assay systems for E1G **12** and PdG **16** including the Ovarian Monitor (section 1.2.3) and related systems.

1.2.2 Immunoassay methods suitable for analysis of E1G, E3-3G, E3-16G and PdG

The immunoassay is an analytical method that depends upon antigen-antibody reactions. The term immunoassay usually refers to a quantitative method for analyzing the immunological properties of analytes.[23] For example, radiolabelled immunoassays use reagents incorporating radioisotopes as tracers to monitor the distribution of free and bound antigen in radioimmunoassays (RIA).

Radioimmunoassays for determining steroid hormone glucuronide concentrations have been reported since 1975.[24] Several steroid glucuronides, including 12-16, were linked directly to a carrier protein by the carboxyl group of the glucuronides. The resultant steroid-glucuronide-BSA complexes were used as antigens in rabbits. The antisera produced bind the steroid glucuronides with high specificity and they can be used to determine the concentrations of steroid glucuronides directly without preliminary hydrolysis. The non-radioactive steroid glucuronide (analyte) and the radio-labeled steroid glucuronide (radioligand) bind to the limited amount of antiserum in a competitive manner. The concentration of free steroid glucuronide (analyte) is calculated from scintillation counting and reference to a standard curve which relates the ratio of bound to free label with the concentration of free hormone. Since the radio-labelled steroid glucuronides were not commercially available they had to be synthesized, usually being prepared from the 6-ene-steroids. Thus the double bond can be reduced with tritium in the presence of palladium on charcoal and tritium can be introduced into the 6 and 7 positions of the steroid glucuronides. Scheme 3 gives an example of the synthesis of radio-labelled steroid glucuronides.
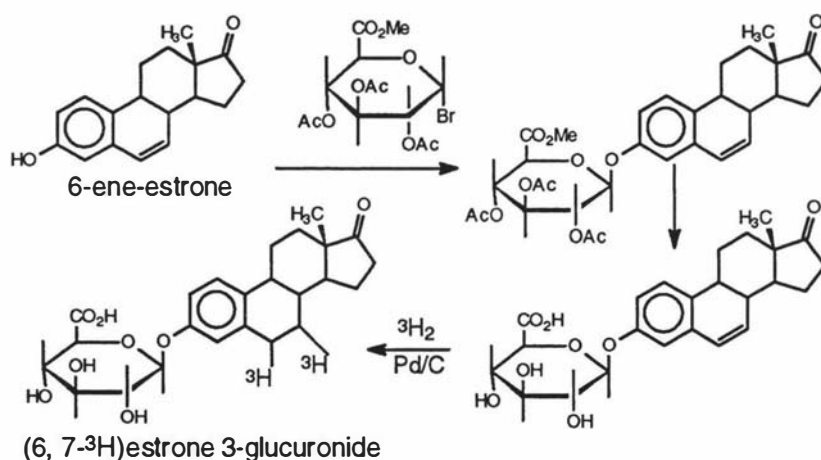
Scheme 3. Synthesis of radio-labelled estrone 3-glucuronide

The chemistry involved in the synthesis was basically the same as for the synthesis of non-radioactive estrone 3-glucuronide **12**, which will be discussed in Chapter 2 (Section 2.1.4.1), except for the extra tritiation step for the radio-labelled estrone 3-glucuronide.

An advantage of radioimmunoassays relative to biological or chemical assays is the high degree of sensitivity obtainable with radiolabelled compounds. The steroid glucuronides may occur in human body fluids in concentrations which range, in small aliquots, from picomoles per litre to micromoles per litre. Radioimmunoassays have the capacity to detect compounds at levels of picomoles per litre or less, well beyond the sensitivity of biological or chemical assay systems. However, there are some problems associated with radioimmunoassays. The disadvantages include the short half-life of the radioactive label, the requirement for special detection equipment and limitations in labelling certain antigens. Also, the bound and free labels have to be separated, which make the radioactivity measurement impractical. In addition, regulations regarding disposal of radioactivity have made the process costly.

More recently, many other immunoassay methods have been developed for the measurement of steroid glucuronides in urine, and are now widely used in research and in the clinical laboratory (Table 1).

Table 1. Immunoassay Methods for Measuring Steroid Glucuronides in Urine

		Ref
Radioimmunoassay (RIA)	Antigen is labelled with a radionuclide for use as the tracer.	24-27
Enzyme Immunoassay (EIA)	An assay procedure based on the reversible and non-covalent binding of an antigen by a specific antibody, in which one of the reactants is labelled with an enzyme.	18, 28-30
Chemiluminescence Immunoassay (CLIA)	Antigen is labelled with a chemiluminescent molecule for use as the tracer.	31, 32
Fluoroimmunoassay (FIA)	Antigen is labelled with a fluorophore for use as the tracer	33

The use of nonisotopically labelled compounds in an immunoassay system has been proposed to avoid many of the problems inherent in radioimmunoassays. Among the nonisotopic immunoassay methods, enzyme immunoassay (EIA) has provided the most convenient means by which the sensitivity and specificity of radioimmunoassay (RIA) can be more generally applied. The reagents and equipment used are relatively cheap, and not associated with special hazards and disposal problems. The enzymes employed for labelling may be stored for long periods of time and enzyme assays are easy to perform often giving colorimetric end-points which can be visually assessed.

Enzyme immunoassays are based on two important biological phenomena. (i): the extraordinary discriminatory power of antibodies, and (ii): the extremely high catalytic power and specificity of enzymes, which may quite often be detectable with great ease at low levels.

Enzyme immunoassays consist thus of a two-pronged strategy: the reaction between the immunoreactants (antibodies with the corresponding antigen) and the detection of that reaction using enzymes, attached to the reactants (hapten-enzyme conjugates) or antibodies (protein-enzyme conjugates), as indicators. There are two general assay types: one in which free and bound label are separated before detection, and one in which the free label can be detected in the presence of the bound label. The assays are termed "Heterogeneous" Enzyme Immunoassays and "Homogeneous" Enzyme Immunoassays respectively.

1.2.3   Homogeneous enzyme immunoassay and the Ovarian Monitor

A "homogeneous" enzyme immunoassay is one which requires no physical separation of bound and free label and was first reported by Rubenstein *et al* in 1972,[34] as an alternative to radioimmunoassays (RIA) and "heterogeneous" enzyme immunoassays. Since it required no purification, extraction or separation of the antibody-bound antigen from the unbound antigen, this revolutionary technique gave the immunoassay much simplicity and the potential to be utilised in home assays.

One of the important features in "homogeneous" enzyme immunoassay systems is that the enzyme activity of the enzyme-hapten conjugates is extensively inhibited by addition of the relevant antibodies. This inhibition is usually inversely proportional to the amount of free hapten in a stochiometric manner. Hence, a measurement of the enzyme activity of a mixture of enzyme and antibody is directly related to the amount of free antigen introduced from a test sample.

Among many different homogeneous immunoassay methods, the first practical, accurate home system for the measurement of estrone glucuronide and pregnanediol glucuronide as markers of fertility, known as the "Ovarian Monitor", has been developed and refined for over twenty years by Professor J. B. Brown and co-workers[18,28] in the Department of Obstetrics and Gynaecology at the University of Melbourne. This system has been validated extensively by many studies including a Word Health Organisation (WHO) trial and is currently used around the world in many countries, both developed and undeveloped. The basis of the test is a homogeneous enzyme immunoassay system in which an anti-steroid estrone glucuronide or pregnanediol glucuronide antibody extensively inhibits the corresponding lysozyme-steroid glucuronide conjugate. As a result, the concentration of E1G **12** or PdG **16** in a urine sample can be determined directly from a simple rate assay without the need for a separation step.

A Stylised Diagram of the Ovarian Monitor

A Stylised Diagram of an Ovarian Monitor Assay Tube and its Constituents
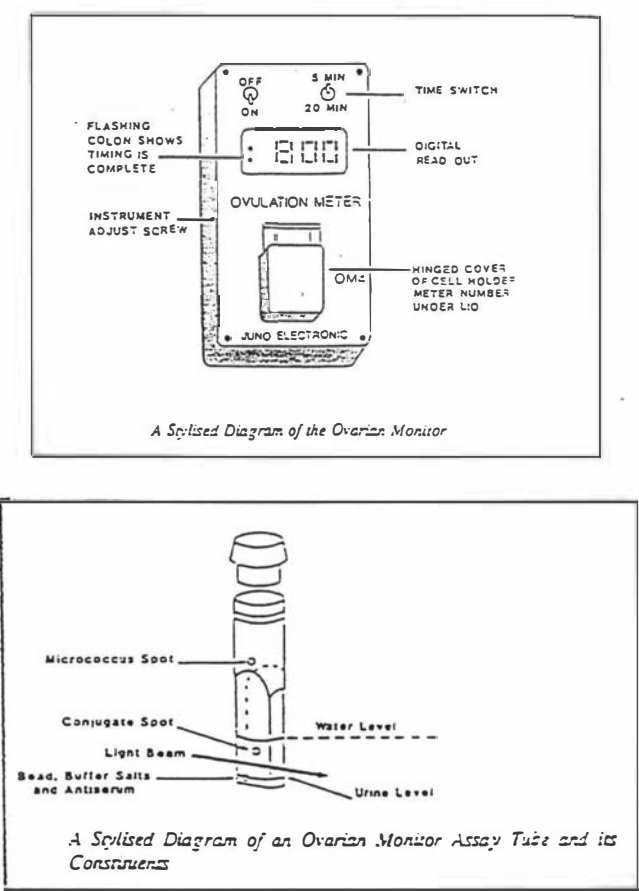
Figure 9. A diagram of the Ovarian Monitor, and a diagram of assay tube and its constituents.

The Ovarian Monitor consists of two important parts; an assay tube and a monitor (Figure 9). In the assay tube, a total of three reactions are performed in the one plastic colorimeter tube which contains the antiserum, enzyme-hormone conjugate and *micrococcus lysodeikticus* (enzyme substrate) placed in exactly measured amounts at different levels on the sides of the tube. This allows the three reactions to be performed serially in a single tube; the Ovarian Monitor has three key functions; (i) as a miniature spectrophotometer measuring and displaying the transmission result; (ii) using an in-built thermostat to control the assay temperature at $40\ ^0C$; (iii) an in-built timer to control the time of the three steps.

The assay process is performed in three steps (Figure 10). The first step is the antigen-antibody reaction; on the time scale of the reactions, the free E1G **12** or PdG **16** in the urine binds irreversibly to the appropriate anti-steroid glucuronide antibody (for E1G or PdG) which is present in a slight excess. Thus, the levels of antibody binding or neutralisation are determined by the E1G or PdG levels in the urine.
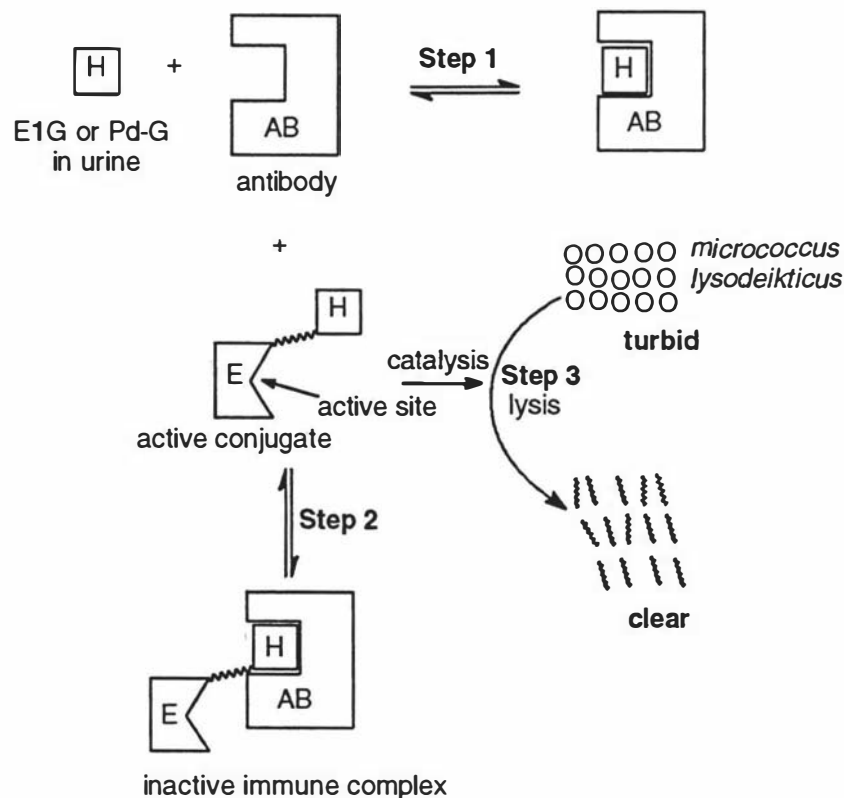
Figure 10. Principle of Homogeneous Enzyme Immunoassay in Ovarian Monitor.

In the second step, the excess antibody, which was not bound by E1G or PdG in the previous step, binds again effectively and irreversibly on the time scale of the experiments to the steroid-enzyme conjugate. The lysozyme conjugate is prepared by the coupling of E1G or PdG *via* their carboxyl groups with amino groups of lysine residues of hen egg white lysozyme (HEWL).[18] The amount of free conjugate remaining at the end of the second step is determined by the amount of free antibody left at the end of the first step, which is determined in turn by the level of E1G or PdG in the urine.

The third step is the *Micrococcus lysodeikticus* reaction. In this step, the free steroid glucuronide-enzyme conjugate remaining after the second step is active to lyse its substrate, *Micrococcus lysodeikticus*, by breaking the peptidoglycan bonds and turning the initially turbid solution clear. The rate of this reaction is measured by the amount of clearing of the turbid solution over fixed time periods. The rate of clearing is determined by the amount of free steroid glucuronide-enzyme conjugate remaining at the end of second step, which is determined in turn by the amount of E1G **12** or PdG **16** in the urine sample.

Thus, a high level of E1G (or PdG) in the urine gives rise to a high level of free lysozyme-steroid glucuronide conjugate and hence a high rate of lysis. Conversely, a low concentration of E1G (or PdG) gives a low level of free conjugate and hence a low rate of lysis. This is shown in a typical standard curve for E1G (Figure 11).[35] Sensitivity is just right in the range of values found in the normal menstrual cycles.

Figure 11. The Standard Curve for Estrogen Glucuronide (E1G, 12)
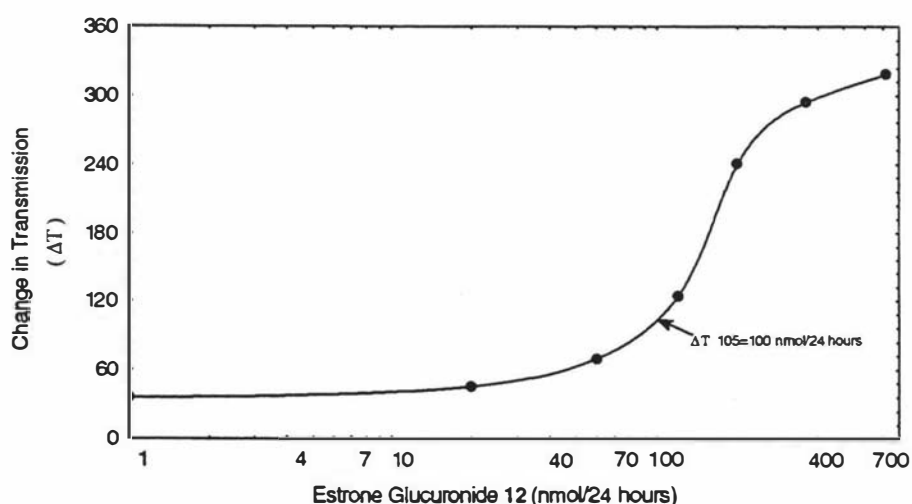
Hence, a simple rate measurement gives a direct measure of the free E1G or PdG concentration and hence direct access to vital hormonal data which signals the state of fertility. For the E1G assay the rate is measured over 20 minutes and for the PdG assay 5 minutes. The women at home can plot their data as change in transmission (ΔT) versus cycle day to accurately and simply determine their menstrual cycle hormonal profile (Figure 12).[35] Figure 12 shows that the beginning of fertility is most likely on day 4 (6 days before the E1G peak day), the most fertile day is day 11 and the end of fertility is given by the pregnanediol glucuronide (PdG) rise on day 14.

Figure 12. Normal menstrual cycle obtained by a woman at home using the Ovarian Monitor
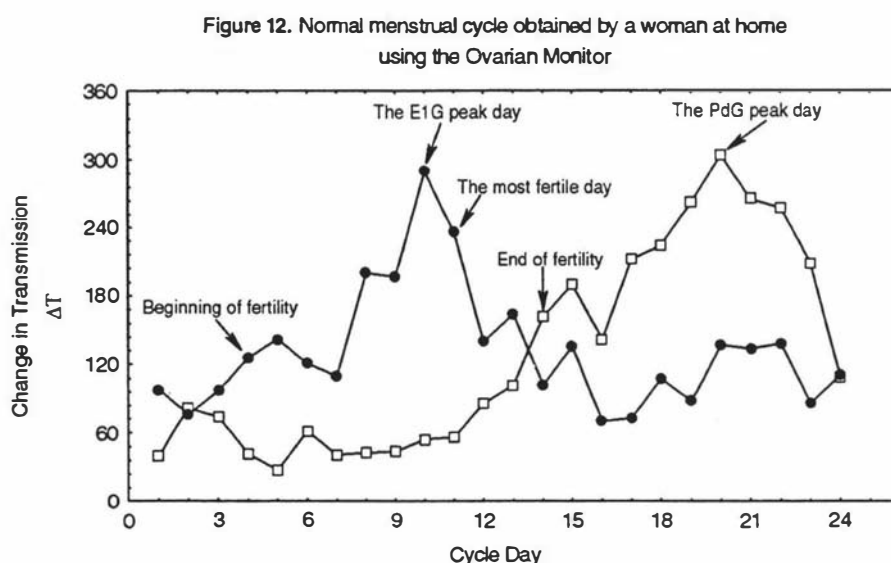
1.2.4 Homogeneous prosthetic group-labelled immunoassay (PGLIA)

In the development of homogeneous enzyme immunoassay systems, some molecules acting with, or upon enzymes, have also been used as immunoassay labels. These assays are called "enzyme-based immunoassays".[36] Such assays depend on the steric hindrance caused by the appropriate antibody attaching itself to the hapten-labelled conjugate, thus modulating the enzyme activity by altering the natural function of the label with the enzyme. These molecules are normally prosthetic groups,[37] enzyme cofactors,[38] substrates[39] and inhibitors.[40] They have all been shown to be suitable for use in immunoassays.
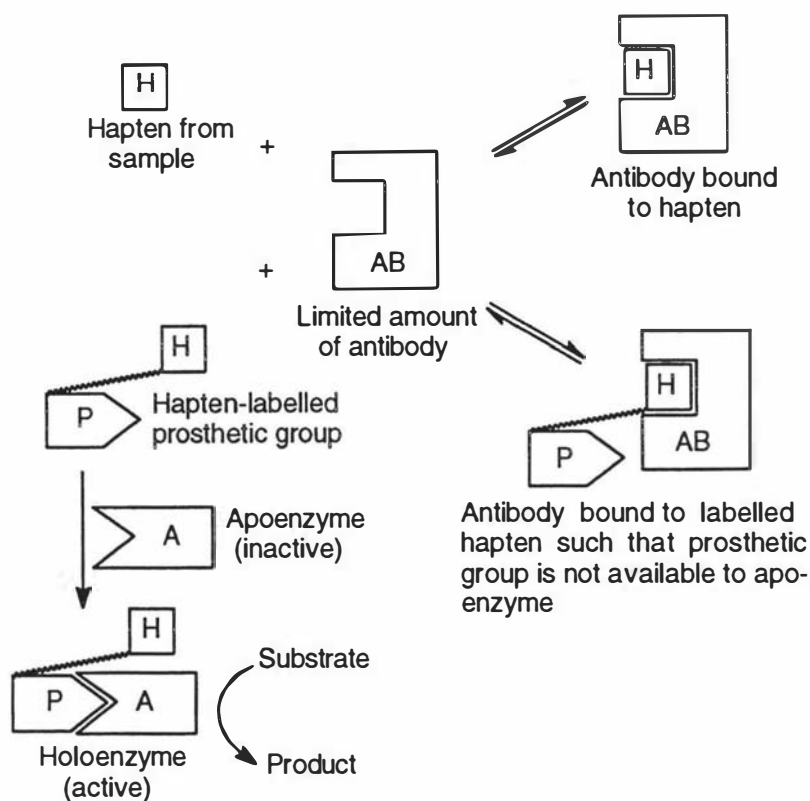
Figure 13. Principle of "Prosthetic Group-Labelled Immunoassay"

The use of a prosthetic group as a label in immunoassay (PGLIA) could lead to the development of sensitive systems as illustrated in Figure 13. Although PGLIA assays have not been used for the measurement of E1G or PdG, the principles involved are relevant to the development of a new system in this thesis. It is necessary to have an understanding of the principle of "PGLIA".

In the first step of PGLIA, the hapten-labelled prosthetic group competes with free hapten from the sample to bind to a limited amount of antibody in solution. A high level of hapten from the sample results in higher binding with the antibody, thus giving rise to a high level of free hapten-labelled prosthetic group left in solution. Hence, the amount of free hapten-labelled prosthetic group is proportional to the amount of hapten from the sample. The second step is the formation of an active holoenzyme after addition of the apoenzyme. The apoenzyme only becomes active when it has been converted into the holoenzyme by binding to the prosthetic group, which is part of the active site of the enzyme. Since antibody bound to the labelled-hapten ensures that the prosthetic group is not available to the apoenzyme, only free hapten-labelled prosthetic group can bind with the apoenzyme to form active holoenzyme, which only then can catalyse the reaction of substrate to product. Therefore, the rate of conversion of substrate to product is determined by the amount

of free hapten-labelled prosthetic group, which is determined in turn by the amount of hapten in the sample.

Prosthetic Group-Labelled Immunoassay (PGLIA) has two potential advantages resulting from the fact that the enzyme is not labelled as it is in normal homogeneous enzyme immunoassays. This allows a wider range of reaction conditions to be used as the prosthetic groups are much more stable than enzymes. The products of these conjugation reactions should also be more specific than reactions involving enzymes, which generally have several comparable functional groups, many of which are likely to react.

Prosthetic Group-Labelled Immunoassay (PGLIA) for the detection of a hapten was first reported by Morris *et al.*[37] They successfully used flavin adenine dinucleotide (FAD) as the prosthetic group, and glucose oxidase as the enzyme, in a colorimetric immunoassay for theophylline. In their method, the prosthetic group (FAD) was joined covalently to the hapten (theophylline) through an appropriate molecular linker (Figure 14) in such a way that the conjugate **17** was able to combine with inactive apoenzyme to form the active holoenzyme.
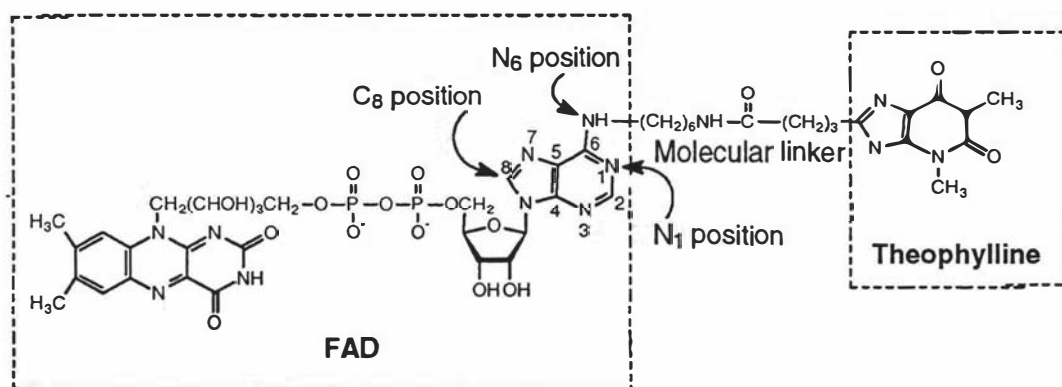
Figure 14. Structure of Theophylline-FAD Conjugate **17**

All the reagents were readily prepared and the assay was rapid, which demonstrated that very reliable results can be obtained within 3 minutes of mixing the components. Also, these assays can be carried out without the need for a separation step because the ability of the prosthetic group-hapten conjugate to regenerate active holoenzyme is substantially inhibited when the labelled hapten is complexed with its antibody. The theophylline-FAD conjugates were found to be stable for at least 12 months when stored appropriately.

The activity of the theophylline-FAD conjugate **17** with apoglucose oxidase shows that the conjugation position of the hapten on the FAD molecule is very important. Binding of the N_6-conjugate to the apoenzyme was much stronger than that of the C_8-conjugate, while the N_1-derivative of FAD had very little activity with apoglucose oxidase[41] (see Figure 14). The properties of the molecular linkers, such as the presence of negatively charged groups in the vicinity of the binding position or some functional groups appended to the binding chain, may inhibit the binding of the FAD conjugate to the apoenzyme. So, the choice of the right binding position and the appropriate molecular linker is one of the most important considerations in making prosthetic group-hapten conjugates, which can be effectively combined with the apoenzyme to form the active holoenzyme. This prosthetic group-labelled immunoassay has also been successfully adapted to a reagent strip format by Tyhach *et al.*[42] Clearly, it could also in principle be adapted to the measurement of E1G, E3-3G, E3-16G and PdG.

1.3 A Search for New Inhibitable Enzyme Systems for Use in Home Assays

1.3.1 The limitation of the Ovarian Monitor system

Despite the success of the Ovarian Monitor system in measuring E1G **12** and PdG **16** (it is as accurate as most laboratory assays and is carried out by women in their homes), there is a perception that the market demands a colour test strip or dipstick type kit to replace the "Ovarian Monitor" for simplicity and economical reasons. The new colour tests, which can be validated against the Ovarian Monitor assay, are expected to be much faster and simpler than the monitor in use, but with the proviso that they must be as accurate as the monitor in order to be of value.

One of the main obstacles to achieve the new colour test strip has been the limitations of the human eye. It can not discriminate between the small increases in colour intensity that occur as fertility begins (about 20% increase per day). Hence, a search for new highly active enzyme systems, instead of using lysozyme, for the preparation of enzyme-steroid glucuronide conjugates for use in home assays for fertility is the main goal of this thesis. If inhibition can be achieved, then the new coloured enzyme could be used in a homogeneous enzyme immunoassay for E1G, E3-3G, E3-16G and PdG. Even if inhibition is not achieved as long as immune reactivity is present in the new enzyme-steroid glucuronide conjugates, which can be linked to a solid phase such as paper or plastic, ELISA (enzyme linked

immunosorbent assay) systems, therefore, can still be developed. It should also be noted that such a system would be generic and applicable to almost any hapten or small molecule.

1.3.2 Horseradish peroxidase (HRP) and HRP-steroid glucuronide conjugates

A variety of enzymes have been used as labels in immunoassays, but horseradish peroxidase (HRP) is one of the most widely used indicator enzymes in the life sciences. HRP has a high molecular stability upon storage when used under various different assay conditions, i.e. variations in pH, ionic strength, buffer types and temperatures.[43] HRP is reasonably cheap and is available in a relatively pure form, and has a carbohydrate content of 10-15%, which can be utilised in certain conjugation reactions. Recently, a recombinant HRP isomer C[44] has also become available, which has high purity and homogeneity. Furthermore, HRP is an ideal enzyme suitable for development in a colour test due to its very high catalytic rate on a variety of substrates to produce a variety of intense colours. Hence, HRP was chosen for the preparation of enzyme-steroid glucuronide conjugates in this thesis rather than glucose oxidase or other enzymes.
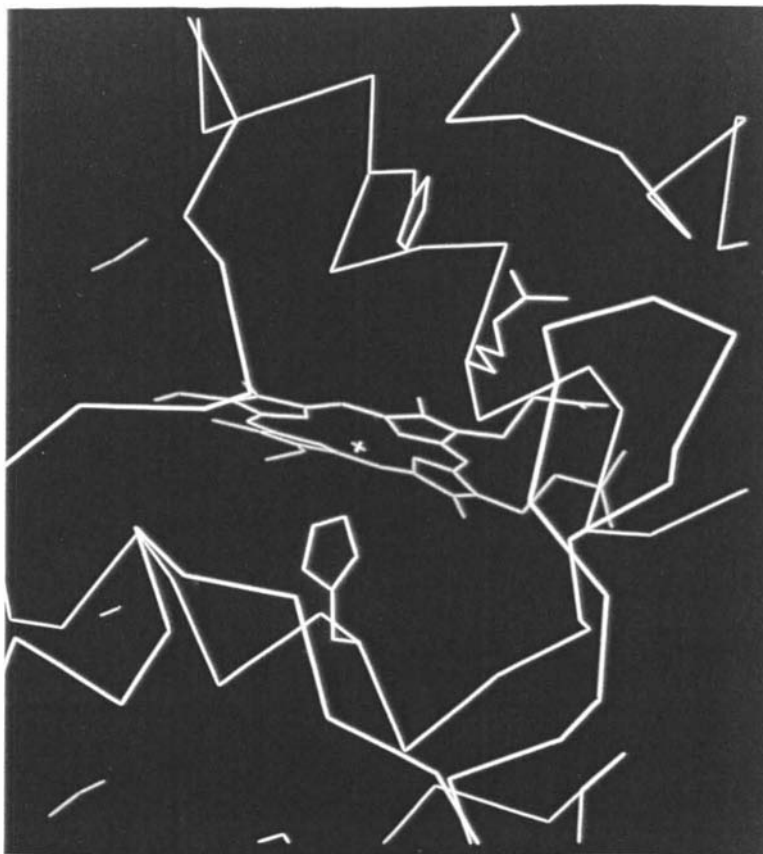
Figure 15. Part of the crystal structure of cytochrome *c* peroxidase indicating the heme group (orange), the iron atom (in the middle of the heme group marked with a +) and three amino acid residues (green).

The components of the HRP molecule can be represented as two parts: protohemin (hemin) and glycoprotein (apoenzyme). Since there is no direct crystal structure of HRP[44] available during the time of writing this thesis, and also all the peroxidases have similar structures, the structure of HRP was examined by using the crystal structure of cytochrome *c* peroxidase as a model (Figure 15).[45] The crystal structure of cytochrome *c* peroxidase indicates that the heme group (orange) is buried in the protein (yellow) and the iron atom (in the middle of the heme group marked with a +) is coordinated with a proximal histidine residue (green below the heme plane). Both distal histidine and arginine residues (both green above the heme plane) function as acid-base catalysts or as a polarizing residue to facilitate the catalytic reaction. The detailed catalytic mechanism of the prosthetic group (heme) and all these three amino acid residues will be discussed in chapter 5.

As the basic requirement of an enzyme immunoassay, the hapten-enzyme conjugates must retain both the catalytic activity of the enzyme and the immune reactivity of the hapten (or alternatively the binding characteristics of the antibody). In general, specific hapten-enzyme conjugates are not available commercially, and careful consideration must be given to the choice of enzyme labels and the methods of conjugate formation.

There are two ways in which enzymes have been employed, directly or indirectly, as immunoassay labels.[36] The direct method for the preparation of enzyme-labelled steroid glucuronide conjugates has been *via* the glucuronic acid moiety, coupled directly with lysine ε-amino groups of the enzymes. There are a number of coupling methods[46,47] available to link enzymes and steroid glucuronides together by this direct method. Rajkowski *et al*[46] used four different enzymes (horseradish peroxidase, urease, alcohol dehydrogenase and glucose-6-phosphate dehydrogenase) to couple to steroid glucuronides by each of the following methods: (i) a carbodiimide method using 1-ethyl-3-(3-dimethylaminopropyl)carbodiimide ·HCl; (ii) a carbodiimide method using 1-cyclohexyl-3-(2-morpholinoethyl)carbo-diimidemethyl-4-toluene sulphonate; (iii) the mixed anhydride method; and (iv) the hydroxysuccinimide/N,N'-dicyclohexylcarbodiimide method. However, only the mixed anhydride method produced an enzyme-labelled product which retained any measurable enzymatic activity and only horseradish peroxidase retained more than 50% of its enzymatic activity.

Recently, estrone glucuronide (E1G) conjugates of hen egg white lysozyme were prepared by both the mixed-anhydride and the hydroxysuccinimide/N,N'-dicyclohexylcarbodiimide (active-ester) coupling procedures in this laboratory.[48] Both methods gave good yields of conjugate but the active-ester procedure gave a more diverse range of products consistent with its greater acylating ability. The purified conjugate material from the active-ester reaction gave over 90% inhibition of the lytic activity in the presence of an estrone glucuronide antibody. When an estrone glucuronide-lysozyme conjugate was used in a homogeneous enzyme immunoassay system the levels of urinary estrone glucuronide encountered in a normal menstrual cycle were easily measured (as in Figure 12). An estrogen conjugate enzyme immunoassay for monitoring pregnancy in the mare has also been reported[49] by using an enzyme conjugate prepared from direct conjugation of estrone glucuronide (E1G) 12 to horseradish peroxidase (HRP). Additionally, March *et al*[47] reported that alkaline phosphatase can be used to make enzyme-steroid glucuronide conjugates, which are both enzymatically and immunologically stable. However, direct conjugation was not the preferred route in this thesis but chemical modification of the carboxyl groups of hemin appeared to give access to a more elegant general synthetic route.

1.3.3 Preparation of HRP-steroid glucuronide conjugates *via* hemin-conjugation

One of the most important characteristics of enzyme-hapten conjugates in homogeneous enzyme immunoassay systems is that the enzyme activity of enzyme-conjugate has to be extensively inhibited by the addition of an antibody. This inhibition property has not been observed in the application of HRP-steroid glucuronide conjugates so far. In order to achieve this inhibition of the conjugate for a new colour test for home use, it is worth trying to design some new specific conjugation methods, to control the location and orientation of the hapten (steroid glucuronides) close to the active site of the enzyme, for the preparation of HRP-hapten conjugates. Even if no inhibition is achieved by this strategy, the new method is still useful since the resulting immunoassay system contains only active steroid glucuronide-HRP conjugates or apo-HRP and no free HRP is present. Therefore, it gives control and reduces non-specific binding by unconjugated HRP in any assay formats.

In theory, hemin-E1G, E3-3G, E3-16G or PdG conjugates can be prepared either by the above direct coupling of the glucuronic acid with the lysine ε-amino groups of the enzymes (direct conjugation), or by linking the glucuronic acid with one

of the carboxyl groups from the hemin (prosthetic group) followed by reconstitution with apo-HRP (indirect conjugation). Since hemin functions as a prosthetic group to govern the enzyme activity of HRP, when steroid glucuronides are coupled to the hemin carboxyl group, the enzyme activity of HRP-steroid glucuronide conjugates are more likely to be inhibited by addition of the anti-steroid glucuronide antibodies due to closeness of the bulky antibody to the active site of the enzyme. Also the PGLIA technique can be applied and compared with the glucose oxidase system.

Furthermore, comparison of the direct conjugation method (protein-conjugation) with the indirect conjugation approach (hemin-conjugation) for the preparation of HRP-steroid glucuronide conjugates shows that the direct conjugation method had also some other problems as well:

(i) Since the enzyme contains both -COOH and $-NH_2$ groups, self-polymerisation of the enzyme can occur with carbodiimide coupling, which causes enzyme cross-linking and denaturation during direct protein conjugation.[50]

(ii) The conjugates need to be separated and purified from the unreacted enzyme and free hapten. But purification of the enzyme-hapten conjugates often affects the sensitivity of the enzyme immunoassay. The presence of free enzyme may cause high background signals. For example, in a solid-phase colour test, free HRP can strongly interfere with the analysis result while unconjugated hapten tends to dilute out the enzyme-labelled form. Hence, the removal of free hapten, or especially unconjugated enzyme, is necessary and very difficult to achieve, sometimes requiring special techniques,[51,52] which take a lot of time and increases the cost.

(iii) The important features of an enzyme-hapten conjugate are its enzymatic activity and immunoreactivity, which are strongly affected by the ratio of hapten to enzyme and the location of the hapten relative to the active site of the enzyme.[53] In theory, the coupling of one hapten per enzyme should be optimal. However, in practice the amount, the location and the orientation of the hapten on the enzyme surface is hard to control during direct protein conjugation, since protein molecules normally contain several different $\varepsilon-NH_2$ groups at different sites on the enzyme.

(iv) Since the efficiency of conjugation of steroid glucuronides with HRP is poor,[46,54] the direct coupling is usually performed by using a large excess of steroid glucuronides and employing concentrated reagents. For example, the conjugations of E1G **12**, E3-16G **14** or PdG **16** with HRP have been achieved by using a 20 to 60

times molar ratio of steroid glucuronides to enzyme.[46] Recently, 11α-hydroxy-progesterone 11-glucuronide was conjugated to HRP by using a very high initial molar ratio of glucuronide to HRP of 300:1.[54] Because steroid hormone glucuronides are very expensive to purchase and hard to synthesise, this direct conjugation greatly increases the cost of the procedure.

Unlike the direct protein conjugation procedure, the hemin-conjugation method for the preparation of HRP-steroid glucuronide conjugates can not only provide important inhibition properties for the enzyme-conjugates, but it can also effectively avoid the above direct protein conjugation problems. First, the steroid glucuronic acid moiety can be coupled to the hemin carboxyl group by an appropriate molecular linker without any cross-linking problems. Secondly, the ratio of the steroid glucuronides to hemin (1:1), the location and the orientation of steroid glucuronides on the enzyme surface are comparably easy to control by using different types and length of molecular linkers between the hemin and the steroid glucuronides. Furthermore, the hemin-steroid glucuronide conjugates should be much more stable in use and in storage, and also much easier to purify and characterise by appropriate analytical techniques than the HRP-steroid glucuronide conjugates.

The use of the hemin-steroid glucuronide conjugates in an enzyme immunoassay could be considered in two ways: It could be used directly in a "prosthetic group-labelled immunoassay (PGLIA)" just as with the FAD-theophylline conjugate **17** (Figure 14). Alternatively, it could be further recombined with the apo-HRP to form active HRP-steroid glucuronide conjugates for use in a normal homogeneous enzyme immunoassay system. Hence, a new approach is provided in this thesis to the synthesis of hemin-E1G, E3-3G, E3-16G and PdG conjugates for use in new assays for urinary E1G, E3-3G, E3-16G and PdG. This can be achieved by coupling hemin acids with the appropriate steroid glucuronic acids using appropriate di-amine molecular linkers, followed by their reconstitution with the apoenzyme to make active HRP-steroid glucuronide conjugates. The major aim of this thesis therefore is to produce these new materials for enzyme immunoassays (both homogeneous and heterogeneous), which will be discussed in the following chapters, as the first step towards new colour tests for the markers of the fertile period.

Chapter 2

Synthesis and Characterisation of Steroid Glucuronides

2.1 Introduction

As a first step in the production of hemin-E1G, E3-3G, E3-16G and PdG conjugates, a ready supply of the different steroid glucuronides is needed as starting materials. In general, there are three sources of steroid glucuronides available; (i) commercial purchase (NZ$10,000 per gram); (ii) extraction from pregnancy urine; and (iii) direct chemical synthesis. Since it is very expensive to purchase the steroid glucuronides and difficult and time-consuming to extract them from pregnancy urine, the chemical synthesis route was taken for preparation of the different steroid glucuronides utilised in this thesis. For the development of colour tests which can serve as markers of the fertile period gram amounts of estrone glucuronide, estriol 3-glucuronide, estriol 16-glucuronide and pregnanediol glucuronide are needed. As discussed in chapter 1 (section 1.1.4) these are the preferred urinary metabolites of serum estradiol and progesterone for measurement.

2.1.1   The types and the sources of steroid glucuronides

A variety of steroid glucuronides have been isolated from natural sources, and their structures may be classified chemically into four different types depending on the nature of the acetal linkage:[55]
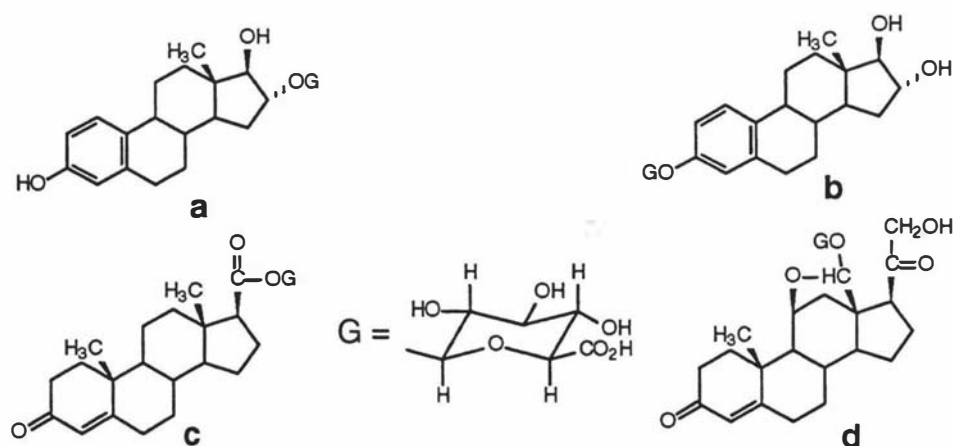
Figure 16. Four different types of steroid glucuronides

(i) alkyl glucuronides in which the linkage to the aglycon moiety involves an alcoholic OH group (**a**); (ii) aryl glucuronides which involve linkage to a phenolic OH group (**b**); (iii) acyl glucuronides involving linkage to a carboxylic acid OH group (**c**); and (iv) "hemiacetal" glucuronides where the linkage to the glucuronide is *via* a hemiacetal OH group (**d**). The structures of these various steroid glucuronides are given in Figure 16. Alkyl and aryl glucuronides are probably the most commonly occurring in nature and only these two types of steroid glucuronides are pertinent to this thesis.

2.1.2   β-Selective O-glycosylation reactions

The most commonly employed method for the synthesis of steroid glucuronides involves the O-glycosylation reaction of a glycosyl donor with an appropriate steroid aglycon under Koenigs-Knorr conditions as a key step.[56-63] From a synthetic standpoint, the efficiency of the O-glycosylation reaction generally involves a high chemical yield, regioselectivity, and stereoselectivity. Among these three criteria, the high regioselectivity was comparatively easy to realise by the selective protection of the hydroxyl group of the glycosyl acceptor. Therefore, many organic chemists have focused on the high chemical yield and high stereoselectivity of the O-glycosylation reactions.

For the synthesis of steroid glucuronides, the correct stereochemistry at the anomeric carbon atom of the glucuronide ring is also essential since the naturally occurring metabolites of estradiol and progesterone all have the β orientation. Thus, any immunoassay system must be designed so that the anti-steroid antibodies, which are raised against synthetic steroid glucuronide protein conjugates, specifically recognise the β form of the steroid glucuronide metabolites. Clearly, if the linkage of the glucuronide ring in the synthetic materials were of α orientation, the antibodies raised by injection of the steroid glucuronide-protein conjugates into sheep would have the wrong stereospecificity. All antibodies so far raised against authentic samples of estrone glucuronide have a high degree of specificity hence the methodology to synthesise and characterise β-glucuronides is an essential pre-requisite for success in this project.

Therefore, in this thesis the chemical synthesis and characterisation of steroid glucuronides will focus on the linkage of a glucuronic acid moiety with the alkyl or aryl hydroxyl groups of steroids to give a β-linked steroid glucuronide. The procedures for synthesising steroid glucuronides using different glycosyl donors and

with particular emphasis on methods appropriate for steroid β-glucuronides will now be reviewed.

2.1.2.1 Different glycosyl donors

(A) Glycosyl halides

The use of glycosyl bromide or chloride as an effective glycosyl donor in the glycosylation reaction was first introduced by Koenigs and Knorr in 1901.[64] In relation to the anomeric stereochemistry of the glycosylation reaction, there are three basic methods which have been developed; (i) the neighbouring group assisted method for construction of a 1,2-*trans*-glycoside such as a β-gluco or α-manno type glycoside; (ii) the anomerisation method[65] for the synthesis of an α-gluco or α-manno type glycoside; and (iii) the heterogenic catalyst method[66] for preparation of a β-mannoglycoside. It is obvious that only method (i) is related to, and most used, in the synthesis of 1,2-*trans*-glycosides such as steroid β-glucuronides. The reaction has been known as the Koenigs-Knorr reaction since that time.

This well-known Koenigs-Knorr method may be described as the coupling of a halosugar with an alcoholic or phenolic group under anhydrous conditions, in the presence of a promoter system. It is generally recognised that orthoesters are the main intermediates in this Koenigs-Knorr reaction. In fact, the use of Koenigs-Knorr reaction conditions is seen by some workers merely as a convenient way of generating an orthoester *in situ* for glycosidation reactions.[67]

The detailed mechanistic studies by Garegg *et al*[67] showed that the chemical yield and the stereochemistry of Koenigs-Knorr reactions are dependent on the following parameters: (i) the structure of the glycosyl halides; (ii) the structure of the alcohol or phenol compounds (glycosyl acceptor); (iii) the promoter used; and (iv) the solvent used. The overall mechanism[67,68] proposed by these workers to account for the glycoside formation in most Koenigs-Knorr reactions is shown in Scheme 4.
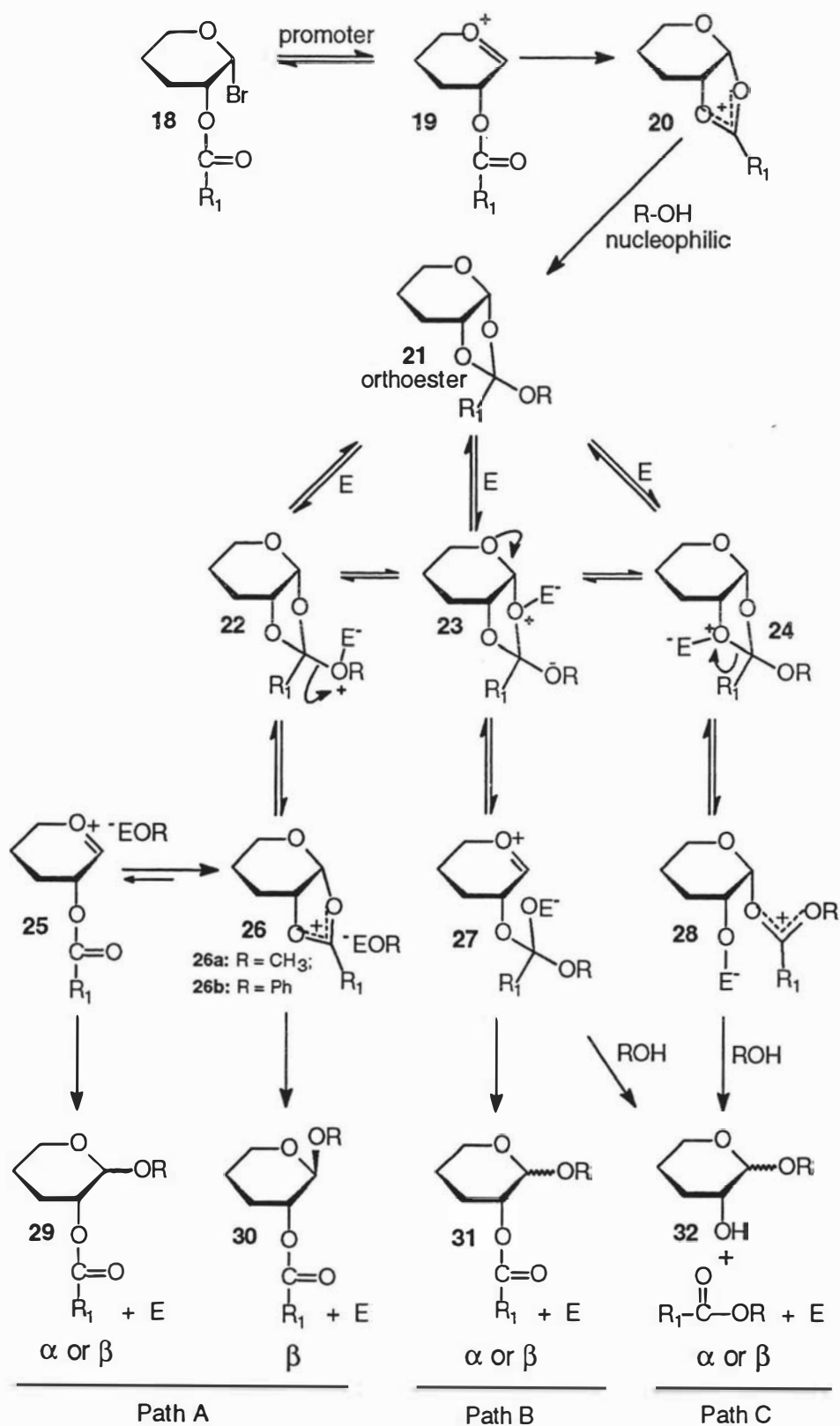
Scheme 4. Possible reaction pathways of glycoside formation
when orthoester 21 reacting with an acid (**E**).

Initially, the glycosyl halide **18** undergoes heterolysis of the carbon-bromine bond assisted by a promoter (halophilic reagent or halide ion acceptor) to form a shielded carbocation **19**, which subsequently forms a 1,2-dioxolenium ion **20** by intermolecular reaction of the neighbouring 2-acetoxy carbonyl oxygen atom with the electron deficient carbon-1. Subsequent nucleophilic reaction of an alcoholic or phenol hydroxyl group with the 1,2-dioxolenium ion **20** results in formation of the orthoester **21**.

There are three possible reaction pathways for acid-catalysed glycoside formation from the orthoester **21**.[67] For most Koenigs-Knorr reactions path A is the main path way, because the cyclic ion pair intermediate **26** is much more stable than the acyclic ion intermediates **27** and **28** in pathways B and C. The cyclic ion pair **26** subsequently forms the β-glucuronide **30** by internal rearrangement, or *via* the acyclic ion **25**, which is in equilibrium with **26**, leading to a mixture of the α and β-glycosides **29**. This is also true for the conversion of acyclic ion **27** to the α and β-glycosides **31** since the alcohols (ROH) can nucleophilically attack the anomeric carbon from both α and β sides of the sugar rings.

Garegg *et al*[67] found that the stereochemistry of Koenigs-Knorr reactions was affected by the structure of the alcohol partner. With alcohols which had either decreased electron density at the alkoxyl oxygen, or some bulky substituents on the adjacent carbon atom, the Koenigs-Knorr reaction was more likely to produce a high proportion of α-glycosides. This can be explained on the basis of scheme 4 as follows: When the oxygen electron density of the counterion (EOR⁻) in the cyclic ion pair intermediate **26** is decreased, or if R is made more bulky, the rate of the β-glycoside yielding reaction (**26** to **30**) is decreased. Reaction by way of the more reactive, but lower concentration, of the acyclic ion **25** then becomes important, thus leading to a higher proportion of α-glycosides.

It also can be seen that on the basis of scheme 4 a low electron density on the oxygen atom (weak base) or for sterically hindered alcohol compounds there will also be a decrease in the yield of the Koenigs-Knorr reactions, because these alcohol compounds function as poor nucleophiles. The higher yield reported[67,69] for glycosidations with benzoylated bromo-sugars, as compared with acetylated bromo-sugars, can be accounted for on the assumption that the side reaction products, 2-OH glycosides **32**, which are formed from the alcoholysis of both acyclic ions **27** and **28** and is an important cause of low yields in normal glycosidation reactions, are avoided. The reason could be due to the better resonance stabilisation[70] of the

benzoylated cyclic ion **26b** than for the acetylated cyclic ion **26a**, which is also more stable than the related acyclic ion pairs **27** and **28** in paths B and C. Hence the pathway **26** to **30** predominates.

The type of acid (E) used, or generated from the promoter system, is also an important factor which influences the rearrangement rate of the cyclic ion pair **26** to the β-glycosides **30**. It seems that strongly acidic species in Koenigs-Knorr reactions give a high β/α ratio in the product, probably as a result of their effect on the oxygen electron density of the counterion (EOR⁻), which strongly stabilises the shielded cyclic ion pair **26**. The influence of the solvent on the product composition is also noteworthy. Because of the higher ionic character of ion pair **25** compared with species **26**, and thus the higher demand for solvation by a polar solvent, polar solvents tend to give higher proportions of α-glycosides *via* pathway A. However, for some special solvents such as nitriles, highly selective β-glycoside synthesis could be achieved by α-nitrilium-nitrile-conjugates as intermediates in glycosylation reactions. The detailed mechanism of nitriles as solvents in glycosylation reactions will be discussed later in this chapter.

So, for the synthesis of 1,2-*trans*-glycosides under classic Koenigs-Knorr conditions, the general choice of reaction conditions should be; (i) strongly basic (high electron density on oxygen), (ii) less sterically hindered alcohol or phenols as glycosyl acceptors, (iii) benzoylated or acetylated halo-sugars as glycosyl donors and, (iv) non-polar solvents, or some special solvents, under acid conditions.

The classical Koenigs-Knorr reactions usually used heavy metals[67-70] as activating reagents and an acid scavenger such as 2,4,6-collidine.[69] Water was generally removed by Drierite and molecular sieves during glycosylation reactions. On the other hand, several Lewis acids produced non-toxic and non-explosive activating reagents and also gave high yields of β-glycosides.[71] Glycosylations of aryl alcohols using a phase-transfer catalyst were also developed for glycosyl bromides or chlorides and provide a facile, stereospecific, and general entry route to β-aryl glycosides.[72] Recently, a simple thermal glycosylation of an alcohol with glycosyl chlorides without using any metal salts has been developed. It was found that a dramatic change in stereoselectivity depended upon the reaction temperature. Relatively lower temperatures favoured β-selective coupling, whereas α-selective reaction occurred at higher reaction temperatures.[73]

The use of glycosyl fluoride as a glycosyl donor was first introduced in 1981.[74] Due to its higher thermal and chemical stability as compared to the lower stability of other glycosyl halides, glycosyl fluoride can be generally purified by an appropriate distillation and even by column chromatography. Suzuki *et al*[75] successfully employed Cp_2MCl_2-$AgClO_4$ (Cp = cyclopentadienyl; M = Zr, Hf) as effective activators of glycosyl fluorides to obtain highly β-selective glycoside linkages.

Scheme 5
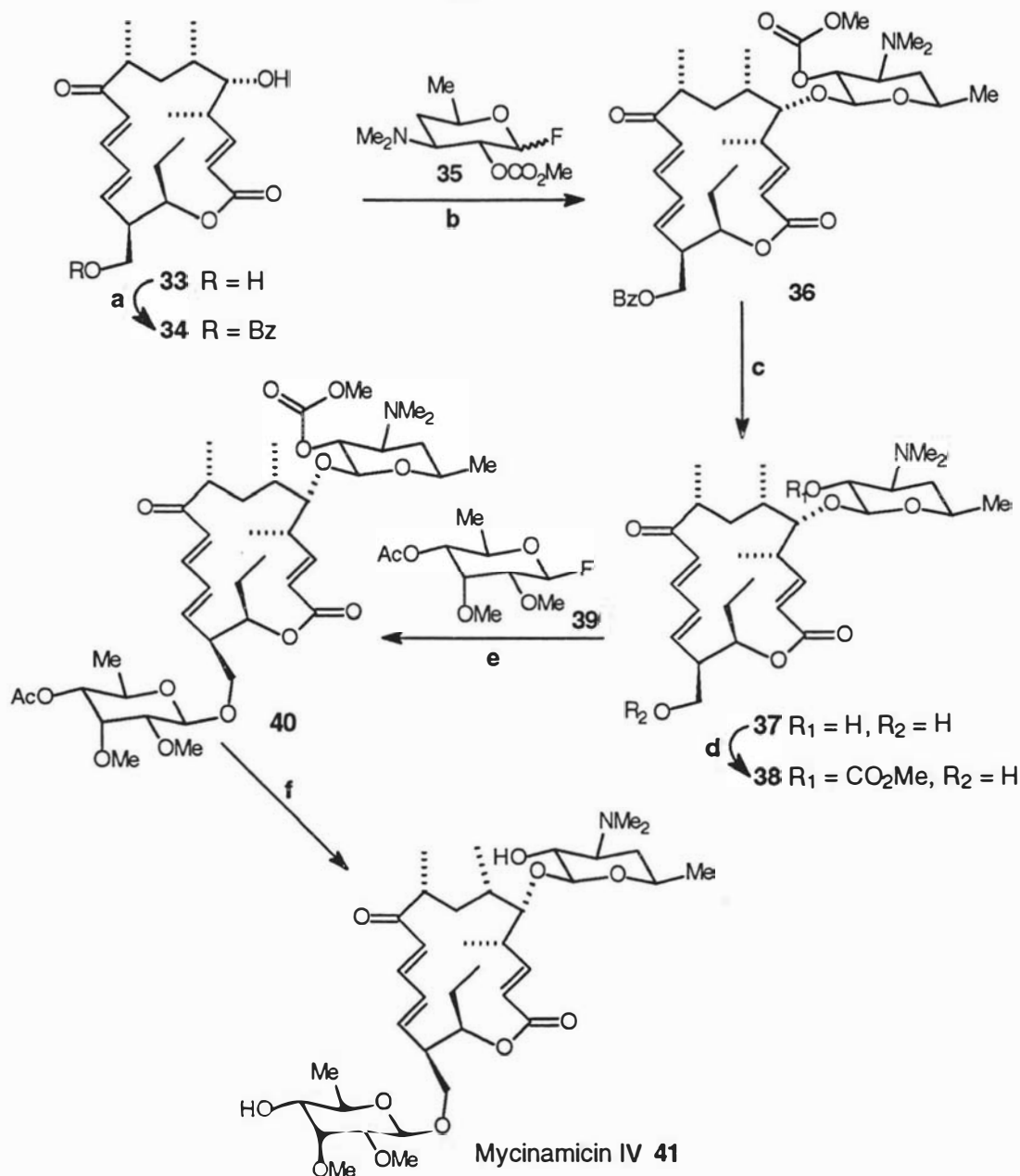
Reagents and conditions: **a)** PhCOCl / Pyridine-CH_2Cl_2, 0 ºC; **b)** Cp_2HfCl_2-$AgClO_4$ / CH_2Cl_2; **c)** Et_3N-H_2O-MeOH (1:1:5), 70 ºC; **d)** $ClCO_2Me$ / CH_2Cl_2, 0 ºC; **e)** Cp_2ZrCl_2 -$AgClO_4$ / C_6H_6, rt, 1 hour; **f)** Et_3N-H_2O-MeOH (1:1:5), rt, 16 hours.
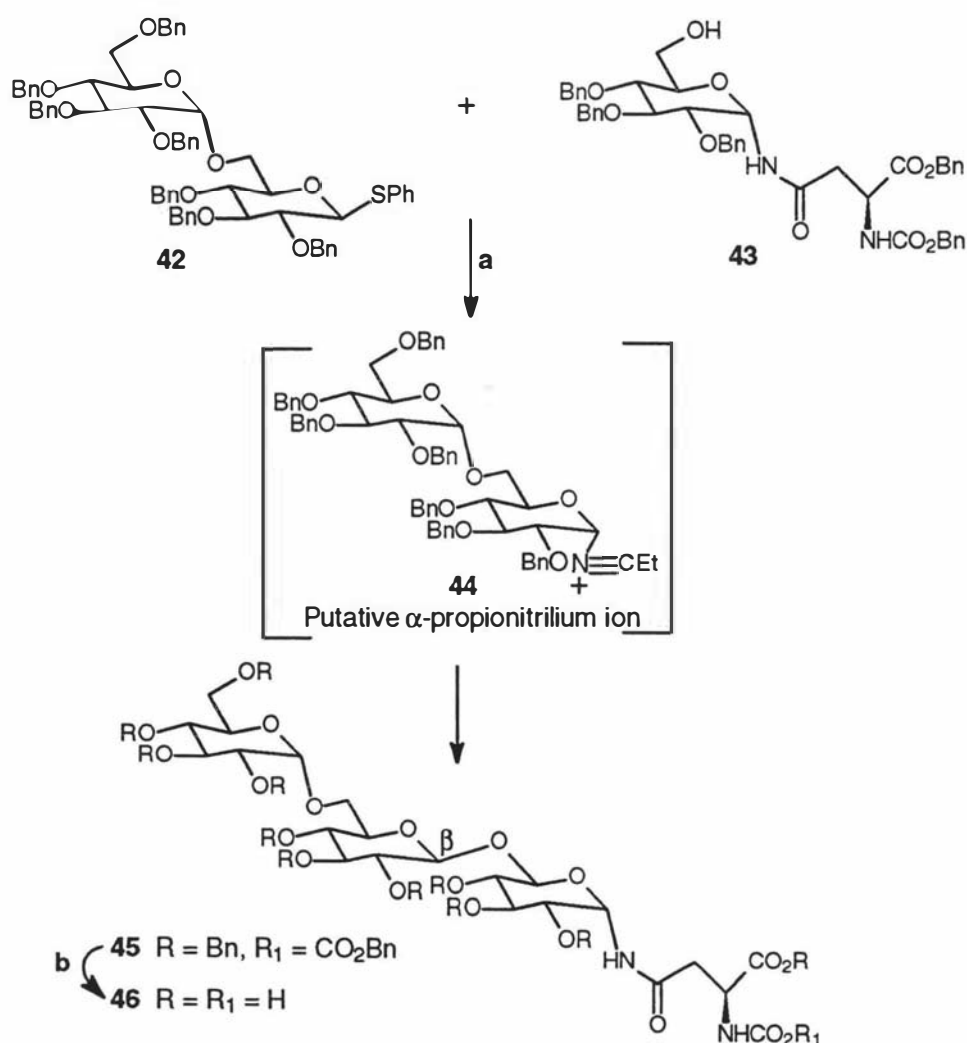
The high β-stereoselectivity was obtained by using shelf-stable glycosyl fluorides and the "non-Koenigs-Knorr" sugars [sugars without a participating group (acyl group) at C(2)-OH, such as compound **39**]. The glycosyl fluorides also provided a useful method for the glycosidation of some basic amino sugars (e.g sugar **35**), which may interfere with the normal glycosidic activation. This activation system was elegantly applied to the synthesis of mycinamicin IV (Scheme 5). Mycinolide IV **33** was benzoylated under controlled conditions to give the selectively mono-protected aglycon **34** in 96% yield. The glycosidation of **34** with glycosyl fluoride **35** in the presence of Cp_2HfCl_2-$AgClO_4$ in CH_2Cl_2 proceeded smoothly to afford **36** in 72% yield with the ratio of α/β products being 1/6. After the separation of the α anomers, the two protecting groups of **36** were detached to give compound **37** in 75% yield. Subsequent treatment of **37** with methyl chloroformate cleanly afforded the alcohol **38**, which then proceeded by means of a second glycosidation with glycosyl fluoride **39** in the presence of Cp_2ZrCl_2-$AgClO_4$ in benzene to furnish glycoside **40** in 86% yield with an excellent stereoselectivity (α/β ratio = 1/26). After the separation, the hydrolytic cleavage of the protecting groups of **40** afforded mycinamicin IV **41**.

(B) Thio-derivatives as glycosyl donors:

The use of thioglycosides in β-glycoside synthesis has attracted considerable attention in recent years.[76-83] The thioglycosides can be prepared conveniently by efficient thiolyses of a sugar ester[84] or reaction of a glycosyl bromide with thiols under phase transfer catalysis conditions.[85] The direct glycosylation of an alcohol with thioglycosides can be accomplished using various thiophilic reagents as promoters. Promotion by methyl trifluoromethanesulfonate (methyl triflate)[76] or by $CuBu_4NBr$/AgOTf[77] is well documented and both give good yields of β-linked derivatives. Nitrosyltetrafluoroborate(NOBF$_4$),[78] an effective activating agent, also gives a reasonably good yield of β-glycosides when a neighbouring group such as acetoxy or an N,N-phthaloylamino group is present at the carbon-2 position. Benzenselenenyl triflate (PhSeOTf), developed by Ito *et al*,[79] has been used also as a powerful activator of thioglycosides for very mild glycosylation reactions. Benzenselenenyl triflate, which was called a "superelectrophilic" activator, can be generated easily from benzenselenenyl chloride and silver triflate. The glycosidation reactions using this reagent proceed with remarkable ease and are completed almost instantaneously, even at -40 ^{o}C. The major products were revealed to be the β-isomers.

N-iodosuccinimide (NIS)/triflic acid (TfOH) assisted activation of thio-glycosides having a participating group at C-2 was found by Veeneman *et al*[80] to be a fast and very high-yielding β-coupling promoter system in thiophilic promoted Koenigs-Knorr reactions. A very similar activation system (NIS/TfOH) was recently employed for the stereocontrolled synthesis of the nephritogenoside core structure **46**.[81] The key to this synthetic strategy was β-selective glycosylation without neighbouring group participation (Scheme 6).

Scheme 6

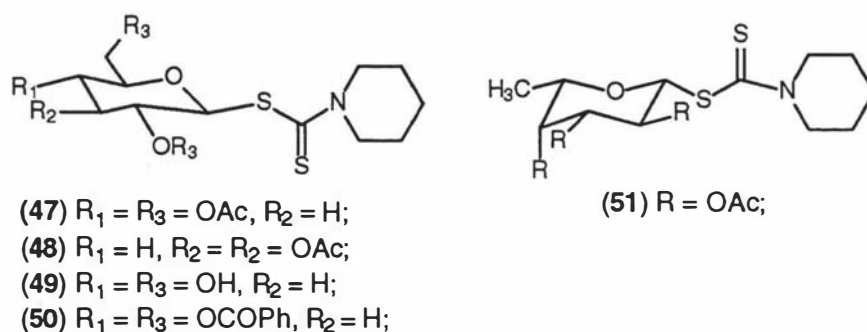Reagents and conditions: **a)** NBS, TfOH,CH₃CH₂CN, -78 ⁰C; **b)** H₂, 20% Pd(OH)₂ /C, THF, EtOH, H₂O, rt.

The coupling of alcohol **43** with 1.5 equivalent of phenyl thioglycoside **42** under the influence of NBS-TfOH in propionitrile at -78 ⁰C proceeded smoothly *via* the putative α-propionitrilium ion **44** to give the trisaccharide **45**, which was hydrogenolysed to furnish the final target compound **46**.

Kihlerg *et al*[82] used silver triflate/bromine as a promoter system in a mild "one-pot" procedure to give O-glycosides in excellent yields with high β or α stereochemical control, even with unreactive and hindered glycosyl acceptors, such as the 4-OH group of glucosamine derivatives. The glycosylation of these sterically hindered alcohols gave 64% yield compared with only 5% by other conventional methods.[86]

During the course of writing this thesis, a stereoselective glycosidation reaction using thioglycosides was reported under mild and neutral conditions by the combined use of N-bromosuccinimide (NBS) and a catalytic amount of various strong acid salts.[83] A combination of NBS with Ph_2IOTf, Bu_4NOTf, or Bu_4NClO_4 was advantageous for β-selective glycosidation with 2-O-acylated or 2-O-benzylated donors by virtue of either the neighbouring group participation or the known solvent effect of acetonitrile (putative α-acetylnitrilium ion or α-nitrilium-nitrile-conjugates, see structure **44**), respectively. More details about the structure of α-nitrilium-nitrile-conjugates will be discussed later in this chapter (Scheme 13).

Recently, a new series of glycosyl donors, acylated glycopyranosyl 1-piperidinecarbodithioates **47-51**[87] (Figure 17), have been prepared by reacting piperidine with sodium hydride and the resulting salt treated with carbon disulphide and then with the appropriate acylated bromo-sugar.

Figure 17

(**47**) $R_1 = R_3 = OAc$, $R_2 = H$;
(**48**) $R_1 = H$, $R_2 = R_2 = OAc$;
(**49**) $R_1 = R_3 = OH$, $R_2 = H$;
(**50**) $R_1 = R_3 = OCOPh$, $R_2 = H$;

(**51**) R = OAc;

These new glycosyl donors are very stable, crystalline, non-hygroscopic compounds, which require no special care in storage or handling and are very useful in 1,2-*trans*-glycosidation reactions.

The sulfoxide-sugar **53**,[88] which was obtained by 3-chloroperoxybenzoic acid (*m*CPBA) oxidation of the corresponding sulphide **52**, has been shown also to be a very powerful glycosyl donor in Koenigs-Knorr reactions (Scheme 7).

Scheme 7
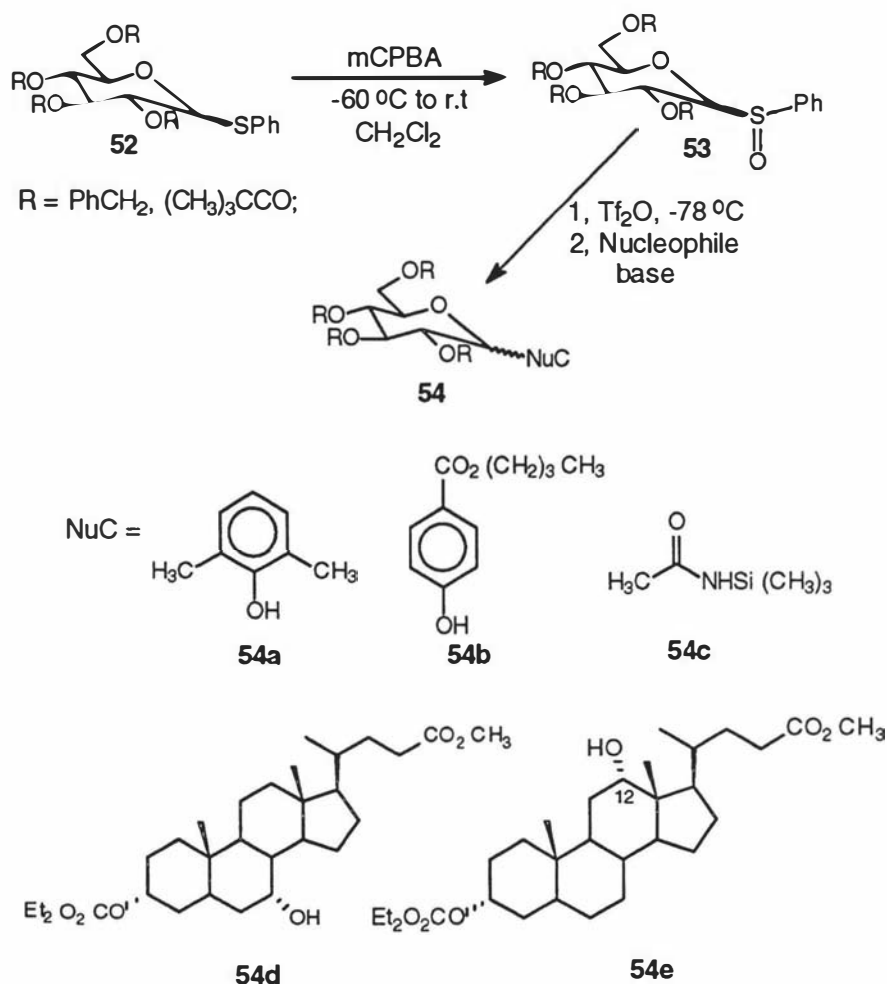
Both hindered and deactivated alcohols or phenols can be glycosylated in good yield by using the sulfoxide glycosyl reagent **53**. The effectiveness of this reaction is shown by the glycosylation of the 12-OH group of steroid derivatives such as compound **54e**, which has strong steric hindrance towards glycosylation. The most striking example of the efficiency of this reaction is the glycosylation of an acetamide on nitrogen (compound **54c**), which could be accomplished only by means of enzymatic catalysis previously.

Since sulfoxide glycosyl donors are much more reactive than the thioglycoside reagents, the selective glycosylation with a sulfoxide glycosyl donor could be achieved when both sulfoxide and thio-functional groups are present in the same

compound. Recently, glycosylation of a phenyl thioglycoside **55** with a phenyl sulfenyl glycoside **57** was shown to occur selectively by virtue of their different activities in glycosylation reactions, which could be effectively used for polysaccharide synthesis and offered some remarkable advantages.[89] An efficient and stereocontrolled synthesis of the nephritogenoside trisaccharide unit **61** by using this selective glycosylation strategy is shown in Scheme 8. The new glycosylation procedure enables complex oligosaccharides to be prepared in a highly convenient and stereoselective manner simply by repeated oxidation of thioglycosides to sulfoxides (reaction condition **a**) and glycosidations with sulfoxide glycosyl donors (reaction condition **b**).

Scheme 8
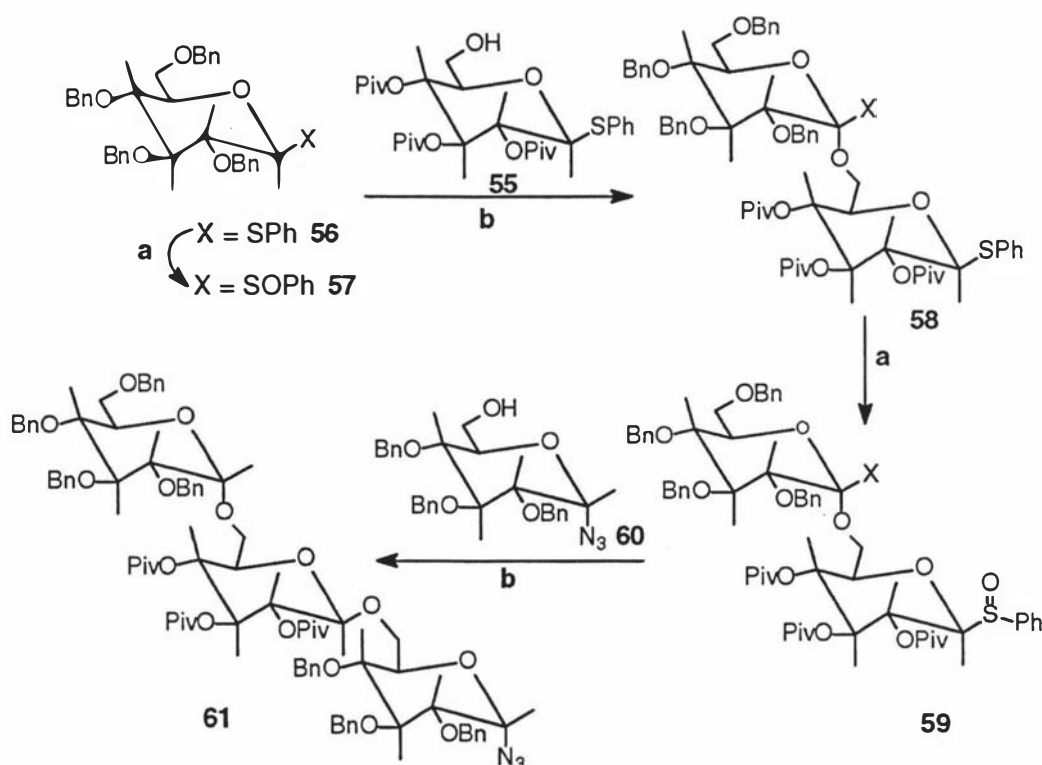
Reagents and conditions: **a)** mCPBA, CH$_2$Cl$_2$, -78 to 10 °C; **b)** Tf$_2$O, DtBP, CH$_2$Cl$_2$ / ether (1:4), -78 to 0 °C;

(C) Phosphorus–derivatives as glycosyl donors:

Newly developed phosphorus containing glycosyl donor groups **62-64** (Figure 18) have been shown by Hashimoto *et al*[90-93] to be very promising alternative promoters for Koenigs-Knorr reactions. Since phosphorus compounds can be easily modified by several kinds of other atoms, a wide variety of leaving groups with different properties can be designed. The glycosyl phosphates **62** can be prepared

easily from the corresponding α-bromo-sugars by silver carbonate-catalysed hydrolysis of glycosyl halides followed by rapid phosphorylation with diphenyl chlorophosphate and DMAP,[94] or simply by reacting the α-bromo-sugar with dibenzyl phosphate in a catalytic two-phase system using tetrabutylammonium hydrogen sulphate as a catalyst.[95]

Figure 18

$R = PhCH_2$ or $PhCO$;
$R' = H$, CO_2Me, CH_2OCH_2Ph, or CH_2OCOPh;

62

$Bz = PhCO$; $R' = H$, or CH_2OCOPh;
$Ts = CH_3PhSO_2$

63

$R = PhCO$, or $PhCH_2$

64
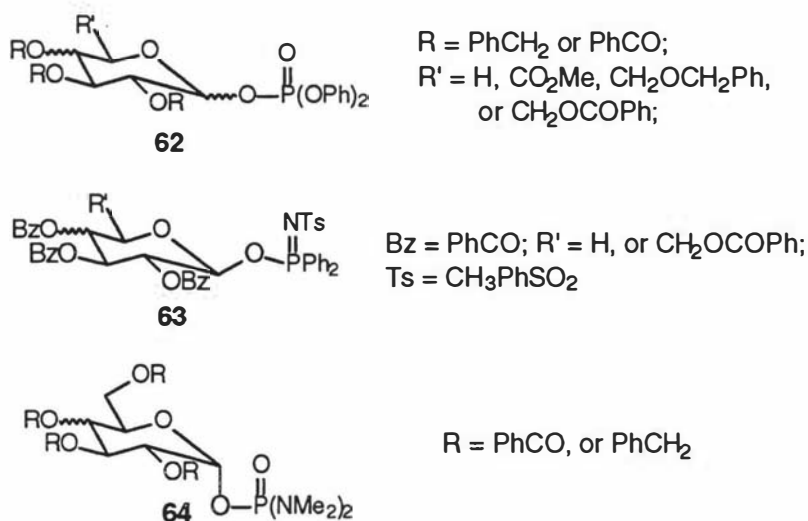
Hashimoto *et al* successfully used different glycopyranosyl phosphates **62**[90] as glycosyl donors for Koenigs-Knorr reactions in the presence of trimethylsilyl triflate (TMSOTf). The reactions gave extremely rapid glycosidation with high β-selectivity with or without neighbouring-group participation. The reaction afforded excellent yields as well. Some steroid compounds, such as estrone,[90] formed β-glucuronide conjugates in very good yield. The glycosidation reactions also showed that the anomeric configuration of the glycosyl donors was not crucial to either the stereochemical outcome or the final yield of the glycosidation reactions. They also reported another mild and rapid glycosidation method *via* benzoyl-protected glycopyranosyl P,P-diphenyl-N-(P-toluenesulfonyl)phosphinimidates **63**.[91] These reagents were prepared by condensation of the 1-O-thallium (I) salts of benzoyl-protected sugar derivatives with P,P-diphenyl-N-(P-toluenesulfonyl)phosphinimidic chloride (TsN=PPh$_2$Cl). Since glycosidation reactions can use boron trifluoride etherate as a promoter and dichloromethane as a solvent, this reaction procedure provides an eminently suitable entry to 1,2-*trans*-glycosides of acid-labile alcohols as well as having the virtue of simplicity.

On the basis of these positive results, they developed other more stable glycopyranosyl donors, benzyl- or benzoyl-protected glycopyranosyl N,N,N',N'-tetramethylphosphoroamidates **64**,[92] which had similar reactivities and stereoselectivities to the glycosyl diphenyl phosphates **62** in glycosidation reactions. However, they are much more stable than glycosyl diphenyl phosphate **62** towards storing and handling.

Scheme 9
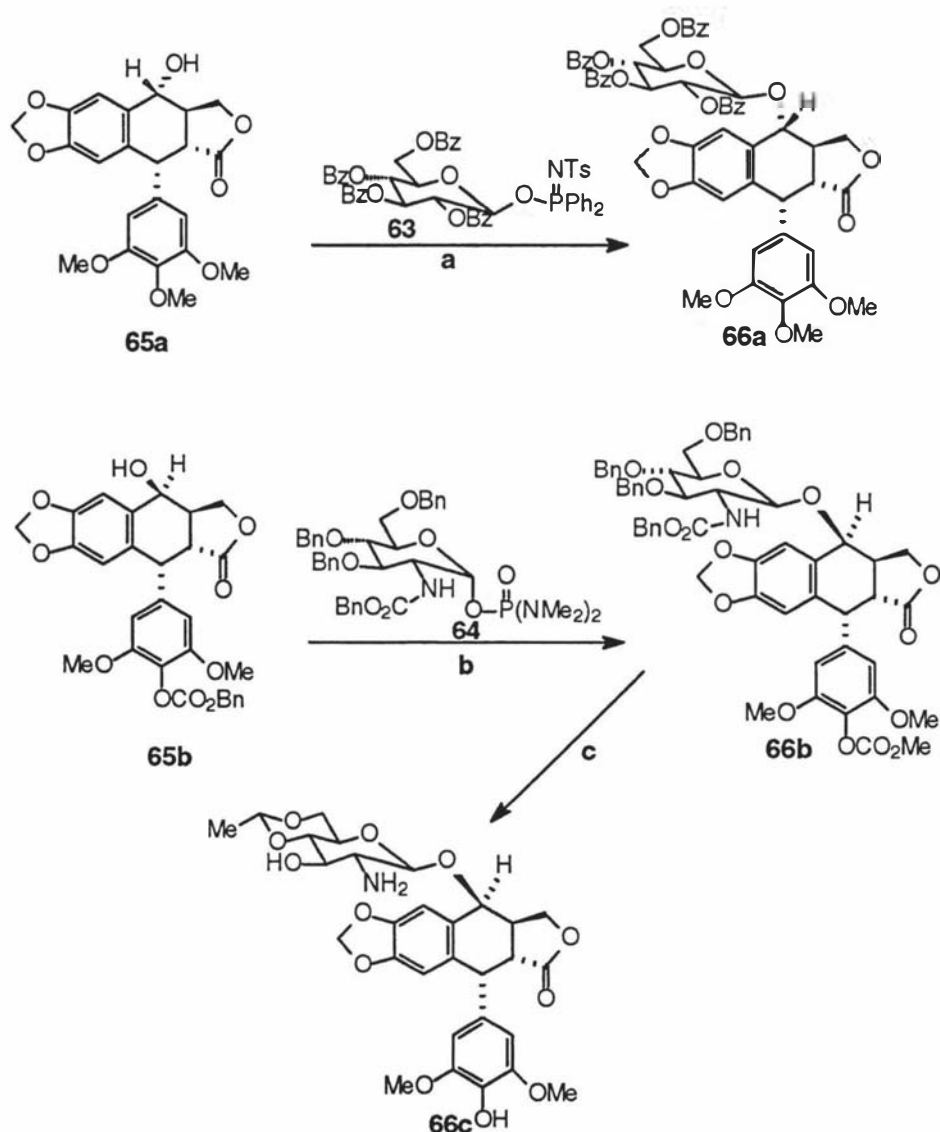
Reagents and conditions: **a**) BF$_3$·OEt$_2$, 4Å molecular sieves, CH$_2$Cl$_2$, -5 °C, 0.5 hour; **b**) BF$_3$·OEt$_2$, 4A molecular sieves, CH$_2$Cl$_2$, -8 °C, 15 min.; **c**) Pd(OH)$_2$/C, MeOH /AcOEt (10:1), 12 hours; MeCH(OEt)$_2$, TsOH, CH$_3$CN, 1 hour.

After a number of variations of the substituents on the phosphorus atom of the leaving groups of glycosyl donors were tried, both glycopyranosyl P,P-diphenyl-N-

(*p*-toluenesulfonyl)phosphinimidate **63** and bis(dimethylamido)phosphate **64** were successfully used as glycosyl donors for the stereocontrolled construction of β-linkages **66** of podophyllotoxin **65a** and **65b** (Scheme 9),[93] which were hard to synthesise by the normal Koenigs-Knorr method or its variations.

Recently, a highly stereocontrolled 1,2-*trans*-β-glycosidation reaction without neighbouring group participation has been developed by the above authors.[96] They used benzyl-protected glycopyranosyl phosphite as a glycosyl donor and boron trifluoride etherate as a promoter. This new method was claimed to exhibit the highest level of 1,2-*trans*-β-selectivity known to date for glycosidation without neighbouring group participation on C-2.

(D) Other variations of glycosyl donors:

Besides the use of the above glycosyl halides, thio- and phosphorous derivatives as glycosyl donors, there have been some other types of glycosyl donors used in Koenigs-Knorr reactions. Among the known 1,2-*trans*-glycosylations the traditional orthoester method suffers from the disadvantage that, besides the desired glycoside **68a** from the direct glycosylation of the starting orthoester **67a**, a second isomeric glycoside **68b** is also obtained by rearrangement (reesterification) of the starting orthoester **67a** to a new orthoester **67b** followed by glycosylation (Scheme 10).[97]

Scheme 10
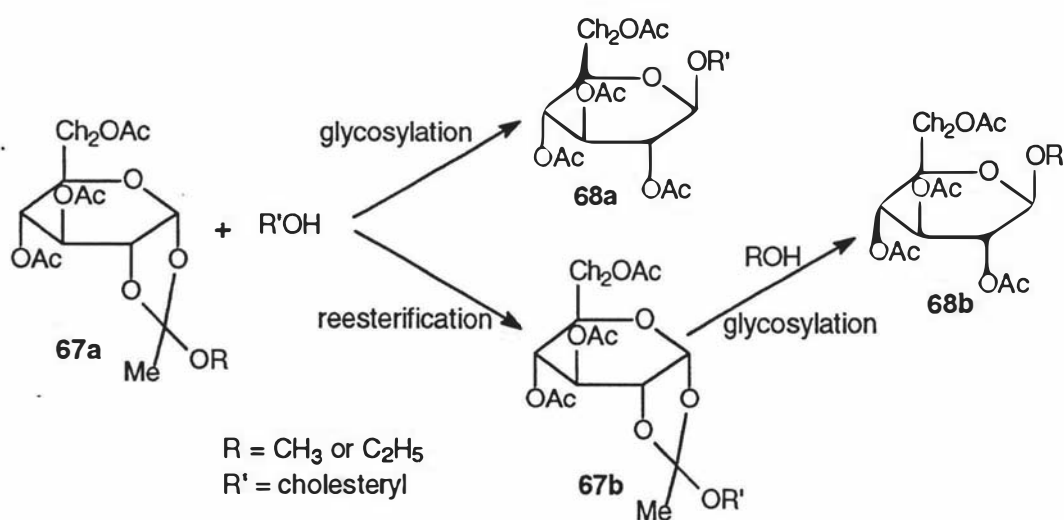
A new type of oximate orthoester of O-pivaloyl glucopyranose **69** as a glycosyl donor, which can avoid the above reesterification problem, has been developed by Kunz *et al*[98] and employed in an effective 1,2-*trans*-glycosylation (Scheme 11).

Scheme 11
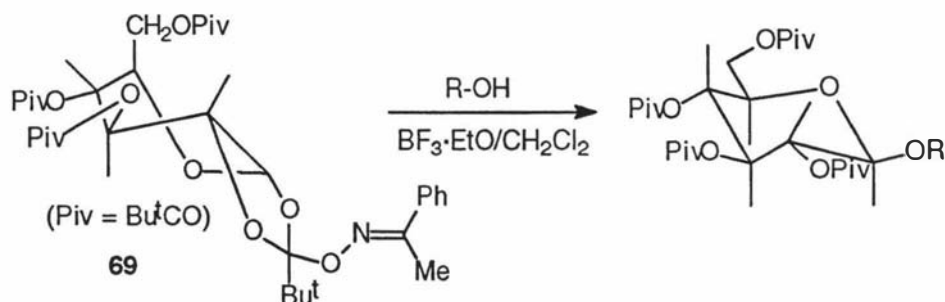
Some complex alcohol and phenols, such as steroid alcohols and estrone, gave very high yields of β-linked products. The oximate orthoester **69** does not give rise to the unwanted side products which are normally produced in orthoester glycosylations, and also allows stereoselective β-glycosylation to take place of both alcoholic and phenolic hydroxyl groups in complex molecules under identical conditions.

Trichloroimidate glycosyl donor is another important type of glycosylation protocol. The thermally and chemically stable trichloroimidate glycosyl donor was easily synthesised from the corresponding 1-hydroxyl sugar by treatment of trichloroacetonitrile in the presence of a base.[99] Up to now, the trichloroimidate-mediated glycosylation has been found to have wide applications in the synthesis of natural products. A typical example of this trichloroimidate method for the β-glycosylation reaction was the synthesis of tigogenyl β-O-cellobioside **72** (Scheme 12).[100]

α-O-Cellobiosyl trichloroacetimidate heptaacetate **70c** was prepared using modified Schmidt conditions (cesium carbonate, CCl_3CN, CH_2Cl_2; then $BF_3 \cdot Et_2O$) from 1-hydroxy-cellobiose heptaacetate **70b** in excellent yield (>90%). Glycosylation of the steroid tigogenin with compound **70c** and zinc bromide as the catalyst at room temperature gave the β-coupling product **71** in 50-60% yield. The tigogenyl β-O-cellobioside **72** could be easily obtained by hydrolysis of compound **71**.

Scheme 12

70 a) R' = α-OAc
  b) R' = α/β-OH
  c) R' = α-OCNHCCL₃

Tigogenin

71

72 (Tigogenyl β-O-cellobioside)
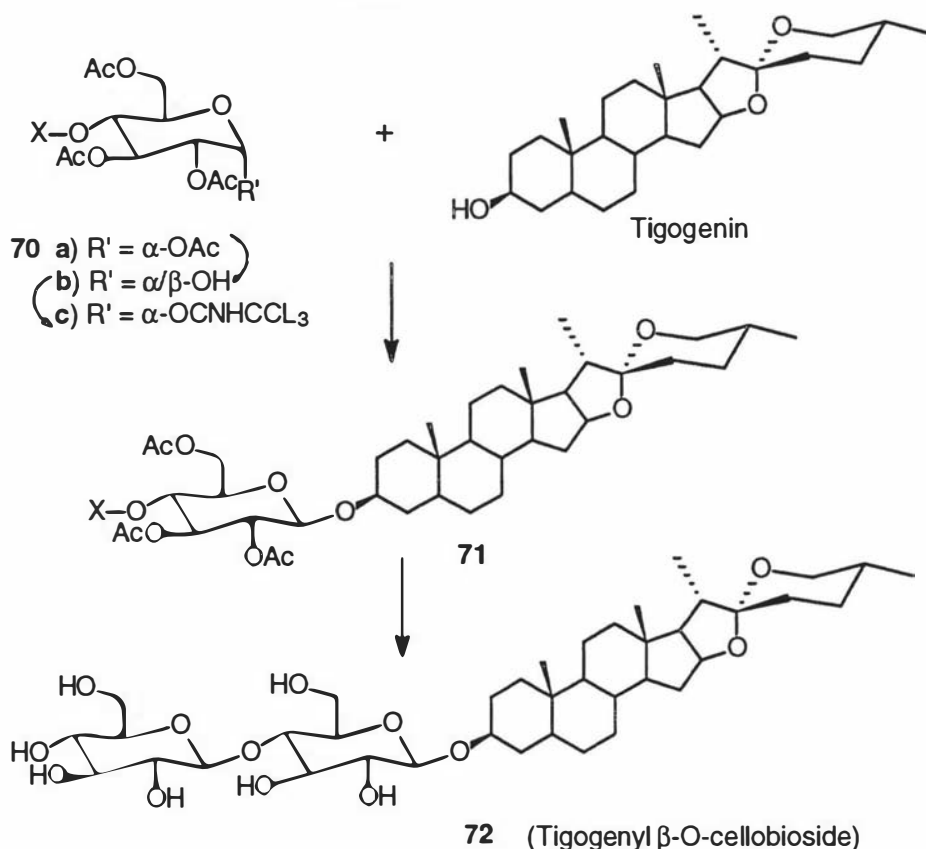
There have been other types of glycosyl donors reported for the β-glycosidations such as glycosyl 2-pyridinecarboxylate[101] and 1-O-acyl sugar.[102]

2.1.2.2 Nitriles as solvents in highly β-selective glycosylation reactions:

The influence of solvents on the stereochemistry of glycosylation reactions is also noteworthy. Besides the general polarity of the solvents, which affects the stabilities of different ion pair intermediates (such as ion pair **25** and **26** in Scheme 4) by solvation, some nitriles react with different glycosyl donors and function as important reaction intermediates to control the stereochemical outcome of the glycosylation reactions. A literature survey reveals that a number of activators have been used for β-glycosylation using nitriles as a solvent. Activators include fluoride (F),[103] methylthio (-SMe),[104] diphenylphosphate [-OP(O)(OPh)₂],[90] p,p-diphenyl-N-(p-toluenesulfonyl)phosphine imidate [-O-P(=NTs)(Ph)₂][105] and trichloroacetimidate [-OC(=NH)CCl₃][106] as leaving groups at the anomeric carbon. The explanation for

these highly β-selective glycosylation reactions using nitriles as solvents is outlined in scheme 13.[106]

Scheme 13
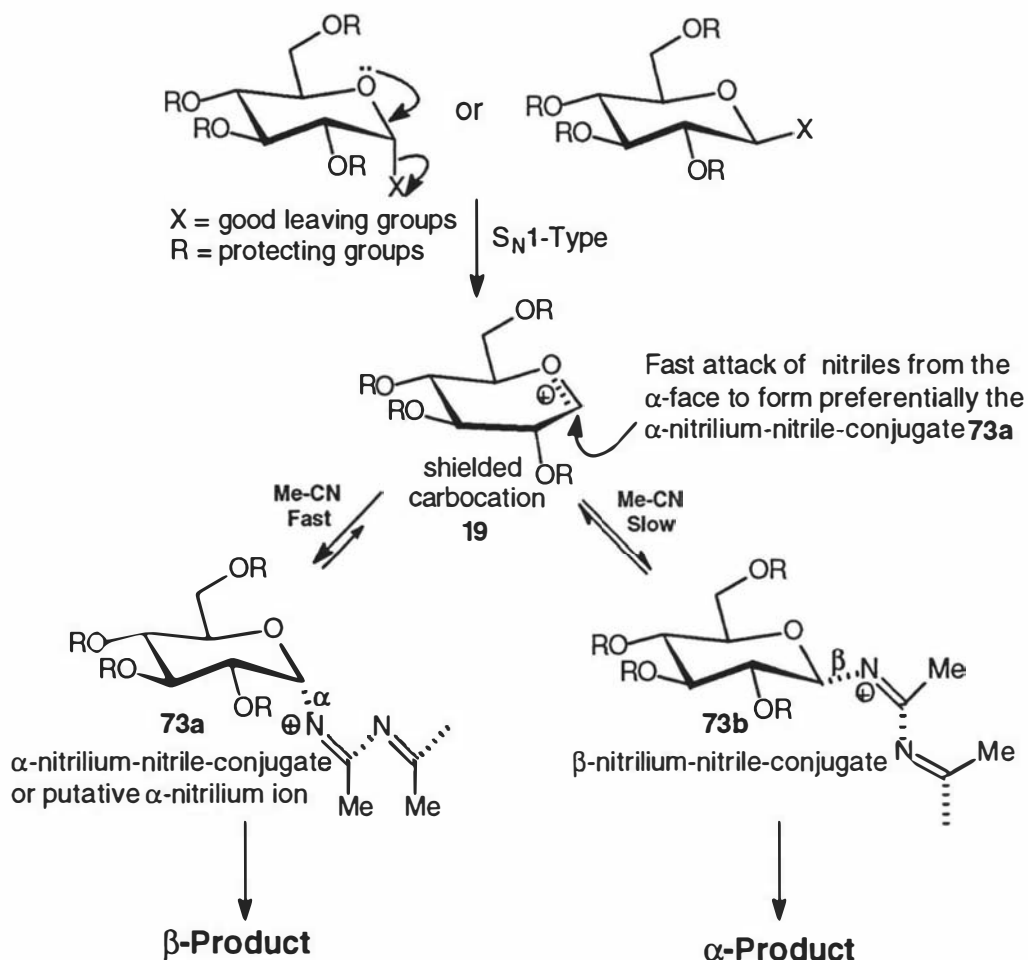
The shielded carbocation **19** as the reaction intermediate (Scheme 4) was generated from the different glycosyl donors, which need excellent leaving groups, under S_N1-type conditions. At very low temperatures, fast attack of solvent nitriles from the α-face of the equatorial ion **19** provided the α-nitrilium-nitrile-conjugate **73a**, which led to the β-coupling products (kinetic control). However, at relatively high temperatures, formation of the thermodynamically more stable β-nitrilium-nitrile-conjugate **73b** is favoured and thus furnished the α-products. Hence, highly selective β-glycosylation reactions in solvents such as nitriles require excellent leaving groups at the anomeric carbon of the glycosyl donors and performance of the glycosylation reaction at low temperatures.

2.1.2.3 Conformational effects in the glycosyl donor and glycosyl acceptor:

The stereoselectivity of the glycosidation reactions are not just affected by the types of leaving group at the anomeric position, the temperature, the solvent, the promoter and the substituents on the sugar. The conformations of the glycosyl donor and acceptor also influence the stereochemical results of glycosylations. For example, the anomeric ratio (α/β) of the glycosides was markedly affected by the anomeric configuration of the glycosyl donors when methylthioglycosides were used for some glycosylations (Scheme 14).[107] The β-thioglycoside **74b** tended to give very high yields of β-glycosides, while the α-anomer **74a** provided mixtures of α and β products.

Scheme 14


74a $R_1 = CO_2Me$, $R_2 = SMe$ ⟶ mixture of α and β-glycosides

74b $R_1 = SMe$, $R_2 = CO_2Me$ ⟶ β-glycosides

ROH = CH_3OH; $CH_3(CH_2)_3OH$; $CH_3(CH_2)_3OH$;

$CH_3(CH_2)_7OH$; $CH_3(CH_2)_{15}OH$; ⟨ ⟩—OH
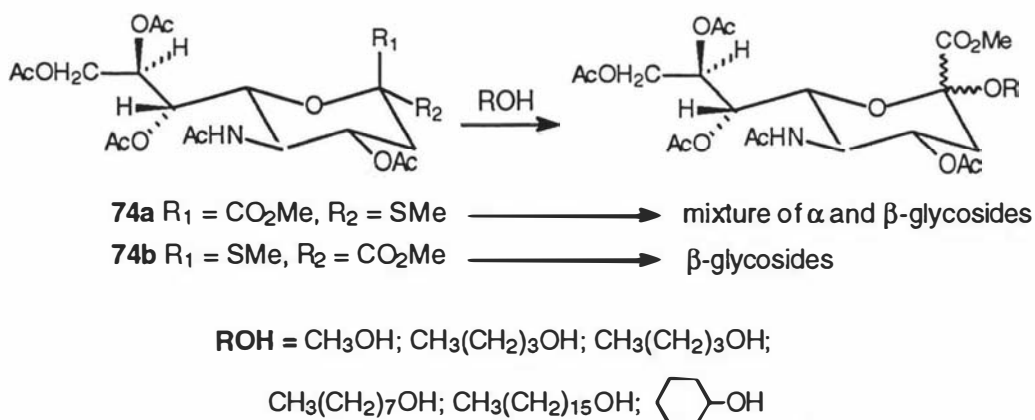
Even if the two glycosyl donors have the same configuration (i.e. the same α or β configuration at the anomeric carbons), different conformational effects from the other parts of the glycosyl donors also resulted in different stereoselectivities in the glycosidation reactions (Scheme 15).[108] The α-selectivity of glycosidation with the conformationally rigid glycosyl donor **75a** possessing a 3,4-O-isopropylidene group was much higher than that of the glycosyl donor **76a**. The stronger repulsion of the 1,3-diaxial interaction between the C-3 substituent and the approaching alcohol from the β-face of the glycosyl donor intermediate **75b** (more steric hindrance) compared with that in the glycosyl donor intermediate **76b** was the main reason for the different stereoselectivities. Hence, the conformationally rigid glycosyl donor **75a** has a higher α-stereocontrol in the glycosylation reaction than does the glycosyl donor **76a**.

Scheme 15
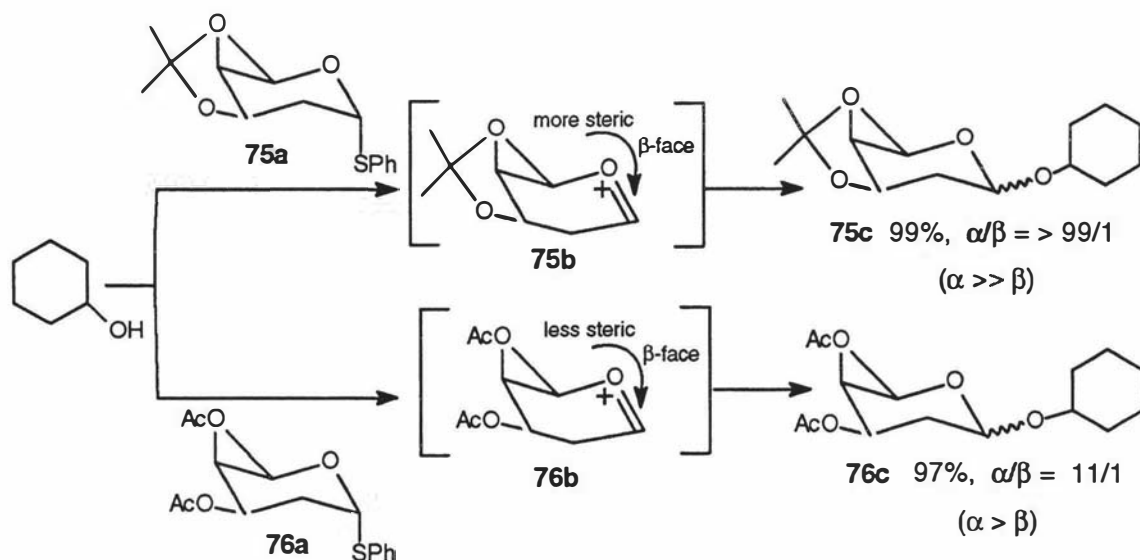
The steric interaction between a glycosyl donor and an acceptor also strongly influenced the stereoselectivities of the glycosidation reactions. For example, for glycosylation of the glycosyl donor 2,3,4-tri-O-benzoyl-6-deoxy-α-D-galactopyranosyl bromide **77a** or its L-isomer **78a** with the glycosyl acceptor **79**, the stereochemical outcome (α/β ratio) of the two glycosylation reactions were quite different (Scheme 16).[109] Although a participating group is present at C-2 of glycosyl donor **77a**, which should be expected to give mainly the β-coupling product from the glycosylation according to the Koenigs-Knorr reaction mechanism, the actual glycosylation product **77c** was predominated by the α-coupling reaction (α/β ratio = 2/1). On contemplating this unusual result we can explain the unexpected stereochemical outcome of the coupling reaction between **77a** and **79** in terms of a sterically mismatched-pair for the β-glycoside transition state **77b**. During the formation of the β-glycoside, considerable steric hindrance arises between the phthalimido group of **79** and the benzoyl ester of **77a** (sterically mismatched-pair, **77b**), but not between the phthalimido group of **79** and the benzoyl ester of the L-isomer **78a** (sterically matched-pair, **78b**). Hence, the glycosylation reaction by the sterically matched-pair **78a** and **79** gave a much higher β-coupling product than that obtained by the sterically mismatched-pair **77a** and **79**.

Scheme 16
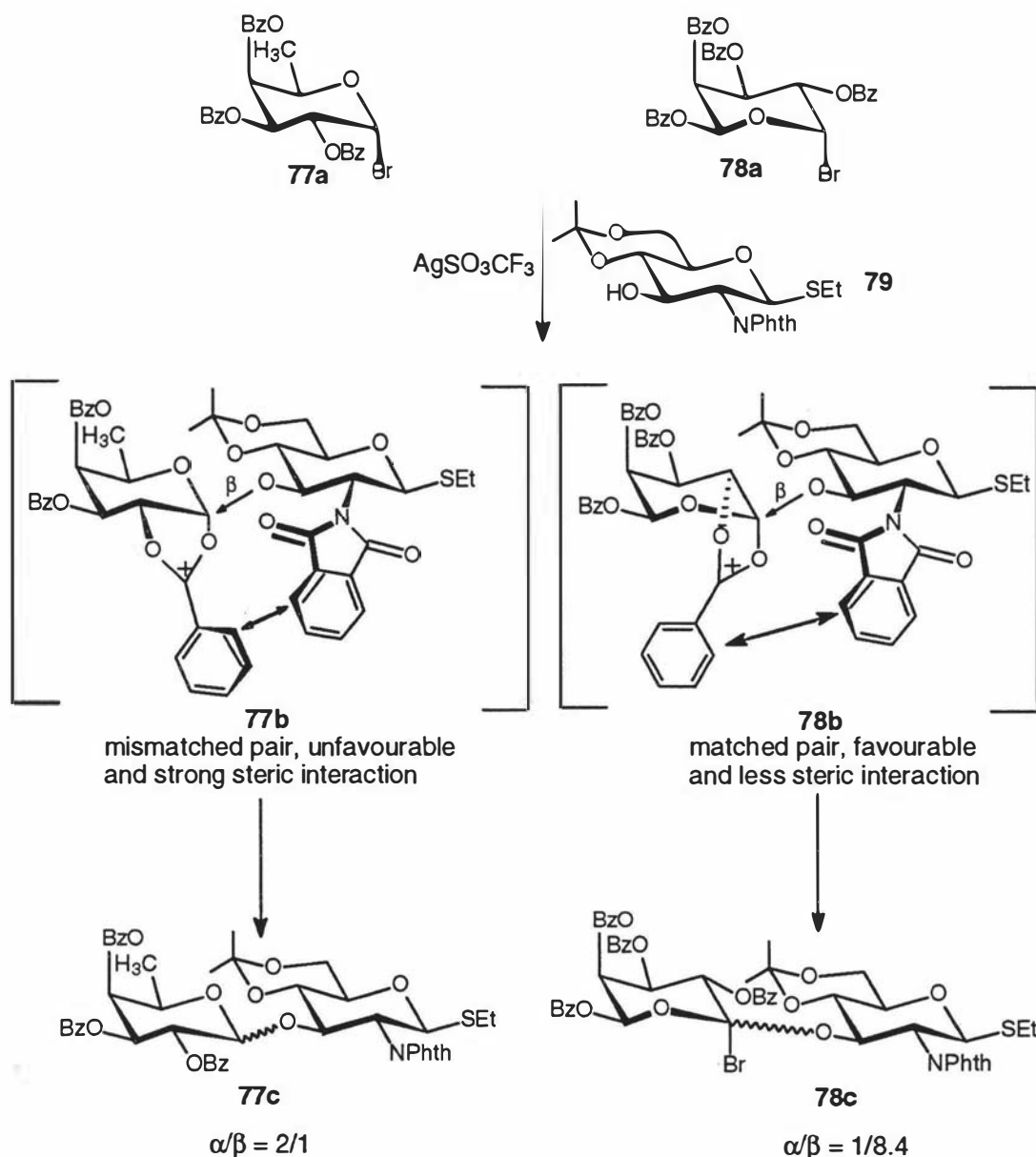
2.1.3 The glycosyl bromide for the synthesis of steroid glucuronides

The employment of a glycosyl bromide or chloride as the reactive glycosyl donor for the synthesis of β-linked steroid glucuronides was first reported by Goebel and Bakers in 1934.[110] Since the glycosyl bromide is more reactive than the chloride, and the steroid aglycons usually have stronger steric hindrance than normal alcohol or phenol compounds, glycosyl bromides have been preferred as intermediates for the synthesis of β-linked steroid glucuronides.

Although some of the above discussed glycosyl fluorides, thioglycosides, phosphorus-derivatives or trichloroimidate glycosyl donors can also give high chemical yields and good β-selectivity in glycosidation reactions, and are more stable than the glycosyl bromides, which were hygroscopic and unstable, these glycosyl donors usually require many extra steps starting from the glycosyl halides, and sometimes special reagents, to prepare. Hence their preparation is not as simple as that for the glycosyl bromides. Furthermore, glycosyl bromides, especially the bromo-sugar **83** which was used in this thesis, have been confirmed and used as effective glycosyl donors for β-coupling with steroid compounds for a long time. They are still being used extensively in recent publications.[61-63,111]

The bromo-sugar **83** can be conveniently prepared from the glucuronolactone **80** by base-catalysed esterification in methanol to give the methyl glucuronide **81**. After acetylation and treatment with 30% hydrobromic acid in acetic acid, the α-bromo-sugar **83** is obtained in reasonable yield (Scheme 17).[112]

Scheme 17
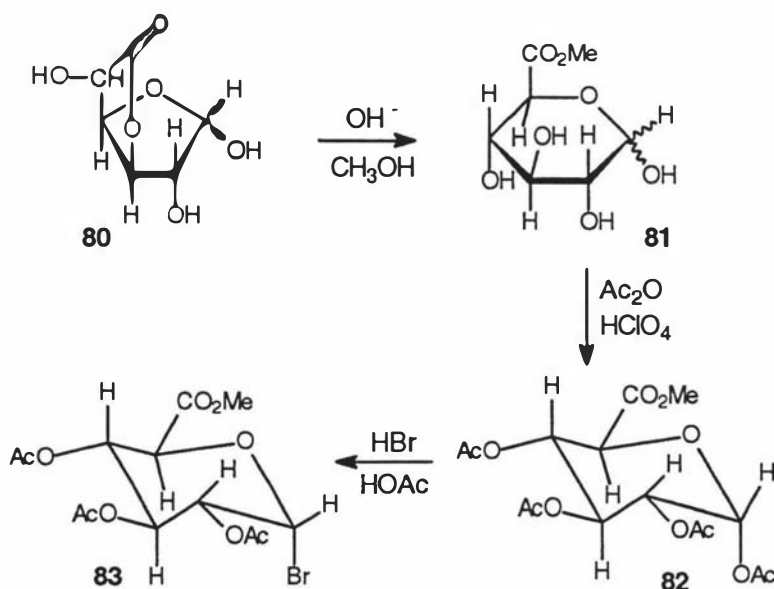
Although there is a new procedure reported[113] for the preparation of glycosyl halides using α-haloenamines under neutral conditions, the above classical method for making bromo-sugar **83** is still the easiest and cheapest procedure. Thus, the bromo-sugar **83** as the main glycosyl donor and the above classical procedure were chosen in the glycosidation reactions for the synthesis of steroid glucuronides in this thesis.

2.1.4 Previous preparations of steroid glucuronides:

2.1.4.1 Preparation of E1G **12**, E3-3G **13** and PdG **16**:

Estrone glucuronide **12** can be prepared simply by the direct glucuronidation of estrone **8** with the bromo-sugar **83** followed by subsequent hydrolysis.[56,60] Pregnanediol 3-glucuronide **16** can also be prepared by Koenigs-Knorr reaction at the carbon-3 position after selective hydrolysis of the 3-acetate group (more labile) of pregnanediol 3,20-diacetate **85**,[114] followed by base catalysed hydrolysis of **87**. Estriol 16α,17β-diester **88** can be prepared easily from estriol **10** by acetylation with acetic anhydride (Ac$_2$O) and a catalytic amount of boron trifluoride etherate in THF at room temperature,[115] or by selective formylation of estriol **10** with 88% formic acid on a steam bath.[60] Hence estriol 3-glucuronide **13** is comparatively easy to synthesise after coupling of the estriol 16α,17β-diester **88** with the bromo-sugar **83** and subsequent hydrolysis (Scheme 18).

2.1.4.2 Synthesis of E3-16G **14** and E3-17G **15**:

The estriol 16- and 17-glucuronides (**14**, **15**) are less readily available because of the difficulty in their syntheses. Historically, Elce *et al*[56] synthesised estriol 16- and 17-glucuronides using estrone **8** as a starting material. Estrone **8** was refluxed in 5% aqueous ethanol with benzyl chloride to give the 3-benzyl ether **90**, which reacted with isopropenyl acetate in the presence of acid to give the enol acetate **91**. The epoxide **92** was obtained by peroxidation of the *enol* acetate **91**, and subsequent acid hydrolysis of the epoxide provided the α-ketol **93**. Estriol 16α-glucuronide **14** was then obtained from the α-ketol **93** by condensation with bromo-sugar **83** to form the steroid 17-oxo-16α-glucuronide tetra-acetate methyl ester **94**. After reduction of the 17-carbonyl group, removal of the protecting groups by hydrogenolysis and alkaline hydrolysis the required estriol 16α-glucuronide **14** was obtained. On the other hand, estriol 17β-glucuronide **15** was prepared by acetylation of the α-ketol **93** at the 16α-position, reduction of the 17-carbonyl group, condensation with bromo-sugar **83** and removal of the protecting groups (Scheme 19).

Scheme 18
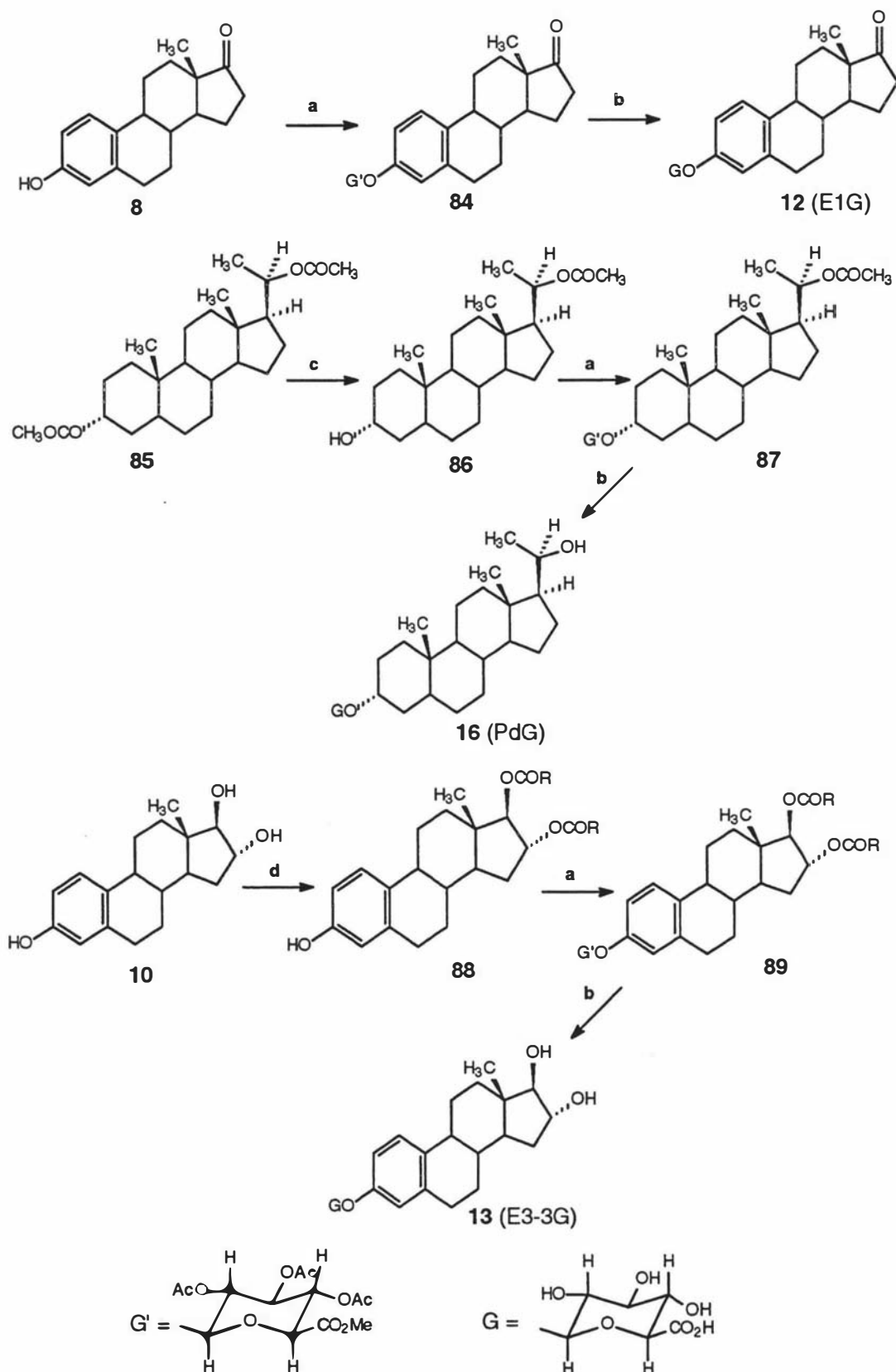
Reagents and conditions: **a)** α-bromosugar / CdCO₃, Toluene, reflux; **b)** NaOH / MeOH, r.t. overnight; **c)** KOH (dilute) / MeOH; **d)** Ac₂O /BF₃·OEt₂, THF, r.t. or 88% of HCOOH on a steam bath.

Scheme 19
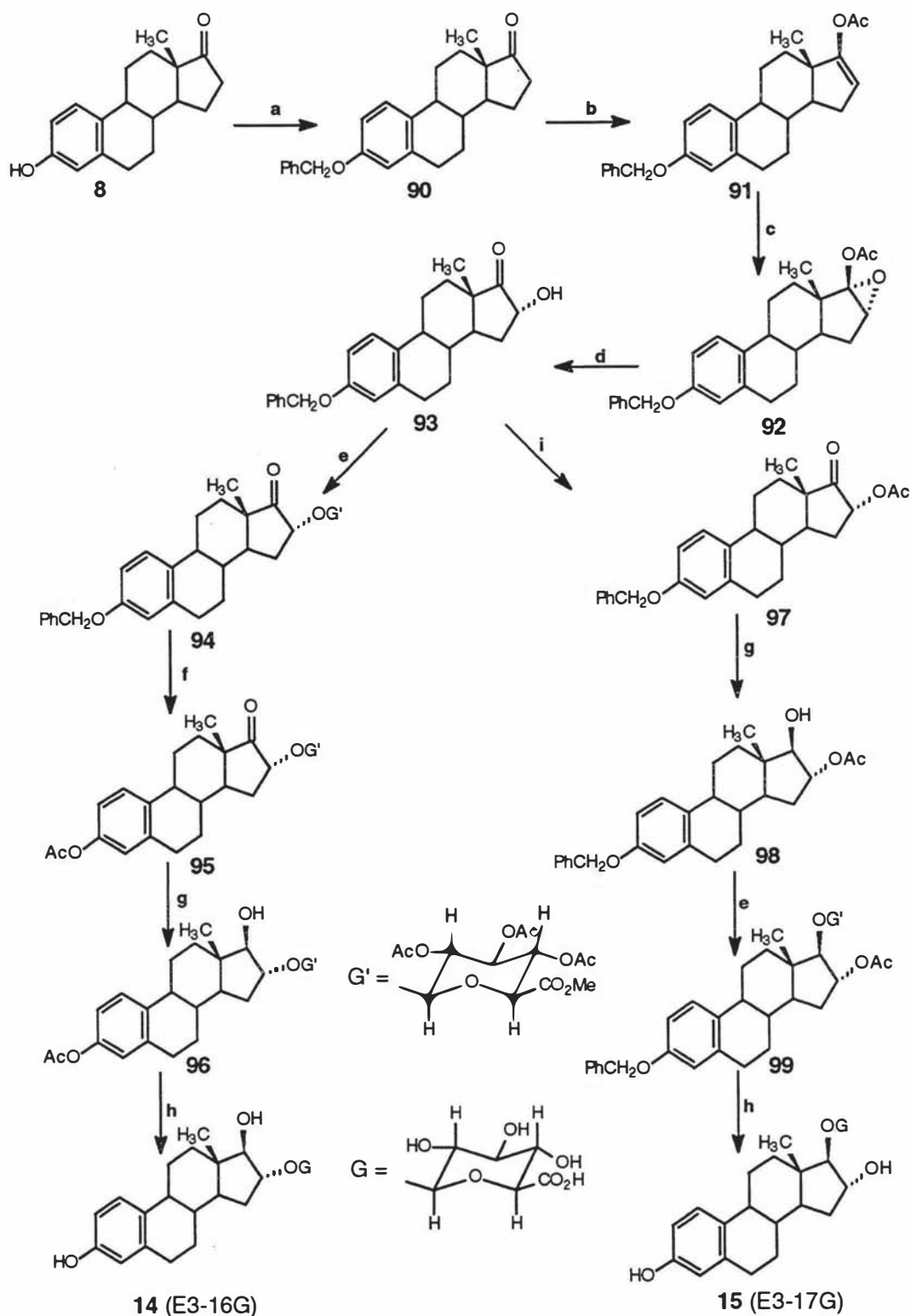
Reagents and conditions: **a)** PhCH₂Cl / K₂CO₃; **b)** isopropenyl acetate / H⁺; **c)** PhCO₃H / PhH; **d)** H₂SO₄ (6N) / acetone / MeOH; **e)** α-bromosugar **83**/Ag₂CO₃ / PhH; **f)** Pd / C, then Ac₂O / pyridine; **g)** NaBH₄ / MeOH; **h)** NaOH / MeOH; **i)** Ac₂O / pyridine, r.t.

The whole synthesis involved many steps and resulted in very low yields of estriol 16- and 17-glucuronides. The same synthetic strategy was adopted by Nambara *et al*[57] to prepare estriol 16- and 17-monoglucuronides, except that the 16α-hydroxyl function in the α-ketol **93** was blocked with a *tert*-butyl rather than with an acyl group for the purpose of avoiding acyl migration in the subsequent reduction with a metal hydride.

More recently, Numazawa *et al*[61] employed a new procedure to synthesise estriol 16-glucuronide **14** *via* an intermediate 2,4,16α-tribromoestrone **100** (Scheme 20).

Scheme 20
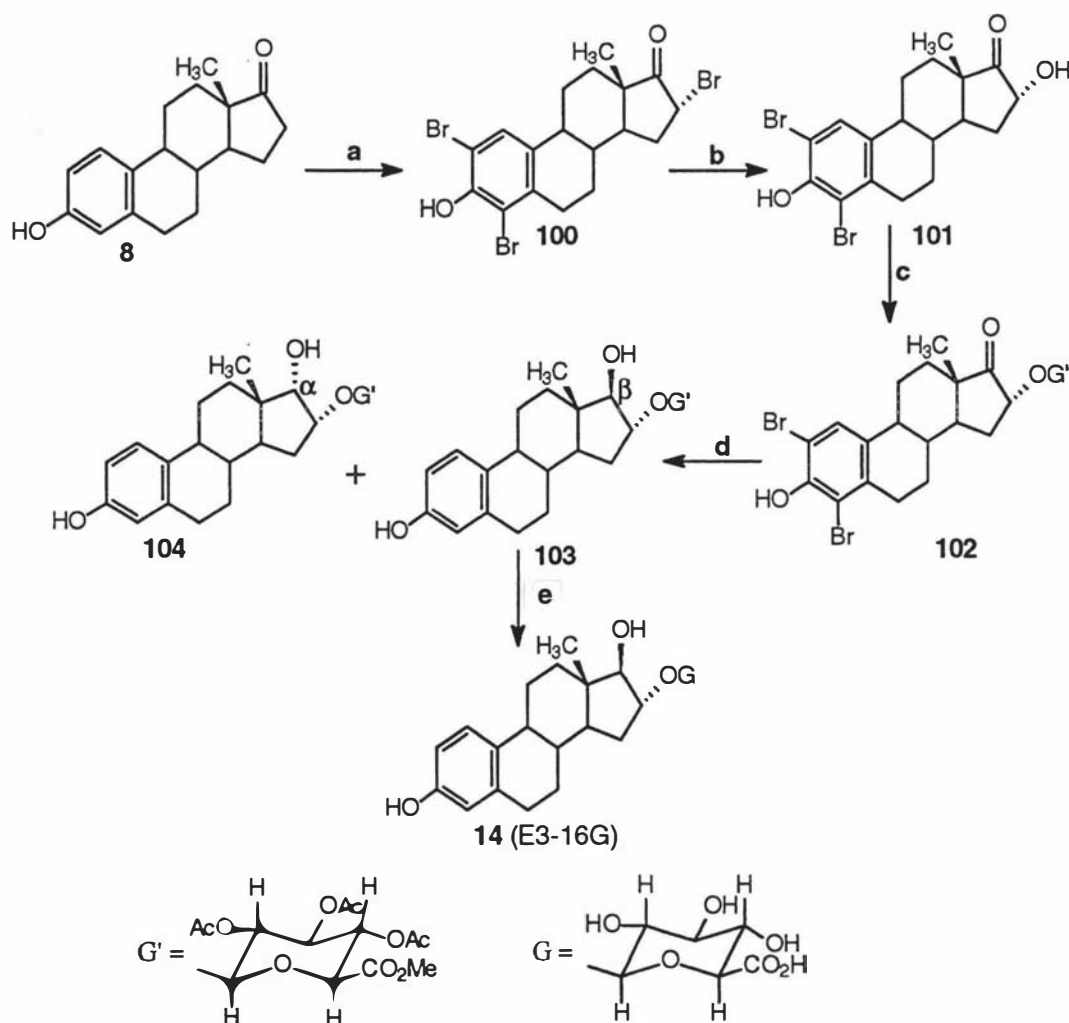
Reagents and conditions: **a)** CuBr$_2$ / MeOH, reflux; **b)** NaOH / 75% aqueous pyridine, r.t. 3 hours; **c)** α-bromosugar / Ag$_2$CO$_3$, benzene; **d)** NaBH$_4$ / PdCl$_2$ / 0 °C; **e)** NaOH / MeOH, r.t. overnight.

They began with bromination of estrone **8** using CuBr$_2$ to get 2,4,16α-tribromoestrone **100**, followed by careful partial hydrolysis to give 2,4-dibromo-3,16α-dihydroxy-estra-1,3,5(10)triene-17-one **101**. Then, they coupled this dibromide-compound **101** with bromo-sugar **83** under Koenigs-Knorr conditions promoted by Ag$_2$CO$_3$ to get the β-coupled product **102**. After reduction of the 17-carbonyl group and hydrolysis of the protecting groups, estriol 16-glucuronide **14** was obtained. The overall yield was much better than that provided by the older method[56,57] starting from estrone. However, this procedure could only be used for the synthesis of estriol 16-glucuronide **14**, not for the general synthesis of estriol monoglucuronides. There were also some problems associated with this procedure as estrone **8** was used as starting material, which will be discussed later.

There is an alternative approach to the synthesis of estriol 16- and 17-glucuronides from estriol **10**. Benstein and co-workers[58] reported a direct glucuronidation of estriol 3-benzyl ether **105** by the Koenigs-Knorr reaction which resulted in the selective formation of the 16-glucuronide. On the other hand, Nambara *et al*[59] reported that the condensation reaction of estriol 3-benzoate **106** with the same bromo-sugar **83** in benzene yielded coupling at both the C-16 and C-17 positions in approximately equal amounts. In chloroform, the main coupling position was found to be at C-17. Since the estriol 16-glucuronide **14** was separated from the 17-isomer **15**, usually by fractional crystallisation, the above methods always produced a low yield of one isomer together with contamination by the other isomer. Hence an effective and simple procedure for the synthesis of estriol 16- and 17-glucuronides is still needed. A new scheme examined in this thesis for preparing the three possible estriol monoglucuronides from estriol **10** is outlined in scheme 21, based on the selective protection and deprotection of the three estriol OH groups, and which also maintains their stereochemical integrity.

For the purpose of further investigation of the synthesis and characterisation of estriol monoglucuronides, needed for the preparation of enzyme conjugates in this thesis, a new scheme for the synthesis of estriol monoglucuronides **13-15** from estriol **10** was developed (Scheme 21). Also the synthesis of estriol 16-glucuronide **14** from estrone **8** was adopted from the literature (Scheme 20)[61] as a comparison. Thus, this chapter is concerned with the synthesis of estrone, estriol and pregnanediol monoglucuronides using the Koenigs-Knorr reactions.

Scheme 21

Proposed synthesis of estriol monoglucuronides **13, 14, 15** from estriol **10**
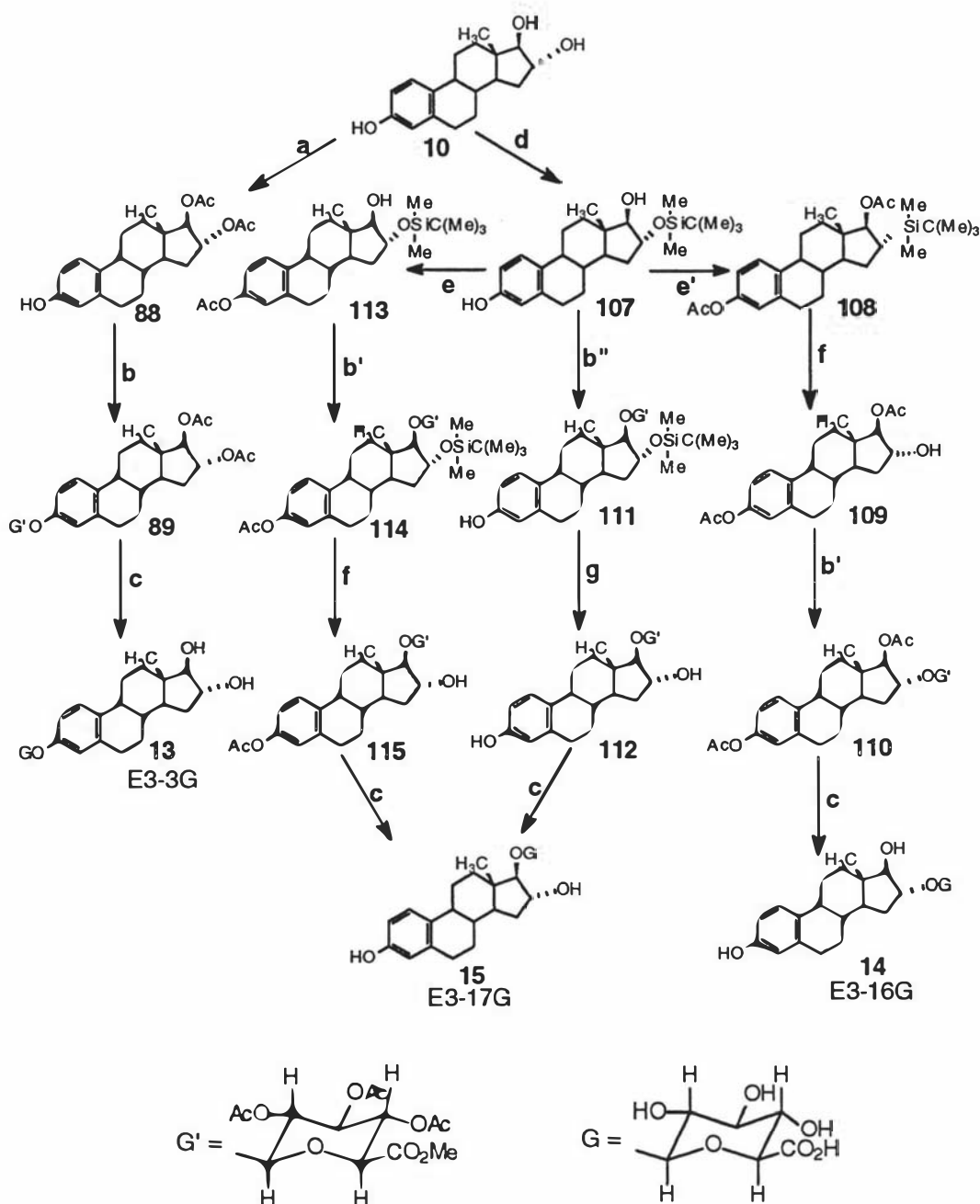
Reagents and conditions: **a)** Cu(OAc)$_2$·H$_2$O / HOAc, reflux; **b)** α-bromosugar (3 eq.) / CdCO$_3$, toluene, reflux, 10 hours; **b'**) α-bromosugar (4 eq.) / CdCO$_3$, toluene, reflux, 10 hours; **b''**) α-bromosugar (2 eq.) / CdCO$_3$, toluene, reflux; **c)** NaOH / MeOH, r.t. overnight; **d)** (CH$_3$)$_3$CSi(CH$_3$)$_2$Cl/imidazole/DMF, -20ºC; **e)** pyridine, Ac$_2$O, 0 ºC, 0.5 hour; **e'**) pyridine, Ac$_2$O, 0 ºC, 48 hour; **f)** HOAc / H$_2$O / THF (4:1:1), r.t. 40 hours; **g)** MeOH, heating.

2.2 Experimental

2.2.1. General details:

Melting points were determined on a Bausch and Lomb microscope hot plate and are uncorrected. Infrared spectra were obtained on a Bio-Rad FTS spectrophotometer as thin films between sodium chloride plates. Absorption maxima are expressed in wavenumbers (cm^{-1}). ^1H Nuclear magnetic resonance spectra were measured at 270 MHz on a JEOL GX 270 spectrometer using tetramethylsilane as an internal standard. Chemical shift values of protons (δ_H) are given in ppm (s = singlet, d = doublet, dd = double doublet, t = triplet and m = multiplet) and coupling constants (J, Hz). Mass spectra (MS) were obtained using a Varian VG70-250S double focusing magnetic sector mass spectrometer with an ionisation potential of 70 eV. Elemental analyses were performed by the microanalytical laboratory, University of Otago, Dunedin, New Zealand.

A Waters associates HPLC system was used with a micro Novapak C_{18} column (150 x 4.6 mm I.D.). This system consisted of two M6000A solvent delivery units, an M680 controller and a U6K universal liquid chromatography injector, coupled to an M450 variable-wavelength UV spectrophotometer and an Omniscribe two-channel chart recorder (Houston Instruments, Austin TX, U.S.A). Detection was carried out at 220 nm for steroid compounds. Flash column chromatography was carried out with silica gel (Merck Kieselgel 60, 230-400 mesh) or aluminium oxide (Merck Aluminiumoxid 90, 70-230 mesh). Amberlite XAD-2 resin (SERVA, 0.3-1 mm) was also used in column chromatography for the purification of steroid glucuronides. Thin-layer chromatography (TLC) was performed using precoated silica gel plates (Merck Kieselgel 60 F_{254}) and the spots were visualised by ultra-violet (UV) fluorescence or by spraying with 10% concentrated sulphuric acid in ethanol and heating at 120 °C for 3 minutes. Solvents were dried and purified according to the methods of Perrin, Perrin and Amarego.[116]

2.2.2. Synthesis of estriol 16α-glucuronide (14) from estrone[61] (scheme 20)

*2,4,16α-Tribromo-3-hydroxy-1,3,5(10)-estratrien-17-one **100***

A solution of estrone **8** (2 g, 7.4 mmol) and $CuBr_2$ (24 g, 14 mmol equiv., predried by heating and stirring at 60-70 °C under high vacuum for 5 hours) in dry MeOH (300 ml) was heated under reflux for 9 hours. TLC was used to monitor the reaction. When TLC showed that no starting material was left and only a tiny amount of by-product (the tetrabromide) had formed, the reaction mixture was poured into ice-water (1 L) and then extracted with $CHCl_3$ (300 ml x 3). The organic layer was dried ($MgSO_4$) and evaporated to give the crude product, which was recrystallised from acetone to give a colourless crystalline solid (3.16 g, 84%), mp, 191-193 °C (Lit.[61] mp, 191-193 °C); δ_H (CDCl_3) 0.93(s, 3H, 18-CH_3), 4.59(m, 1H, 16β-H), 7.40(s, 1H, aromatic).

*2,4-Dibromo-3,16α-dihydroxy-1,3,5(10)-estratrien-17-one **101***

To a solution of compound **100** (300 mg, 0.58 mmol) in 8 ml of 75% aqueous pyridine was added aqueous NaOH (1 ml, 1.75 mmol). The reaction mixture was then set aside at room temperature for 3 hours. TLC (hexane/EtOAc, 2:1) was used to monitor the reaction. When the TLC plate showed no starting material **100** (R_F = 0.60) and only the product **101** (R_F = 0.23) was formed, the reaction mixture was poured into 1% HCl (200 ml, pH = 6), and then extracted with EtOAc (100 ml x 3). The organic layer was washed with water, dried over $MgSO_4$ overnight and evaporated to give the crude product (280 mg), which was recrystallised from acetone to give a white solid (215 mg, 82%), mp, 205-206 °C (Lit.[61] mp, 205-206 °C); δ_H (CDCl_3) 0.995(s, 3H, 18-CH_3), 4.44(m, 1H, 16β-H), 5.91(s, 1H, 3-OH), 7.40(s, 1H, aromatic). When the reaction mixture was poured into 1% HCl (30 ml) or 1.5% HCl (300 ml), very low yields of product were obtained in both cases (80 mg, 30% or 85 mg, 32.3%).

*Methyl tetra-O-acetyl glucopyranuronate **82***

The title compound was prepared from glucuronolactone **80** according to the procedure described by Bollenback *et al*,[112] except that sodium was used in the reaction instead of sodium methoxide. The product **82** was obtained in 50% yield as pure white crystals, mp, 176-178 °C, (Lit.[112] mp, 176.5-178 °C); δ_H (CDCl_3) 2.04(s,

3H, OCOCH$_3$), 2.05(s, 6H, 2OCOCH$_3$), 2.12(s, 3H, OCOCH$_3$), 3.75(s, 3H, COOCH$_3$), 4.18(d, J = 9.16 Hz, 1H, 5'-H), 5.12-5.16(m, 3H, 2',3',4'-H), 5.77(d, J = 7.69 Hz, 1H, 1'-H).

Methyl 1-bromo-1-deoxy-2,3,4-tri-O-acetyl-α-D-glucopyranuronate 83

The title compound was prepared from methyl tetra-O-acetyl glycopyranuronate **82** according to the procedure described by Bollenback *et al*[112] in 89% yield as colourless crystals, mp, 106-107 °C (Lit.[112] mp, 106-107 °C); δ$_H$ (CDCl$_3$) 2.059(s, 3H, OCOCH$_3$), 2.064(s, 3H, OCOCH$_3$), 2.11(s, 3H, OCOCH$_3$), 3.77(s, 3H, COOCH$_3$), 4.58(d, J = 10.25 Hz, 1H, 5'-H), 4.84-4.89(dd, 1H, 2'-H), 5.24(t, 1H, 3'-H), 5.62(t, 1H, 4'-H), 6.65(d, J = 4.03 Hz, 1H, 1'-H);

Methyl 1-thiophenyl-1-deoxy-2,3,4-tri-O-acetyl-α-D-glucopyranuronate 119

α-Bromosugar **83** (300 mg, 0.765 mmol) and Bu$_4$NHSO$_4$ (260 mg) were dissolved in solvent EtOAc (3 ml). The solution was stirred vigorously at room temperature. After addition of Na$_2$CO$_3$ (1 M, 3 ml) and PhSH (15 drops, excess), the solution was continuously stirried for another 0.5 hour. TLC showed the reaction was completely finished. EtOAc (50 ml) was added to the reaction mixture, and the organic phase was washed with Na$_2$CO$_3$ (1 M, 30 ml x 3), Water (30 ml x 2), brine (30 ml) and dried over MgSO$_4$ overnight. The EtOAc was removed under reduced pressure to afford an oil, which was precipitated by adding EtOH (20 ml). The crude solid was recrystallised twice from EtOH to give pure product as white crystals (305 mg, 94% yield). The structure of product was confirmed by ^{1}H NMR. δ$_H$ (CDCl$_3$) 2.00(s, 3H, OCOCH$_3$), 2.02(s, 3H, OCOCH$_3$), 2.09(s, 3H, OCOCH$_3$), 3.77(s, 3H, COOCH$_3$), 4.04(d, J = 9.7 Hz, 1H, 5'-H), 4.74(d, J = 10.1 Hz, 1H, 1'-H), 4.97(t, 1H, 2'-H), 5.18-5.28(m, 2H, 3'- and 4'-H), 7.33-7.53(m, 5H, phenyl).

Methyl 2,4-dibromo-3-hydroxy-17-oxo-1,3,5(10)-estratrien-16α-yl-2,3,4-tri-O-acetyl-β-D-glucopyranosuronate 102

A typical experimental procedure for the coupling reaction of compound **101** with methyl 1-bromo-1-deoxy-2,3,4-tri-O-acetyl-α-D-glucopyranuronate **83** was as follows;[61,117] Dried CdCO$_3$ (615 mg, 3.75 mmol) was added to a solution of compound **101** (379 mg, 0.85 mmol) in anhydrous toluene (40 ml), and the suspension was concentrated to approximately 25 ml by distillation to remove moisture. After distillation, the solution of methyl 1-bromo-1-deoxy-2,3,4-tri-O-

acetyl-α-D-glucopyranuronate **83** (1.08 g, 2.73 mmol) in anhydrous toluene (20 ml) was added dropwise by syringe, keeping the addition rate the same as the rate of distillation. Finally, the whole reaction mixture was refluxed for 5 hours. The precipitate was then removed by filtration and washed with CH_2Cl_2. The filtrate and washings were combined and evaporated under reduced pressure. The solid residue was purified by dissolving it in acetone/water (1:4, 100 ml), and extraction with EtOAc (100 ml x 3). The organic layer was washed with water, dried over $MgSO_4$ and evaporated to give crude product (914 mg), which was twice recrystallised from CH_2Cl_2/MeOH (1:1, 30 ml) to give a pure white solid (310 mg, 48%); mp, 250 °C (Lit.[61] mp, 250 °C); δ_H (CDCl$_3$) 0.92(s, 3H, 18-CH$_3$), 2.03(s, 6H, 2OCOCH$_3$), 2.07(s, 3H, OCOCH$_3$), 3.75(s, 3H, COOCH$_3$), 4.10(dd, 1H, 16β-H), 4.49(d, J = 7.69 Hz, 1H, 5'-H), 4.83(d, J = 7.69 Hz, 1H, 1'-H), 5.03(t, 1H, 2'-H), 5.23-5.34(m, 2H, 3' and 4'-H), 5.86(s, 1H, 3-OH), 7.38(s, 1H, aromatic).

Compound **102** was also prepared by using two different promoter catalysts for the coupling reactions as described below:

(i) Ag_2CO_3 as catalyst; As described in the reference procedure,[61] pure compound **102** (25 mg, 36.5% yield, mp, 250 °C) was obtained from the reaction of 2,4-dibromo-3,16α-dihydroxy-1,3,5(10)estratriene **101** (40 mg, 0.094 mmol) with methyl 1-bromo-1-deoxy-2,3,4-tri-O-acetyl-α-D-glucopyranuronate **83** (220 mg, 0.56 mmol), catalysed by anhydrous Ag_2CO_3 (250 mg, 0.893 mmol) in dry benzene (20 ml). The melting point and ^{1}H-NMR spectrum of the product were identical with that of compound **102** made by the $CdCO_3$ method.

(ii) AgOTf as catalyst; A solution of compound **101** (100 mg, 0.225 mmol) and 4Å molecular sieves (powder, 0.5 mg) in dry CH_2Cl_2 (20 ml) was cooled down to -25 °C, and stirred for 15 minutes. AgOTf (200 mg) was added in two portions. After stirring at -25 °C for 40 minutes, the reaction temperature was slowly increased to 0 °C and the reaction mixture kept at 0 °C for 1 hour. Then the reaction mixture was diluted with CH_2Cl_2 (25 ml), filtered, washed with $NaHCO_3$, H_2O and dried over $MgSO_4$. Evaporation of the solvent under reduced pressure and purification of the residue by flash chromatography, using hexane/EtOAc (1:1), afforded the compound **102** (40 mg, 40% yield, mp, 250 °C); The ^{1}H-NMR spectrum was identical as above.

Methyl 3,17β-dihydroxy-1,3,5(10)estratrien-16α-yl-2,3,4-tri-O-acetyl-β-D-gluco-pyranosiduronate 103 and methyl 3,17α-dihydroxyl-1,3,5(10)estratrien-16α-yl-2,3,4-tri-O-acetyl-β-D-glucopyranosiduronate 104

Compound **102** (175 mg, 0.23 mmol) was treated with $NaBH_4$ (50 mg, 1.35 mmol) in the presence of $PdCl_2$ (100 mg, 0.376 mmol) as described by the reference procedure.[61] After the reaction, TLC (CH_2Cl_2/EtOAc, 2:1) showed that no starting material **102** (R_F = 0.86) was left and that two products (**103**, R_F = 0.54 and **104**, R_F = 0.68) had formed. Separation of the reaction mixture by flash chromatography, using CH_2Cl_2/EtOAc (2:1) as solvent gave pure compound **103** (96 mg, 70%) and pure compound **104** (40 mg, 30%).
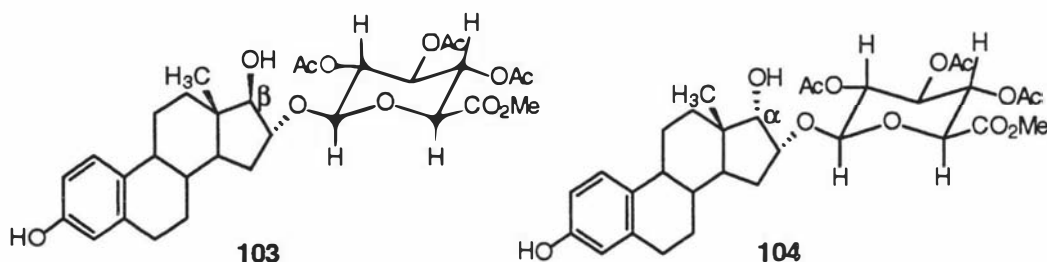
For compound **103** (white solid); mp, 229-231 °C, (Lit.[61] mp, 229-231 °C); High resolution EIMS m/z, 604.2529 (M)$^+$ (Calculated for $C_{31}H_{40}O_{12}$, 604.2520); IR ν_{max}, 3,423 cm^{-1} (OH), 1,745 cm^{-1} (C=O); δ_H (CDCl$_3$/CD$_3$OD, 20:1) 0.80(s, 3H, 18-CH$_3$), 2.04(s, 3H, OCOCH$_3$), 2.05(s, 3H, OCOCH$_3$), 2.06(s, 3H, OCOCH$_3$), 3.67(d, J = 5.13 Hz, 1H, 17α-H), 3.78(s, 3H, COOCH$_3$), 3.95(m, 1H, 16β-H), 4.12(d, J = 9.52 Hz, 1H, 5'-H), 4.61(d, J = 7.69 Hz, 1H, 1'-H), 5.01(t, 1H, J = 8.06 and 9.15 Hz, 2'-H), 5.17-5.32(m, 2H, 3' and 4'-H), 6.55-7.13(m, 3H, aromatic).

For compound **104** (white solid); mp, 216-219 °C; High resolution EIMS m/z, 604.2563 (M)$^+$ (Calculated for $C_{31}H_{40}O_{12}$, 604.2520); IR ν_{max}, 3,423 cm^{-1} (OH), 1,721 and 1,755 cm^{-1} (CO); δ_H (CDCl$_3$) 0.72(s, 3H, 18-CH$_3$), 2.04(s, 3H, 2OCOCH$_3$), 2.06(s, 3H, OCOCH$_3$), 3.73(d, J = 4.39 Hz, 1H, 17β-H), 3.77(s, 3H, COOCH$_3$), 4.07(d, J = 9.53 Hz, 1H, 5'-H), 4.38(m, 1H, 16β-H), 4.46(d, J = 8.06 Hz, 1H, 1'-H), 5.05(t, 1H, J = 8.43 and 8.42 Hz, 2'-H), 5.18-5.33(m, 2H, 3' and 4'-H), 6.55-7.17(m, 3H, aromatic);

3,17β-Dihydroxy-1,3,5(10)-estratrien-16α-yl-β-D-glucopyranosiduronic acid 14

Compound **103** (47 mg, 0.079 mmol) was dissolved in MeOH (12 ml) and aqueous NaOH (1 ml, 2 M) was added. The reaction mixture was then set aside at room temperature with stirring overnight. When TLC (EtOAc/EtOH/HOAc, 3:1:1) showed no starting material **103** was left, the reaction mixture was poured into ice/water (40 ml) and titrated to pH = 8. After evaporation of MeOH under reduced pressure, the glucuronide solution was passed through an Amberlite XAD-2 resin column, and the product was eluted with 50% aqueous MeOH. The glucuronide solution was then titrated to pH = 2.5 and stood overnight to give compound **14** as fine crystals (23.5 mg, 65% yield); mp, 217-223 °C, (Lit.[118] 223-224 °C);

HPLC; Product **14** (0.5 mg) was dissolved in CH_3CN/H_2O (3:7) and 0.05 ml of the resulting solution was loaded onto a Novapak C_{18} reverse phase column (solvent A: $H_2O/CH_3CN/HCOOH$, 80:20:0.1; solvent B: $H_2O/CH_3CN/HCOOH$, 10:90:0.1, flow rate 1 ml/min, linear gradient from 20 to 70% solvent B over 60 minutes). A wavelength of 220 nm and sensitivity of 2.0 were used for the detection of estriol 16-glucuronide **14** (retention time: 20 minutes) (Figure 19).
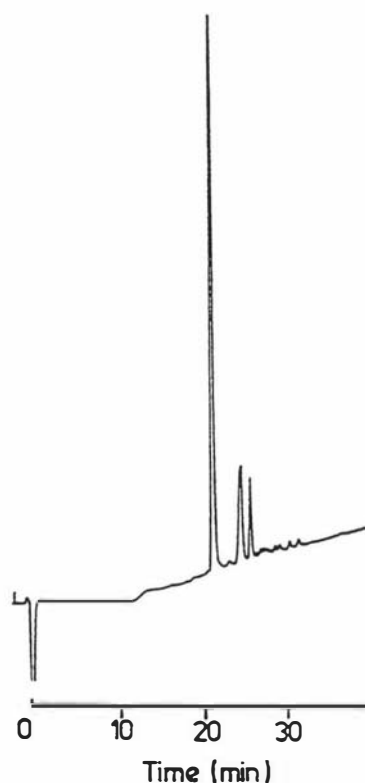
Figure 19. HPLC Analysis of estriol 16-glucuronide **14**, prepared from estrone **8** according to scheme 20,[61] showing the product **14** (retention time: 20 minutes) and a small amount of impurities.

For compound **14**: FABMS, m/z 465 (MH)$^+$, High resolution EIMS, 446.1935 (M-H$_2$O)$^+$ (Calculated for C$_{24}$H$_{30}$O$_8$, 446.1941); δ_H (CD$_3$OD) 0.79(s, 3H, 18-CH$_3$), 3.23-3.31(m, 1H, 2'-H), 3.42(t, 1H, 3'-H), 3.53(t, 1H, 4'-H), 3.63(d, J = 5.31 Hz, 1H, 17α-H), 3.86(d, J = 9.79 Hz, 1H, 5'-H), 4.11(m, 1H, 16β-H), 4.38(d, J = 7.83 Hz, 1H, 1'-H), 6.47-7.07(m, 3H, aromatic).

2.2.3. Preparation of estriol monoglucuronides from estriol[117] (Scheme 21)

2.2.3.1 Estriol 3-glucuronide (E3-3G) **13**

16α,17β-Diacetoxy-1,3,5(10)-estratrien-3-ol 88

A mixture of estriol **10** (60 mg, 0.208 mmol) and copper (II) acetate monohydrate (1 g)[119] in acetic acid (3 ml) was stirred under refluxing for 20 hours. TLC (hexane/EtOAc, 2:1) showed a major product **88** (R$_F$ = 0.33) and a small amount of a mixture of estriol 16α- and 17β-monoacetate **116, 117** (R$_F$ = 0.17). The solvent was then removed under reduced pressure, and the residue poured into H$_2$O (20 ml) and extracted with Et$_2$O (25 ml x 2). The ethereal solution was washed successively with aqueous NaHCO$_3$ and H$_2$O, dried, and concentrated. Purification of the residue by flash chromatography on Al$_2$O$_3$, using hexane/EtOAc (1:1), afforded compound **88** (45 mg, 58%) as a pure white solid. mp, 173-175 °C, (Lit.[115] 173-175 °C). IR ν_{max} 3,414 cm^{-1} (3-OH), 1,742 and 1,713 cm^{-1} (C = O, C-16,17-diacetate); δ_H (CDCl$_3$) 0.84(s, 3H, 18-CH$_3$), 2.06(s, 3H, OCOCH$_3$), 2.10(s, 3H, OCOCH$_3$), 5.00(d, J = 5.59 Hz, 17α-H), 5.18(m, 1H, 16β-H), 5.36(s, 1H, 3-OH), 6.57-7.14(m, 3H, aromatic).

If the above reaction mixture was stirred under refluxing for only 4 hours, the major product was the mixture of **116** and **117** (47 mg, 58%; including 60% of **116** and 40% of **117**). δ_H (CDCl$_3$) 0.86(s, 3H, 18-CH$_3$), 2.11(s, 3H, OCOCH$_3$), 2.15(s, 3H, OCOCH$_3$), 3.50(s, 0.6H, 17β-OH from **116**), 3.63(d, J = 4.48 Hz, 0.6H, 17α-H from **116**), 3.89(s, 0.4H, 16α-OH from **117**), 4.18(m, 0.4H, 16β-H from **117**), 4.28(d, J = 4.48 Hz, 0.4H, 17α-H from **117**), 4.81-4.86(m, 0.6H, 16β-H from **116**), 5.33(s, 1H, 3-OH), 6.56-7.15(m, 3H, aromatic).

116   **117**
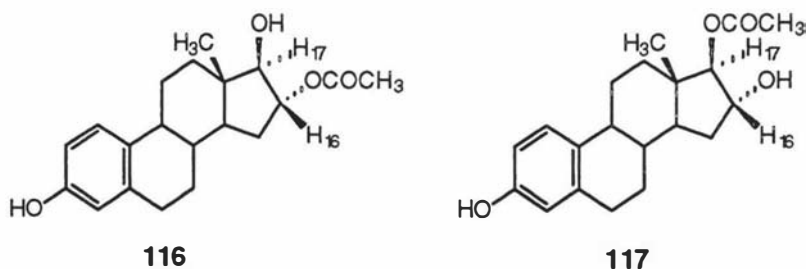
Methyl 16α,17β-diacetoxy-1,3,5(10)-estratrien-3-yl-2,3,4-tri-O-acetyl-β-D-glucopy-ranosiduronate 89

The coupling reaction was performed by a procedure similar to that used in the preparation of **102**, except that a longer refluxing time (10 hours) was used for compound **88** (400 mg) instead of 5 hours refluxing as for compound **101**. The purification of the residue by flash chromatography on Al_2O_3, using hexane/EtOAc (1:1) (R_F = 0.40 for compound **89**) as eluent, gave compound **89** as white crystals (420 mg, 57%); mp, 196-198 °C; δ_H (CDCl$_3$) 0.84(s, 3H, 18-CH$_3$), 2.040(s, 3H, OCOCH$_3$), 2.049(s, 3H, OCOCH$_3$), 2.053(s, 3H, OCOCH$_3$), 2.057(s, 3H, OCOCH$_3$), 2.09(s, 3H, OCOCH$_3$), 3.74(s, 3H, COOCH$_3$), 4.16(d, J = 9.53 Hz, 1H, 5'-H), 5.00(d, J = 5.86 Hz, 1H, 17α-H), 5.09(d, J = 7.32 Hz, 1H, 1'-H), 5.19(m, 1H, 16β-H), 5.27-5.35(m, 3H, 2', 3' and 4'-H), 6.71-7.21(m, 3H, aromatic).

16α,17β-Dihydroxy-1,3,5(10)-estratrien-3-yl-β-D-glucopyranosiduronic acid 13

The hydrolysis reaction was performed by a procedure similar to that used in the preparation of **14**. Compound **13** (90 mg, 64% yield) was obtained from compound **89** (210 mg, 0.309 mmol) as fine crystals; mp, 237-240 °C; (Lit.[57] 213-220 °C). Analysis calculated: $C_{24}H_{32}O_9$: C, 62.5; H, 6.95; Found: C, 61.73, H, 6.95; FABMS m/z, 464 (M)$^+$; δ_H (DMSO-d$_6$) 0.66(s, 3H, 18-CH$_3$), 3.17-3.24(m, 4H, 2', 3', 4' and 17α-H), 3.81(m, 2H, 5' and 16β-H), 4.61(d, J = 4.76 Hz, 1H, OH, disappeared after addition of D$_2$O), 4.68(d, J = 4.46 Hz, 1H, OH, disappeared after addition of D$_2$O), 4.95(d, J = 7.33 Hz, 1H, 1'-H), 5.21(d, 1H, OH, disappeared after addition of D$_2$O), 5.39(d, J = 4.76 Hz, 1H, OH disappeared after addition of D$_2$O), 6.68-7.19(m, 3H, aromatic).

2.2.3.2 Estriol 16α-glucuronide (E3-16G) **14**:

16α-(tert-Butyldimethylsilyloxy)-1,3,5(10)-estratrien-3,17β-diol **107**

Compound **107** was prepared from estriol **10** by selective protection of the 16α-hydroxyl group with *tert*-butyldimethylsilyl chloride according to established literature procedures[120] in 82% yield. For compound **107** (white solid), mp, 193-194 °C; (Lit.[120] 194 °C). IR ν_{max} 3,563 cm^{-1} (OH), 3,316 cm^{-1} (OH); δ_H (CDCl$_3$) 0.06 (s, 6H, -SiMe$_2$), 0.73 (s, 3H, 18-CH$_3$), 0.87 (s, 9H, -SiCMe$_3$), 3.30 (s, 1H, 17β-OH), 3.46 (d, 1H, J = 5.49 Hz, 17α-H), 4.06 (m, 1H, 16β-H), 4.66 (s, 1H, 3-OH), 6.49-7.08 (m, 3H, aromatic);

3,17β-Diacetoxy-16α-(tert-butyldimethylsilyloxy)-1,3,5(10)-estratriene **108**

Compound **108** was prepared from compound **107** by acetylation with Ac$_2$O and pyridine according to established literature procedures[120] in 93% yield. For compound **108** (fine crystals) mp, 110-112 °C; (no melting point reported[120]). IR ν_{max} 1,766 and 1,744 cm^{-1} (C = O, C-3,17-diacetate); δ_H (CDCl$_3$) 0.03 (d, 6H, -SiMe$_2$), 0.77 (s, 3H, 18-CH$_3$), 0.88 (s, 9H, -SiCMe$_3$), 2.09 (s, 3H, OCOCH$_3$), 2.28 (s, 3H, OCOCH$_3$), 4.30 (m, 1H, 16β-H), 4.84 (d, 1H, J = 5.59 Hz, 17α-H), 6.78-7.28 (m, 3H, aromatic).

3,17β-Diacetoxy-1,3,5(10)-estratriene-16α-ol **109**

A typical experimental procedure for the desilylation of the 16α-*tert*-butyl-dimethylsilyl group was as follows.[121] Compound **108** (239 mg) was dissolved in 15 ml of solvent mixture (HOAc/H$_2$O/THF, 3:1:1), and stirred for 40 hours at room temperature. After adding 100 ml of ether (Et$_2$O), the organic layer was separated, washed with ice-cooled NaHCO$_3$ and water, and dried over MgSO$_4$. Removal of the solvent under reduced pressure afforded a white solid which was purified by flash chromatography using hexane/EtOAc (2:1) as eluent to give compound **109** as a white solid (177 mg, 97% yield). mp, 140 °C; (Lit.[120] mp, 132 °C). IR ν_{max} 3,503 cm^{-1} (16β-OH), 1,751 and 1,719 cm^{-1} (C=O, 3,17-diacetate); δ_H (CDCl$_3$) 0.86(s, 3H, 18-CH$_3$), 2.15(s, 3H, OCOCH$_3$), 2.28(s, 3H, OCOCH$_3$), 3.76(s, 1H, 16α-OH), 4.16(m, 1H, 16β-H), 4.28(d, J = 4.48 Hz, 1H, 17α-H), 6.80-7.28(m, 3H, aromatic).

Methyl 3,17β-diacetoxy-1,3,5(10)estratriene-16α-yl-2,3,4-tri-O-acetyl-β-D-glucopyranosiduronate 110

The coupling reaction was performed by a procedure similar to that used in the preparation of **102**, except that the purification of the oily residue was carried out by flash chromatography using hexane/EtOAc (1:1) as eluent instead of by recrystallisation in acetone/water and CH_2Cl_2/MeOH as for compound **102**. Compound **110** was obtained from compound **109** (170 mg, 0.46 mmol) as a white solid (250 mg, 80% yield); mp, 170-173 °C; Analysis calculated, $C_{35}H_{44}O_{14} \cdot 2/3H_2O$: C, 59.99; H, 6.52; Found: C, 59.96; H, 6.24; δ_H (CDCl$_3$) 0.75(s, 3H, 18-CH$_3$), 2.02(s, 3H, OCOCH$_3$), 2.03(s, 3H, OCOCH$_3$), 2.05(s, 3H, OCOCH$_3$), 2.06(s, 3H, OCOCH$_3$), 2.28(s, 3H, 3-OCOCH$_3$), 3.77(s, 3H, COOCH$_3$), 3.96(d, J = 9.70 Hz, 1H, 5'-H), 4.25(m, 1H, 16β-H), 4.56(d, J = 7.46 Hz, 1H, 1'-H), 4.95-4.98(m, 2H, 2' and 17α-H), 5.22-5.25(m, 2H, 3' and 4'-H), 6.77-7.26(m, 3H, aromatic).

3,17β-Dihydroxy-1,3,5(10)-estratrien-16α-yl-β-D-glucopyranosiduronic acid 14

The hydrolysis reaction was performed by a procedure similar to that used in the preparation of **14** from compound **103**. Compound **14** was obtained from compound **110** (48 mg, 0.07 mmol) as fine crystals (27 mg, 65%); mp, 223-224 °C; (Lit.[118] mp, 223-224 °C).
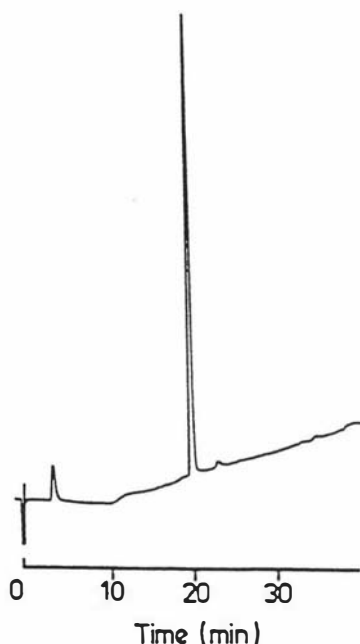
Figure 20. HPLC Analysis of estriol 16-glucuronide **14**, prepared from estriol **10** according to the present scheme (21),[117] showing the pure product **14** (retention time: 20 minutes).

HPLC showed that product **14** was pure (Figure 20) (HPLC conditions are the same as conditions in Figure 19). For compound **14**: Analysis calculated, $C_{24}H_{32}O_9 \cdot 4H_2O$: C, 53.72; H, 7.51; Found: C, 53.77; H, 6.82; FABMS m/z, 464 (M)+; δ_H (CD$_3$OD) 0.79(s, 3H, 18-CH$_3$), 3.25-3.34(m, 1H, 2'-H), 3.41(t, 1H, 3'-H), 3.54(t, 1H, 4'-H), 3.64(d, J = 5.49 Hz, 1H, 17α-H), 3.79(d, J = 9.53 Hz, 1H, 5'-H), 4.10(m, 1H, 16β-H), 4.36(d, J = 7.69 Hz, 1H, 1'-H), 6.47-7.07(m, 3H, aromatic). Product **14** was identical with an authentic sample of estriol 16α-glucuronide, FABMS, m/z, 464 (M)+, High resolution EIMS, 446.1931 (M-H$_2$O)+ (Calculated for $C_{24}H_{30}O_8$, 446.1941) and the ^{1}H-NMR spectrum, obtained from pregnancy urine (J. B. Brown, University of Melbourne, personal communication) in every respect (Figure 21).
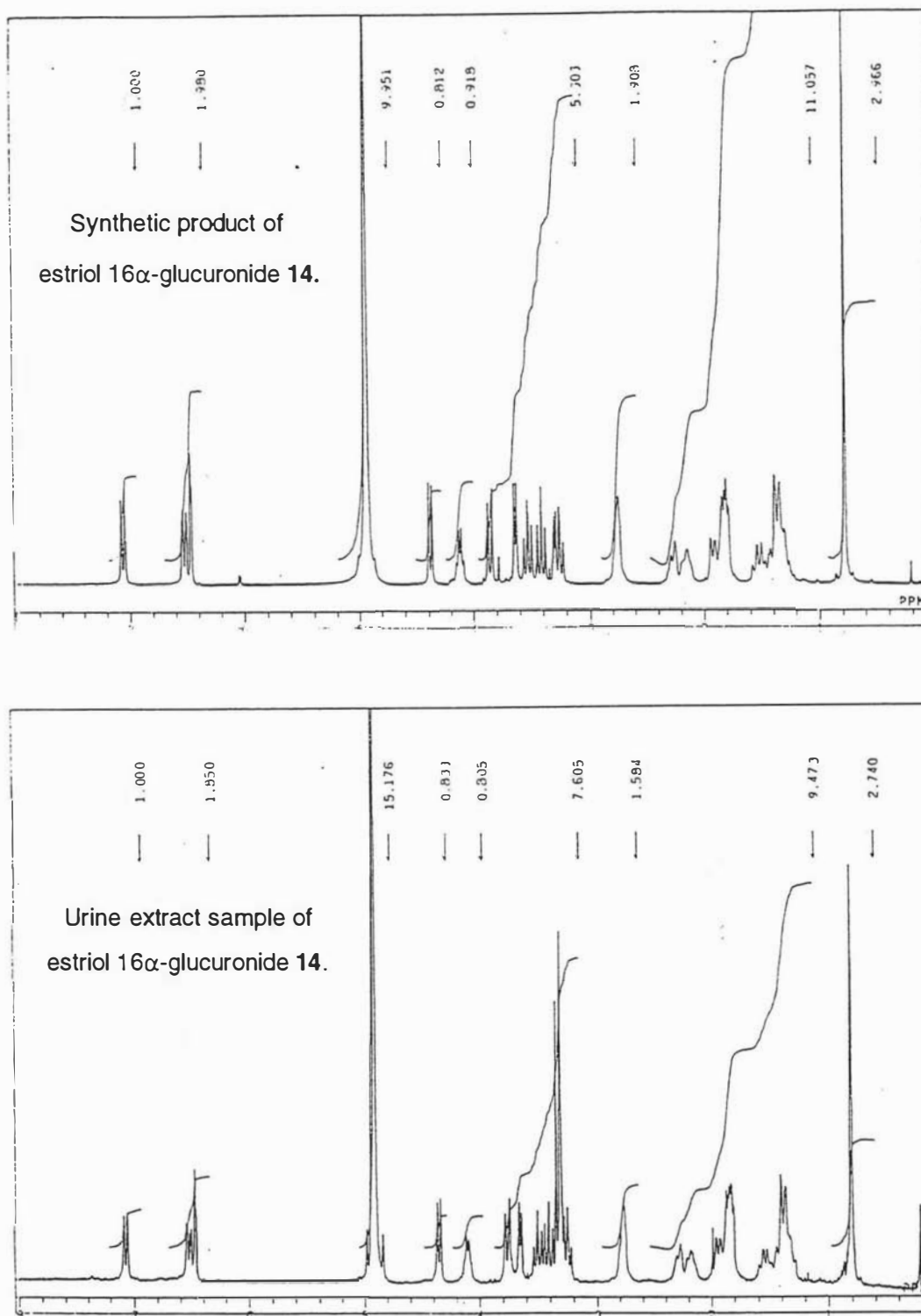
Figure 21. ^1H NMR Spectra of estriol 16α-glucuronide **14** (CD$_3$OD) from both a urine extract sample and the synthetic product showing two spectra which are basically the same, except the urine sample contains a strong H_2O peak at position δ = 3.3.

2.2.3.3 Estriol 17β-glucuronide (E3-17G) **15**:

Methyl 3-hydroxy-16α-(tert-butyldimethylsilyloxy)-1,3,5(10)-estratriene-17β-yl-2,3,4-tri-O-acetyl-β-D-glucopyranosiduronate 111

The coupling reaction was performed by a procedure similar to that used in the preparation of **110**, except that a 2 molar ratio of methyl 1-bromo-1-deoxy-2,3,4-tri-O-acetyl-α-D-glucopyranuronate **83** to compound **107** was used instead of a 4 molar ratio as for compound **109** and there was no refluxing time after addition of the methyl 1-bromo-1-deoxy-2,3,4-tri-O-acetyl-α-D-glucopyranuronate **83**. Compound **111** was obtained from compound **107** (370 mg, 0.92 mmol) as a light-yellow solid (285 mg, 47%). Attempts to crystallise compound **111** were unsuccessful because the *tert*-butyldimethylsilyl group of compound **111** was easily removed in solvent methanol (MeOH) by heating gently, and also by standing at room temperature for 24 hours. Hence compound **112** was obtained as pure crystals in this way. The IR, ^{1}H-NMR and melting point were identical with product **112** made by deprotection of **111** under weak acid conditions (HAc/H$_2$O/THF, 3:1:1).[121]

Methyl 3,16α-dihydroxy-1,3,5(10)-estratrien-17β-yl-2,3,4-tri-O-acetyl-β--D-glucopyranosiduronate 112

The desilylation reaction was performed by a procedure similar to that used in the preparation of compound **109**. Compound **112** was obtained from compound **111** (220 mg) as colourless crystals (160 mg, 85% yield). mp, 216-218 °C; (Lit.[57] mp, 207-212 °C). Analysis calculated; C$_{31}$H$_{40}$O$_{12}$·H$_2$O: C, 59.79; H, 6.79; Found: C, 59.71; H, 6.60; High resolution EIMS, 604.2519773 (M)$^+$ (Calculated for C$_{31}$H$_{40}$O$_{12}$, 604.2519772). δ_H (CDCl$_3$) 0.74 (s, 3H, 18-CH$_3$), 2.04 (s, 3H, OCOCH$_3$), 2.05 (s, 3H, OCOCH$_3$), 2.08 (s, 3H, OCOCH$_3$), 3.34 (d, J = 5.22 Hz, 1H, 17α-H), 3.71 (s, 1H, 16α-OH), 3.77 (s, 3H, COOCH$_3$), 4.11 (d, J = 9.33 Hz, 1H, 5'-H), 4.22 (m, 1H, 16β-H), 4.59 (d, J = 7.83 Hz, 1H, 1'-H), 5.09 (t, 1H, 2'-H), 5.25-5.30 (m, 2H, 3' and 4'-H), 5.77(s, 1H, 3-OH), 6.56-7.11 (m, 3H, aromatic).

3,16α-Dihydroxy-1,3,5(10)-estratrien-17β-yl-β-D-glucopyranosiduronic acid 15

The hydrolysis reaction was performed by a procedure similar to that used in the preparation of **14**. Compound **15** was obtained from compound **112** and **115** as fine crystals in 65% or 64% yield respectively; mp, 245-247 °C; (Lit.[59] mp, 241 °C);

Analysis calculated; $C_{24}H_{32}O_9 \cdot 3.5H_2O$: C, 54.64; H, 7.45; Found: C, 54.19; H, 7.37; FABMS m/z, 465 (MH)$^+$. δ_H (CD$_3$OD) 0.87(s, 3H, 18-CH$_3$), 3.25-3.34(m, 1H, 2'-H), 3.41(t, 1H, 3'-H), 3.48(d, J = 4.76 Hz, 1H, 17α-H), 3.54(t, 1H, 4'-H), 3.88(d, J = 9.53 Hz, 1H, 5'-H), 4.18(m, 1H, 16β-H), 4.43(d, J = 7.69 Hz, 1H, 1'-H), 6.46-7.06(m, 3H, aromatic).

3-Acetoxy-16α-(tert-butyldimethylsilyloxy)-1,3,5(10)-estratrien-17β-ol 113

Protection of the 3-hydroxy group in compound **107** was performed by an acetylation procedure similar to that used in the preparation of compound **108**, except that the reaction was stirred at 0 °C (ice-cooled bath)[115] for 0.5 hour instead of at room temperature for 40 hours. After extracting with ethyl acetate (EtOAc) (20 ml x 2), the organic layer was dried over magnesium sulphate (MgSO$_4$) overnight. Removal of the solvent under reduced pressure afforded a white solid that was purified by flash chromatography using hexane/EtOAc (3:1) as eluent to give compound **113** as a white solid (48 mg, 87% yield); mp, 190-192 °C; Analysis calculated, $C_{26}H_{40}O_4Si \cdot 1/2H_2O$: C, 68.83; H, 9.11; Found: C, 68.93; H, 8.91; IR, v_{max} 3,617 and 3,594 cm^{-1} (17β-OH), 1,754 cm^{-1} (C = O, 3-acetate); δ_H (CDCl$_3$) 0.06 (s, 3H, -SiCH$_3$), 0.07 (s, 3H, SiCH$_3$), 0.75 (s, 3H, 18-CH$_3$), 0.89 (s, 9H, -SiCMe$_3$), 2.25 (s, 3H, 3-OCOCH$_3$), 3.44 (s, 1H, 17β-OH), 3.54 (d, J = 5.86 Hz, 1H, 17α-H), 4.06 (m, 1H, 16β-H), 6.75-7.26 (m, 3H, aromatic).

Methyl 3-acetoxy-16α-(tert-butyldimethylsilyloxy)-1,3,5-(10)estratrien-17β-yl-2,3,4-tri-O-acetyl-β-D-glucopyranosiduronate 114

The coupling reaction was performed by a procedure similar to that used in the preparation of **110**. Compound **114** was obtained from compound **113** (45 mg, 0.10 mmol) as a white solid (53 mg, 69%); mp, 212-214 °C; Analysis calculated, $C_{39}H_{56}O_{13}Si$: C, 61.55; H, 7.42; Found: C, 61.39; H, 7.37; δ_H (CDCl$_3$) 0.04 (s, 3H, -SiMe), 0.08 (s, 3H, -SiMe), 0.72 (s, 3H, 18-CH$_3$), 0.88 (s, 9H, -SiCMe$_3$), 2.02 (s, 3H, OCOCH$_3$), 2.03 (s, 3H, OCOCH$_3$), 2.06 (s, 3H, OCOCH$_3$), 2.28 (s, 3H, 3-OCOCH$_3$), 3.66 (d, J = 5.5 Hz, 17α-H), 3.73 (s, 3H, COOCH$_3$), 3.98 (d, J = 9.89 Hz, 1H, 5'-H), 4.10 (m, 1H, 16β-H), 4.64 (d, J = 7.7 Hz, 1'-H), 5.02 (t, 1H, 2'-H), 5.22-5.26 (m, 2H, 3' and 4'-H), 6.78-7.28 (m, 3H, aromatic). FABMS m/z, 761 (M)$^+$.

Methyl 3-acetoxy-16α-hydroxy-1,3,5(10)-estratrien-17β-yl-2,3,4-tri-O-acetyl-β-D-glucopyranosiduronate 115

The desilylation reaction was again performed by a procedure similar to that used in the preparation of **109**. Compound **115** was obtained from compound **114** (50 mg) as a white solid (33 mg, 78% yield); mp, 225-227 °C; (Lit.[59] mp, 222-224 °C). δ_H (CDCl$_3$) 0.76 (s, 3H, 18-CH$_3$), 2.04 (s, 3H, OCOCH$_3$), 2.05 (s, 3H, OCOCH$_3$), 2.08 (s, 3H, OCOCH$_3$), 2.28 (s, 3H, 3-OCOCH$_3$), 3.34 (d, J = 5.13 Hz, 1H, 17α-H), 3.49 (s, 1H, 16α-OH), 3.78 (s, 3H, COOCH$_3$), 4.12 (d, J = 9.53 Hz, 1H, 5'-H), 4.26 (m, 1H, 16β-H), 4.60 (d, J = 8.06 Hz, 1'-H), 5.09 (t, 1H, 2'-H), 5.23-5.31 (m, 2H, 3' and 4'-H), 6.78-7.27 (m, 3H, aromatic).

2.2.3.4 Hydrolysis of estriol 16α- and 17β-glucuronides **(14, 15)** with β-glucuronidase:

A solution of the estriol glucuronide **14** or **15** (15 mg) and β-glucuronidase (E.C.3.2.1.31 Sigma Co., 5 mg, 14000 Fishman Units) in 0.1M-acetate buffer (pH = 4.6, 30 ml) was incubated at 38 °C for 24 hours. The incubated mixture was extracted with EtOAc (30 ml x 3), washed with water, dried over MgSO$_4$, and evaporated to give a white solid. The solid was crystallised from aqueous MeOH (1:1) to give estriol **10** (7 mg) and (6 mg) as colourless plates, mp, 279-284 °C, from enzymatic digestion of **14** and **15** respectively. The products were identical with an authentic sample of estriol in every respect.

2.2.4. Preparation of estrone glucuronide 12 and pregnanediol Glucuronide 16

2.2.4.1 Estrone glucuronide (E1G) **12**:

Methyl 17-oxo-1,3,5(10)-estratrien-3-yl-2,3,4-tri-O-acetyl-β-D-glucopyranosiduronate 84

The coupling reaction was performed by a procedure similar to that used in the preparation of **89**. The purification of the solid residue by flash chromatography on Al$_2$O$_3$, using hexane/EtOAc (2:1) as eluent, gave compound **84** as white crystals (117 mg, 54%) from estrone **8** (100 mg, 0.37 mmol) and methyl 1-bromo-1-deoxy-2,3,4-tri-O-acetyl-α-D-glucopyranuronate **83** (440 mg, 1.11 mmol). For compound **84**, mp, 228-231 °C; δ_H (CDCl$_3$) 0.90(s, 3H, 18-CH$_3$), 2.042(s, 3H, OCOCH$_3$), 2.049(s, 3H, OCOCH$_3$), 2.054(s, 3H, OCOCH$_3$), 3.74(s, 3H, COOCH$_3$), 4.15-

4.18(m, 1H, 5'-H), 5.11(d, J = 7.33 Hz, 1H, 1'-H), 5.23-5.35(m, 3H, 2', 3' and 4'-H), 6.73-7.23(m, 3H, aromatic).

17-Oxo-1,3,5(10)-estratrien-3-yl-β-D-glucopyranosiduronic acid **12**

The hydrolysis reaction was performed by a procedure similar to that used in the preparation of **14**. Compound **12** (40 mg, 62%) was obtained from compound **84** (85 mg, 0.145 mmol) as fine crystals; mp, 165-168 °C; (Lit.[122] mp, 165-168 °C).

HPLC result showed that product **12** was pure (Figure 22) (HPLC conditions are the same as conditions in Figure 19).
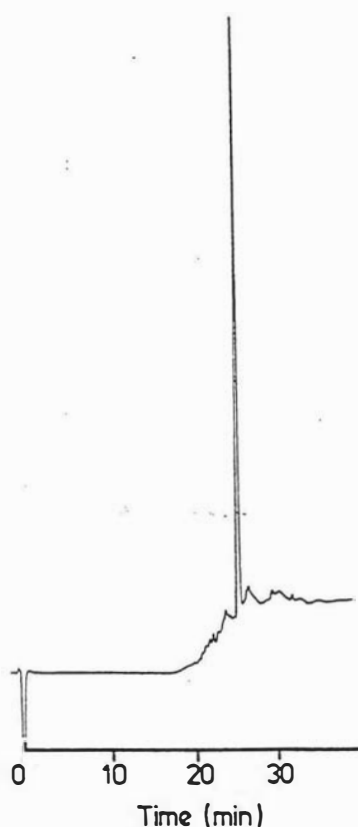
Figure 22. HPLC Analysis of estrone 3-glucuronide (E1G) **12** showing the pure product (retention time: 26 minutes).

For compound **12**: FABMS m/z, 446 (M)$^+$ ($C_{24}H_{30}O_8$); δ_H (acetone-d$_6$) 0.89(s, 3H, 18-CH$_3$), 3.47-3.74(m, 2H, 2' and 3'-H), 3.71(t, 1H, 4'-H), 4.06(d, J = 9.53 Hz, 1H, 5'-H), 5.06(d, J = 7.32 Hz, 1H, 1'-H), 6.78-7.23(m, 3H, aromatic).

2.2.4.2 Pregnanediol 3-glucuronide (PdG) **16**:

Methyl   20α-acetoxy-5β-pregnane-3α-yl-2,3,4-tri-O-acetyl-β-D-glucopyranosiduro-nate 87

The coupling reaction was performed by a procedure similar to that used in the preparation of **110**. Compound **87** was obtained from compound **86** (60 mg, 0.166 mmol, provided by Mr Mark Smales by partial hydrolysis of compound **85**) as a white crystalline powder (58 mg, 52%); mp, 176-179 °C. (Lit.[114] 177-180 °C). δ_H (CDCl$_3$) 0.64(s, 3H, 18-CH$_3$), 0.90(s, 3H, 19-CH$_3$), 1.21(d, J=6.22 Hz, 3H, 21-CH$_3$), 2.01(s, 3H, OCOCH$_3$), 2.02(s, 6H, 2OCOCH$_3$), 2.05(s, 3H, OCOCH$_3$), 3.59(m, 1H, 3β-H), 4.88-5.00(m, 2H, 20α and 2'-H), 5.18-5.30(m, 2H, 3' and 4'-H).

20α-Hydroxy-5β-pregnane-3α-yl-β-D-glucopyranosiduronic acid 16

The hydrolysis reaction was performed by a procedure similar to that used in the preparation of **14**. Product **16** was obtained from compound **87** (50 mg, 0.092 mmol) as fine crystals (25 mg, 55%); mp, 194-196 °C (Lit.[114] 194-197 °C). δ_H (CD$_3$OD) 0.66(s, 3H, 18-CH$_3$), 0.94(s, 3H, 19-CH$_3$), 1.18(d, J = 6.23 Hz, 3H, 21-CH$_3$), 3.19(t, 1H, 2'-H), 3.37(t, 1H, 3'-H), 3.51(t, 1H, 4'-H), 3.77(d, J = 9.90 Hz, 1H, 5'-H), 4.44(d, J = 7.69 Hz, 1H, 1'-H).

2.3 Results and Discussion

2.3.1. The synthesis of estriol monoglucuronides

In recent years, considerable attention has been directed to the biomedical problems associated with the metabolism and physiological role of estrogen conjugates in the human feto-placental unit. The importance of estriol monoglucuronide synthesis, therefore, has attracted increasing consideration. This stems largely from the growing awareness that their role in the body is not merely one of detoxification, but they also play important roles as starting materials for the preparation of protein- or enzyme-conjugates in immunoassays.

2.3.1.1 Comparison of estrone **8** with estriol **10** as a starting material for the synthesis of estriol monoglucuronides

Estriol monoglucuronides can be prepared either from estrone **8** or estriol **10**. Compared with the results of this thesis, the previous synthesis of estriol 16α-glucuronide **14** from estrone **8** (scheme 20)[61] is shown to have some disadvantages. First of all, the bromination of estrone **8** revealed difficulties in preventing the formation of the 2,4,16,16-tetrabromide derivative as a by-product. When the reaction time was not long enough, the reaction gave the required 2,4,16-tribromide **100** plus some mono- and di-bromides as by-products. If the bromination reaction was continued too long, the reaction always produced the 2,4,16,16-tetrabromide as the main product. Hence, the brominated product had to be purified many times by repeated recrystallization and the final yield of pure product was not as high as that reported in the literature.[61] Secondly, the hydrolysis of the 2,4,16-tribromide **100** to the dibromide **101** was difficult to control and it required the use of large amounts of dilute acid aqueous solution (1% HCl, 200 ml) to get a good yield of product **101** (82%). If 1.5% HCl (300 ml) was used for the same hydrolysis reaction as above, a very low yield of product **101** was obtained (32.3%). The reason for this low yield is probably that the acidity of 1.5% HCl was too high for the hydrolysis of 2,4,16-tribromide **100**. Furthermore, the reduction of the 17-carbonyl group presented another problem, since it always produced 30% of the 17α-isomer **104** which had to be isolated by column chromatography despite literature claims that only the 17β-isomer should be formed.

The new procedure described in this chapter (see Scheme 21) represents a simpler way to synthesise estriol 3-, 16- and 17-monoglucuronides (**3**, **14** and **15**) from estriol **10** in three to five steps each and in acceptable overall yields (21% for estriol 3-glucuronide **13**; 39% for estriol 16α-glucuronide **14** and 25% for estriol 17β-glucuronide **15**). The procedure makes use of the fact that estriol **10** reacts with *tert*-butyldimethylsilyl chloride specifically at the 16α-OH group. This is probably a result of steric hindrance by the C_{18}-methyl group adjacent to the 17β-OH group and a lower nucleophilic strength of the phenolic 3-OH group which raises the activation energy for reaction at this position due to electron delocalisation of the OH group lone pairs of electrons. Once the 16α-OH group is protected, it is then possible to selectively acetylate the 3- and 17-OH groups, which makes it possible to control the site of glucuronidation completely (scheme 21). For example, complete acetylation followed by deprotection of the 16α-OH group leads to glucuronidation at the 16α-OH position.

The glucuronidation reactions with protected estriol derivatives gave higher yields than starting from comparable 16α-hydroxy-17-oxo-derivatives as is necessary when beginning with estrone. From the mechanistic studies of Koenigs-Knorr reactions (Scheme 4), it can be seen that the orthoester **21**, which is the most important intermediate, results from the nucleophilic reaction of an alcohol or phenol with the 1,2-dioxolenium ion **20**. Consistent with this view, as discussed in the introduction of this chapter, it is generally found that alkoxyl oxygen atoms with low electron density or sterically hindered alcohols, both of which are expected to be poor nucleophiles, usually decrease the yields of Koenigs-Knorr reactions.

Elce *et al*[56] observed a variation in the yield of glucuronide formation dependent upon the position of the hydroxyl group, and the steric and electronic influence of the neighbouring groups in steroid compounds. For example, condensation of the bromo-sugar **83** with the 16α-hydroxy-17-one **93** gave a low yield of the estriol 16α-glucuronide derivative regardless of the spatial availability of the 16α-hydroxyl group. This low yield can be attributed to the withdrawal of electrons by the adjacent 17-carbonyl group resulting in the 16α-hydroxyl group being less nucleophilic than an ordinary secondary hydroxyl group. For the synthesis of the estriol 17β-glucuronide derivative, the coupling reaction of the bromo-sugar **83** with the 17β-hydroxy-16-one compound **118**, appeared to be influenced by both steric (18-CH_3) and electronic effects (C_{16} = O). A very low yield of the 17-glucuronide derivative was obtained in this instance. Since there is no adjacent carbonyl group in the protected estriol derivatives in the present procedure, the free hydroxyl group is

more nucleophilic and hence higher yields were obtained in the glucuronidation reactions.
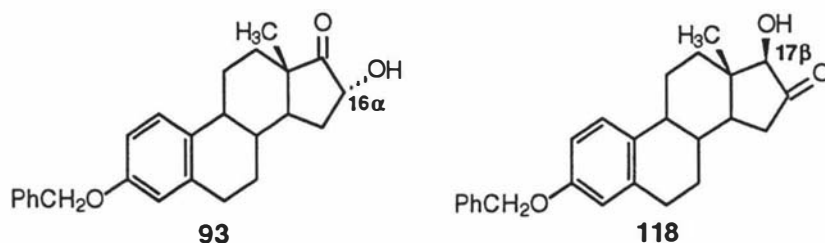
By comparison of the two HPLC results (Figure 19 and 20), it also can be seen that estriol 16α-glucuronide **14**, which was made from estriol **10** according to the present procedure (Scheme 21), was of higher purity than the product **14** prepared from estrone **8**.

There was another advantage in using estriol **10** as a starting material rather than using estrone **8**. The usual synthesis of estriol 16- and 17-glucuronides from estrone involves many steps including the glucuronidation of the 16α-hydroxy-17-oxo derivatives and reduction of the 17-carbonyl group. The reduction of the 17-carbonyl group often produces significant quantities of the 17α-isomer,[56] which significantly decreases the yield. For example, in the present work during the synthesis of estriol 16α-glucuronide **14** from estrone **8** according to the literature procedure,[61] 30% of methyl 3,17α-dihydroxy-1,3,5(10)estratriene-16α-yl-2,3,4-tri-O-acetyl-β-D-glucopyranosiduronate **104** (17α-isomer) and 70% of methyl 3,17β-dihydroxy-1,3,5(10)-estratriene-16α-yl-2,3,4-tri-O-acetyl-β-D-glucopyranosiduronate **103** (17β-isomer) were obtained, although there was no 17α-isomer **104** reported in the literature procedure.[61]
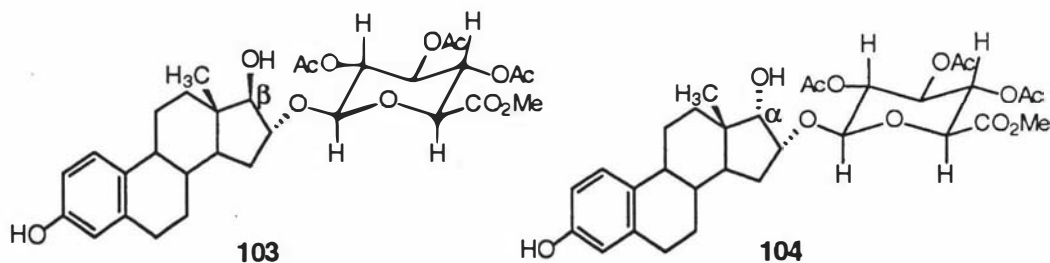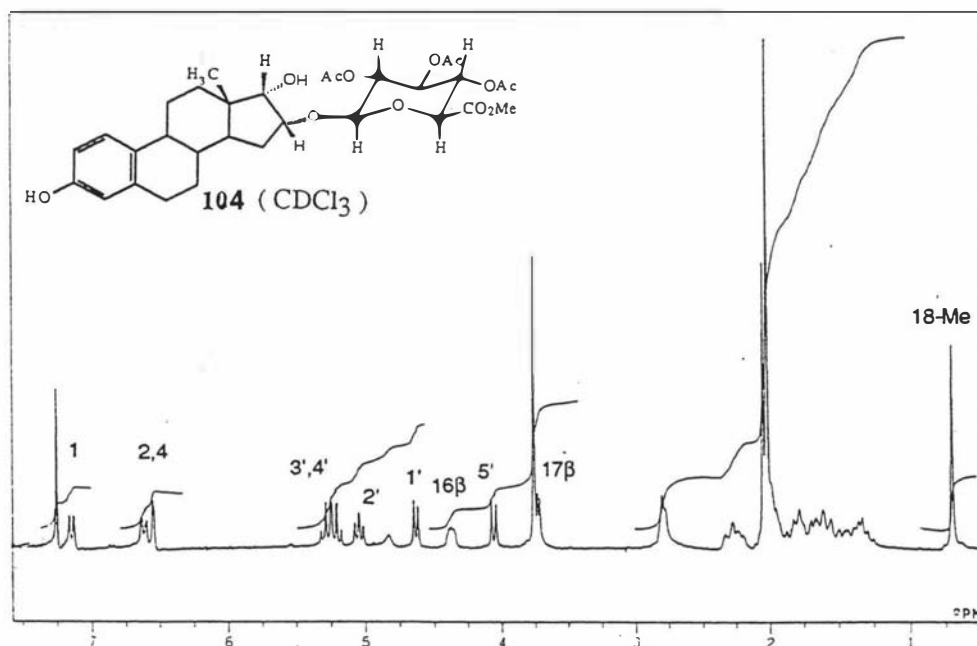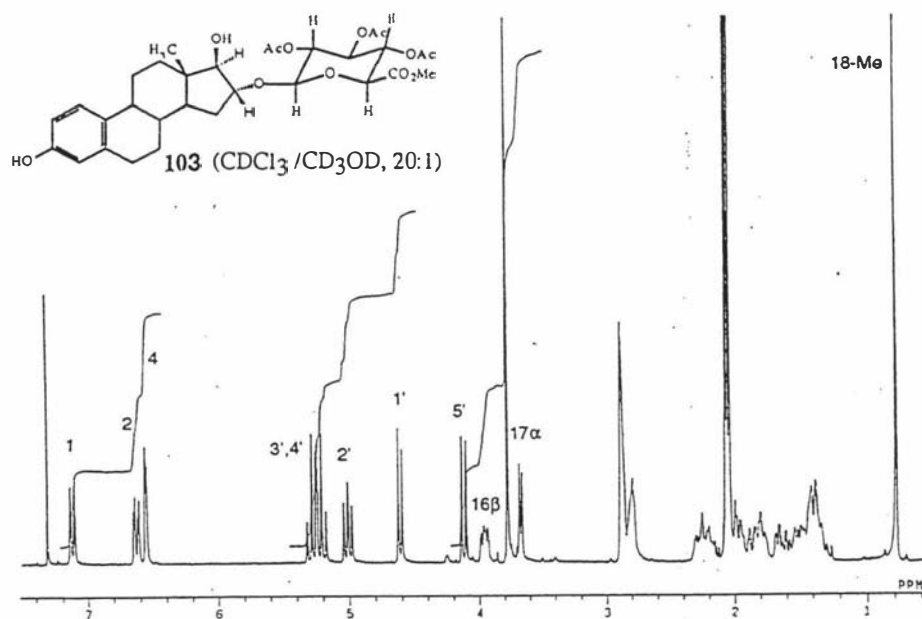
Figure 23. Comparison of the ¹H NMR spectra of compounds **103** and **104** showing the major differences between these two stereo-isomers. In the 17β-isomer **103**, the 16β-proton is upfield of the 5'-proton, while in the 17α-isomer **104**, the 16β-proton appears downfield of the 5'-proton position.

Both isomers were characterised and confirmed by spectroscopy and accurate mass spectra (see experimental section). The major difference between the α and β isomers was reflected in the ^{1}H-NMR spectra shown in Figure 23. In the 17α-isomer **104**, the 16β-proton appeared as a multiplet at 4.38 ppm and downfield of the 5'-H position, while in the 17β-isomer **103**, the 16β-proton was upfield of the 5'-H position as a multiplet at 3.95 ppm (Figure 23).

Since the stereochemistry at carbon-16 and carbon-17 is known in the D-ring when estriol **10** is used as a starting material and is preserved during subsequent reactions, the problem of obtaining the unwanted 17α-isomer during the reduction of the 17-carbonyl group is avoided. Also, it should be noted that determination of the absolute stereochemistry of these positions in the five-membered D-ring of steroids after reduction of the 17-oxo group is difficult by spectroscopic techniques. A spectroscopic technique for determining the absolute stereochemistry in ring D will be discussed later in chapter 3.

The present method also has advantages over other previous procedures using estriol **10** as a starting material,[58,59] since the direct glucuronidation of a 3-protected estriol (**105** or **106**) always produced a mixture of the 16- and 17-glucuronides, which were difficult to separate. Especially, it was difficult on a preparative scale to get pure estriol 16α- or 17β-glucuronides. Also, it is difficult to get high yields of 3-protected estriols.[115] Furthermore, recent results[63] showed that the selective formation of estriol monoglucuronide derivatives did not occur at the C-16 or C-17 position with direct glucuronidation, which was inconsistent with the previous results.[58]

Scheme 21 therefore provides a very simple procedure, which can selectively synthesise estriol 3-, 16- and 17-glucuronides in comparatively high yields without the separation and purification problem. This procedure also preserves the D-ring stereochemistry and location of the glucuronide linkage, which is important for estriol monoglucuronides for use in biological systems as in the present work. By selectively protecting and deprotecting the different hydroxyl groups of estriol in a controlled sequence, the new method also provides an opportunity for further manipulation of estriol and opens the way for the synthesis of a wide range of estriol derivatives.

2.3.1.2 Purification of steroid glucuronides in their free acid forms

It was especially notable that all of the steroid glucuronides which were synthesised in this thesis were transformed to the free acid form by titrating the sodium salt solution, obtained after alkaline hydrolysis of the protected steroid glucuronide esters, to pH = 2.5. Although the glycosidic bonds of the steroid glucuronides, being acetal linkages, are always acid-sensitive,[123] the glycosidic linkage seems quite stable at this pH value at least for short period of time. This procedure not only afforded the free acid, which is the necessary form of the steroid glucuronides for later amidation reactions, but also provided a useful method for the purification of steroid glucuronides. Since the free acids of steroid glucuronides are normally insoluble in water, unlike the sodium salts, they can be separated comparatively easy from aqueous solution, which retains the low molecular weight reagents and sodium salts in aqueous solution, to obtain a pure steroid glucuronide product. The sodium salt form of the steroid glucuronides usually requires many repeated crystallisations from methanol in order to obtain a pure product, which results in significant loss of valuable products.

The free acid forms of the steroid glucuronides showed some differences in solubility. Estrone glucuronide **12** was very soluble in either acetone or methanol. However steroidal alicyclic glucuronides (estriol 16- and 17-glucuronides **14, 15** and pregnanediol glucuronide **16**) were soluble in methanol but not in acetone. Estriol 3-glucuronide **13** dissolved in neither acetone nor methanol, and was only soluble in DMSO as a solvent.

2.3.1.3 Selective protection and deprotection reactions in estriol derivatives

Attempts to synthesise estriol $16\alpha,17\beta$-diacetate **88** by selective acetylation using acetic anhydride and a catalytic amount of boron trifluoride etherate in THF[115] were unsuccessful, giving complex product mixtures. $BF_3 \cdot Et_2O$ is very active and is hard to control when it is used as a catalyst in acetylation reactions. However, successful acetylation to produce the required estriol $16\alpha,17\beta$-diacetate **88** was achieved by simply refluxing estriol **10** in acetic acid in the presence of copper (II) acetate monohydrate.[119] After four hours refluxing, the reaction gave a mixture of estriol 16α- and 17β-monoacetate (**116, 117**) in a ratio of 3:2 as the main products. The higher yield of acetylation product at the 16α-OH group compared with the 17β-OH group probably resulted from the fact that the 17β-OH group is sterically hindered by the 18-CH_3 group. The estriol monoacetates were slowly converted to the

16α,17β-diacetate **88** by further refluxing and after 20 hours a reasonable yield (58%) of estriol 16α,17β-diacetate **88** was obtained.
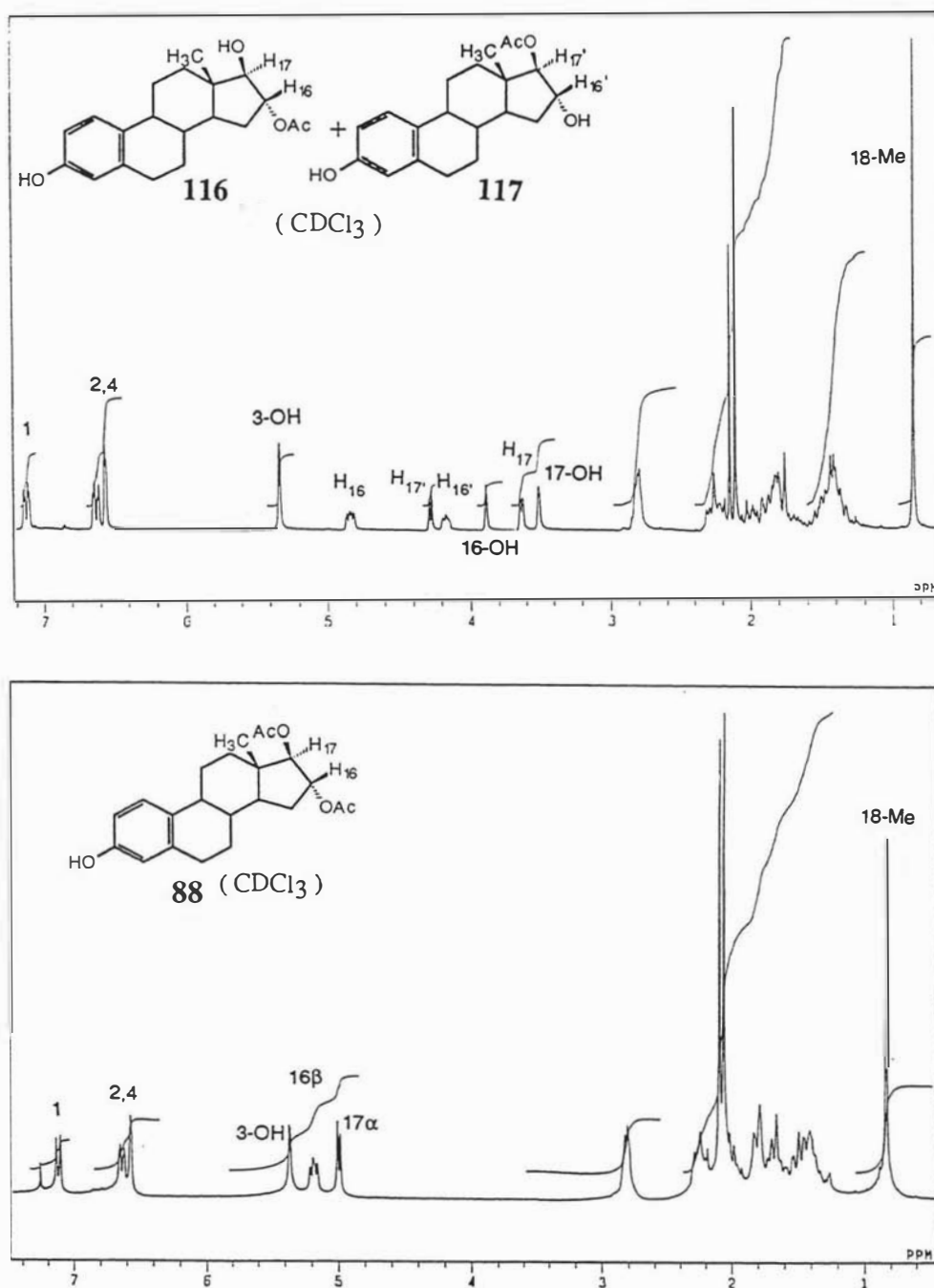
Figure 24. Comparison of two ¹H NMR spectra of mono-acetylated products (**116, 117**) and the di-acetylated product **88** showing the chemical shifts of 16β- and 17α-protons in compound **88** being much higher than those in mono-acetylated compounds (**116, 117**).

Some differences between estriol 16α,17β-diacetate and the two monoacetates are shown in Figure 24 by comparing the two ¹H-NMR spectra. With estriol **10** as a reference compound,[61] the monoacylation of the 16α-OH or 17β-OH groups produced a downfield shift at the 16β-proton of 0.8 ppm (4.03 to 4.83) in compound **116** or of the 17α-proton by 0.78 ppm (3.5 to 4.28) in compound **117**. Small downfield shifts for neighbouring protons were also produced as well (0.13 ppm for the 17α-proton in **116** and 0.15 ppm for the 16β-proton in **117**). However, when both the 16α-OH and 17β-OH groups were acylated, large downfield shifts were observed at the 16β- and 17α-protons (1.15 and 1.5 ppm) respectively (Figure 24).

Since acetic acid and copper (II) acetate monohydrate are both very cheap, and the reaction is very easy to control simply by refluxing, this new method offers a simple, economical and selective acetylation procedure for aliphatic hydroxyl groups in the presence of phenolic hydroxyl groups. Also, because there is no 3-acetylation product, this method obviously has advantages over other selective acetylation methods to prepare estriol 16α,17β-diacetate **88** as an intermediate for the synthesis of estriol 3-glucuronide **13**.

An interesting observation made during the synthesis of compound **112** (scheme 21) was the ease of deprotection of the *tert*-butyldimethylsilyl group in compound **111**. The usual reagent for the cleavage of a silyl ether is tetra-n-butylammonium fluoride. However in the current work, removal of the *tert*-butyldimethylsilyl group using the weak acid solution (HAc/H₂O/THF)[121] gave a much higher yield than deprotection by fluoride ion as described in the literature.[120] It is possible that tetra-n-butylammonium fluoride functions as a strong base in THF and causes 1,2-migration of the acyl group,[124] which significantly decreases the chemical yield. It is also noted that the *tert*-butyldimethylsilyl group in compound **111** could be removed simply by dissolution in MeOH and gentle heating. The reason is probably that the steric interaction between the two large functional groups at carbon-16 and carbon-17 (the carbohydrate moiety and the silyl protecting group) makes the silyl ether unstable and hence the silyl group was easily removed from the steroid compound **111**.

111
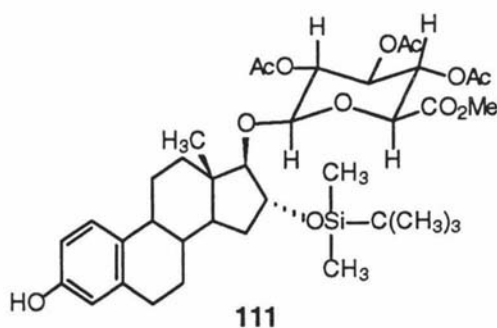
2.3.2. Koenigs-Knorr reactions for the synthesis of steroid glucuronides

During the course of this work, some interesting aspects of the glucuronidation reactions were noted. Estriol has been proved to be a useful model for a comparison of the relative reactivities of the different types of hydroxyl groups towards the O-glycosylation reactions (i.e. regioselectivity of the glucuronidation reactions).

2.3.2.1 Selective β-glycosidation between aliphatic and phenolic hydroxyl groups of steroids

β-Glycosidation is one of the key reactions in the synthesis of the different steroid glucuronides. When two different aliphatic hydroxyl groups were present in the same steroid compound as in estriol, selective glucuronidation of one of those under Koenigs-Knorr conditions could be achieved, using $CdCO_3$ as a catalyst, as a result of differing degrees of steric hindrance. For example, the Koenigs-Knorr reaction of the 2,3-protected 2-hydroxyestriol with bromo-sugar **83** using $CdCO_3$ gave a mixture of the 16α- and 17β-coupling products in a ratio of 7:1.[58] This presumably reflects the fact that the 16α-OH position is less sterically hindered compared with the 17β-OH group of estriol derivatives. Recently, Lugemwa *et al*[111] reported that reaction of β-estradiol with tri-O-acetyl-α-D-xylopyranosyl bromide in the presence of sodium hydroxide provided exclusively the 3-O-glucuronide in modest yield (45%). Since the aromatic hydroxyl group of β-estradiol is much more nucleophilic than the secondary hydroxyl group at carbon-17 under basic conditions (non-Koenigs-Knorr condition), protection of the 17β-OH group was not necessary. However, there is no previous report concerning the preferential selection of the

Koenigs-Knorr reaction for an alcoholic hydroxyl group in the presence of a phenolic hydroxyl group under neutral conditions.

In the present work, estriol 17β-glucuronide **15** could be synthesised in reasonable yield (47%) by direct glucuronidation of compound **107** (Scheme 21), in which both types of hydroxyl group were available. The result showed that the alcoholic 17β-hydroxyl group was much more reactive than the phenolic hydroxyl group in this compound despite the fact that there was a bulky *tert*-butyldimethylsilyl group at the 16α-OH position and a methyl group at the carbon-18 position. Hence estriol 17β-glucuronide **15** could be prepared without the need to protect the 3-OH group. This selectivity can be employed in the synthesis of other steroid glucuronides as well, such as estradiol 17β-glucuronide derivatives, by using the same procedure.

This selectivity of the Koenigs-Knorr reaction for an alcoholic hydroxyl group rather than for a phenolic hydroxyl group probably results from different electron densities at the alkyl and phenolic oxygen atoms under neutral conditions. For the phenol compounds (glycosyl acceptors), the lone-pair electrons of the phenolic oxygen atom are delocalised at the aromatic ring through the conjugation system. Hence, the lower electron density at the phenolic hydroxyl group causes it to function as a much poorer nucleophile than does the alcoholic hydroxyl group, which gives the great difference in reactivity observed between them under Koenigs-Knorr conditions.

2.3.2.2 Glycosyl donors for the synthesis of steroid glucuronides

As discussed earlier, the nature of the glycosyl donor and the promoter are the most crucial factors in determining the chemical yield and stereochemistry of the Koenigs-Knorr reactions. For most of the Koenigs-Knorr reactions used in the synthesis of steroid glucuronides, methyl 1-bromo-1-deoxy-2,3,4-tri-O-acetyl-α-D-glucopyranuronate **83** (α-bromosugar) was the glycosyl donor. This was easily prepared and showed good chemical reactivity and β-selectivity in the glycosidation reactions as reported in the literature. However, this reagent is not stable and can be stored at 0 °C for only a few weeks before it turns black although this can be recrystallised. An attempt was made therefore to use a more stable glycosyl donor for preparing estrone glucuronide **12**. β-Phenylthioglucuronide **119**, which was easily prepared from methyl 1-bromo-1-deoxy-2,3,4-tri-O-acetyl-α-D-glucopyranuronate **83** under phase transfer conditions[85] (Scheme 22), was chosen. However the coupling reaction with **8** was unsuccessful, giving no product.

Scheme 22

83　　　　　　　　　　**119**
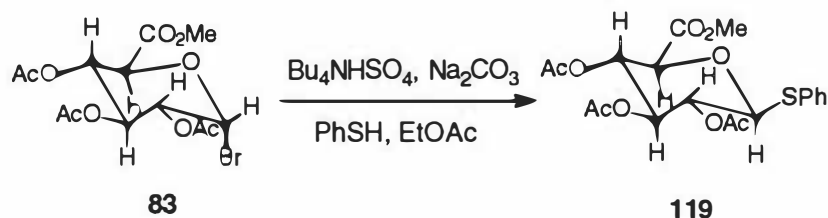
It is obvious that the β-phenylthioglucuronide **119** was not as reactive as the bromo-sugar **83** for the glucuronidation of the steroid compounds under the present conditions. The search for more stable, but reactive, and easily prepared glycosyl donors for the synthesis of steroid glucuronides is still one of the challenges in the field of carbohydrate synthesis. Although some glycosyl fluorides, thioglycosides or phosphrous-derivatives gave high chemical yields and good β-selectivity in glycosidation reactions, and are more stable than the glycosyl bromides, these glycosyl donors usually need many extra steps and some special reagents to prepare. In addition they are usually prepared from the halo-sugar anyway.

Recently, 2-phenylsulphonyl cyclic ethers **120** have been shown to undergo facile displacement of the sulphonyl group by alcohols under very mild conditions, in the presence of magnesium bromide etherate and sodium bicarbonate in tetrahydrofuran, to give good yields of the corresponding acetals **121**.[125] Some glycosidations can be achieved by using carbohydrate derivatives of the sulphone (Scheme 23).

Scheme 23

120　　　　　　　　　　**121**
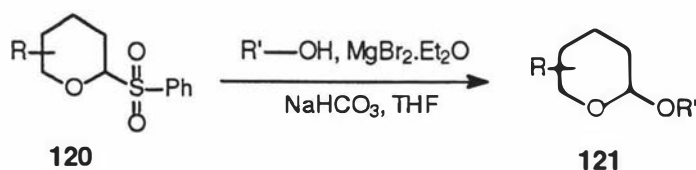
Previous research indicated that the anomeric sulphoxides, such as **53** (scheme 7)[88] and **57** (scheme 8),[89] were more reactive than the anomeric sulfide analogues **52** (scheme 7) or **56** (scheme 8) as glycosyl donors in Koenigs-Knorr reactions. A reasonable explanation for this behaviour can be obtained from the mechanism of the Koenigs-Knorr reactions (Scheme 4). The orthoester **21** results from the nucleophilic reaction of an alcohol or phenol with the 1,2-dioxolenium ion **20**, which is associated with an electron deficient anomeric carbon atom. Generally, the less the electron density at the anomeric carbon, the faster the Koenigs-Knorr reactions. The anomeric sulfoxide **53** or **57** has much less electron density at the anomeric carbon than does the anomeric sulfide **52** or **56** due to the electron withdrawing nature of the S=O group. Hence, glycosyl sulphoxide donors are expected to be more reactive than the glycosyl sulfide analogues towards glycosylation reactions.

In theory, the anomeric sulphone **120** should be even more reactive than both glycosyl sulfoxides (**53, 57**) and sulfides (**52, 56**) as the glycosyl donor in Koenigs-Knorr reactions, because of the strong electron withdrawing effect at the anomeric carbon by the sulphonyl group (O=S=O). Furthermore, the sulphonyl group is a well known good leaving group in organic chemistry, and the anomeric sulphone **120** should be prepared easily by oxidation from the corresponding sulfide. It should also be worth attempting to prepare an anomeric sulphone glycosyl donor from the reaction of bromo-sugar **83** with a sulphone salt under phase transfer conditions.[85] However, the yield and the stereochemical outcome of this glycosyl donor in Koenigs-Knorr reactions needs further investigation. No further attempt was made in this thesis for new glycosyl donors because bromo-sugar **83** gave good yields of β products and was easy to prepare from the protected sugar. Obviously a stable but active glycosyl donor would be an advantage.

2.3.2.3 Different promoters for the β-glycosidations of steroid glucuronides

Both Ag_2CO_3 and $CdCO_3$ are widely used as catalysts and acid acceptors in the Koenigs-Knorr reactions for the synthesis of steroid glucuronides. Ag_2CO_3 is a traditional catalyst and has been used for many years. In 1971, $CdCO_3$ was introduced by Bernstein and co-workers[60] as a new catalyst for the Koenigs-Knorr synthesis of aryl glucuronides. A few years ago, $CdCO_3$ was also successfully used in the Koenigs-Knorr reactions of steroidal alicyclic glucuronides for the synthesis of 2-hydroxyestriol monoglucuronides.[62] Recently, Shimada et al[63] concluded that $CdCO_3$ is not suitable for the synthesis of estriol 16- and 17 monoglucuronides because of the

low yields in their experiments. But from the results of the present research, a different conclusion can be drawn.

In the present work, comparing Ag_2CO_3 and $CdCO_3$ in Koenigs-Knorr reactions, the use of $CdCO_3$ appears to have some advantages over Ag_2CO_3. Firstly, it is more convenient to use $CdCO_3$ as a promoter in the Koenigs-Knorr reactions than using Ag_2CO_3. It is generally recognised that water plays a detrimental role in the Koenigs-Knorr reactions; anhydrous solvent and completely dried reagents and reaction vessels are necessary prerequisites for a successful reaction. When Ag_2CO_3 is used as a catalyst, it has to be freshly prepared. Since it is hard to dry after preparation and also difficult to remove moisture from the solvent, the Koenigs-Knorr reactions sometimes give low yields of product. For example, in the present work compound **102** was prepared by reaction of 2,4-dibromo-3,16α-dihydroxy-1,3,5(10)estratriene **101** with bromo-sugar **83** catalysed by Ag_2CO_3 in benzene in 36.5% yield, compared with 48% yield when using $CdCO_3$ (see experimental). When $CdCO_3$ was used in glucuronidation reactions, the commercial reagent could be used directly without any purification. All the compounds and the solvent (toluene) could be easily and thoroughly dried by azeotropic distillation to remove moisture before starting the reaction. It is thus easier to control the reaction under scrupulously anhydrous conditions. During this work, $CdCO_3$ has been used as a catalyst in the Koenigs-Knorr reaction and stored in a desiccator over long periods of time. All the steroid glucuronides **12-16** in this thesis were made by using this catalyst directly without any purification.

It is obvious that the previous low yield[63] reported for Koenigs-Knorr reactions catalysed by $CdCO_3$ resulted from the use of improper reaction conditions. Azeotropic distillation to remove moisture before starting the coupling reaction is crucial to the success of these reactions. Secondly, $CdCO_3$ catalysed Koenigs-Knorr reactions showed some selectivity in the preferential glucuronidation of an alcoholic hydroxyl group in the presence of a phenolic hydroxyl group[117] and selective glucuronidations between 16α- and 17β-hydroxyl groups subject to different steric hindrance.[62] This selectivity has not been observed when Ag_2CO_3 was used as a catalyst. Furthermore, certain bromosugars tend to be unstable in the presence of silver-based catalysts but the Cd-based promoters, as "softer" non-oxidising metal cation forms, are more stable in the glycosidation reactions.[126]

2.3.3 Summary

In summary, estrone glucuronide **12**, estriol monoglucuronides **13-15** and pregnanediol glucuronide **16** have been successfully synthesised as described in this chapter. In particular, a new scheme for the synthesis of estriol monoglucuronides **13-15** from estriol (Scheme 21) provides a simple procedure and good yields of pure products based on the protection and deprotection of hydroxyl groups, glucuronidation, and hydrolysis. This new synthetic route also retains the original stereochemical integrity of the estriol, and thus produces the estriol monoglucuronides with the correct stereochemistry. Additionally, the methodologies used in the synthesis and purification of steroid glucuronides as the free acid forms in this chapter can be extended to the synthesis and purification of general drug glucuronides. Since glucuronidation is an important metabolic pathway in mammals and is responsible for the urinary and biliary excretion of a large number of drugs, the synthesis of different drug glucuronides will be found to have very wide applications. For example, drug glucuronides can be used as analytical standards for HPLC, drug addicts, "dope" testing of athletes, racehorses, animal pharmaceutical residues, and the detection of toxins or pollutants in our environment.

Chapter 3

X-Ray Crystal Structure Analysis and NMR Investigation of
Estriol 16- and 17-Monoglucuronide Derivatives

3.1 Introduction

Although estriol monoglucuronides are important as human metabolites of estradiol, and have been synthesised by different methods, the knowledge of the position and configuration of the glycoside linkage between estriol and the carbohydrate moiety awaits the availability of appropriate standards. The stereochemical integrity of these linkages is nevertheless important in the chemical synthesis of steroid glucuronides to use in the analysis of biological fluids. If the stereochemistry is incorrect, recognition by stereospecific binding proteins is seriously impaired. There are no detailed NMR studies on estriol monoglucuronides and so far there has been no X-ray structural analysis on any of the estriol monoglucuronides reported in the literature.

Previously, in order to establish conclusively the exact conjugation-position in Koenigs-Knorr glucuronidation of estriol 16- and 17-glucuronides **14**, **15**, it was necessary to convert the glucuronide products into different derivatives either by the use of diazomethane[118] or an appropriate oxidation procedure.[59] As a general procedure diazomethane has been used extensively for the esterification of the C-6'-carboxyl group of steroid glucuronides. However, Neeman *et al*[118] made use of diazomethane in a rather unique fashion for determining the structure of urinary estriol 16α-glucuronide **14**. Treatment of estriol 16-glucuronide with diazomethane gave the 3, 6'-dialkylated steroid derivative **122** and further treatment of this material with diazomethane and a strong acid catalyst, boron trifluoride etherate, gave the fully methylated methyl ester **123**. Cleavage of the sugar **123** was achieved by refluxing with 4M hydrochloric acid in 10% aqueous ethanol which afforded estriol dimethyl ether **124** in 81% yield (Scheme 24). The resulting estriol dimethyl ether **124** was shown to be identical with synthetic 3,17β-dimethoxy-1,3,5(10)estratriene-16α-ol **124**, and to be different from the 3,16α-dimethoxy isomer.

Scheme 24
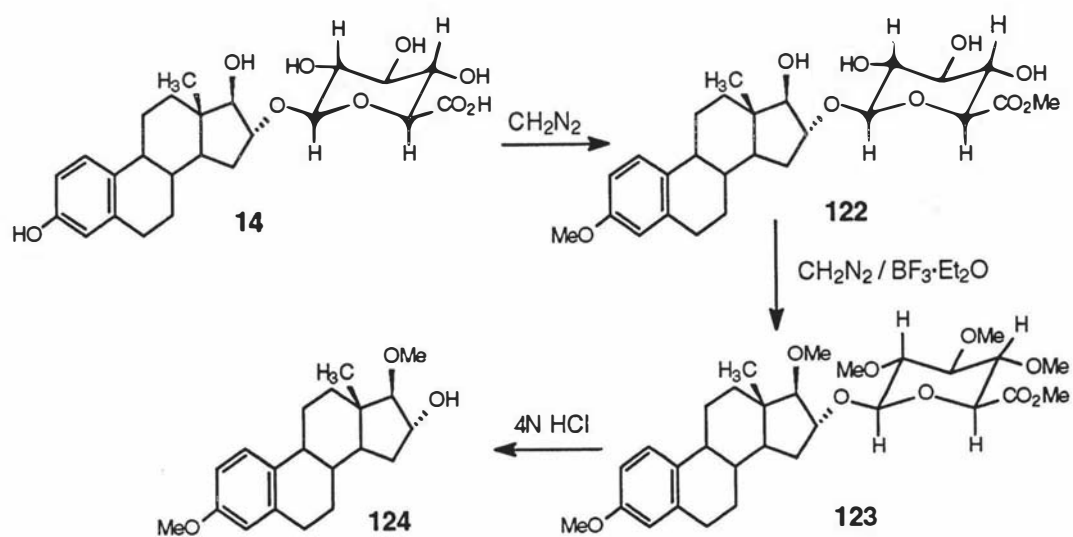
Scheme 25
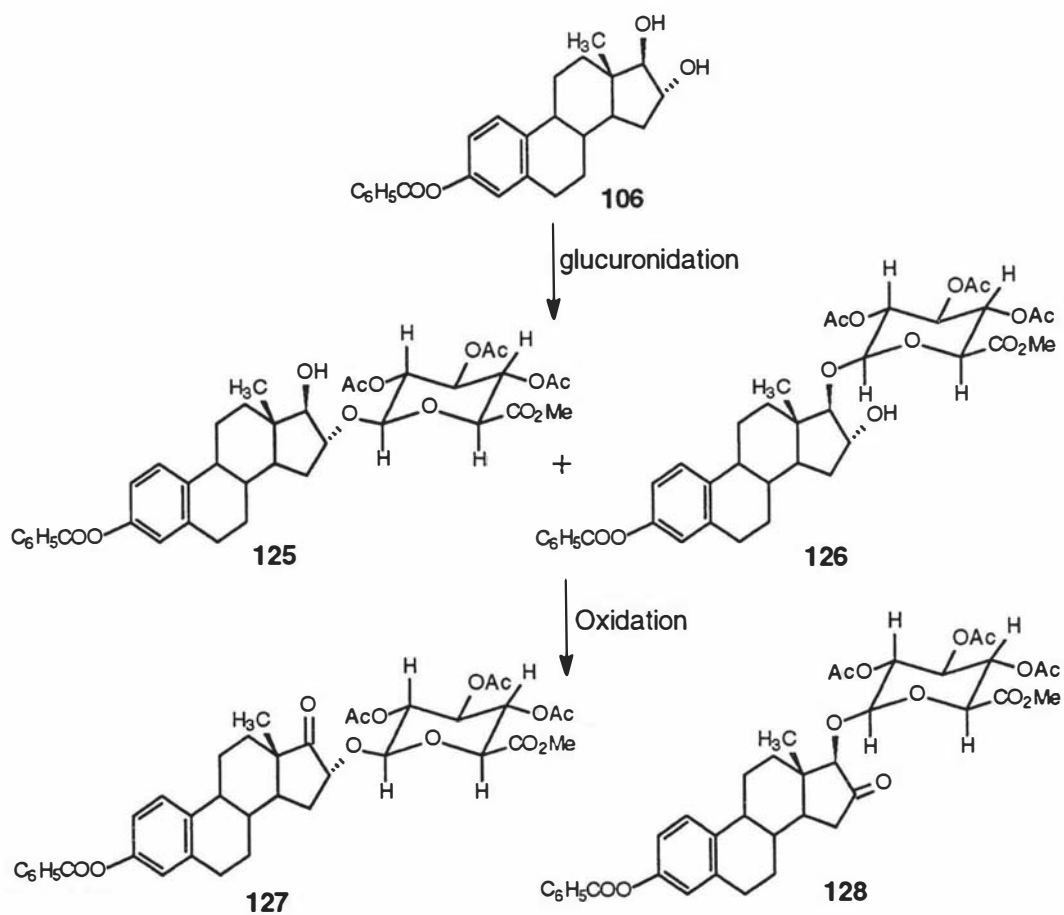
The structural assignment was also confirmed by converting the glucuronidation products **125, 126** into the 16- or 17-ketol glucuronide derivatives **127, 128** respectively by Jones oxidation (Scheme 25).[59] Inspection of the nuclear magnetic resonance spectra revealed that a 17α proton signal in the 17-glucuronide **128** appeared at 4.03 ppm as a singlet, while a 16β-proton signal in the 16-glucuronide **127** appeared at 4.48 ppm as a multiplet. Thus, exclusive glucuronidation at either the 16- or 17-position was demonstrated by the ^{1}H-NMR comparisons of the derivatives.

There are no direct spectroscopic, or other, methods to identify these isomers reported in the literature. Also, there is another problem which was related to the determination of the configuration of the glycosidic linkage. Since the usual synthetic routes from estrone **8** to estriol 16α- and 17β-glucuronide (**14, 15**) involve the reduction of the 17-carbonyl group as the key step, the reduction reactions introduce the possibility of isomerisation and epimerisation at the 16 and 17 carbon centres. However, unlike the situation for six-membered rings, the determination of relative stereochemistry at C-16 and C-17 in the 5-membered D-ring of steroids is difficult to judge solely from the ^{1}H NMR chemical shift data and the magnitude of the coupling constants (J) for the 16 and 17 protons (H_{16}-H_{17}) (Table 2, Section 3.3.2). There is no way to distinguish the 16-glucuronides from the 17-glucuronide derivatives or the α-isomer from the β-isomer on the basis of the ^{1}H NMR chemical shifts and the coupling constants alone. For example, there was no clear trend in the magnitude of the coupling constants to distinguish a *cis* arrangement from a *trans* arrangement of the 16 and 17 hydrogen atoms. The *trans* arrangement ($R_2 = R_4 = H$) (Table 2, Section 3.3.2) in compounds **10, 14, 15, 103, 108, 112, 114** and **115** gave a range of coupling constants from 4.76-6.0 Hz whereas the *cis* arrangement ($R_2 = R_5 = H$) of compound **104** also gave a similar value (4.39 Hz).

The hydrolysis of both the estriol 16- and 17-glucuronides with β-glucuronidase (see section 2.2.3.4), which is the most common enzymatic hydrolysing reagent for the identification of estriol monoglucuronides, confirmed the β orientation for the linkage of the carbohydrate moiety with the estriol skeleton. Since the enzymatic action of β-glucuronidase is only positive towards the β_2-linkages in compounds **14** and **15**, this diagnostic method only confirms the β configuration with respect to the glucuronide ring. No such simple test is available to confirm the orientation of the β_1-linkage in compound **15** or the α-linkage shown in compound **14** (Scheme 26).[127] These linkages are also of vital importance for the structural recognition of steroid glucuronides by binding proteins.

Scheme 26
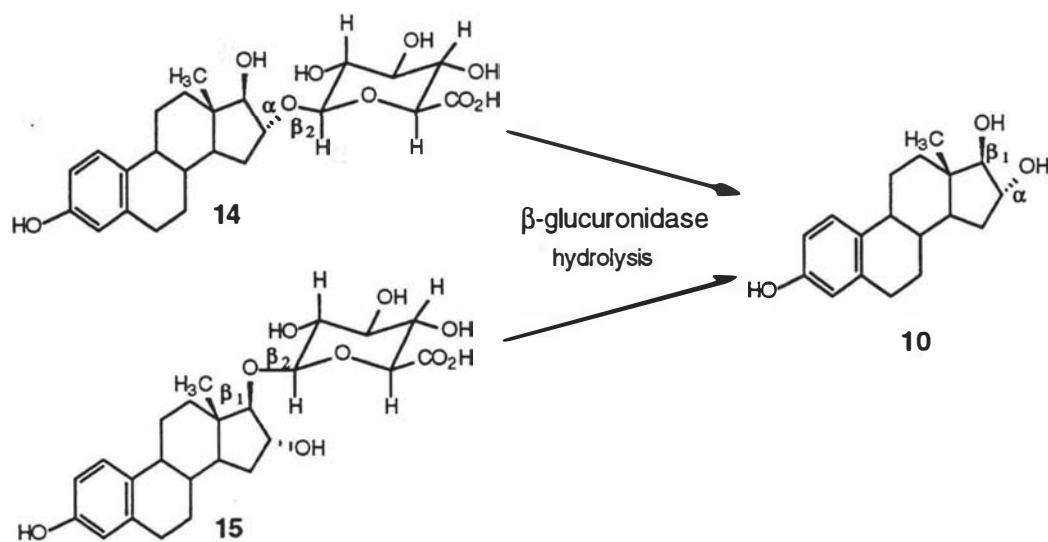
We have developed a synthetic procedure for the preparation of estriol glucuronides starting from estriol and utilising selective protection and deprotection of the three hydroxyl groups of estriol (Scheme 21, Chapter 2).[117] In this method the stereochemistry at the C-16 and C-17 positions of the D-ring should be preserved and hence the compounds synthesised serve as standards for the assignment of ^{1}H and ^{13}C NMR chemical shifts. Furthermore, as discussed above, since the hydrolysis of estriol monoglucuronides with β-glucuronidase and the determination of the proton coupling constants J (H_{16}-H_{17}) do not reveal the stereochemistry of the D-ring itself[127] (Section 3.3.1), X-ray structural analysis is desirable to confirm the stereochemistry of these compounds. Because of the difficulty experienced in obtaining suitable crystals from estriol 17β-glucuronide **15**, and also since the stereochemistry of the free glucuronide **15** and its ester **112** were the same,[127] the absolute configurations at all stereochemical centres are identical before and after hydrolysis (Scheme 27). Therefore, the X-ray structure analysis was undertaken for compound **112**, which was more easily crystallised, to confirm that the absolute configuration at all stereocentres was maintained during synthesis. Also, in this chapter, the general spectroscopic differences between the estriol 17β- and 16α-glucuronide derivatives are established on the basis of their ^{13}C NMR data, in conjunction with the 2D-NOESY technique.

Scheme 27
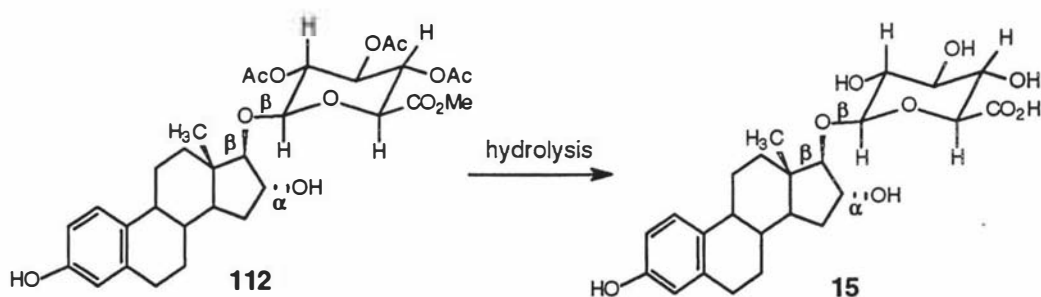
3.2 Experimental

3.2.1. Nuclear magenetic resonance investigation

Proton 2D-COSY (^{1}H-^{1}H) and 2D-NOESY spectra were measured at 270 MHz on a JEOL GX 270 spectrometer using CDCl$_3$ or CD$_3$OD as solvent and tetramethylsilane as an internal standard. ^{13}C Nuclear magnetic resonance spectra were recorded at 67.8 MHz using a JEOL GX270 spectrometer. ^{13}C Nuclear magnetic resonance data are expressed in ppm downfield from tetramethylsilane as an internal reference.

Estriol **10** was purchased from Sigma Chemical Company and used without purification. The syntheses of the estriol 16- and 17-glucuronide derivatives (**14, 15, 104, 105, 110, 112, 114** and **115**) have been described in Chapter 2.

3.2.2 X-ray determination of compound 112

Colourless crystals of methyl 3,16α-dihydroxy-1,3,5(10)-estratrien-17β-yl-2,3,4-tri-O-acetyl-β-D-glucopyranouronate **112** were obtained by the slow evaporation of methanol.

112
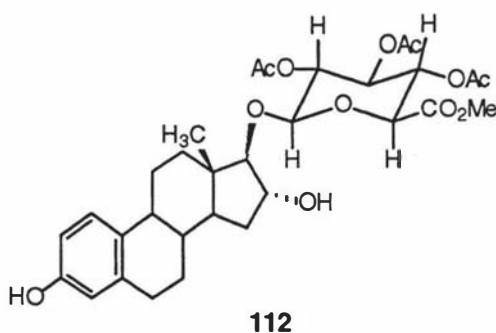
Crystal Data: $C_{31}H_{40}O_{12} \cdot H_2O$, M = 623.68, orthorhombic, space group $P2_12_12_1$, a = 13.712(2), b = 13.961(2), c = 17.019(2) Å, U = 3257.8(7) Å (from the least-squares setting angles of 23 reflections; $16.97 < \theta < 29.31^0$), Cu-K_α-radiation, λ = 1.5418 Å, Z = 4, D_c = 1.233 g cm^{-3}, $F(000)$ = 1288, μ(Cu-Kα) = 7.6 cm^{-1}, colourless crystals: size 0.36 x 0.23 x 0.21mm.

Data collection and processing: Enraf-Nonius CAD4 diffractometer at 293 K, ω-2θ scan mode, ω scan angle $(1.30 + 0.14 \tan \theta)^0$, variable scan speed (2.06-8.24^0 min^{-1}), maximum count time 90 seconds, 3859 reflections measured ($1.0 < \theta < 22.0^0$, $\pm h, \pm k, +l$; $22.0 < \theta < 52^0, +h, +k, +l$; $52 < \theta < 65^0, -h, -k, -l$). The intensities of three standard reflections were monitored every two hours of X-ray exposure time and showed a maximum loss in intensity of 3.7%. Of the reflections measured 2774 were unique [merging R_{int} = 0.025] after data were corrected for Lorentz and polarisation effects, crystal decay and absorption effects (psi-scans;[128] maximum and minimum transmission factors 0.9998 and 0.9187 respectively).

Structure analysis and refinement: Structure solution was by direct methods.[129] Full-matrix least-squares refinement with anisotropic thermal motion was assumed for all non-hydrogen atoms except those of the water molecule. Hydrogen atoms were in calculated positions (C-H 0.96 Å). At convergence R and R_w were 0.066 and 0.078 respectively for the 396 parameters refined using the 1989 data for which $F^2 > 2\sigma(F^2)$. The function minimised was $\Sigma w(|Fo| - |Fc|)^2$ with $w^{-1} = [\sigma^2(F_o) + 0.004071F_o{}^2]$. Computations were performed with the MolEN package,[128] SHELXS-76[129] and SHELX 86[130] programs.

Additional material available from the Cambridge Crystallographic Data Centre comprises thermal parameters, H-atom coordinates and a full listing of bond distances and angles.

3.3 Results and Discussion

3.3.1   General characterisation of steroid glucuronides by NMR spectroscopy

In the present work, all the steroid glucuronides were characterised by the ^{1}H-NMR and ^{13}C-NMR techniques. For all the steroid glucuronides **12-16** (Figure 7, Chapter 1, section 1.1.3), the aromatic protons (1-, 2- and 4-H in the A ring of the estrogens), the 18-CH$_3$ group and the 1'- to 5'-protons of the glucuronic acid moiety were assigned unambiguously by ^{1}H-^{1}H 2D-COSY spectra. The assignment of the chemical shift positions for the 16β- and 17α-protons of the estriol monoglucuronides **13**, **14**, **15** were made on the basis of their different splitting patterns. For example, the 17α-proton appeared as a doublet due to splitting by the single neighbouring 16β-H group and the 16β-proton as a multiplet caused by splitting from both the single 17α-H group and the pair of protons on C15, and the correlation between the 16β- and 17α-protons in 2D-COSY spectra (Figures 25-29).

For example, in the 2D-COSY spectrum (Figure 27) of estriol 16α-glucuronide **14**, the two aromatic protons (1-H and 2-H) of the A ring appeared as a pair of doublets at 7.06 and 6.53 ppm by splitting each other, and showed a correlation between them. The third aromatic proton (4-H) of the A ring was easily recognised by its single peak (6.47 ppm) and showed no cross correlations with the other protons. The 18-methyl group could be simply identified as a singlet (0.79 ppm) and again had no cross correlation with the other protons. For the 1'- to 5'-protons of the glucuronic acid ring, since the anomeric carbon (1'-C) is directly linked to the two oxygen atoms, the anomeric proton (1'-H) always has a higher chemical shift value than that of the 5'-proton (5'-H). The correlations of 1'-H (4.38 ppm) with 2'-H (3.27 ppm), 2'-H with 3'-H (3.42 ppm), 3'-H with 4'-H (3.53 ppm) and 4'-H with 5'-H (3.86 ppm) were all clearly recognisable in the spectrum. The *trans*-relationship of the protons (1'- to 5'-H) was demonstrated by the large coupling constants for all the neighbouring protons ($J_{1',2'}$, $J_{2',3'}$, $J_{3',4'}$ and $J_{4',5'} > 7.8$ Hz), which confirmed the basic structure of the glucuronic acid ring. In particular, the large coupling constant of the 1'- and 2'-protons ($J_{1',2'} = 7.83$ Hz) established that the glucuronic acid ring is β-linked[131] to the steroid moiety, which is consistent with the experimental result of hydrolysis of estriol 16α- and 17β-glucuronides by β-glucuronidase (Section 2.2.3.4). The assignment of the 16β- and 17α-protons was based on their different splitting patterns as discussed above, and the 17α-proton appeared as a doublet (3.63 ppm) showing a cross correlation with the 16β-proton as a multiplet at 4.11 ppm in the 2D-COSY spectrum (Figure 27).
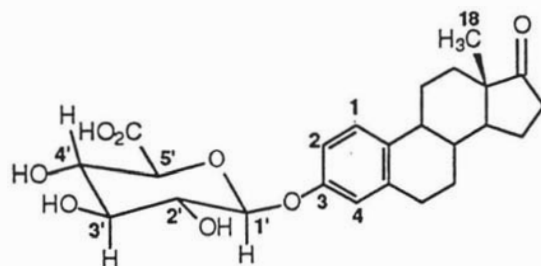
Estrone 3-glucuronide (E1G) **12**
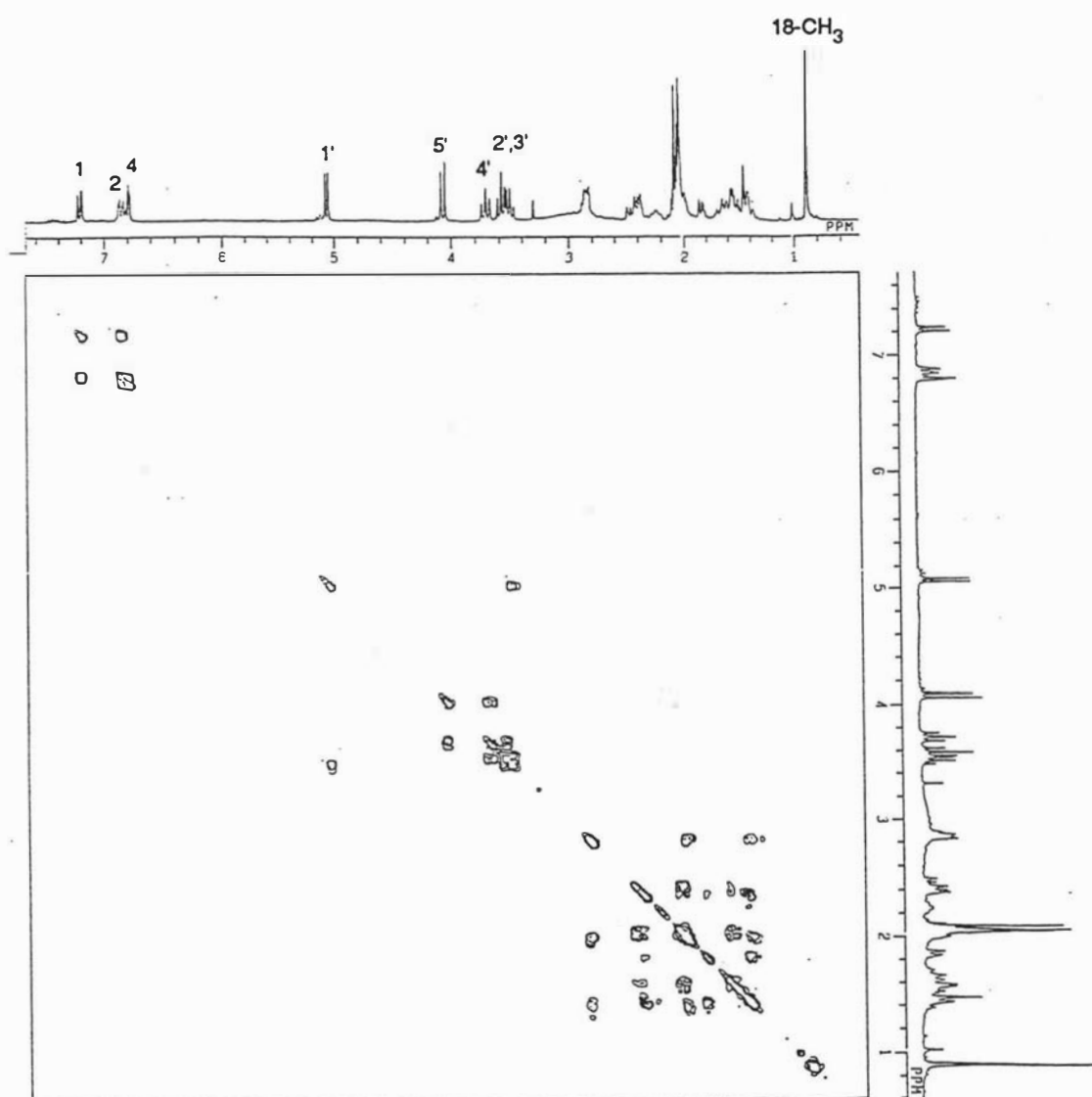
Figure 25. ^{1}H-^{1}H 2D-COSY spectrum of estrone 3-glucuronide (E1G) **12**
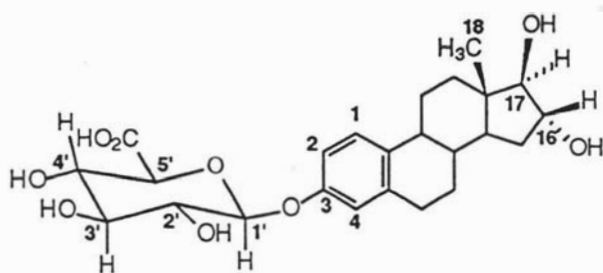
Estriol 3-glucuronide (E3-3G) **13**
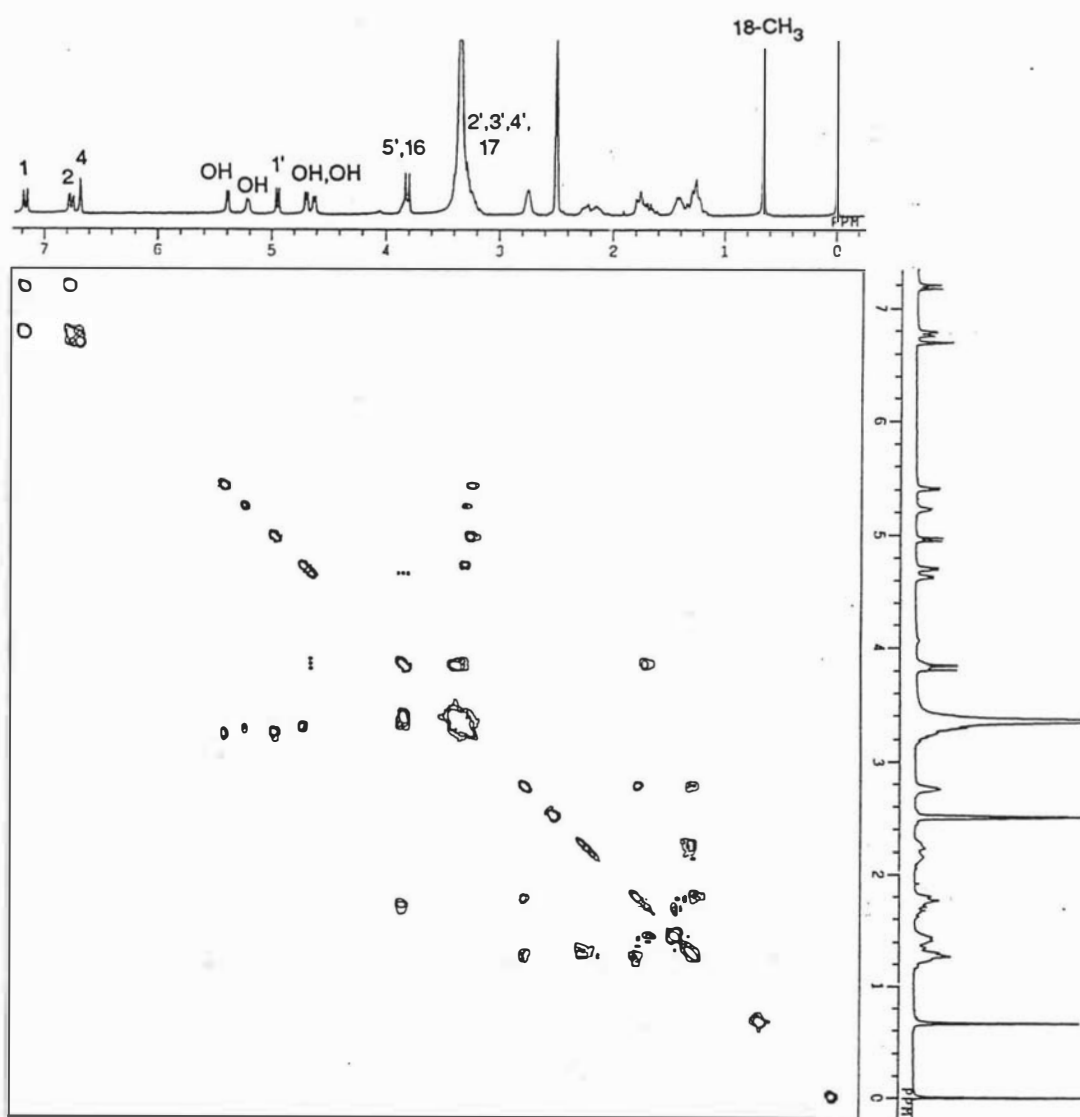
Figure 26. ¹H-¹H 2D-COSY spectrum of estriol 3-glucuronide (E3-3G) **13**
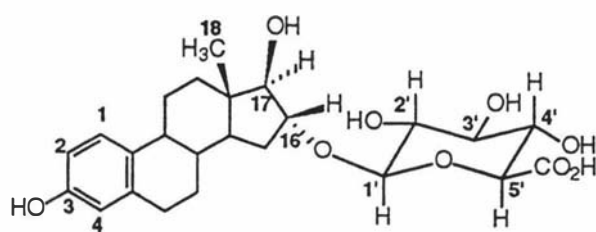
Estriol 16α-glucuronide (E3-16G) **14**
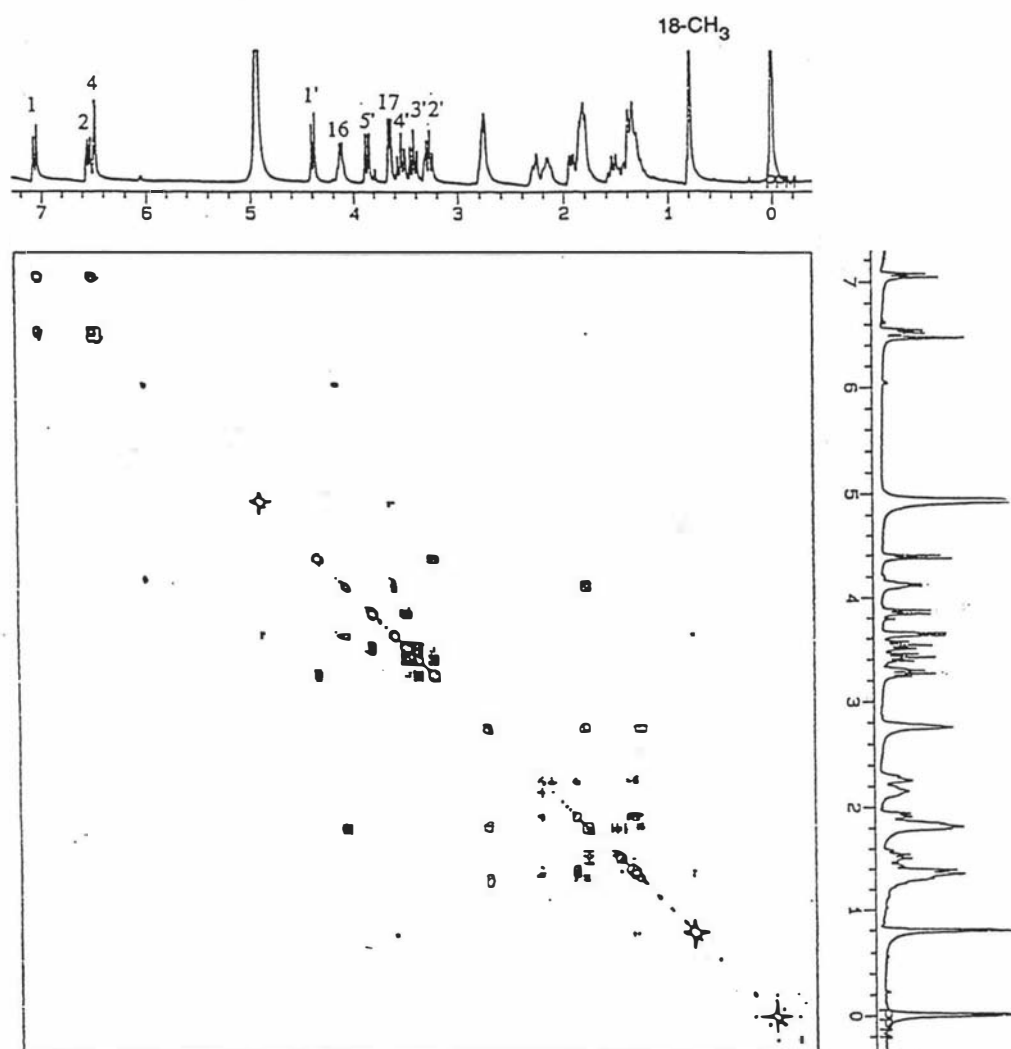
Figure 27. ^{1}H-^{1}H 2D-COSY spectrum of estriol 16α-glucuronide (E3-16G) **14**

Estriol 16β-glucuronide (E3-16G) **15**

estriol 17β-glucuronide (E3-17-G)
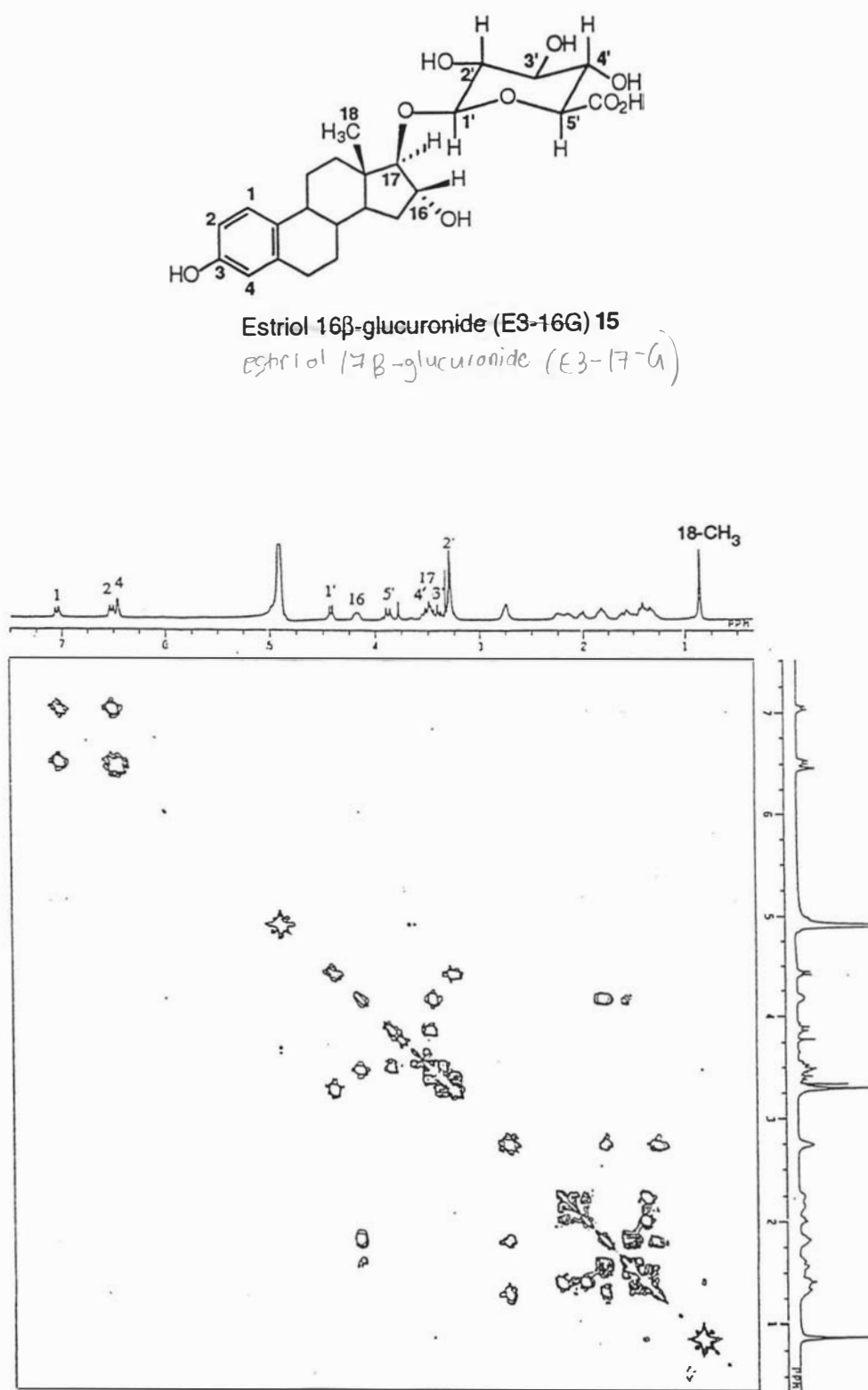
Figure 28. ¹H-¹H 2D-COSY spectrum of estriol 17β-glucuronide (E3-17G) **15**
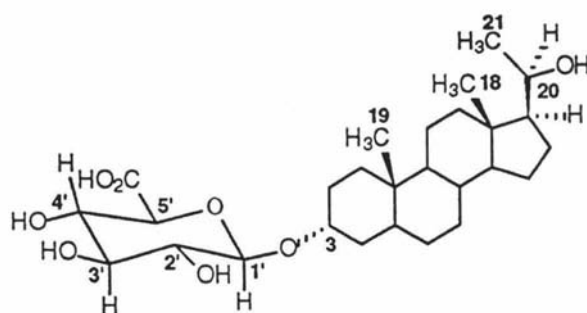
Pregnanediol 3-glucuronide (PdG) **16**
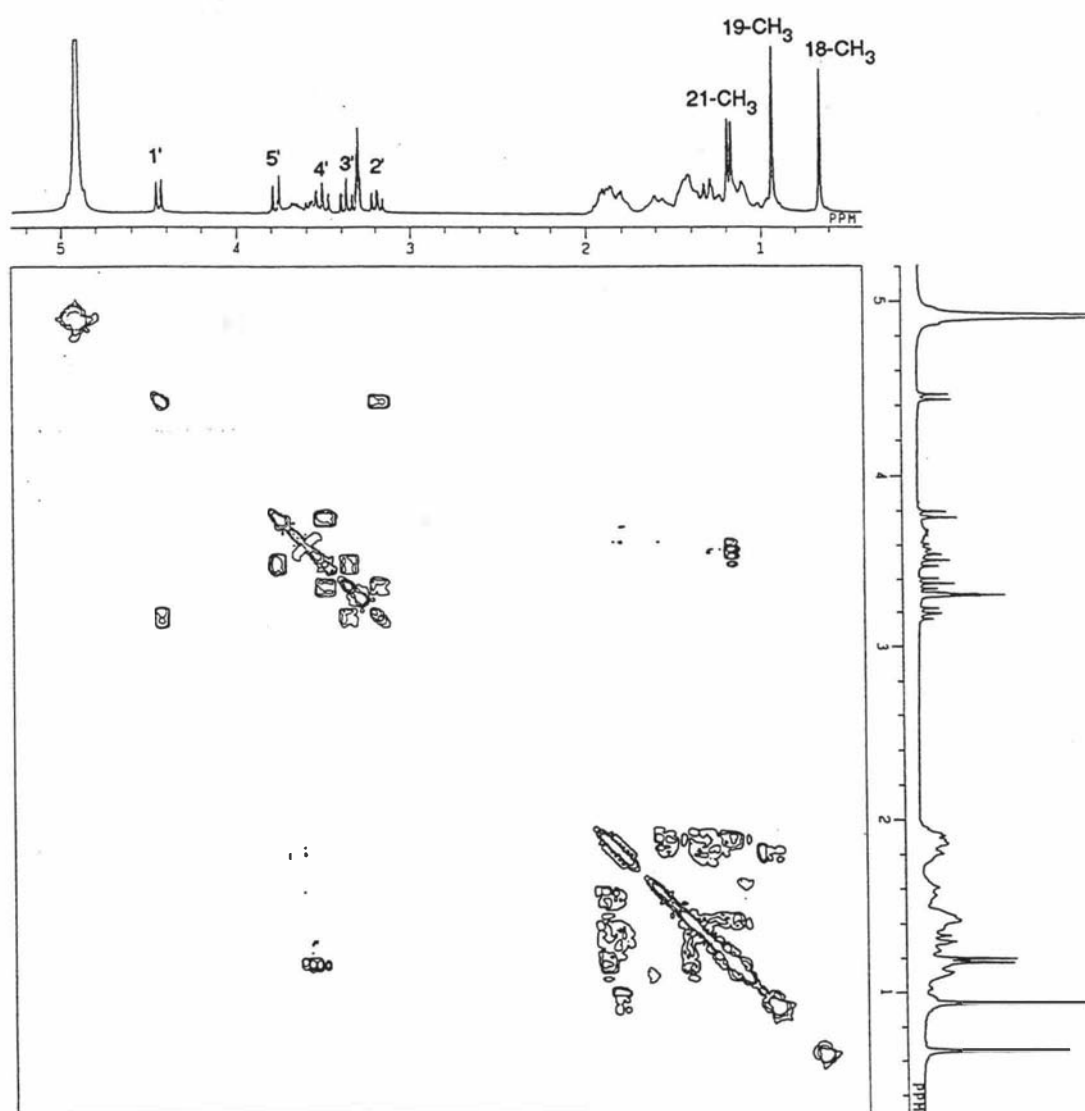
Figure 29. ¹H-¹H 2D-COSY spectrum of pregnanediol 3-glucuronide (PdG) **16**

For all the other steroid glucuronides **12-13**, **15-16**, the procedure for assignment of the three aromatic protons of the steroid A ring, the 1'- to 5'-protons of the glucuronic acid moiety and the 16β- and 17α-protons were made on a similar basis to the above assignment. For example, in the 2D-COSY spectrum of estrone 3-glucuronide **12** (Figure 25), two correlated aromatic protons (1-H and 2-H) appeared at 7.20 and 6.85 ppm respectively, while the aromatic 4-proton occured at 6.80 ppm as a singlet. The correlations of 1'-H (5.06 ppm) with 2'-H (3.61 ppm), 3'-H (3.61 ppm) with 4'-H (3.71 ppm), and 4'-H with 5'-H (4.06 ppm) were obvious in the spectrum. The large coupling constant (J, 7.32 Hz) of the 1'-proton with the 2'-proton also showed that the linkage of glucuronide to the estriol was β. The correlation of 2'-H and 3'-H was hidden due to both protons appearing at the same position (3.61 ppm). The 18-methyl group appeared as a singlet at 0.89 ppm (Figure 25).

For estriol 3-glucuronide **13**, the three aromatic protons showed the same correlation and similar chemical shift values as for **12**, which occured at 7.19 ppm (1-H), 6.77 ppm (2-H) and 6.70 ppm (4-H). Although the 2'-, 3'-, 4'-protons of the glucuronic acid ring and the 17α-proton appeared at the same chemical shift position (3.21 ppm), and the 5'-proton was covered by the 16β-proton at 3.81 ppm, the correlations of 1'-H (4.95 ppm) with 2'-H (3.21 ppm), 4'-H (3.21 ppm) with 5'-H (3.81 ppm) and 16β-H (3.81 ppm) with 17α-H (3.21 ppm) were all apparent in the spectrum (Figure 26). The large coupling constant (J, 7.33 Hz) for 1'-H and 2'-H confirmed the β-linkage of the steroid glucuronide. The fact that all four sugar OH groups disappeared after addition of D_2O into the sample in DMSO and resulted in only one doublet being present in the range of 4 ~ 5 ppm, corresponding to the 1'-proton, was also helpful in confirming the assignment of the 1'-proton of the glucuronide ring (Figure 26).

In the case of estriol 17β-glucuronide **15**, the chemical shift positions of the three aromatic protons (1-, 2- and 4-H) and the 18-CH_3 group were similar to those of the other steroid glucuronides (Figure 28). The assignment of 1'-H to 5'-H was also based on a variety of correlations of 1'-H (4.43 ppm) with 2'-H (3.30 ppm), 2'-H with 3'-H (3.41 ppm), 3'-H with 4'-H (3.54 ppm), and 4'-H with 5'-H (3.88 ppm). The β-linkage of the glucuronide to estriol was also shown by the large coupling constant ($J_{1',2'}$ = 7.69 Hz). Both the 16β- and 17α-protons in the 17β-glucuronide **15** revealed that these two protons were correlated and were assigned to the resonance at 3.48 ppm (17α-H, doublet) and 4.18 ppm (16β-H, multiplet) respectively (Figure 28).

In the 2D-COSY spectrum of PdG **16** (Figure 29), there were no aromatic protons. The five protons (1'-H to 5'-H) of the glucuronic acid ring were established again on the basis of following correlations: 1'-H (doublet, 4.44 ppm) with 2'-H (triplet, 3.19 ppm); 2'-H with 3'-H (triplet, 3.37 ppm); 3'-H with 4'-H (triplet, 3.51 ppm); 4'-H with 5'-H (doublet, 3.77 ppm). The large coupling constant ($J_{1',2'}$ = 7.69 Hz) showed the β-linkage between glucuronide ring and steroid moiety. The 18- and 19-CH_3 group of the steroid appeared as singlets at 0.66 and 0.94 ppm, respectively, and both methyl groups had no correlations with the other protons. However, the 21-CH_3 group occured as a doublet at 1.18 ppm due to its splitting by the 20-proton (Figure 29).

Comparing the ^{1}H-NMR spectra of these steroid glucuronides, all the protons from the carbohydrate moiety showed very similar chemical shift positions for the aryl glucuronides **12, 13** and for the steroidal alicyclic glucuronides **14, 15, 16**. The main difference between the aryl and alicyclic glucuronides was reflected in the anomeric-proton (1'-H) of the aryl glucuronides **12, 13** which had higher chemical shift values than those of the alicyclic glucuronides **14, 15, 16**. The reason probably can be attributed to the decreased electron density of the anomeric carbon (1'-C) by electron withdrawal through conjugation in the aryl glucuronides **12** and **13**.

It is important to identify the exact conjugation position of the glucuronide ring to estriol for steroid compounds such as estriol 16- or 17-glucuronide. However, there were only small differences in the ^{1}H-NMR chemical shift values between the estriol 16- and 17-glucuronides **14, 15**. Compared with the 16α-glucuronide **14**, the 17α-proton in the 17β-glucuronide **15** was shifted upfield by about 0.2 ppm (from 3.64 to 3.48 ppm). In the 16α-glucuronide **14**, the 17α-proton was observed as a doublet situated downfield of the sugar 4'-H position, but in the 17β-glucuronide, the 17α-proton doublet was upfield of the sugar 4'-H position (triplet) and covered one of the three peaks arising from the 4'-proton (Figure 30). These chemical shift values are in good agreement with those reported for the 16α- and 17β-glucuronides of 2,3-protected 2-hydroxyestriol.[62] The other differences between the two isomers were that the position of the 16β-H, 18-CH_3, 1'-H and 5'-H signals were shifted downfield by nearly 0.1 ppm in the 17β-isomer **15** compared with the 16α-isomer **14**.
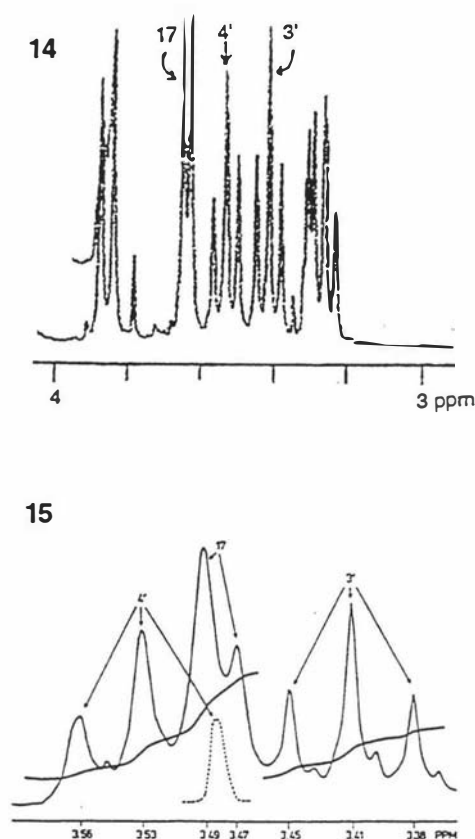
Figure 30. Comparison of two ^{1}H NMR spectra of estriol 16- and 17-glucuronides (**14, 15**) in the chemical shift ranges of 3 to 4 ppm.

Another important observation made from the 2D-NOESY spectra for all the estriol 16- and 17-glucuronide derivatives was the cross correlation of the 17α-proton with the anomeric proton (1'-H) of the sugar ring which only occurred in the 17β-glucuronide derivatives. For example, in the 2D-NOESY spectrum of estriol 17-glucuronide derivatives, the 17α-proton (3.34 ppm in both compounds **112** and **115**) always showed a cross correlation with the 1'-proton (assigned to 4.59 ppm in **112** and 4.60 ppm in **115**) of the sugar ring (Figure 32). The cross correlation between the 17α-proton of the steroid moiety and the 1'-proton of sugar ring resulted from the closeness of these two protons in space, which was further confirmed by the X-ray crystal analysis of compound **112** (Section 3.3.3). However, no cross correlations were observed for any of the 16α-glucuronide derivatives between the 17α- or 16β-proton and the protons of the glucuronide ring (Figure 31). This difference also provides a very useful indicator for distinguishing between the estriol 16- and 17-glucuronide derivatives.
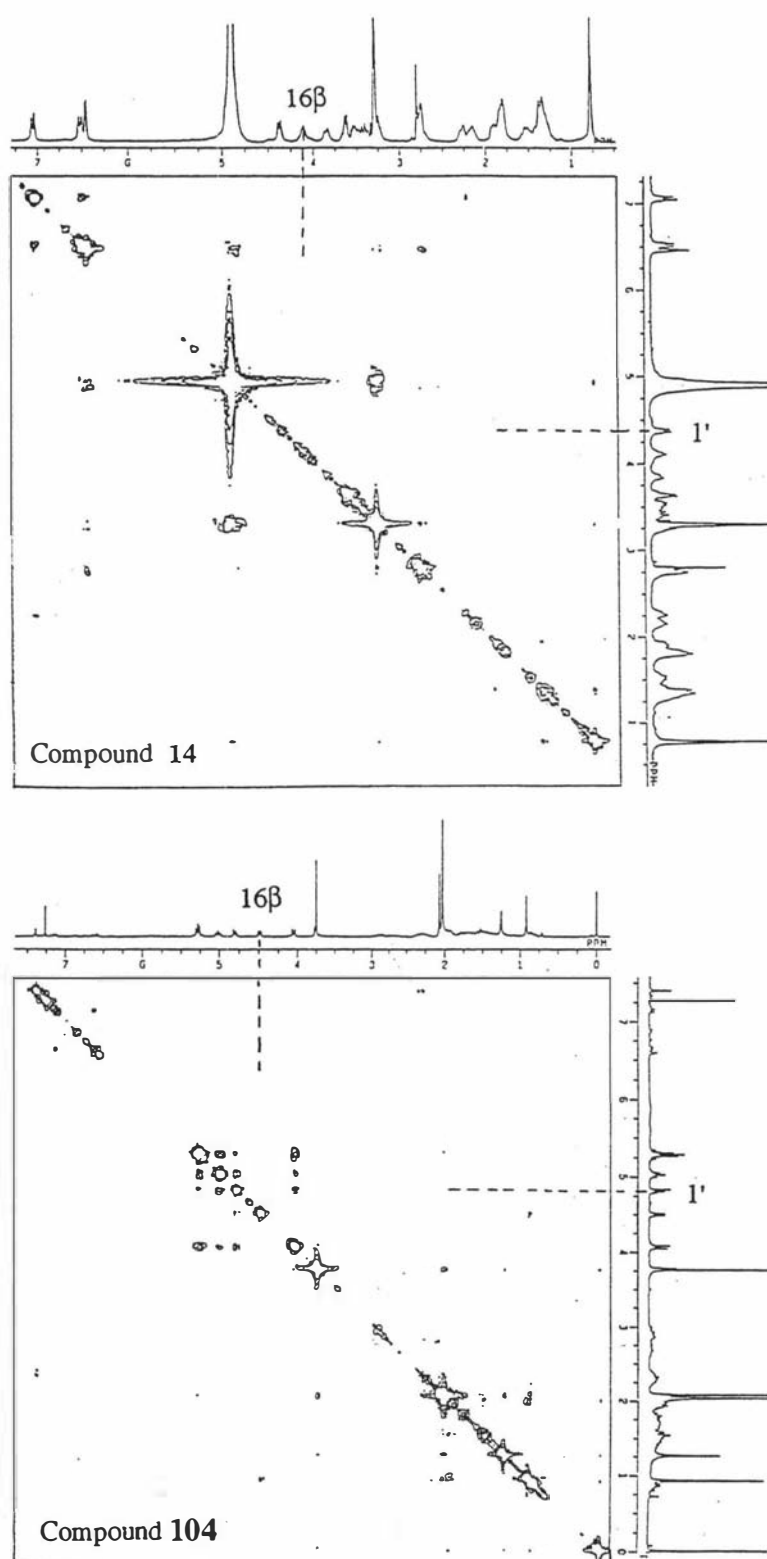
Figure 31. 2D-NOESY spectra of estriol 16α-glucuronide derivatives (**14** and **104**) showing no cross correlations between the 16β- or 17α-proton and the protons of the glucuronide ring.
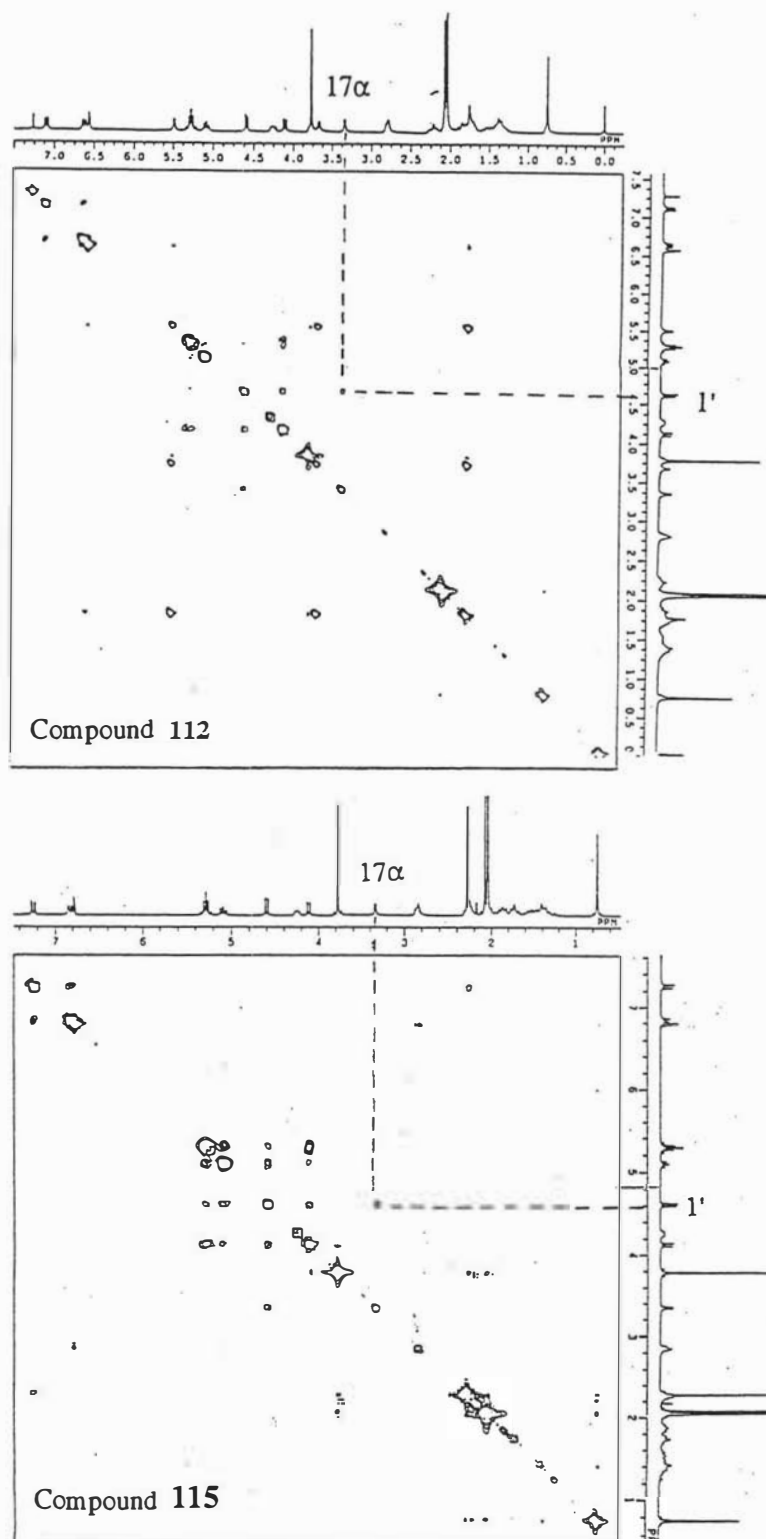
Figure 32. 2D-NOESY spectra of estriol 17β-glucuronide derivatives (**112** and **115**) showing the correlations of the 17α-proton from the estriol moiety with the anomeric proton (1'-H) of the glucuronide ring.

From the above discussion, it can be seen that there were only small differences in the proton NMR chemical shift values between the estriol 16- and 17-glucuronides **14, 15**. Also, the coupling constants between the 17α- and 16β-protons for all of the estriol 16- and 17-glucuronide derivatives were similar (Table 2, Section 3.3.2). Hence, it was necessary to characterise the estriol 16- and 17-glucuronide derivatives by ^{13}C NMR analysis since carbon-13 chemical shifts are much more sensitive to the configuration or conformational changes of the different steroids than the proton chemical shifts.[132] Also, larger differences in the ^{13}C chemical shift patterns in different steroid glucuronides should be expected in theory.[133] Although the stereochemistry of all the estriol 16α- or 17β-glucuronide derivatives are regarded as known since the synthesis started from the 16α-silylether of estriol,[117] the following ^{13}C NMR investigation was carried out to establish the general spectroscopic differences between the estriol 16α- and 17β-glucuronide derivatives.

3.3.2 Glycosidic linkage-induced chemical shifts for C-16 and C-17 from ^{13}C NMR[133]

The structures of the compounds with known stereochemistry at carbon 16 and 17 are given in Table 2. Compounds (**14, 15, 110, 112, 114** and **115**) were synthesised from estriol (scheme 21)[117] and compounds (**103, 104**) were prepared from estrone (scheme 20).[61] The ^{13}C NMR chemical shifts of estriol **10**, estradiol-17β **9** and compound **129** were taken as a basis for comparison.

Since all of the chemical shift values for the three aromatic protons (1-, 2- and 4-H of the A ring), the 16- and 17-protons, the 18-CH$_3$ group and the 1'- to 5'-protons of the glucuronide ring were accurately assigned by 2D-COSY analysis (Figures 25-29), the ^{13}C-^{1}H HETCOR technique was used to assign the corresponding ^{13}C chemical shifts. In the ^{13}C-^{1}H HETCOR spectra, every proton could be correlated with the related carbon atom to which it is bonded, to determine the associated carbon chemical shift values of the steroid glucuronides. Therefore, carbon atoms from the estriol skeleton (C-1, 2, 4, 16, 17 and 18) and carbon atoms from the carbohydrate moiety (C-1', 2', 3', 4' and 5') were assigned unambiguously by ^{13}C-^{1}H HETCOR analysis. Figures 33 and 34 give examples of the ^{13}C-^{1}H HETCOR spectra for the estriol 16α- and 17β-glucuronides.

Table 2. The Structures of Estriol Monoglucuronide Derivatives
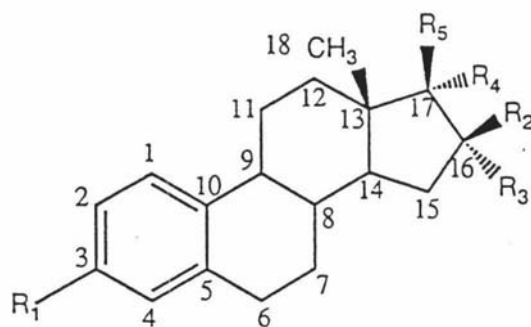
Compound	R_1	R_2	R_3	R_4	R_5	$J (H_{16}-H_{17})$[117](Hz)
112	OH	H	OH	H	OG'	5.22
15	OH	H	OH	H	OG	4.76
115	$OCOCH_3$	H	OH	H	OG'	5.13
114	$OCOCH_3$	H	OS	H	OG'	5.5
103	OH	H	OG'	H	OH	5.13
14	OH	H	OG	H	OH	5.49
110	$OCOCH_3$	H	OG'	H	$OCOCH_3$	-----
104	OH	H	OG'	OH	H	4.39
10	OH	H	OH	H	OH	6.0[61]
9	OH	H	H	H	OH	-----
129	OH	H	H	H	CH_2OH	-----
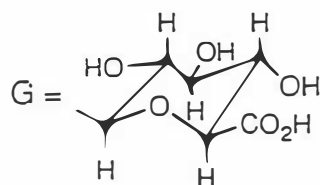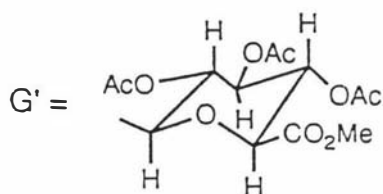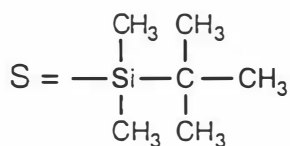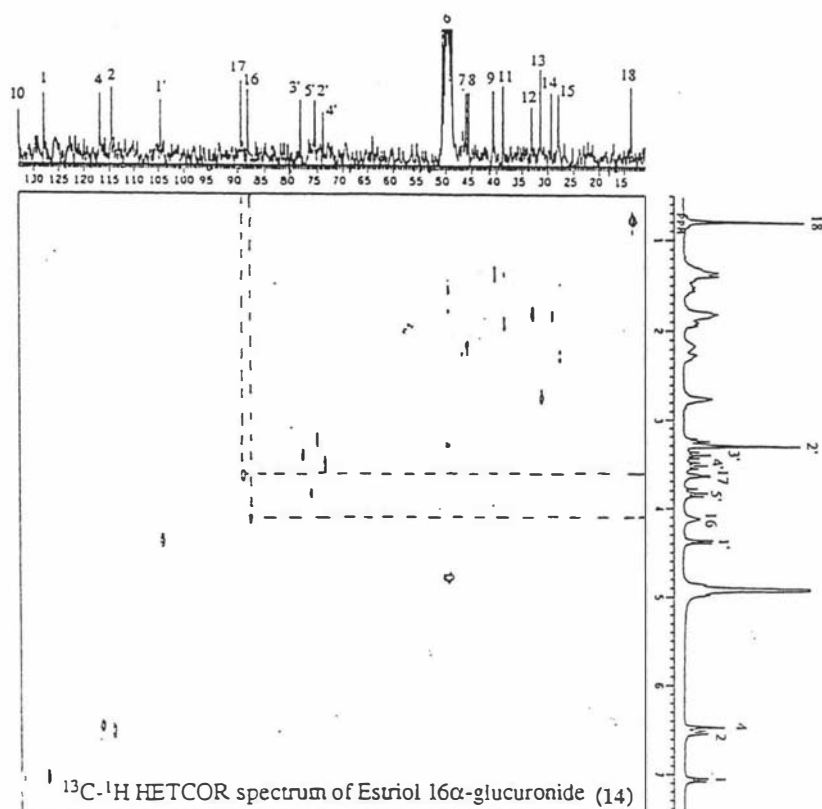
Figure 33. ^{13}C-^{1}H HETCOR spectrum of estriol 16α-glucuronide **14** establishing the chemical shift positions for carbon atoms C-1, 2, 4, 16, 17, 18 and C-1' to C-5' of glucuronic acid, and showing the small difference (1.09 ppm) in ^{13}C chemical shifts between C-16 and C-17.
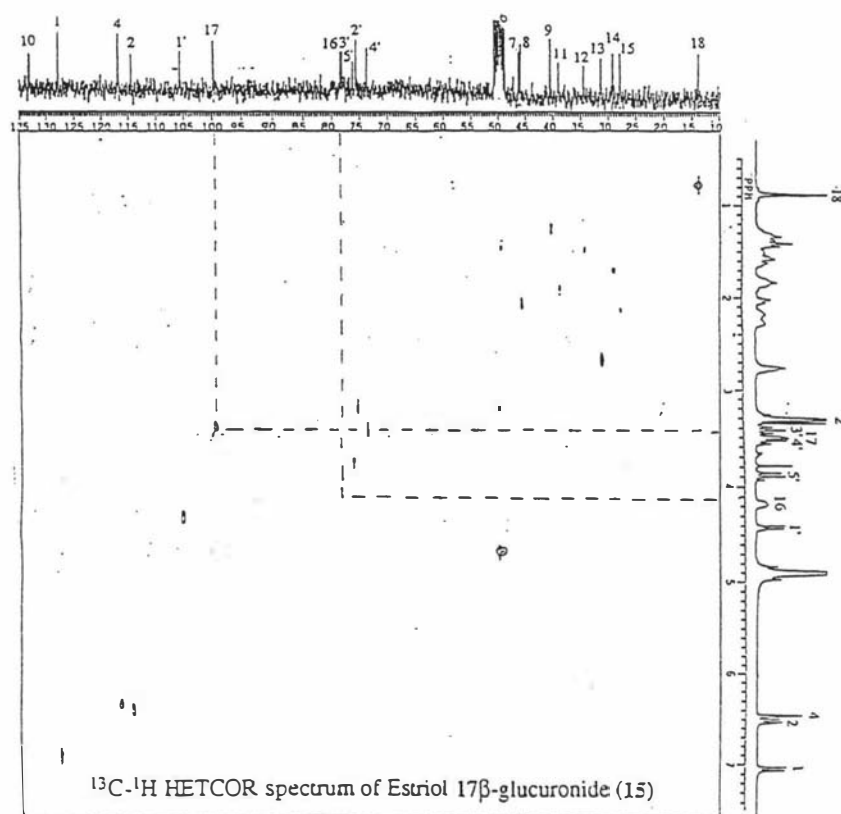
Figure 34. ^{13}C-^{1}H HETCOR spectrum of estriol 17β-glucuronide **15** establishing the chemical shift positions for carbon atoms C-1, 2, 4, 16, 17, 18 and C-1' to C-5' of glucuronic acid, and showing the large difference (21.22 ppm) in ^{13}C chemical shifts between C-16 and C-17.

In the ^{13}C-^1H HETCOR spectrum of estriol 16α-glucuronide **14** (Figure 33), three aromatic carbon atoms were assigned from the following correlations: C-1 (127.9 ppm) with 1-H (7.19 ppm), C-2 (114.5 ppm) with 2-H (6.85 ppm), and C-4 (116.8 ppm) with 4-H (6.80 ppm). Carbon-18 (13.72 ppm) was also correlated with the 18-CH_3 group (0.79 ppm). The correlations of C-1' to C-5' of the glucuronic acid ring with the related 1'- to 5'-protons were all clearly recognisable in the spectrum, i.e. C-1' (104.7 ppm)/1'-H (4.38 ppm), C-2' (75.63 ppm)/2'-H (3.27 ppm), C-3' (78.42 ppm)/3'-H (3.42 ppm), C-4' (74.02 ppm)/4'-H (3.53 ppm), and C-5' (76.41 ppm)/5'-H (3.86 ppm). The identification of C-16 (88.39 ppm) and C-17 (89.48 ppm) was also based on their correlation with the 16β-proton (4.11 ppm) and 17α-proton (3.63 ppm) respectively. The difference in chemical shift values between C-16 and C-17 was only 1.09 ppm (Figure 33).

For estriol 17β-glucuronide **15**, the process of assignment of all three aromatic carbon atoms, C-16, 17, 18, and C-1' to C-5' of the glucuronic acid moiety was essentially the same as the above procedure for estriol 16α-glucuronide. Their correlations and assignments are clearly shown in Figure 34, i.e. C-1 (127.9 ppm)/1-H (7.06 ppm), C-2 (114.5 ppm)/2-H (6.52 ppm), C-4 (121.6 ppm)/4-H (6.46 ppm), C-1' (105.6 ppm)/1'-H (4.43 ppm), C-2' (75.69 ppm)/2'-H (3.30 ppm), C-3' (78.40 ppm)/3'-H (3.41 ppm), C-4' (73.79 ppm)/4'-H (3.54 ppm), C-5' (76.32 ppm)/5'-H (3.88 ppm), C-16 (78.60 ppm)/16β-H (4.18 ppm), C-17 (99.82 ppm)/17α-H (3.48 ppm), C-18 (13.95 ppm)/0.87 ppm). The difference in chemical shift values between C-16 and C-17 in compound **15** was 21.22 ppm (Figure 34).

For all the other estriol 16- and 17-glucuronide derivatives, the determination of the above carbon atoms was made on exactly the same basis as for compounds **14** and **15**. The assignment of the remainder of the carbon atoms of the estriol glucuronide derivatives were made by comparison of their ^{13}C-NMR spectra with those of similar derivatives reported in the literature.[127,134] The chemical shifts observed showed good agreement with literature values. The complete list of ^{13}C-NMR chemical shift values is given in Table 3.

Table 3: ^{13}C NMR Chemical Shift Values (ppm) of Steroid Compounds

C	Compounds
	112	15	115	114	103	14	110	104	10
1	126.7	127.9	126.2	121.6	127.9	127.9	126.3	126.5	127.9
2	112.7	114.5	118.6	----	114.5	114.5	118.6	112.7	114.5
3	153.6	156.7	----	----	156.8	156.7	148.4	153.5	156.8
4	115.3	116.8	121.6	118.7	116.8	116.8	121.5	115.2	116.9
5	138.1	139.5	148.5	138.2	----	139.5	137.9	138.1	139.6
6	47.54	----	47.63	47.52	----	----	47.86	----	----
7	44.03	46.29	44.03	----	46.00	46.06	44.49	46.19	46.14
8	43.77	45.94	44.03	43.63	45.65	45.60	43.63	43.37	45.83
9	37.98	40.59	37.64	37.78	40.64	40.70	37.69	38.62	40.82
10	132.1	133.2	138.2	121.6	133.1	133.2	137.5	132.6	133.3
11	36.77	39.03	36.77	34.35	39.66	38.80	38.89	31.88	38.83
12	32.22	34.54	32.31	----	38.68	33.30	31.39	31.01	35.72
13	29.49	31.10	29.40	26.90	31.40	31.43	29.31	29.63	31.46
14	27.01	29.24	26.90	25.89	29.38	29.35	26.89	27.99	29.35
15	25.74	27.89	25.57	25.72	27.94	27.97	25.60	25.66	28.00
16	76.60	78.60	75.99	76.30	88.68	88.39	84.43	83.50	79.55
17	100.2	99.82	100.3	96.67	89.14	89.48	87.22	78.67	91.41
18	12.64	13.95	12.64	12.61	13.66	13.72	12.99	17.16	13.66
1'	101.7	105.6	101.8	100.7	101.8	104.7	100.5	100.7	----
2'	71.15	75.69	71.19	72.42	73.67	75.63	71.27	71.10	----
3'	71.96	78.40	71.96	71.73	77.27	78.42	72.02	72.00	----
4'	68.74	73.79	68.77	69.70	71.69	74.02	69.40	69.29	----
5'	71.27	76.32	71.33	73.00	74.25	76.41	72.85	73.54	----
6'	170.2	173.6	170.5	----	172.1	172.2	170.2	170.2	----
OAc	20.62	----	20.62	----	21.44	----	20.85	20.62	----
	20.62		20.62		21.29		20.62	20.62	
	20.60		20.11		21.23		20.44	20.50	
C=O	169.5	----	169.4	----	----	----	170.1	169.4	----
	169.1						169.8	169.3	
	167.0						3x169	167.0	
OCH$_3$	53.21	----	53.19	52.70	----	----	52.84	53.13	----

The principal difference between the estriol 16α- and 17β-glucuronide derivatives is clearly seen in the ^{13}C chemical shift values of carbon-16 and 17 (see Table 3). With estriol **10** as a reference, the glycosidic linkage produced a downfield shift on the carbon to which it was linked, and an upfield shift on the neighbouring carbon atom. Thus from the values of Table 3, it can be established that carbon-16 and 17 are significantly affected by the glycosidic linkage.

Introduction of a 17β-carbohydrate moiety deshielded carbon-17 with differing magnitudes for compounds (**112, 15, 115** and **114**) (8.79, 8.41, 8.80 and 5.26 ppm, respectively), whereas all the carbon-16 atoms were shielded (2.95, 0.95, 3.56 and 3.25 ppm, respectively). For the 16α-glucuronide derivatives (**103, 14, 110** and **104**), on the other hand, all of the carbon-16 atoms were deshielded (9.13, 8.84, 4.88 and 3.95 ppm, respectively) while the carbon-17 atoms were shielded (2.27, 1.93, 4.19 and 12.74 ppm, respectively). Hence, the glycosidic linkage at the C-17β-OH group caused the chemical shifts of carbon-17 to become even larger, and those of carbon-16 to become smaller, whereas the glycosidic linkage at the C-16α-OH group increased the chemical shift of carbon-16 significantly, while those of carbon-17 decreased. Since carbon-17 is downfield of carbon-16 in estriol, the overall substituent effect caused relatively large differences (over 20 ppm) to the chemical shifts between carbon-16 and 17 for the estriol 17β-glucuronide derivatives (Figure 34), and very small differences (less than 5 ppm) for all the estriol 16α-glucuronide derivatives (Figure 33). This difference is obvious in the figures (Table 3). This major difference is thus diagnostic in distinguishing between the estriol 16- and 17 glucuronide derivatives. It is also noted that for all of the *trans*-compounds (16β-H,17α-H) (**103, 14** and **110**), the chemical shift values of carbon-17 were larger than those of carbon-16, but for the only *cis*-compound **104** (16β-H, 17β-H) in the series this difference was reversed (C-16 > C-17). Thus, inspection of these data is useful in identifying *cis* or *trans* isomers as well as the position of attachment of the glucuronides in the D-ring.

3.3.3 X-ray structural analysis of estriol glucuronide derivative 112[133]

The molecular structure of **112**, as determined by X-ray crystallography,[135] using the numbering system is shown in Figure 35, Atomic coordinates and selected bond distances and angles are given in Tables 4 and 5 respectively. The structure clearly confirms that the stereochemistry at carbon 17 is the β configuration as anticipated from the synthetic route adopted and as indicated by the 2D-NOESY spectrum of the 17β-glucuronide derivatives.
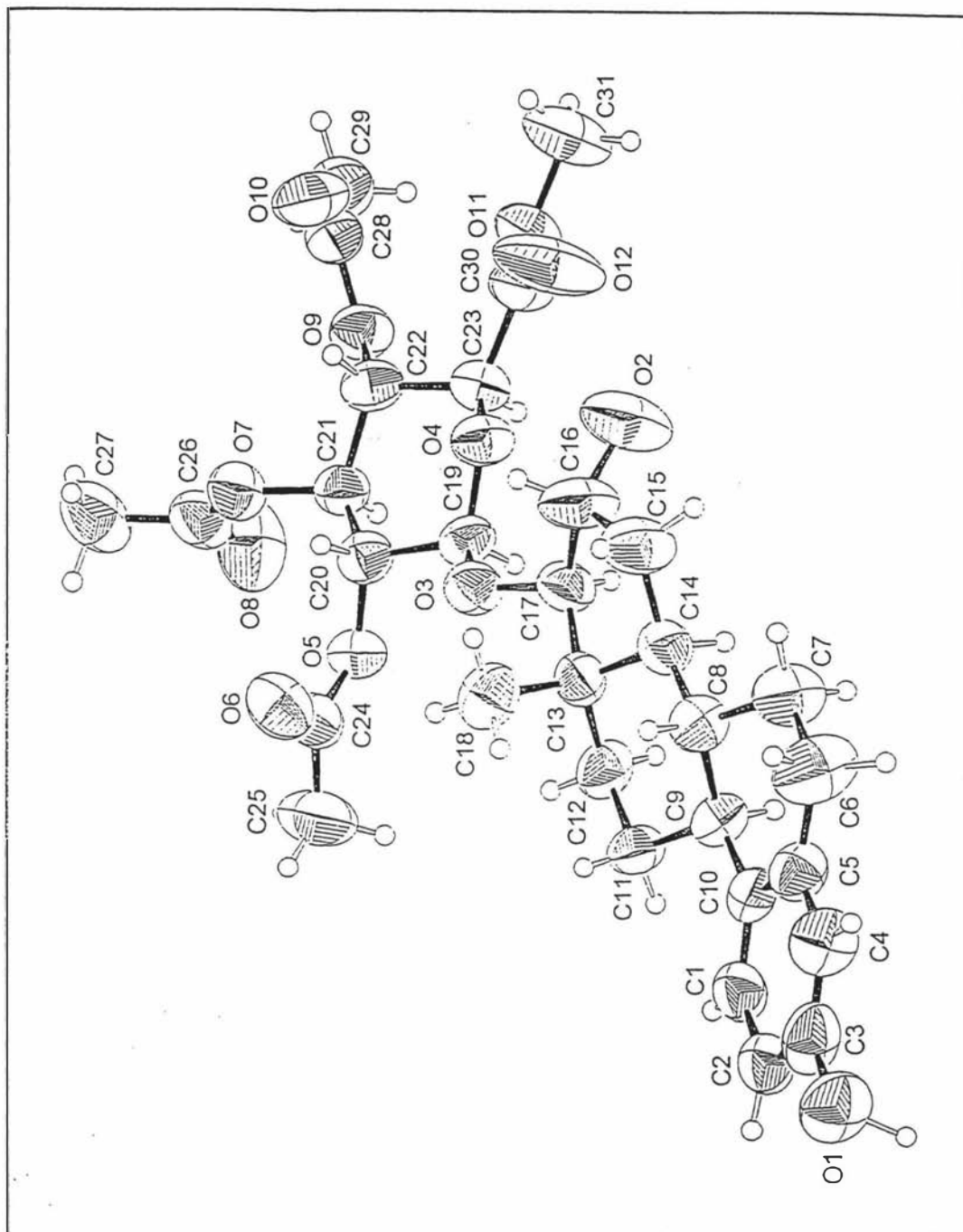
Figure 35. Zortep[135] diagram of $C_{31}H_{40}O_{12} \cdot H_2O$ (**112**) showing the numbering system. Hydrogen atoms are labelled according to the atoms to which they are attached. Thermal ellipsoids have been drawn at the 50% probability levels except for hydrogens where arbitrary levels have been used.

Table 4

Atom Coordinates for $C_{31}H_{40}O_{12} \cdot H_2O$ (**112**)

Atom	X / a	Y / b	Z / c
O (1)	0.2535 (5)	0.2512 (5)	-0.1102 (4)
O (2)	-0.0169 (5)	-0.5043 (5)	-0.1433 (6)
O (3)	-0.2133 (4)	-0.3658 (4)	-0.1642 (4)
O (4)	-0.2271 (4)	-0.5254 (4)	-0.1459 (3)
O (5)	-0.4204 (4)	-0.3478 (4)	-0.1328 (3)
O (6)	-0.3895 (6)	-0.2595 (5)	-0.2410 (5)
O (7)	-0.5146 (4)	-0.5174 (4)	-0.1964 (3)
O (8)	-0.6212 (5)	-0.5083 (8)	-0.0983 (5)
O (9)	-0.4355 (4)	-0.6839 (4)	-0.1224 (4)
O (10)	-0.3871 (6)	-0.7849 (5)	-0.2183 (5)
O (11)	-0.2526 (5)	-0.7615 (4)	-0.0791 (4)
O (12)	-0.1356 (6)	-0.6876 (5)	-0.1439 (8)
O (13)	-0.1538 (9)	-0.0764 (8)	-0.4303 (7)
O (14)	-0.3158 (51)	-0.0480 (40)	0.0145(36)
C (1)	0.0608 (7)	0.0813 (6)	-0.0663 (6)
C (2)	0.1093 (7)	0.1676 (7)	-0.0745 (6)
C (3)	0.2043 (8)	0.1674 (8)	-0.0994 (6)
C (4)	0.2453 (8)	0.0808 (8)	-0.1189 (6)
C (5)	0.1977 (6)	-0.0050 (7)	-0.1098 (5)
C (6)	0.2496 (7)	-0.0947 (8)	-0.1333 (9)
C (7)	0.1931 (7)	-0.1863 (7)	-0.1191 (7)
C (8)	0.0879 (6)	-0.1736 (6)	-0.1357 (5)
C (9)	0.0449 (6)	-0.0985 (5)	-0.0786 (5)
C (10)	0.1016 (6)	-0.0058 (6)	-0.0858 (4)
C (11)	-0.0653 (6)	-0.0862 (6)	-0.0877 (6)
C (12)	-0.1195 (6)	-0.1818 (7)	-0.0833 (6)
C (13)	-0.0808 (6)	-0.2507 (6)	-0.1430 (5)
C (14)	0.0280 (6)	-0.2661 (6)	-0.1291 (6)
C (15)	0.0538 (7)	-0.3519 (7)	-0.1814 (8)
C (16)	-0.0393 (8)	-0.4148 (6)	-0.1784 (8)
C (17)	-0.1147 (6)	-0.3555 (6)	-0.1344 (6)
C (18)	-0.1048 (7)	-0.2157 (7)	-0.2276 (5)
C (1')	-0.2698 (7)	-0.4354 (6)	-0.1288 (5)
C (2')	-0.3709 (6)	-0.4296 (6)	-0.1631 (5)
C (3')	-0.4319 (6)	-0.5160 (6)	-0.1438 (5)
C (4')	-0.3770 (6)	-0.6096 (5)	-0.1544 (5)
C (5')	-0.2794 (6)	-0.6013 (5)	-0.1097 (5)
C (6')	-0.2125 (7)	-0.6882 (6)	-0.1165 (6)
C (7')	-0.4218 (7)	-0.2680 (6)	-0.1778 (7)
C (8')	-0.4755 (11)	-0.1908 (7)	-0.1315 (9)
C (9')	-0.6060 (7)	-0.5137 (7)	-0.1662 (8)
C (10')	-0.6794 (7)	-0.5148 (8)	-0.2262 (8)
C (11')	-0.4297 (8)	-0.7712 (7)	-0.1593 (7)
C (12')	-0.4851 (9)	-0.8436 (7)	-0.1115 (8)

Table 5

Selected Bond Distances (Å) and Angles (^{o}) for $C_{31}H_{40}O_{12} \cdot H_2O$ (**112**)

Bond Distances

C(1)-C(2)	1.38 (1)	O(3)-C(17)	1.45 (1)
C(1)-C(10)	1.38 (1)	O(3)-C(1')	1.38 (1)
C(2)-C(3)	1.37 (1)	O(4)-C(1')	1.42 (1)
C(3)-C(4)	1.37 (2)	O(4)-C(5')	1.42 (1)
C(4)-C(5)	1.37 (1)	O(5)-C(2')	1.43 (1)
C(5)-C(6)	1.49 (1)	O(5)-C(7')	1.35 (1)
C(5)-C(10)	1.38 (1)	O(6)-C(7')	1.17 (1)
C(6)-C(7)	1.52 (1)	O(7)-C(3')	1.45 (1)
C(7)-C(8)	1.48 (1)	O(7)-C(9')	1.35 (1)
C(8)-C(9)	1.55 (1)	O(8)-C(9')	1.18 (1)
C(8)-C(14)	1.54 (1)	O(9)-C(4')	1.42 (1)
C(9)-C(10)	1.52 (1)	O(9)-C(11')	1.37 (1)
C(9)-C(11)	1.53 (1)	O(10)-C(11')	1.18 (1)
C(11)-C(12)	1.53 (1)	O(11)-C(6')	1.32 (1)
C(12)-C(13)	1.50 (1)	O(11)-C(13')	1.44 (1)
C(13)-C(14)	1.53 (1)	O(12)-C(13')	1.15 (1)
C(13)-C(17)	1.54 (1)	C(1')-C(2')	1.51 (1)
C(13)-C(18)	1.56 (1)	C(2')-C(3')	1.50 (1)
C(14)-C(15)	1.53 (1)	C(3')-C(4')	1.52 (1)
C(15)-C(16)	1.55 (1)	C(4')-C(5')	1.54 (1)
C(16)-C(17)	1.52 (1)	C(7')-C(8')	1.53 (2)
O(1)-C(3)	1.36 (1)	C(9')-C(10')	1.43 (1)
O(2)-C(16)	1.42 (1)	C(11')-C(12')	1.40 (2)

Table 5 (continued)

Bond Angles

C(2)-C(1)-C(10)	123.3(0.9)	C(13)-C(17)-O(3)	109.9(0.6)
C(1)-C(2)-C(3)	119.1(1.0)	C(16)-C(17)-O(3)	114.0(8)
C(2)-C(3)-C(4)	117.7(0.9)	C(17)-O(3)-C(1')	116.0(0.7)
C(2)-C(3)-O(1)	120.7(1.1)	C(1')-O(4)-C(5')	111.3(0.6)
O(1)-C(3)-O(4)	121.4(1.0)	O(3)-C(1')-C(2')	108.0(0.7)
C(3)-C(4)-C(5)	123.1(0.9)	O(3)-C(1')-O(4)	107.6(0.6)
C(4)-C(5)-C(6)	118.4(0.8)	O(4)-C(1')-C(2')	110.3(0.6)
C(4)-C(5)-C(10)	119.6(0.9)	C(1')-C(2')-C(3')	112.6(0.7)
C(6)-C(5)-C(10)	121.8(0.8)	C(1')-C(2')-O(5)	109.9(0.7)
C(5)-C(6)-C(7)	114.9(0.8)	C(3')-C(2')-O(5)	107.4(0.6)
C(6)-C(7)-C(8)	111.5(0.9)	C(2')-C(3')-C(4')	112.8(0.6)
C(7)-C(8)-C(9)	109.5(0.7)	C(2')-C(3')-O(7)	108.2(0.6)
C(7)-C(8)-C(14)	114.0(0.8)	C(4')-C(3')-O(7)	107.7(0.6)
C(9)-C(8)-C(14)	108.7(0.6)	C(3')-C(4')-C(5')	107.8(0.6)
C(8)-C(9)-C(10)	109.4(0.6)	C(3')-C(4')-O(9)	107.6(0.6)
C(8)-C(9)-C(11)	113.0(0.7)	C(5')-C(4')-O(9)	110.8(0.7)
C(1)-C(10)-C(9)	121.7(0.7)	C(4')-C(5')-O(4)	106.2(0.6)
C(1)-C(10)-C(5)	116.9(0.8)	C(4')-C(5')-C(6')	115.1(0.7)
C(5)-C(10)-C(9)	121.4(0.8)	O(4)-C(5')-C(6')	104.8(0.7)
C(9)-C(11)-C(12)	112.2(0.7)	C(2')-O(5)-C(7')	117.5(0.7)
C(11)-C(12)-C(13)	110.8(0.7)	O(5)-C(7')-C(8')	107.2(1.0)
C(12)-C(13)-C(14)	109.4(0.7)	O(5)-C(7')-O(6)	126.9(0.9)
C(12)-C(13)-C(17)	116.0(0.7)	C(8')-C(7')-O(6)	125.9(1.0)
C(12)-C(13)-C(18)	110.6(0.7)	C(3')-O(7)-C(9')	119.4(0.7)
C(14)-C(13)-C(17)	98.4(0.7)	O(7)-C(9')-O(8)	122.6(0.9)
C(14)-C(13)-C(18)	113.3(0.7)	O(7)-C(9')-C(10')	112.2(1.0)
C(17)-C(13)-C(18)	108.8(0.7)	O(8)-C(9')-C(10')	125.1(1.0)
C(8)-C(14)-C(13)	113.1(0.7)	C(4')-O(9)-C(11')	116.1(0.7)
C(8)-C(14)-C(15)	119.3(0.7)	O(9)-C(11')-C(12')	108.6(1.0)
C(13)-C(14)-C(15)	104.3(0.7)	O(9)-C(11')-O(10)	124.3(0.9)
C(14)-C(15)-C(16)	103.5(0.7)	C(12')-C(11')-O(10)	127.0(1.0)
C(15)-C(16)-C(17)	105.5(0.7)	C(5')-C(6')-O(11)	109.2(0.8)
C(15)-C(16)-O(2)	109.5(0.9)	C(5')-C(6')-O(12)	125.1(0.9)
C(17)-C(16)-O(2)	114.7(1.0)	O(11)-C(6')-O(12)	125.4(0.9)
C(13)-C(17)-C(16)	105.4(0.7)	C(6')-O(11)-C(13')	116.3(0.8)

Table 6 (a)

Planes of "Best Fit" for $C_{31}H_{40}O_{12} \cdot H_2O$ 112

The equations are of the form $AX + BY + CZ = D$

	A	B	C	D
Plane 1	-0.2944	0.1349	-0.9641	0.9605
Plane 2	-0.3099	0.1074	-0.9447	0.9297
Plane 3	-0.3016	0.1120	-0.9468	1.5502
Plane 4	0.1290	-0.1499	-0.9802	2.7735
Plane 5	-0.3199	0.0858	-0.9436	0.9101
Plane 6	-0.0104	0.1791	-0.9838	1.1458

Table 6 (b)

Deviations of Atoms (Å) from Planes of "Best Fit" for $C_{31}H_{40}O_{12} \cdot H_2O$ 112

(Atoms defining the plane are marked with an asterisk)

Atom	Plane 1	Plane 2	Plane 3	Plane 4	Plane 5	Plane 6
C(1)		0.00(1)			-0.01(1)*	
C(2)					0.01(1)*	
C(3)					-0.01(1)*	
C(4)	0.06(1)				0.02(1)*	
C(5)	0.00*	-0.05(1)*			-0.02(1)*	
C(6)	0.00*	0.01(1)*			0.02(1)	
C(7)	-0.17(1)	-0.11(1)			-0.07(1)	
C(8)	0.54(1)	-0.62(1)	0.00(1)*	0.01(1)*	0.68(1)	
C(9)	-0.06(1)	0.00(1)*	-0.62(1)		0.04(1)	
C(10)	0.00*	0.01(1)*			0.02(1)*	
C(11)	0.55(1)	0.63(1)	0.00(1)*			
C(12)			0.00(1)*	-1.21(1)		
C(13)			0.70(1)	-0.01(1)*		
C(14)	0.50(1)	0.63(1)	0.00(1)*	-0.01(1)*		
C(15)				1.08(1)		
C(16)				1.00(1)		
C(17)				0.01(1)*		
C(1')						- 0.04(1)*
C(2')						0.56(1)
C(3')						0.03(1)*
C(4')						-0.03(1)*
C(5')						-0.77(1)
O(4)						0.02(1)*

Table 7

Selected Torsion Angles (°) for $C_{31}H_{40}O_{12} \cdot H_2O$ **112**

(The range of values reported for molecules **9**, **10** and **129** is included for comparison[136-138])

Ring A			Ring B		
Bond	**112**	Range	Bond	**112**	Range
C(1)-C(2)-C(3)-C(4)	3.2(1.1)	-0.7→1.6	C(5)-C(6)-C(7)-C(8)	37.7(1.0)	36.3→-48.0
C(2)-C(3)-C(4)-C(5)	-4.3(1.1)	-0.1→-2.3	C(6)-C(7)-C(8)-C(9)	-62.9(0.9)	-63.2→-64.9
C(3)-C(4)-C(5)-C(10)	5.2(1.1)	0.7→1.8	C(7)-C(8)-C(9)-C(10)	56.3(0.8)	51.1→59.9
C(4)-C(5)-C(10)-C(1)	-4.9(1.0)	-2.5→1.4	C(8)-C(9)-C(10)-C(5)	-26.8(.8)	-22.5→-30.8
C(5)-C(10)-C(1)-C(2)	4.2(1.0)	1.6→-0.7	C(9)-C(10)-C(5)-C(6)	2.7(0.9)	-0.6→5.8
C(10)-C(1)-C(2)-C(3)	-3.4(1.1)	1.1→-1.3	C(10)-C(5)-C(6)-C(7)	-7.2(1.1)	-6.4→-17.6

Ring C			Ring D		
Bond	**112**	Range	Bond	**112**	Range
C(8)-C(9)-C(11)-C(12)	52.2(0.7)	-52.0→56.1	C(13)-C(14)-C(15)-C(16)	-34.4(0.8)	-32.2→-36.1
C(9)-C(11)-C(12)-C(13)	-55.7(0.8)	-35.1→-55.9	C(14)-C(15)-C(16)-C(17)	7.1(0.9)	2.7→10.1
C(11)-C(12)-C(13)-C(14)	58.4(0.8)	55.7→58.3	C(15)-C(16)-C(17)-C(13)	22.3(0.9)	19.8→27.8
C(12)-C(13)-C(14)-C(8)	-60.1(0.8)	-59.8→-62.8	C(16)-C(17)-C(13)-C(14)	-42.5(0.8)	-38.0→-46.0
C(13)-C(14)-C(8)-C(9)	55.2(0.7)	57.9→60.2	C(17)-C(13)-C(14)-C(15)	47.1(0.7)	44.4→48.6
C(14)-C(8)-C(9)-C(11)	-50.8(0.7)	-51.3→-56.7			

Sugar Ring		Miscellaneous	
Bond	**112**	Bond	**112**
C(1')-C(2')-C(3')-C(4')	-44.6(0.8)	C(13)-C(17)-C(16)-O(2)	143.0(0.8)
C(2')-C(3')-C(4')-C(5')	50.9(0.7)	C(13)-C(17)-C(16)-C(15)	22.3(0.9)
C(3')-C(4')-C(5')-O(4)	-62.2(0.7)	O(3)-C(17)-C(16)-O(2)	-96.3(0.9)
C(4')-C(5')-O(4)-C(1')	70.9(0.7)	O(3)-C(17)-C(16)-C(15)	143.0(0.8)
C(5')-O(4)-C(1')-C(2')	-64.0(0.7)	H(16)-C(16)-C(17)-H(17)	137.1(1.3)
O(4)-C(1')-C(2')-C(3')	48.8(0.8)		

Ring A has the expected aromaticity with bond distances of 1.37(1)-1.38(1) Å, torsion angles (see Table 6) close to the ideal value of zero and no significant deviations (Table 7) from the plane of best fit through atoms C(1)-C(5), C(10). The non-planar geometries associated with rings B, C, and D are also as expected by comparison with other similar steroid molecules **9**, **10** and **129**. The torsion angles calculated for these rings are all very close to, or lie within, the ranges reported for the two crystallographically independent molecules found in each of estriol **10**,[136] estradiol-17β **9**,[137] and compound **129**[138] (see Tables 2 and 7).

The torsion angles and planes of "best fit" data support the description of the chair arrangement for ring C and a geometry similar to that of a half-chair for ring B. The chair nature of the carbohydrate ring is also established from the data presented in Tables 6 and 7. All of the hydrogen substituents on the ring occupy axial sites so that those attached to adjacent carbon atoms adopt *trans* positions with respect to one another. The larger non-hydrogen ring substituents lie in the equatorial positions. The *trans* relationship of all adjacent protons observed in the latter ring is in accordance with the large coupling constants (> 7.0 Hz) obtained by ^{1}H NMR.[117,133]

Two intermolecular approaches are observed between O-1 and O-11 of a second molecule and between O-8 and the partially weighted water molecule O-14 at distances of 3.23 and 3.13 Å respectively. These may be contrasted with other similar steroid molecules[136-138] which lack the bulky substituent at C-17 but where shorter H-bonding contacts, in the range 2.62-2.98 Å, are observed.

Of greatest interest are the arrangement adopted by the substituents on ring D. The carbohydrate moiety is attached in the β-position so that O-3 is in the *trans* position relative to O-2. Steric pressure between H-17 and H-1', which are *cis* to one another, is relieved by slight twists about the O(3)-C(17) and O(3)-C(19) bonds so that a contact distance of 2.24 Å is achieved. This close approach is reflected in the cross correlation of the anomeric proton (H-1') and H-17 proton in 17β-glucuronide derivatives, which was observed in the 2D-NOESY spectrum (Figure 32). Atoms H-16 and H-17 take up β and α positions respectively and give rise to a torsion angle of 137^0 for H(16)-C(16)-C(17)-H(17).

A quantitative description of steroid ring D puckering and conformation in terms of the maximum angle of torsion φ_m (geometrical parameter) and the "phase angle" of pseudorotation Δ (conformation parameter) was introduced by Altona *et al*[139] to describe flexible 5-membered rings. Thus, the five dihedral torsional angles
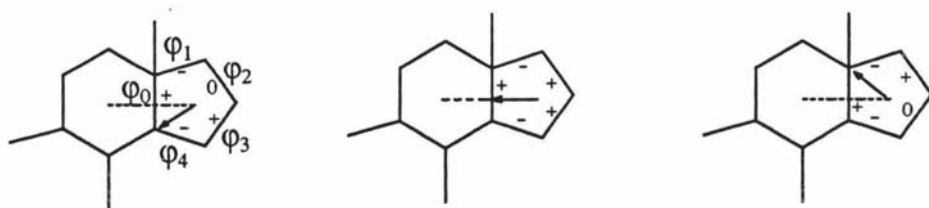
$(\varphi_0, \varphi_1, \varphi_2, \varphi_3$ and $\varphi_4)$ of the steroid ring D can be used for the caculation of the phase angle value Δ (Figure 36, Equation 1). The zero point on the Δ scale is defined in Figure 36. The maximum angle of torsion φ_m can also be caculated from Equation 2 (Figure 36).

$$\tan\frac{\Delta}{2} = \frac{(\varphi_2+\varphi_4)-(\varphi_1+\varphi_3)}{3.0777\varphi_0}$$

(Equation 1)

$$\varphi_0 = \varphi_m\cos\frac{\Delta}{2}$$

(Equation 2)

(+, - or 0 signs indicate that the torsional angle takes a positive, negative or zero value).

$\Delta = -36^0$ $\Delta = 0^0$ $\Delta = +36^0$

C(14) envelope   half-chair   C(13) envelope

Figure 36. Pseudorotation itinerary of ring D, from phase angle $\Delta = -36^0$ to $\Delta = +36^0$, showing the signs of the torsional angles

Hence, according to the above two equations for φ_m and Δ from the literature,[139] a calculation from the torsion angles of ring D in compound **112** was performed as follows:

For compound **112** (Table 7): $\varphi_0 = C(17)-C(13)-C(14)-C(15) = 47.1^0$

$\varphi_1 = C(16)-C(17)-C(13)-C(14) = -42.5^0$

$\varphi_2 = C(15)-C(16)-C(17)-C(13) = 22.3^0$

$\varphi_3 = C(14)-C(15)-C(16)-C(17) = 7.1^0$

$\varphi_4 = C(13)-C(14)-C(15)-C(16) = -34.4^0$

$$\tan\frac{\Delta}{2} = \frac{(\varphi_2+\varphi_4)-(\varphi_1+\varphi_3)}{3.0777\varphi_0} = \frac{(22.3-34.4)-(-42.5+7.1)}{3.0777 \times 47.1} = 0.16$$

$$\frac{\Delta}{2} = 9.1^0$$

Therefore, $\Delta = \mathbf{18.2^0}$

$$\varphi_0 = \varphi_m\cos\frac{\Delta}{2} \qquad \varphi_m = \varphi_0 / \cos\frac{\Delta}{2} = 47.1\cos\frac{18.2}{2} = \mathbf{47.7^0}$$

From the above caculations (giving a maximum torsion angle $\varphi_m = + 47.7^0$ and a phase angle $\Delta = 18.2^0$), the torsion angles for ring D in compound **112** show that it adopts an arrangement intermediate between the C(13) envelope and half chair conformations since its phase angle (Δ) of 18.2^0 is between 0^0 and $+36^0$.
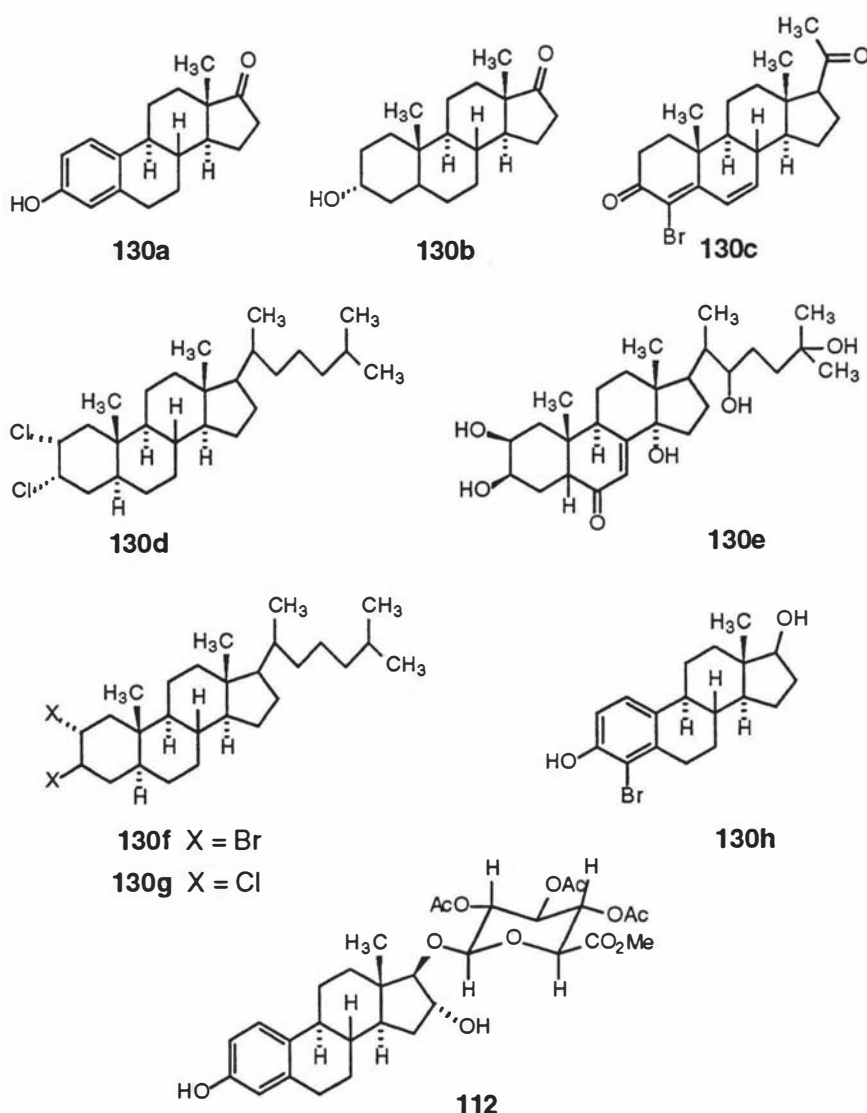
Figure 37. Structures of steroids (**130a-130h**)[139] and estriol 17-glucuronide derivative**112**[133]

A comparison of compound **112** with other steroids in the literature[139] was undertaken and is shown in Figure 37 and Table 8. Despite the fact that the large carbohydrate moiety (glucuronide ring) was attached to the 17-OH group, the maximum torsion angle (φ_m), phase angle (Δ), and the C/D torsion angles (φC, φD) of compound **112** are all typical of other 17 substituted steroids with no significant differences. The maximal torsional parameter (φ_m) of all steroid rings D is relatively

constant (47 ^{0}), although a slight tendency to increase with increasing phase angle (Δ) is noted. These observations are in agreement with the suggestion that the nature of the C-16 or C-17 substituent has no discernible influence on the actual geometry adopted for ring D.[139,140]
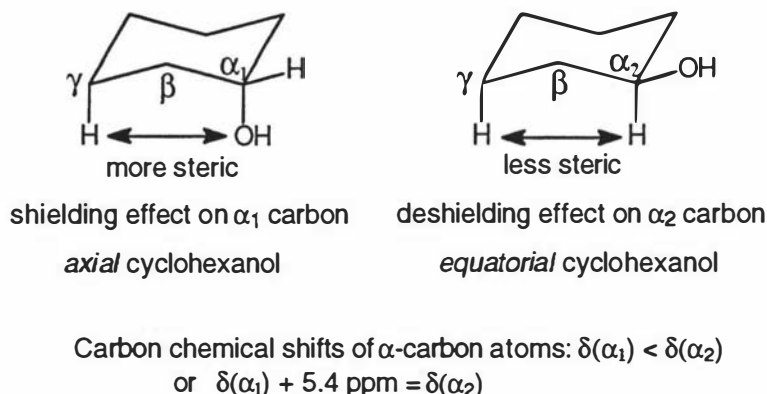
Table 8. Maximum torsional angle (φ_m) and phase angle of pseudorotation Δ for ring D, and the torsional angles (φC, φD) about the C/D junction of steroids

	130a	130b	130c	130d	130e	130f	130g	130h	112	standard value
φ_m	42.3^0	44.9^0	46.2^0	46.7^0	48.2^0	46.6^0	50.1^0	49.9^0	47.7^0	46.7^0
Δ	-39.8^0	-7.9^0	+2.1^0	+7.9^0	+10.7^0	+15.4^0	+16.1^0	+21.1^0	+18.2^0	
φC	69.6^0	59.0^0	62.2^0	60.0^0	60.0^0	58.7^0	61.8^0	64.3^0	60.1^0	55.8^0
φD	39.8^0	44.9^0	46.2^0	47.0^0	48.6^0	46.8^0	49.9^0	49.5^0	47.1^0	44.0^0

Despite the fact that the nature of the C-16 and C-17 substituents has little effect on the overall geometry of ring D there are nevertheless obvious significant substituent-dependent differences in the ^{13}C NMR shift positions. For example, the C-17 ^{13}C NMR shift for 3,17β-dihydroxyestra-1,3,5(10)-triene (estradiol-17β **9**) is 81.93 ppm[132] and the corresponding shift for the 3,17β-ditetrahydropyranyl ether derivative of estradiol-17β is 84.24 ppm.[134] When compared with the chemical shift differences for the bulkier substituents in compounds **112, 15, 114-115** and estriol **10** in the present work (Table 3) it appears that steric interactions play an important role in controlling the substituent effects in ^{13}C-NMR.[132]

To understand how the C-16 or C-17 substituents affect the carbon chemical shifts in the ring D of steroids it is necessary to have an understanding of substituent effects upon carbon chemical shifts in a normal cyclohexane or cyclopentane ring. In previous studies, it was found that the steric effects, in particular the γ-carbon atom and their axial hydrogens (Figure 38), appears to be important for the shielding of the α-carbon atom chemical shift. For example, when an *axial* OH group was introduced into cyclohexane, the steric interaction between the OH group and the *axial* γ-proton caused shielding of the α-carbon by 5.4 ppm when compared to the α-carbon of an *equatorial* OH group in cyclohexanol (Figure 38).

more steric   less steric

shielding effect on α_1 carbon   deshielding effect on α_2 carbon

axial cyclohexanol   *equatorial* cyclohexanol

Carbon chemical shifts of α-carbon atoms: $\delta(\alpha_1) < \delta(\alpha_2)$

or $\delta(\alpha_1) + 5.4\ ppm = \delta(\alpha_2)$

Figure 38 α-Carbon (α_1) of axial cyclohexanol is shielded by 5.4 ppm in its ^{13}C chemical shift compared to the α-carbon (α_2) of equatorial cyclohexanol.

For the five-membered cyclopentane ring, the substituent effects are similar, but there is lesser steric hindrance compared with the six-membered cyclohexane ring. From Figure 38, it is clearly shown that the more axial the substituent is, the more steric compression the substituent supplies. Therefore, more shielding or less deshielding is produced for the carbon atom to which the substituent is linked, and thus its ^{13}C NMR chemical shift value becomes smaller.

In steroids, the ring D substituents are never truly axial or equatorial but for all of the estriol 16α- and 17β-glucuronide derivatives in the present work, the large carbohydrate moiety is likely to take up a more equatorial position than does a normal OH group to avoid strong hindrance from the large sugar ring with the *axial* γ-protons (Figure 38). The large carbohydrate group also forces the neighbouring OH group in estriol monoglucuronide derivatives to a more axial position than a normal OH group would occupy. Therefore, the carbon atom (C-16 or C-17) is deshielded when attaching to a carbohydrate moiety due to it occupying a more equatorial or more stable position. On the other hand, the neighbouring carbon atom (C-17 or C-16) is shielded, as a result of the OH group necessarily being more axial, and existing more steric influence. Consequently the effect of the bulkier geometry gives rise to the differing shielding or deshielding effects in ^{13}C chemical shifts of carbon-16 and 17.[132] Because of the flexibility of ring D the precise details of the steric effects leading to the individual shifts are unclear and await further three dimensional structure determinations.

3.3.4 Summary

In summary, estrone glucuronide **12**, the estriol monoglucuronides **13-15** and pregnanediol glucuronide **16** were characterised by ^{1}H-^{1}H 2D-COSY, 2D-NOESY and ^{1}H-^{13}C HETCOR spectra in this chapter. The results unambiguously showed the β-linkage of the glucuronide ring with the steroid moiety in all of the steroid glucuronides. The conjugation positions of the glucuronic acid to estriol, such as estriol 16- or 17-glucuronide, were distinguished from their ^{13}C chemical shift values and the proton 2D-NOESY spectra. The crystal structure analysis of one estriol 17-glucuronide derivative also confirmed that the absolute configuration at all stereocentres was maintained during synthesis. Hence, the steroid glucuronides, synthesised in chapter 2, can be used with certainty for the preparation of different protein-conjugates for raising antibodies in immunoassays or for the synthesis of horseradish peroxidase conjugates *via* hemin modification, which will be discussed in the next chapter.

Chapter 4

Synthesis of Hemin Conjugates with Steroid Glucuronides

4.1 Introduction

As discussed in Chapter 1, this thesis aims to explore a new method for preparing horseradish peroxidase-steroid glucuronide conjugates (HRP-E1G, HRP-E3-3G, HRP-E3-16G and HRP-PdG), which can be achieved by the conjugation of the appropriate steroid glucuronide with hemin IX (the prosthetic group of HRP), followed by reconstitution with the apo-protein to form active HRP-steroid glucuronide conjugates indirectly. The synthesis of the different hemin-steroid glucuronide conjugates requires an appropriate molecular linker to bind the steroid glucuronides and the hemin together. This can be achieved by the utilisation of a bifunctional cross-linker, which is a very important strategy widely used for the conjugation of small molecules to proteins or other molecular probes.[141-150]

4.1.1 Bifunctional cross-linkers

A reagent which can couple different molecules is called a bifunctional cross-linking reagent. Bifunctional cross-linking reagents usually have two reaction sites in the molecules and there are two types of compounds, homobifunctional and heterobifunctional cross-linking reagents. Since bifunctional cross-linking reagents are often used in aqueous media, the availability of water-soluble bifunctional cross-linking reagents with flexible dimensions is becoming more important these days.

The properties of the bifunctional cross-linker, including its length and shape, may affect the binding of the hemin-steroid glucuronide conjugates with the apo-protein, the enzymatic activity of the new semi-synthetic enzyme and the recognition of the steroid glucuronides by stereospecific binding proteins such as anti-steroid glucuronide antibodies. Bifunctional reagents and their methodologies have been widely used for antibody production, drug delivery, protein immobilisation and studies of enzymes and receptors.[148] Some of these bifunctional linkers and procedures are of utmost importance and have attracted great attention in recent years.

For example, a heterobifunctional linking reagent **134** containing a masked aldehyde group and an acyl hydrazide was synthesised and used for the coupling of glycopeptides and other amino-containing compounds to proteins.[141] The reaction scheme for the preparation of this bifunctional reagent having a hydrazide group at one end and an acetal group at the other and its application is shown in scheme 28.
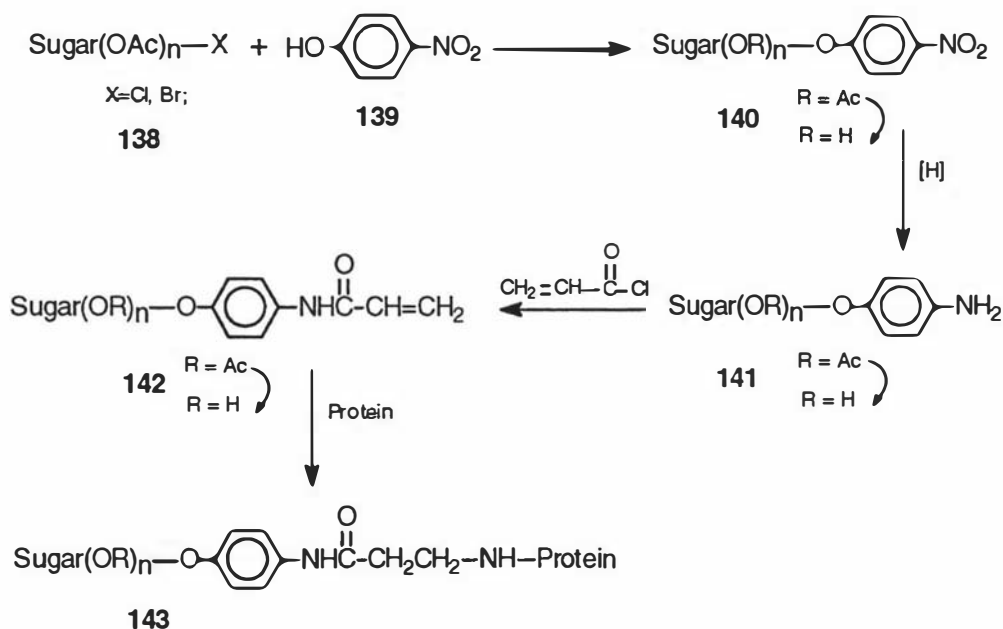
Scheme 28
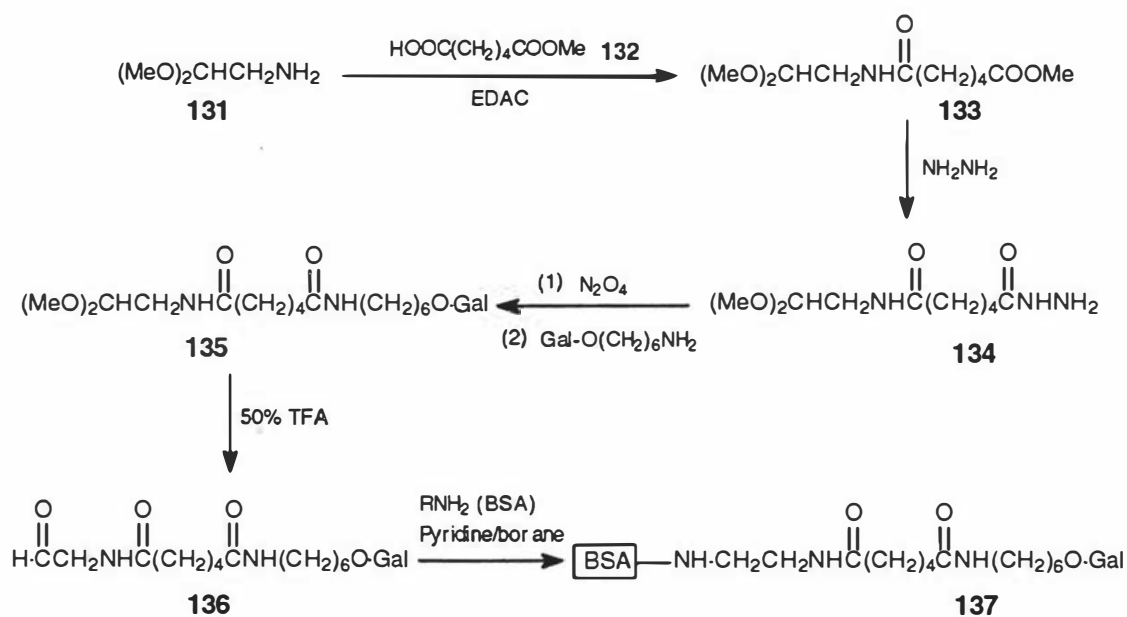
The coupling of the aminoacetaldehyde dimethyl acetal **131** to the adipic acid methyl monoester **132** was achieved using 1-ethyl-3-(3'-dimethylaminopropyl)carbo-diimide (EDAC) in dichloromethane. Subsequent aminolysis of compound **133** with hydrazine afforded the bifunctional linking compound **134**, which is very stable and can be stored indefinitely at room temperature. To couple a glycopeptide to a protein the linking reagent is first attached to the glycopeptide *via* acyl azide coupling, then the acetal is converted back to an aldehyde group by 50% trifluoroacetic acid (TFA) catalysed deprotection. Finally, the aldehyde group is coupled to proteins *via* the ε-amino groups forming an imine linkage, which can be reduced with pyridine-borane to the stable amine functionality. This procedure was successfully used for the conjugation of a triantennary glycopeptide to BSA with a very efficient coupling yield (~ 85%).

p-Nitrophenol **139**, a simple organic molecule, can also be used as a bifunctional linker for the preparation of artificial carbohydrate protein conjugates.

Roy *et al*[142] used halo-sugar derivatives **138** as glycosyl donors to link to *p*-nitrophenol **139** under phase transfer conditions with tetrabutylammonium hydrogen sulphate (TBAHS) and sodium hydroxide. The resultant *p*-nitrophenyl glycoside **140** was then reduced to the corresponding *p*-aminophenyl glycoside **141**. The N-acryloylation of the *p*-aminophenyl glycoside **141** with acryloyl chloride and triethylamine afforded the desired β-N-acryloylphenyl glycoside **142** in excellent yields. These conjugated precursors **142** can be coupled efficiently to proteins *via* Michael addition with amine functional groups of proteins (Scheme 29) or alternatively directly polymerised with acryloyl-type monomers to form polymer-bonded carbohydrates.

Scheme 29

ω-Methoxycarbonylalkyl thiols **147**[143] are examples of another type of heterobifunctional linker for the coupling of carbohydrates to either proteins or derivatized silica gel matrices (Scheme 30). All 3-bromo-2-(bromomethyl) mono- to tetrasaccharide glycosides (dibromoisobutyl glycoside or DIB β-glycoside) **146** were prepared by $BF_3 \cdot Et_2O$-mediated glycosylation of 3-bromo-2-(bromomethyl)propanol (DIBOL) **145** with 1-O-acetyl saccharides **144**. Treatment of the DIB glycosides **146** with the bifunctional linker, ω-methoxycarbonylalkyl thiol **147**, gave the spacer-armed bis-sulphide sugar **148**. Oxidation of the sulphide **148** with *m*-chloroperbenzoic acid afforded the corresponding bis-sulfone sugar **149**. After transformation of the

esters into the corresponding, strongly acylating, acylazides the spacer-armed glycosides were coupled to proteins or derivatized silica gel particles to provide artificial glycoproteins **150** and glycoparticles **151**. Artificial glycoproteins **154** and glycoparticles **155** can also be prepared from the allylic bromide glycoside **152** by using the same type of heterobifunctional linker **147** and similar coupling procedures (scheme 30).

Scheme 30
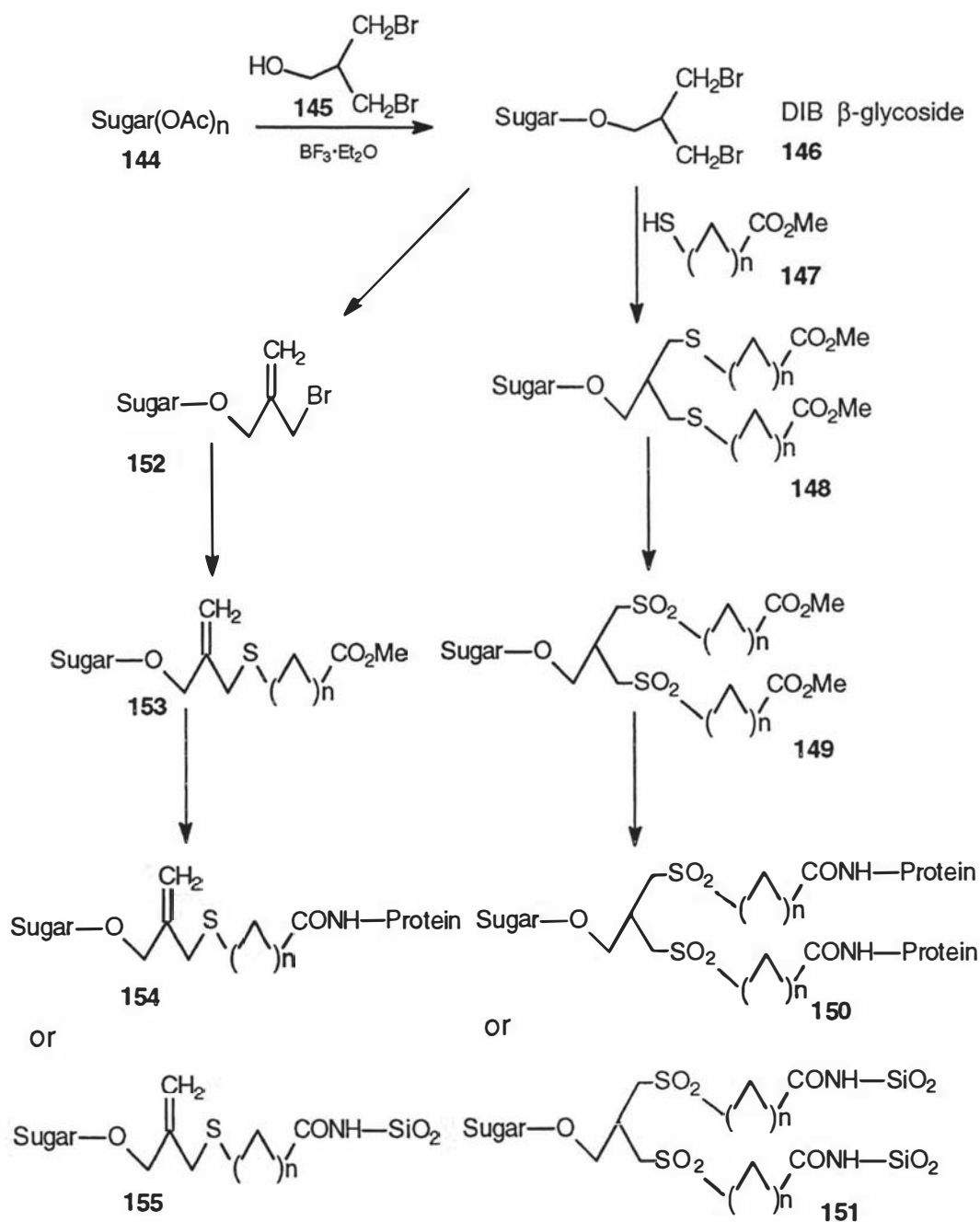
N-γ-maleimidobutyryloxy succinimide ester (GMBS) **158** is a stable hetero-bifunctional crosslinker for immobilisation of antibodies on inorganic supports. Bhatia *et al*[144] utilised GMBS **158** as a crosslinker for attaching antibodies to silica surfaces in three steps (scheme 31).

Scheme 31
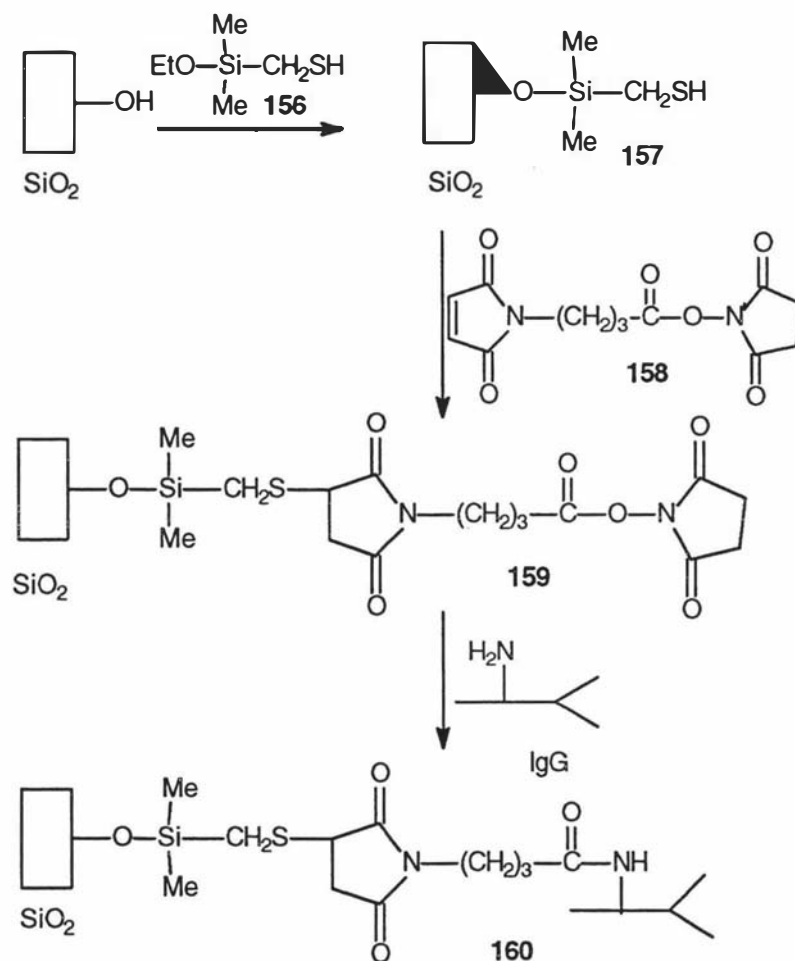
The first step was cleaning of the silica surfaces with acid and coating with a silane film by silanization of the hydroxyl groups on the silica surface with a 2% solution of mercaptomethyldimethylethoxysilane (MDS) **156** in dry toluene, or with other silanes. The second step was the treatment of the silanized substrate **157** with the heterobifunctional crosslinker **158**. The thiol group on the thiol-terminal films **157** reacts specifically and covalently with the maleimide region of the heterobifuntional crosslinker GMBS **158** in organic solvents, leaving the succinimide residue of GMBS available for protein attachment. Immobilisation of the antibody was the last step, which was achieved by reaction of the active succinimide ester residue of **159** with

terminal amino groups of the protein in an aqueous solution through the formation of a stable amide bond.

The same strategy was also adopted by Janda *et al*[145] to immobilise catalytic antibodies on glass beads. The results showed that the catalytic antibodies immobilised on an inorganic support retained the same activity and stereoselectivity as they exhibited in solution.

Heterobifuntional polyethylene glycol (PEG) derivatives are also important examples of crosslinkers. Since they are inexpensive, water soluble, and also available in a variety of lengths either commercially, or from the phase-transfer synthesis of oligoethylene glycols by addition of ethyleneoxy units to α,ω-diols,[146] heterobifunctional PEG derivatives show great potential as crosslinking reagents. For example, monoallyl diethylene glycol 161[147] was used as a heterobifunctional linker in the synthesis of spacer-armed glycosides. These can be coupled to proteins or polymers for use as immunogens or immunoadsorbants for affinity chromatography. The monoallyl diethylene glycol 161 was easily prepared from diethylene glycol and allyl chloride or bromide under phase-transfer conditions. Glycosylation of the monoallyldiethylene glycol 161 was achieved by a variety of methods for the different glycosyl donors, as shown in scheme 32.
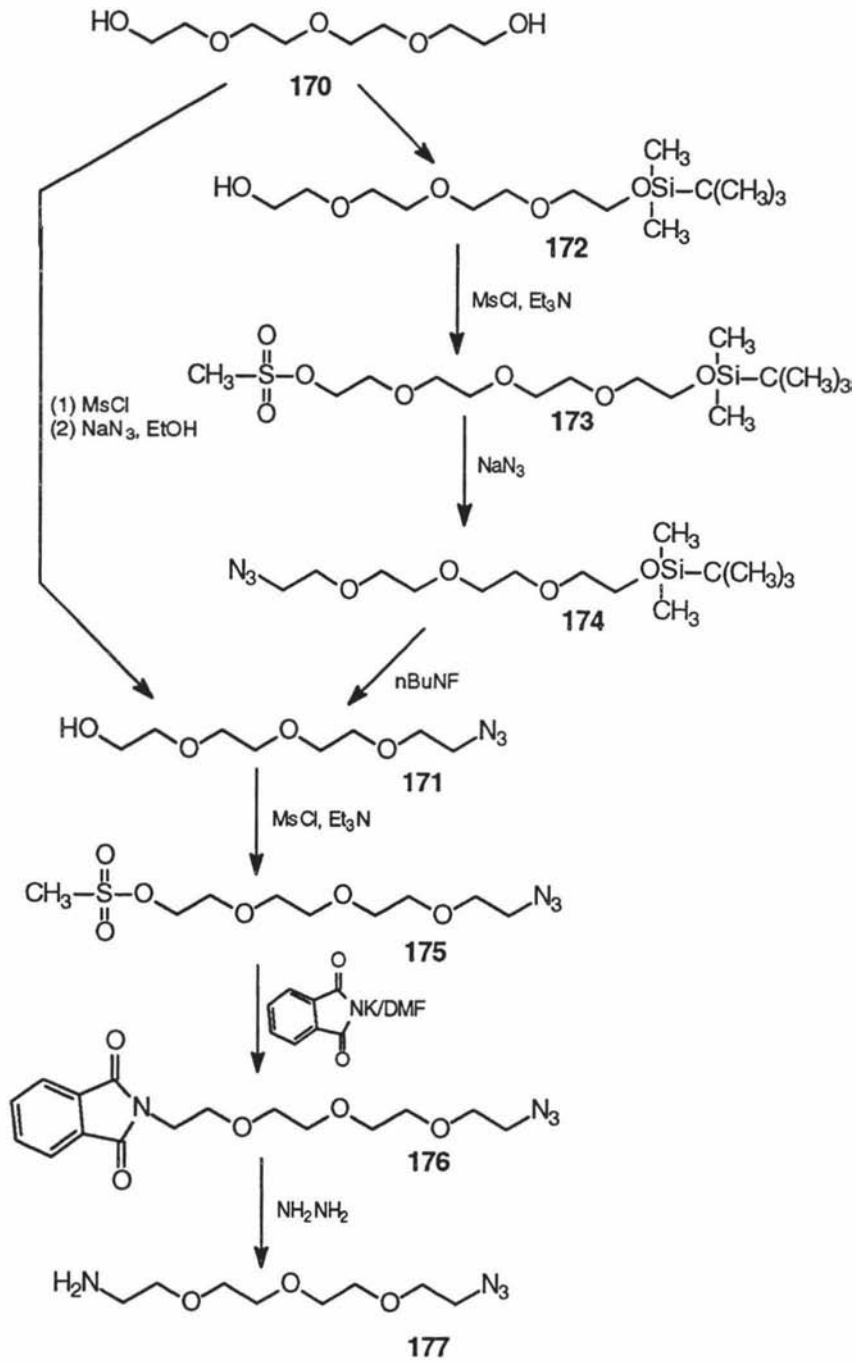
Scheme 32
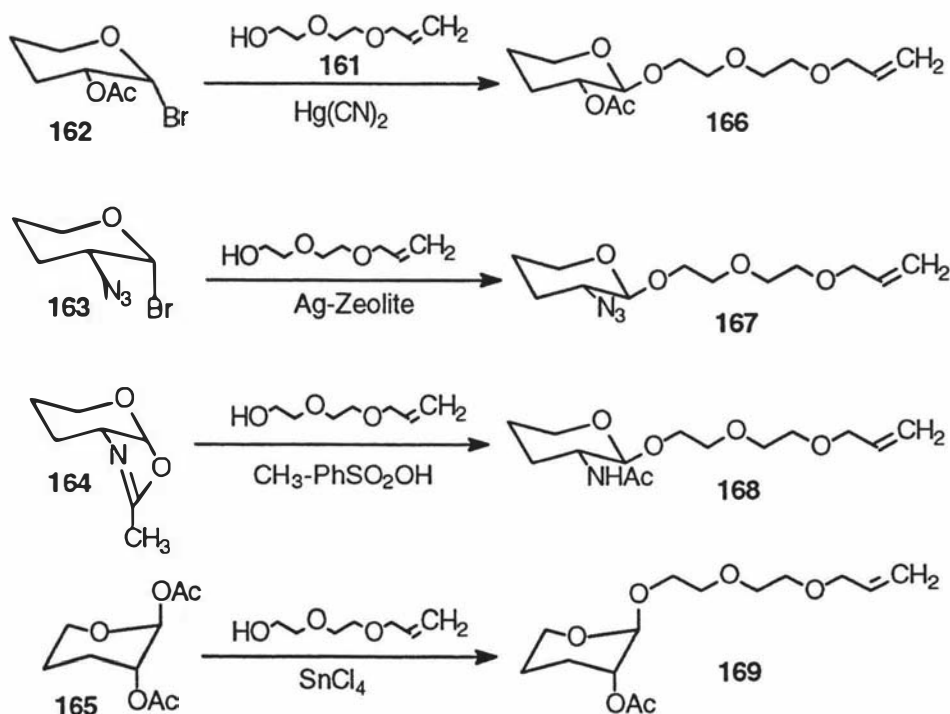
The glucopyranosyl bromide **162** or **163** was found to link to the bifunctional reagent **161** in the presence of mercuric cyanide or silver zeolite. The coupling of the oxazoline glycosyl donor **164** to the bifunctional linker **161** was better catalysed with p-toluenesulfonic acid, while for glycosyl donor **165** tin tetrachloride was a suitable promoter for the glycosylation reaction. At the other end of the bifunctional linker in all the spacer-armed glycosides (**166-169**), the allylic double bond can be copolymerized with acrylamide to form synthetic polymerised oligosaccharides or easily transformed into an aldehyde by passing ozone through the solution. The resulting aldehyde can then be coupled to proteins by reductive amination with sodium cyanoborohydride.

A new heterobifunctional PEG derivative **177**, which contains an amine group at one end and an azide group at the other end, was prepared recently by Bertozzi *et al.*[148] The bifunctional compound **177** was prepared from commercially available tetraethylene glycol **170** by two methods (scheme 33).

The first method involves mesylation (MsCl, Et$_3$N) of **170** followed by reaction with sodium azide in ethanol to give the azido alcohol **171** as a viscous oil in 44% yield. Alternatively, azido alcohol **171** was synthesised by monosilylation of the diol compound **170**, followed by mesylation of compound **172**. Treatment of the resulting compound **173** with sodium azide in ethanol and desilylation of compound **174** gave the desired product **171**. Azido alcohol **171** was mesylated and subjected to a Gabriel amine synthesis to give the azido amine **177** as a heterobifunctional linker. The free amine of compound **177** can be conjugated to biological molecules directly by an amide linkage (or *via* the corresponding isothiocyanate). After conjugation, the azide group at the other end of linker **177** can be reduced to an amine by mild, biocompatible reagents, for conjugation to other molecules.

The bifunctional linker **177** has been used successfully for the synthesis of a mannose-fluorescein conjugate **182** (scheme 34). The C-glycoside of mannose **178** was ozonized and reduced with zinc/acetic acid to give aldehyde **179** and reductive amination of compound **179** with the bifunctional linker **177** gave the mannose-linker conjugate **180**. Reduction of the azide **180** using 1,3-propanedithiol, followed by debenzylation (Na, liquid NH$_3$) and reaction with fluorescein isothiocyanate (FITC) provided the mannose-fluorescein conjugate **182**.

Scheme 33

Scheme 34
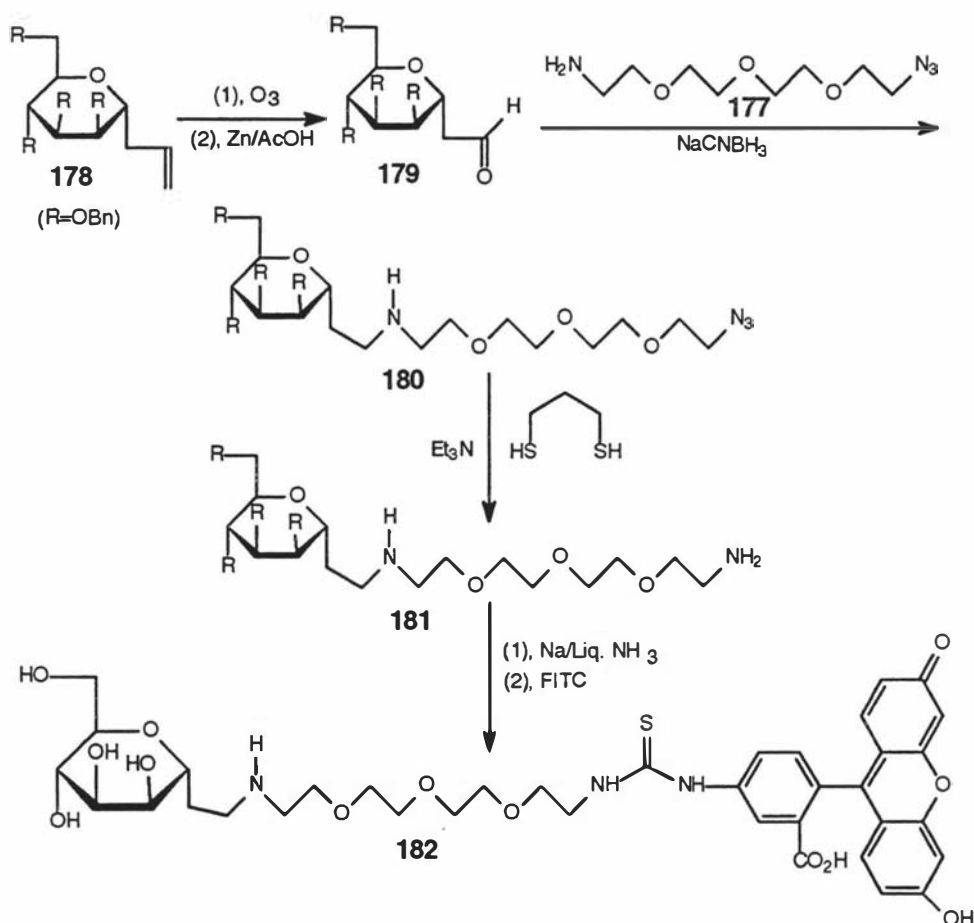
Some simple amino acids can be used also as bifunctional linkers for the conjugation of two different molecules. L-Lysine **183** was successfully used as a bifunctional linker for the linkage of steroid drugs to the side-chain of a polymer for the studies of drug delivery by Pleurdeau *et al* (Scheme 35).[149]

The amino-acid group of L-lysine **183** was blocked by forming a biscopper-lysine complex **184**, and the free amine functional group of the lysine complex **184** was linked to the drug moiety by reacting the chloroformate derivatives of the steroid **185**. After removal of the copper the lysine-steroid conjugates **187** can be attached to the side-chains of a polymer by two different methods. The first involves the synthesis of a methacrylic monomer **189** by reacting methacryloyl chloride **188** with the amino acid moiety of the conjugate **187** and subsequent polymerisation. The second method depends upon chemical modification of a polymer with the lysine-steroid conjugates **187** by forming a stable amide linkage between the carboxyl group of the polymer and the amine functionality of the amino acid drug moiety (Scheme

35). Both polymers **190** and **191**, after attachment of steroid drugs, can be used for the pharmacological testing of drug delivery.

Scheme 35
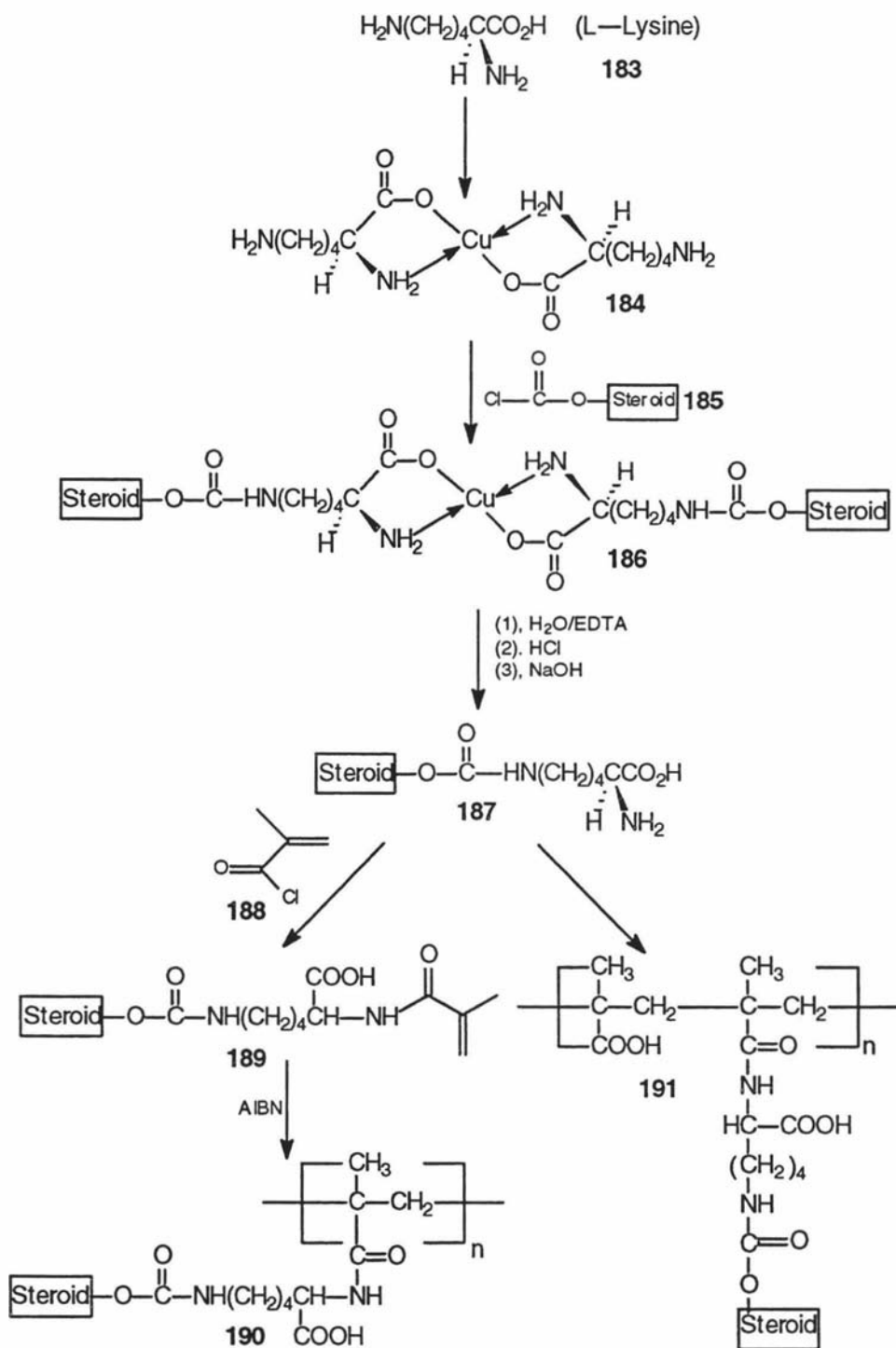
The bifunctional reagent is not just a crosslinking reagent, but also functions as a suitable spacer arm to minimise the steric interaction between the two molecules which are linked together. γ-Aminobutyric acid **193** was used as a spacer arm for the design and synthesis of a new fluorogenic HIV protease substrate **199**, which was based on the concept of resonance energy transfer between a fluorophore and an acceptor chromophore linked by an HIV protease specific substrate peptide.[150] Scheme 36 outlines the synthetic route for this new substrate **199**.

Scheme 36
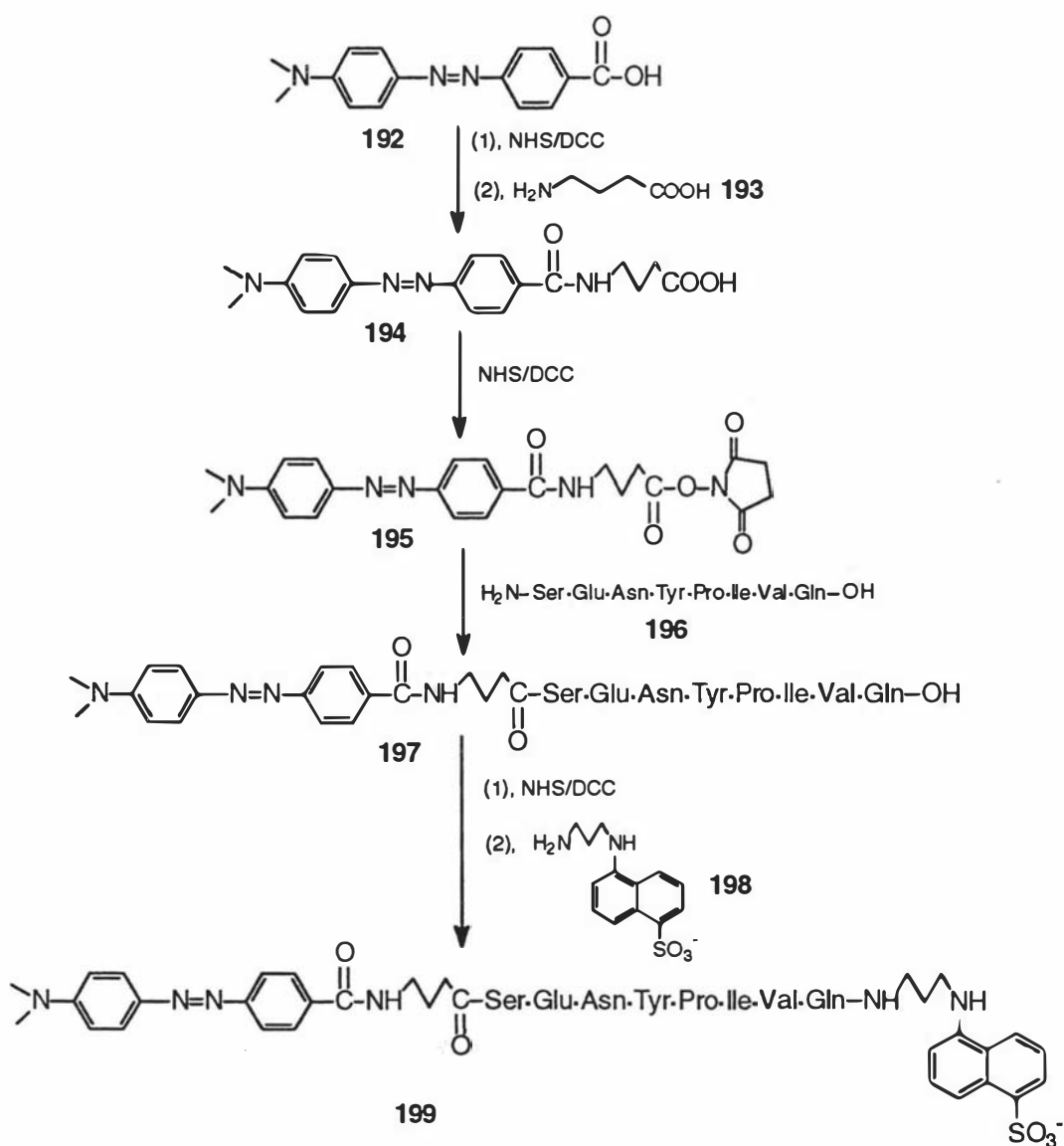
4-(4'-Dimethylaminobenzenazo)benzoic acid (BABCL) **192** was attached to the γ-aminobutyric acid spacer **193** by a standard peptide linkage. The conjugation of the spacer-armed DABCL moiety **194** with peptide **196** was achieved through another standard N-hydroxysuccinimide active ester **195** to give the coupling product **197**. The main purpose of using the bifunctional spacer linker **193** here is to minimise

potential steric problems involving the DABCL group and the protease active site. Coupling of the amino group in 5-(2'-aminoethyl)aminonaphthlene sulfonic acid (EDANS) **198** to the peptide C-terminus was accomplished by using 1-ethyl-3-(3'-dimethylaminopropyl)carbodiimide (EDAC) in the presence of N-hydroxy-succinimide and provided a new fluorogenic HIV protease substrate **199**, which can be used for sensitive, continuous measurement of HIV protease activity.

4.1.2 The choice of the bifunctional linker for the preparation of steroid glucuronide-hemin conjugates

It can be seen from the above discussion that different bifunctional linkers can been prepared and used for different purposes. For this Ph.D. project, a suitable bifunctional linker is needed to join a variety of steroid glucuronides (E1G **12**, E3-3G **13**, E3-16G **14** and PdG **16**) and protoporphyrin IX or the iron derivative (known as hemin IX) together. The common attachment positions for both steroid glucuronides and porphyrin molecules are carboxyl groups from the carbohydrate moiety of the glucuronides and the propionic acid side-chains (6 and 7) of the porphyrin compounds. Hence, the requirement of two amino groups at both ends of a bifunctional crosslinker is essential for the conjugation strategy. It is obvious from the previous discussion that the heterobifunctional PEG derivative **177** and amino acids, such as L-lysine **183**, are potentially suitable crosslinkers for achieving the above coupling because they can be used to join the steroid glucuronides and porphyrin or hemin derivatives by two amide linkages in a controlled sequence.

Early research on the reconstitution of the horseradish peroxidase apo-protein with modified hemins as probes for horseradish peroxidase has established that the free hemin carboxyl groups are important for efficient binding to apo-horseradish peroxidase and generation of a highly active enzyme.[151] For example, when the enzyme was reconstituted with protoheme monomethyl ester instead of hemin IX itself it showed only 20% of the activity of the native enzyme, and the enzyme containing the protohemedimethyl ester showed no peroxidase activity at all.[152] On this basis it has been concluded that coupling to these carboxyl groups seriously compromises or even eliminates the enzymatic activity and little further work has been reported. The crystal structure of cytochrome *c* peroxidase (Figure 39),[45] which is presumed to have a similar structure to the active site of HRP, clearly shows that the two hemin propionic acid groups, in particular the 7-propionic acid side chain, are involved in a variety of salt bridges with amino acid residues of the apo-protein and serve to stabilize the local geometry of the protein.
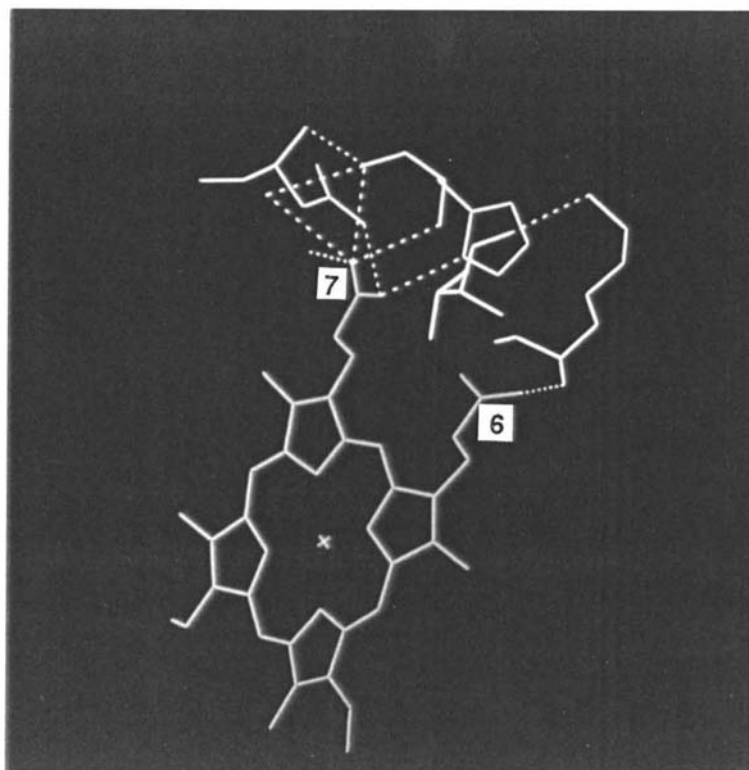
Figure 39. The interactions of hemin propionate side chains with the apo-protein, taken from the crystal structure of cytochrome *c* peroxidase, which indicates that the hemin 6- and 7-propionic acid groups (yellow) are involved in a variety of salt bridges or hydrogen-bonding (green) with amino acid residues of the apo-protein.

From Figure 39, the hemin 7-propionic acid group appears to be more important than the 6-propionic acid group towards the binding of the hemin with the apo-protein. In HRP, this 7-propionic acid group is involved in a hydrogen bond with an asparagine (Asn 175) residue of the apo-protein, and modification of this carboxylic acid group would destroy the stabilisation of the enzyme. Hence, it is likely that a higher enzymatic activity would be obtained if the hemin modification is carried out only at the 6-propionate side chain and the 7-propionic acid group is maintained. Perhaps even better the introduction of an extra carboxyl group in the modified synthetic hemin into a similar spatial location to that the hemin 6-propionic acid group occupied in the native hemin may be beneficial. Therefore, L-lysine **183** was chosen as the first crosslinker for the preparation of steroid glucuronide-hemin conjugates in this thesis, as shown in Figure 40. It was hoped that the extra carboxyl group, which is introduced by the L-lysine linker **183**, can compensate in terms of cofactor binding for the loss of the hemin IX carboxyl group due to the necessary

formation of the amide linkage. The other important factor, which also affects binding of modified hemins with the apo-protein, is the length of the bifunctional linkers. Obviously, they have to be long enough to fit in with the apo-protein structure without serious non-bonding or salt bridge interactions which will disrupt the tertiary structure.
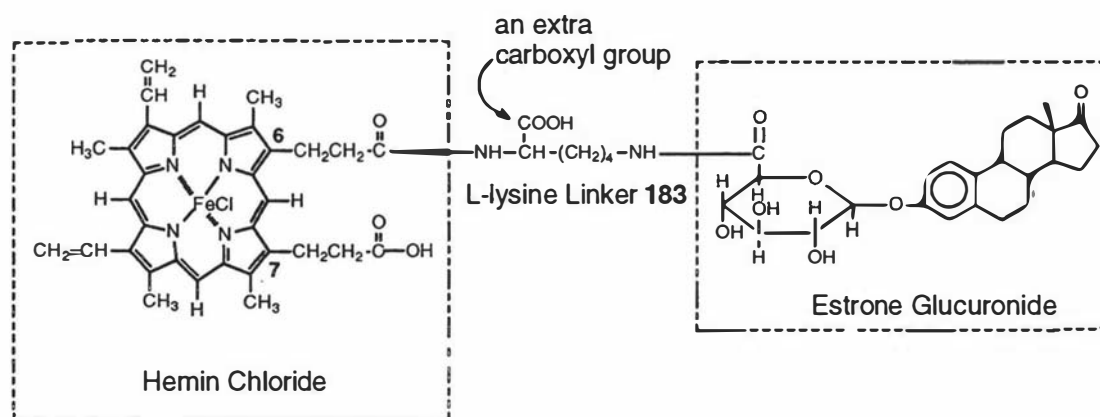
Figure 40. Structure of a hemin conjugate with estrone glucuronide

### 4.1.3 Acylation of amino-acid derivatives

Having chosen L-lysine **183** as the first bifunctional linker for the conjugation of the chosen steroid glucuronides and hemin IX, the obvious structural linkage between the hemin and the steroid glucuronides moiety is mainly involved the two amide reactions. One is the reaction of the carboxyl group from the glucuronides with the ϵ–NH_2 group from L-lysine **183**, which can be performed by standard peptide-forming reactions. The other is the reaction of the hemin carboxyl groups with the α–NH_2 group of L-lysine **183**. To meet the structural requirement of maintaining the hemin 7-propionic acid group free (Figure 40), it is essential to couple the α–NH_2 group of L-lysine **183** with only one of the two hemin carboxyl groups (mono-coupling). If this coupling reaction was started with the hemin mono-ester (with one propionic acid protected), it would be inconvenient to recover the free propionic acid group by deprotection in such a complicated conjugate (see structure in Figure 40) after the amide-forming reaction. The same is true for the acylation of the α-amino acid of the L-lysine **183** and inconvenience would also result from the necessity to deprotect a protected α-amino acid. Therefore, ideally both the selective amidation of an unprotected α-amino acid and the mono-coupling reaction of one of the two hemin carboxyl groups are needed for a successful achievement of the synthesis (Figure 41). This requires careful attention to the reagents and reaction conditions.
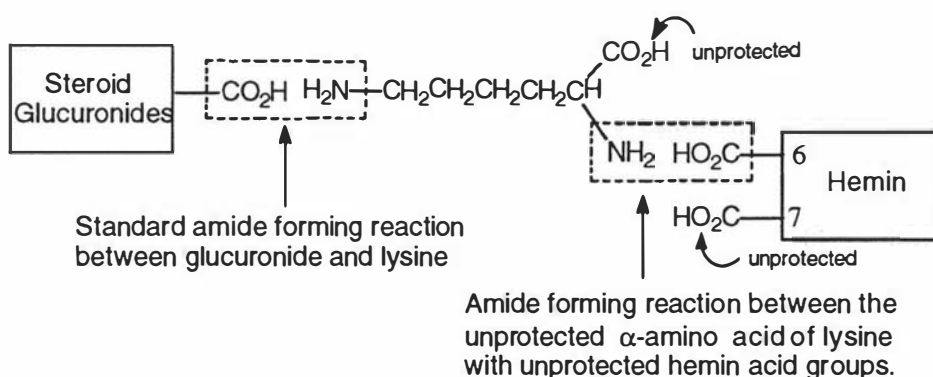
Figure 41. Two amide forming reactions involved in the
synthesis of hemin-steroid glucuronide conjugates.

In the literature, the general methods for the acylation of unprotected α-amino
acid derivatives have mainly involved two approaches, which include the acyl
chloride and different active ester methodologies. The activation of carboxylic acids
by conversion to the corresponding acyl chloride, followed by reaction with α-amino
acids under Schotten-Baumann conditions is the simplest approach and played an
important role in the infancy of peptide synthesis. In recent years, this method has
been greatly improved by using mixed solvents and now is mainly used for the
synthesis of long-chain N-acylaminocarboxylic acids by reaction of amino acids with
long-chain aliphatic acid halides. This method has appeared in several patents.[153]

The active ester method, utilising succinimidyl (ONSu) **200** or *p*-nitrophenyl
esters (ONp) **201**, which allows the formation of an amide bond under very mild
conditions, is known to be useful for peptide synthesis or chemical modification of
proteins. The reaction of a *p*-nitrophenyl active ester **201** with an amino acid **202**
proceeds because of activation of the carbonyl carbon of the ester group by the
electron-withdrawing effect of the *p*-nitro group as shown in scheme 37.[154] The
aminolysis of active esters **201** proceeds through a bimolecular mechanism that
involves the formation and decomposition of a tetrahedral addition intermediate **203**.
The reaction of the active esters **201** with α-amino acids leading to the corresponding
N-acyl-α-amino acid **204**[154] product competes with the hydrolysis reaction of the
active esters **201**. The same was also true for amino acid acylations with the active
succinimidyl ester (ONSu) **200**.[155]
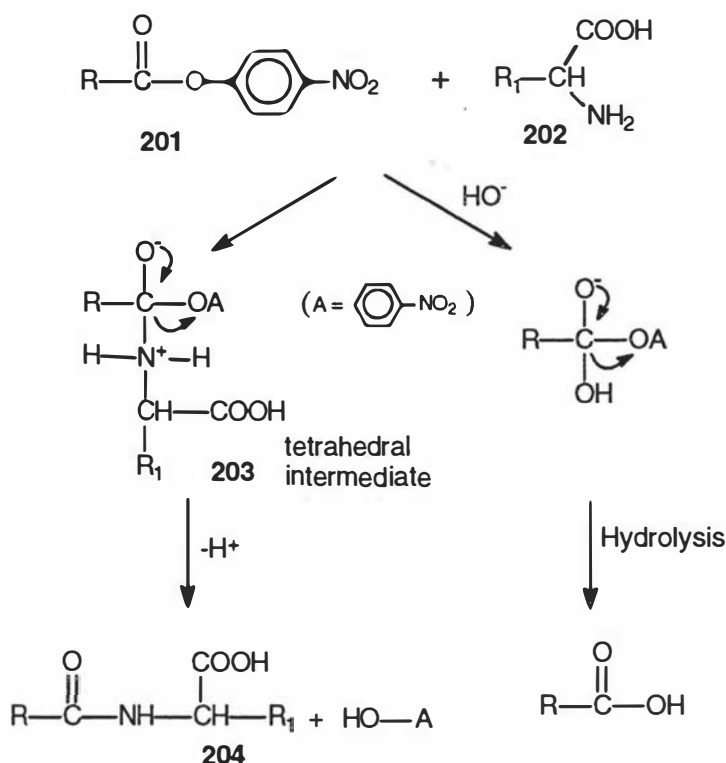
Scheme 37. Aminolysis and hydrolysis of nitrophenyl active esters **201** with an α-amino acid **202**

The ε-amino group of lysine in peptides has been successfully acylated with fatty acid p-nitrophenyl esters in the presence of 1-hydroxybenzotriazole (HOBt) in organic solvents in the synthesis of fatty acid acyl *S.cerevisiae* mating pheromone analogues.[156] The results showed that the fatty acid acyl group does not influence coupling of the peptide fragments as a result of its long fatty acid chain.

Scheme 38
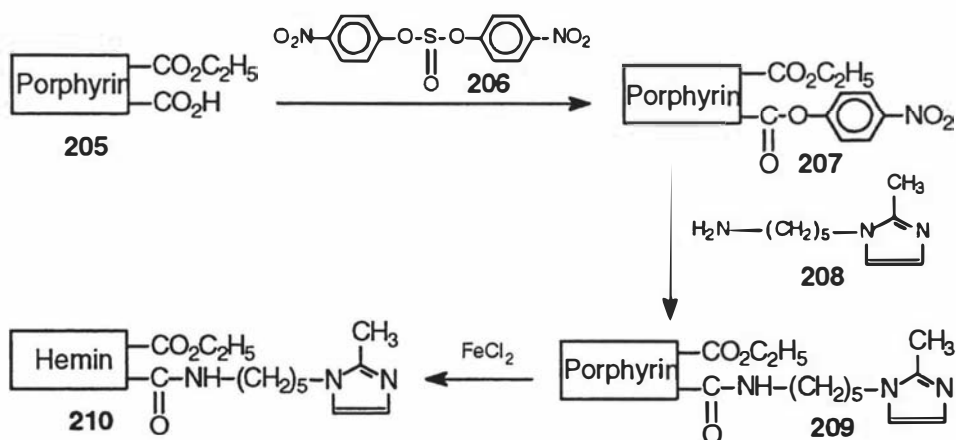
The porphyrin monocarboxylic acid p-nitrophenyl ester **207** was also used for the preparation of hemin derivatives having a 2-methylimidazole ligand with an N-

pentylamine side chain, as shown in scheme 38.[157] The porphyrin mono-acid *p*-nitrophenyl ester **207** was prepared from the reaction of the prophyrin mono-ester **205** and bis(*p*-nitrophenyl)sulphite **206** in a mixture of DMF and pyridine. After the coupling reaction of the active ester **207** with 1-(5-aminopentyl)-2-methylimidazole, followed by incorporation of iron ions into the porphyrin derivative **209**, the required hemin derivatives **210** were obtained. These hemin derivatives **210** can be used for oxygen binding studies.

Recently, (*p*-hydroxyphenyl)dimethylsulfonium methyl sulphate active ester **211** (Figure 42) was reported as a very mild, selective and water-soluble acylating reagent for amino acids, peptides, and proteins.[158] This water-soluble acylating reagent has been successfully used for the synthesis of long-chain N-acylaminocarboxylic acids[159] and some peptides used as synthetic sweeteners.[160]
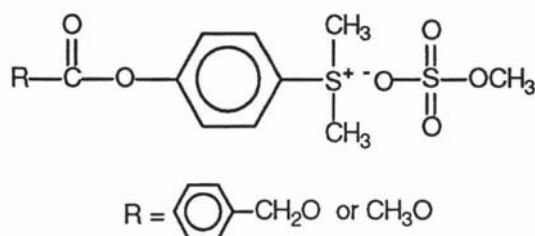
Figure 42 Structure of water-soluble acylating reagents **211**

4.1.4 The strategy and the methods of synthesis of hemin-steroid glucuronide conjugates

For the synthesis of hemin conjugates with the steroid glucuronides of interest in this thesis (Scheme 39), the first convenient step is the blocking of the α-amino acid group of the L-lysine **183** by forming a biscopper-lysine complex **184**. The free amine functional group at the other end of lysine **184** can be conjugated to steroid glucuronides directly by standard amide linkage reactions to form steroid glucuronide-L-lysine conjugates (**212, 213**). After removal of the copper the α-amino acid of the lysine-steroid conjugates (**214, 215**) becomes available for hemin attachment. Hence, the second amidation reaction between the hemin carboxyl groups and the ϵ-amino group of the L-lysine **183** will link the steroid compounds and hemin together to make the final conjugates (**232, 233**). In this second amidation reaction, protoporphyrin IX **216** and hemin IX **227** were both used as starting materials since modification of the protoporphyrin IX **216** allows NMR data to be easily acquired and hemin derivatives (**232, 233**) can be obtained by insertion of Fe^{2+} ions into the related protoporphyrin IX conjugates (**225, 226**). However, hemin derivatives (**232, 233**) can
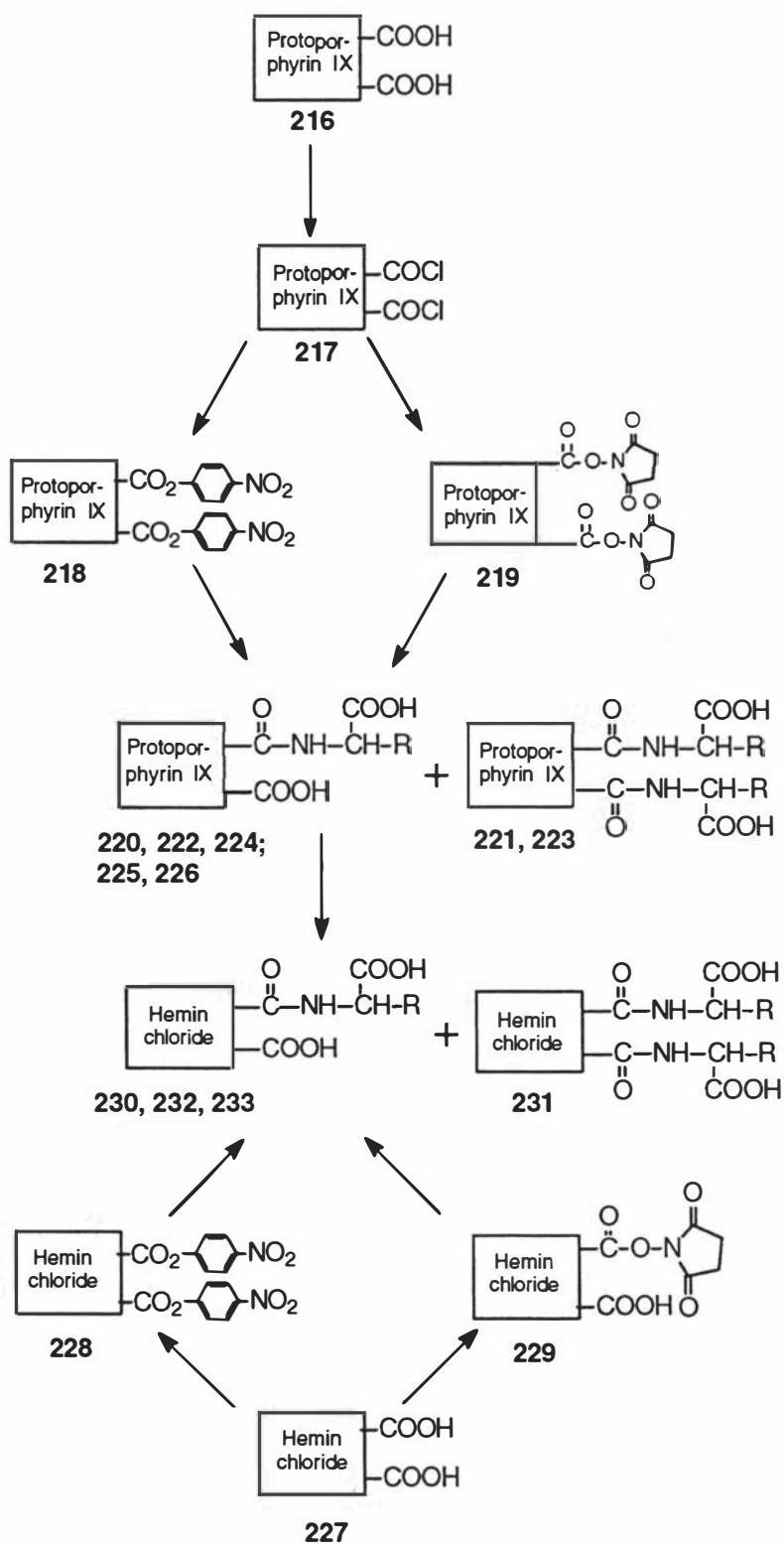
also be prepared by direct conjugation of lysine-steroid glucuronides (**212, 213**) with hemin IX **227**. Since ultimately it is the hemin which is required for production of a semi-synthetic HRP, and also it is cheaper and more stable than protoporphyrin IX **216**, it is preferable to use hemin IX **227** as a starting material.

Previously, the synthesis of monoacylated porphyrin or hemin derivatives always started from the porphyrin monoesters such as **205** (Scheme 38),[157] which took more reaction steps and resulted in overall low yields. Hence, it is ideal to prepare the different monoconjugates of protoporphyrin IX or hemin with steroid glucuronides starting from the protoporphyrin IX **216** or hemin IX **227** directly. In this thesis, the coupling step was focused on the selective mono-amidation reaction of one of the two protoporphyrin IX or hemin carboxyl groups with the α-amino group of unprotected α-amino acid derivatives. This is the important structural requirement of a steroid glucuronide-hemin conjugate capable of re-insertion into the HRP apo-protein (Chapter 5, section 5.1.2).

Hence, the work described in this chapter concentrates mainly on the selective mono-amidation reaction. Since the protoporphyrin IX or hemin derivatives are usually not water-soluble, water-soluble acylating reagents such as compound **211** are not suitable for this acylation reaction. Therefore, two different protoporphyrin IX or hemin active esters, p-nitrophenyl esters (ONp) (**218, 228**) and succinimidyl (ONSu) (**219, 229**), were investigated instead. Different reagents and reaction conditions were also investigated (Scheme 40). Protoporphyrin IX p-nitrophenyl ester **218** or succinimidyl ester **219** was prepared by activation of protoporphyrin IX **216** to the corresponding acyl chloride **217** (oxalyl chloride/CH_2Cl_2, reflux), followed by reaction with p-nitrophenol or N-hydroxysuccinimide in the presence of base at room temperature. Alternatively, the hemin IX p-nitrophenyl ester **228** or its mono-succinimidyl ester **229** was directly synthesised from the reaction of hemin IX **227** with p-nitrophenol or N-hydroxysuccinimide catalysed by dicyclohexylcarbodiimide (DCC) at different temperatures. The porphyrin IX and hemin mono-conjugated products (**225-226, 232-233**) were obtained from the selective mono-coupling reactions of porphyrin IX or hemin IX with controlled amounts of the different steroid glucuronides. Since only the anti-estrone glucuronide and anti-pregnanediol glucuronide antibodies were available at the time of writing of this thesis, the hemin-glucuronide conjugates (**232, 233**) were primarily prepared from the estrone glucuronide **12** and pregnanediol glucuronide **16**. Some unprotected α-amino acids were first used as model compounds for initial research into this selective mono-amidation reaction.

Scheme 39

Synthesis of hemin-steroid glucuronide conjugates **232, 233**

Steroid glucuronide = Estrone β-glucuronide (E1G) **12**
or
Pregnanediol β-glucuronide (PdG) **16**

Reagents and conditions: **a**,CuCO$_3$, reflux: **b**,steroid glucuronide / DCC / NHS / DMF, bis-copper-L-lysine/dilute NaHCO$_3$, r.t. for 12 hours; **c**, Chelex 100 resin/50% aqueous MeOH, r.t. for 3 hours; **d**, bis p-nitrophenyl)ester of protoporphyrin IX /Et$_3$N / DMF, r.t overnight; **e**, FeCl$_2$ / DMF-CH$_3$CN, reflux for 0.5 hour; **f**, p-nitrophenol /DCC / pyridine, r.t. overnight; **g**, bis (p-nitrophenyl)ester of hemin / Et$_3$N / DMF, r.t. overnight.

Scheme 40

R = α-amino acids (DL- or L-phenylalanine, L-tryptophan and L-arginine)
or steroid glucuronide-L-lysine conjugates **214, 215**

4.2 Experimental

4.2.1. General details
see **2.2.1 Experimental.**

The same HPLC system was used as that described in section 2.2.1 Experimental except that a micro µBondapak C18 column (300 x 4.6 mm I.D.) and three different solvent systems were used. Solvent I: **A** CH$_3$OH/Na$_3$PO$_4$ (0.01 M, pH = 6.85) 200:300, **B** THF/CH$_3$OH/Na$_3$PO$_4$ (0.01 M, pH = 6.85) 70:240:60; Solvent II: **A** CH$_3$CN/H$_2$O/H$_3$PO$_4$ 300:200:0.5, **B** CH$_3$CN/H$_2$O/n-BuOH/H$_3$PO$_4$ 100:50:350:0.5; Solvent III: **A** CH$_3$OH/H$_2$O/HOAc 300:200:5, **B** CH$_3$OH/HOAc 500:5. A new HPLC system was used for the isolation of hemin mono-conjugate of estrone glucuronide from hemin. Column Type: VYDAC, 218TP54 Protein and Peptide C18; Solvent IV: **A** THF, **B** CH$_3$OH/H$_2$O/HOAc 300:200:5, **C** CH$_3$OH/HOAc 500:5.

Additionally, a SMART^{TM} FPLC system using a µRPC C$_2$/C$_{18}$ PC3.2/3 column (Solvent V: **A** H$_2$O/CH$_3$CN/NaCl/HCO$_2$H 10:90:1:0.5, **B** H$_2$O/CH$_3$CN /NaCl/HCO$_2$H 40:60:1:0.5) was used for the analysis of the steroid glucuronide-L-lysine conjugates and a gel filtration column (Sephadex G-15, 150 mm x 18 mm), which was generously provided by the Separation Science Unit, Massey University, was also connected to an FPLC system for the purification of porphyrin-steroid glucuronide conjugates. Chelex 100 resin was received as a gift from Mrs Heather Baker, and the reversed phase Sep-Pak cartridges were generously provided by Mr Dick Poll. Electronic absorption spectra were recorded on a Hewlett-Packard model 8452A diode-array spectrophotometer. Absorption maxima (λ_{max}) are expressed in nanometres (nm).

4.2.2 Synthesis of steroid glucuronide-L-lysine conjugates

4.2.2.1 *Preparation of bis-copper-L-lysine chelate 184*

The bis-copper-L-lysine chelate **184** was prepared by an established literature procedure.[161] L-lysine monohydrochloride salt **183** (20 g) was dissolved in distilled water (200 ml) and the solution heated under reflux. While refluxing, an excess of copper carbonate (30 g) was added gradually until the solution was saturated. The

mixture was allowed to reflux gently for another 0.5 hour and the unreacted copper carbonate was removed by gravity filtration using whatman #1 paper. The blue filtrate was evaporated to dryness using a freeze drier and the blue residue was recrystallized from acetone/water to give a blue solid **184**.

4.2.2.2 *N-17-oxo-1,3,5(10)estratriene-3-yl-β-D-glucopyranosiduronyl-L-lysine* **214**

To a solution of estrone 3-glucuronide **12** (52 mg, 0.1165 mmol) in dry DMF (2 ml) was added 1,3-dicyclohexylcarbodiimide (60 mg, 0.29 mmol) and N-hydroxy-succinimide (30 mg, 0.26 mmol). The solution containing the active N-succinimide ester of estrone 3-glucuronide **12** was stirred for 0.5 hour at room temperature and used in the next step without further purification.

A solution of bis-copper-L-lysine chelate **184** (25 mg) and $NaHCO_3$ (50 mg) in water (2 ml) was added to the above DMF solution containing the activated ester. The resulting mixture was stirred at room temperature overnight (12 hours). The reaction mixture was added to 50 ml of water, neutralized to pH = 6 using 1M HCl and the white precipitate (N, N-dicyclohexylurea) was filtered off to give a blue solution of product **212**. A small amount of the blue solution of **212** was taken for Mass Spectral analysis; FABMS for compound **212**: m/z, 575 (M-Cu/2)$^+$.

The blue solution of compound **212** was added to MeOH (50 ml) and Chelex 100 resin (2 g, prewashed by 1M acetic acid and deionized water)[162] and stirred at room temperature for 3 hours. The resin was filtered and washed with 50% of aqueous MeOH (20 ml x 3) to get a colourless solution. After removing the MeOH under reduced pressure the aqueous solution was freeze dried overnight to give a white solid (140 mg). The white solid was dissolved in a mixture of MeOH (4 ml) and H_2O (40 ml), and purified by XAD-2 chromatography. The solution was passed through the XAD-2 column and washed with water (100 ml) to remove unreacted L-lysine and sodium chloride. The starting material **12** (5 mg) was eluted from the column with 50% of aqueous MeOH and the product was eluted from the column with pure MeOH. After removing solvent (MeOH) a white solid was obtained, which was recrystallized from methanol to give product **214** as fine crystals (43 mg, 64% yield); mp, 225-228 ^{0}C;
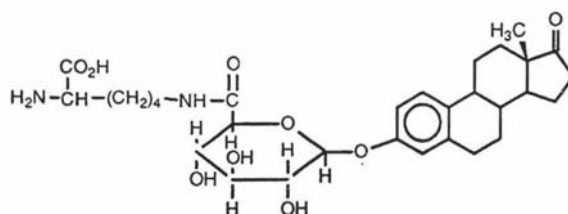
214

The purity of the product was checked by HPLC; Product **214** (0.5 mg) was dissolved in CH_3CN/H_2O (3:7) and 0.01 ml of the resulting solution was loaded onto a µRPC C_2/C_{18} PC3.2/3 column in a SMART^{TM} FPLC system (Solvent V: flow rate: 0.24 ml/min; gradient: 0 to 20 minutes, a linear gradient of solvent B from 30% to 50%; 20 to 23 minutes, a linear gradient of solvent B from 50% to 100%; 23 to 25 minutes, 100% of B). A wavelength of 280 nm was used for the detection of product **214** (retention time: 10.25 minutes) and starting material **12** (retention time: 15.07 minutes) (Figure 43a). FABMS for compound **214**: m/z, 575 (M)$^+$ ($C_{30}H_{42}O_9N_2$) (Figure 43b).

4.2.2.3 *N-20α-hydroxy-5β-pregnane-3α-yl-β-D-glucopyranosiduronyl-L-lysine 215*

Compound **215** was prepared by a procedure similar to that used in the preparation of **214**. Product **215** was obtained from pregnanediol glucuronide PdG **16** (48 mg, 0.097 mmol) as a white solid (24 mg, 40% yield). The reaction also gave a small amount of starting material **16** (6 mg, 12.5%).
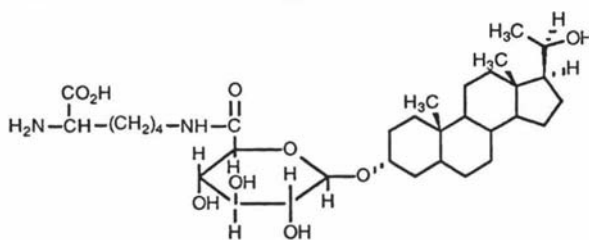
215

The product **215** was analysed by HPLC (SMART^{TM} system) under similar conditions to those used for the detection of compound **214**, except that a different gradient (Solvent V: 0 to 23 minutes, a linear gradient of solvent B from 30 to 50%; 23 to 25 minutes, a linear gradient of solvent B from 50 to 100%) was used for the purification of compound **215**. Compound **215** (retention time: 7.72 minutes, 91.5%) and starting material **5** (retention time: 1.89 minutes, 8.5%) were monitored at a wavelength of 280 nm (Figure 44a). FABMS for compound **215**: m/z, 625 (M)$^+$ ($C_{33}H_{56}O_9N_2$) (Figure 44b).
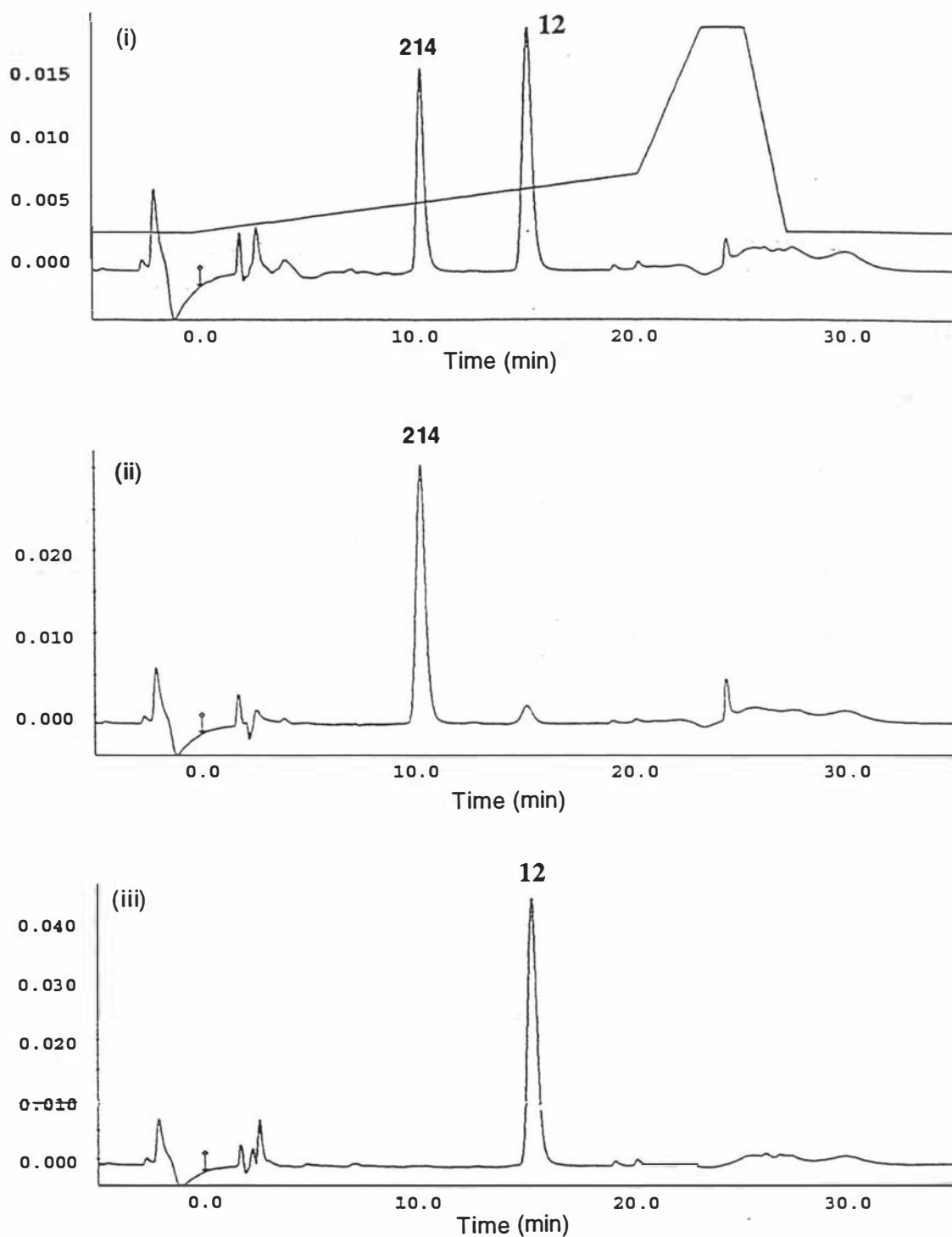
Figure 43a. (i) HPLC of mixture (1:1) of estrone glucuronide **12** (retention time: 15.07 minutes) and N-17-oxo-1,3,5(10)estratriene -3-yl-β-D-glucopyranosiduronyl-L-lysine **214** (retention time: 10.25 minutes); (ii) HPLC of product **214** showing a very small amount of **12** present; (iii) HPLC of estrone glucuronide **12**.
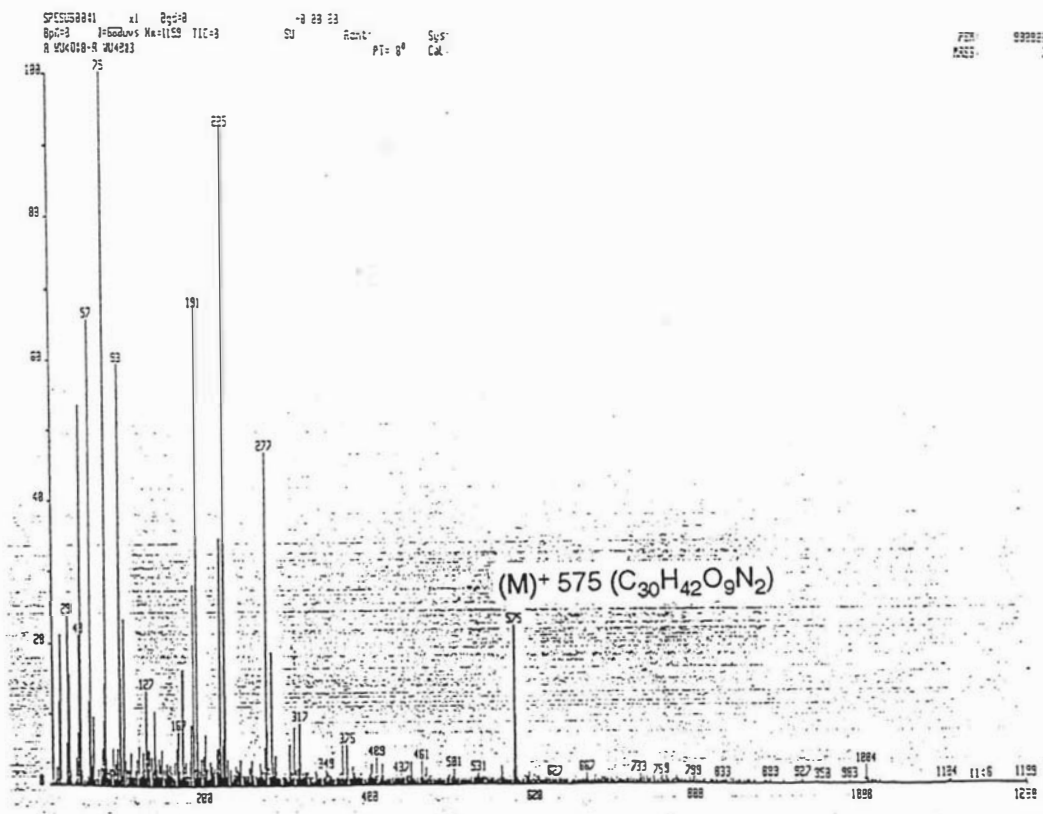
Figure 43b. FAB mass spectrum of N-17-oxo-1,3,5(10)estratriene -3-yl-β-D-glucopyranosiduronyl-L-lysine **214** (M)$^+$ 575 (C$_{30}$H$_{42}$O$_9$N$_2$).
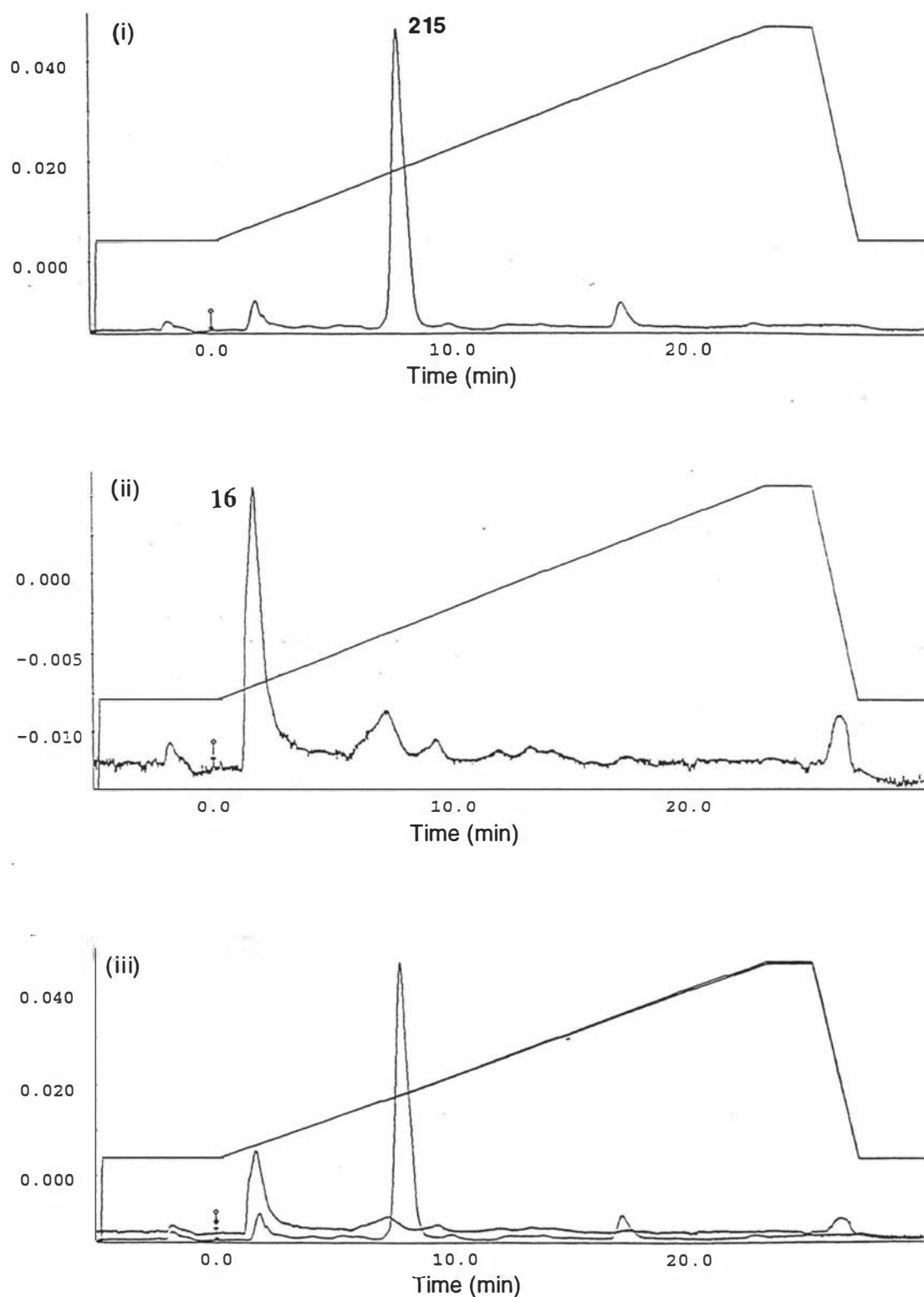
Figure 44a. (i) HPLC of N-20α-hydroxy-5β-pregnane-3α-yl-β-D-glucopyranosiduro-nyl-L-lysine **215** (retention time: 7.72 minutes) showing a very small amount of starting material **16** present; (ii). HPLC of pregnanediol glucuronide **16** (retention time:1.89 minutes); (iii) Overlay display of two HPLC spectra of (i) and (ii).
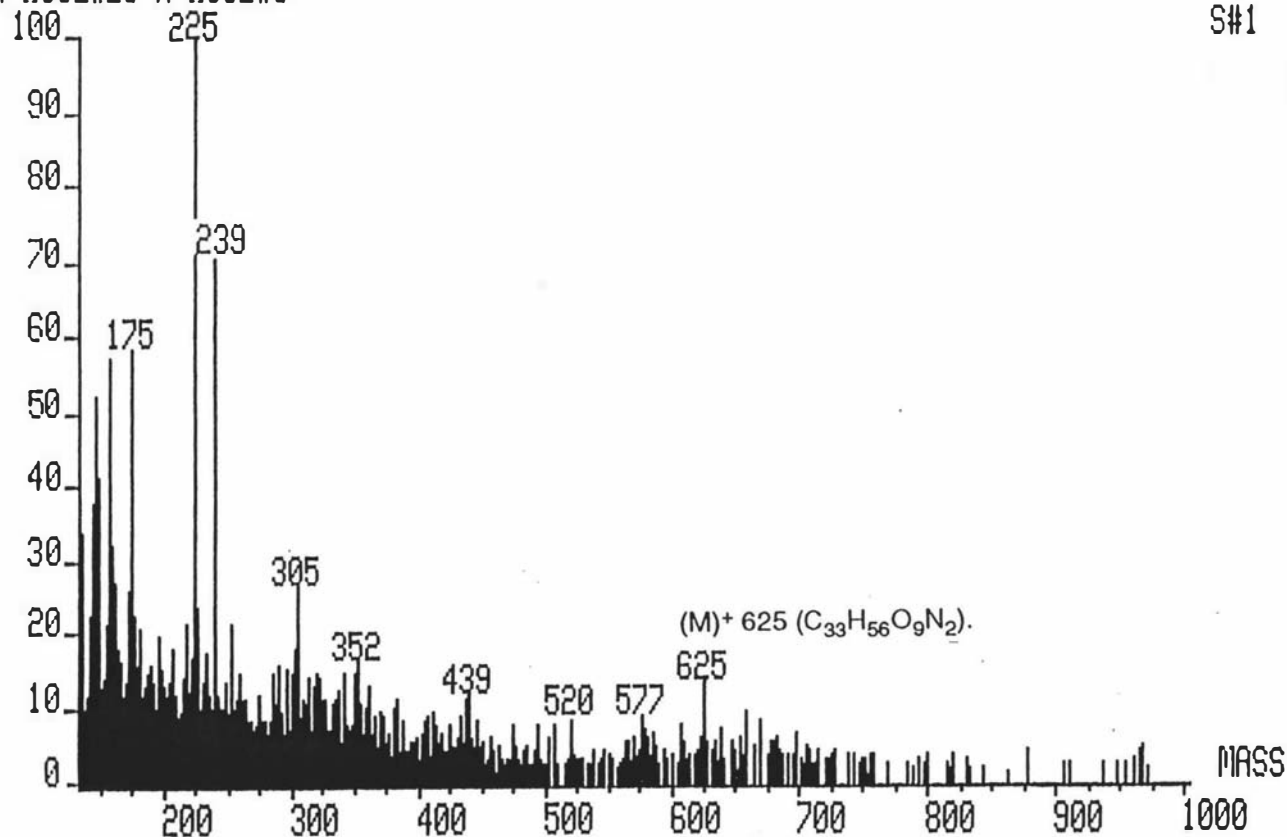
Figure 44b. FAB mass spectrum of N-20α-hydroxy-5β-pregnane-3α-yl-β-D-gluco-pyranosiduronyl-L-lysine **215** (M)+ 625 ($C_{33}H_{56}O_9N_2$).

4.2.3 Synthesis of conjugates of protoporphyrin IX with amino acids and steroid glucuronide derivatives

4.2.3.1 *7,12-Diethenyl-3,8,13,17-tetramethyl-21H,23H-porphin-2,18-dipropionic acid chloride 217*[163]

7, 12-Diethenyl-3, 8, 13, 17-tetramethyl-21H, 23H-porphin-2, 18-dipropionic acid **216** (25 mg, 0.044 mmol) was dissolved in dry CH_2Cl_2 (10 ml). Oxalyl chloride (0.2 ml) was added dropwise to the above solution by syringe under refluxing. After further refluxing for 15 minutes, solvent was distilled off from the mixture under reduced pressure and the residue dried further under high vacuum for 0.5 hour to give 7, 12-diethenyl-3, 8, 13, 17-tetramethyl-21H, 23H-porphin-2, 18-dipropionic acid chloride **217** as a black solid (34 mg), which was used for the next step without purification.

4.2.3.2 *Di-p-nitrophenyl 7, 12-Diethenyl-3,8,13,17-tetramethyl-21H, 23H-porphin-2, 18-di-propionate 218*

Compound **217** (34 mg) was added to dry methylene chloride (10 ml) and the mixture was stirred at 0 ^{0}C (ice bath) while adding a solution of *p*-nitrophenol (12.4 mg, 0.089 mmol) in acetone (1 ml) and pyridine (0.5 ml) over 10 minutes. The reaction mixture was stirred at room temperature for a further 1 hour. TLC on silica (CH_2Cl_2/CH_3COCH_3 2:1) showed the major product was **218** (R_F = 0.6). Solvent was removed from the reaction mixture under reduced pressure and the residue was dried under high vacuum before redissolving in methylene chloride (40 ml). The resulting solution in CH_2Cl_2 was filtered to remove insoluble residues and washed with CH_2Cl_2 (5 ml x 2). The solvent was removed from the combined filtrate and the residue was purified by flash chromatography, using CH_2Cl_2/CH_3COCH_3 (2:1) as solvent, to afford pure product **218** (32 mg, 90%). Electronic spectrum (λ_{max}, chloroform): 274 nm, 408 nm, 508 nm, 542 nm, 578 nm, 630 nm; IR, v_{max} (chloroform): 3303 cm^{-1} (NH), 3012 cm^{-1} (unsaturated C-H), 1755 cm^{-1} (C=O, dinitrophenyl ester), 1520 cm^{-1} (asymmetric ArNO$_2$), 1342 cm^{-1} (symmetric ArNO$_2$); High resolution FABMS, 805.298578780 (MH)$^+$ (calculated for $C_{46}H_{41}N_6O_8$, 805.29858781); δ_H (CDCl$_3$) 10.23, 10.17, 10.08 and 10.00 (4s, 4H, 5,10,15,20-H), 8.23-8.34(m, 2H, 2 =CH), 7.84-7.89(m, 4H, aromatic), 6.68-6.75(m, 4H, aromatic), 6.20-6.43(m, 4H, 2 CH$_2$=), 4.43(t, 4H, 2CH$_2$), 3.72, 3.71, 3.63 and 3.62(4s, 12H, 4CH$_3$), 3.43(t, 4H, 2CH$_2$).

Compound **218** was also prepared by the following methods:

7, 12-Diethenyl-3, 8, 13, 17-tetramethyl-21H, 23H-porphin-2, 18-dipropionic acid **216** (50 mg, 0.089 mmol) and *p*-nitrophenol (30 mg, 0.22 mmol) were dissolved in dry pyridine (10 ml) and the solution was stirred at 0 ^{0}C (ice bath) for 0.5 hour, before thionyl chloride (0.05 ml) was added dropwise to the above cold solution by syringe. After further stirring at 0 ^{0}C for 0.5 hour the reaction mixture was poured into ice water (100 ml) to yield a precipitate. The mixture was then centrifuged to collect the solid, which was washed with cold water twice to remove pyridine and excess *p*-nitrophenol. The residue was dissolved in acetone (30 ml) and dried over $MgSO_4$ overnight. The acetone solution was passed through a short silica gel column and eluted with CH_2Cl_2/CH_3COCH_3 (2:1) to give a clear red solution. After evaporation of the solvent under reduced pressure the fine black solid (25 mg, 35% yield) was obtained. mp > 250 ^{0}C. The TLC, electronic and ^{1}H-NMR spectrum of the product were identical with **218** prepared by the previous method.

4.2.3.3 *Protoporphyrin IX-Phenylalanine conjugates 220, 221a and 221b*

To a solution of freshly prepared compound **218** (16 mg, 0.02 mmol) in dry DMF (2 ml) were added DL-phenylalanine (3.9 mg, 0.024 mmol) and Et_3N (0.025 ml). The reaction mixture was then stirred at room temperature overnight. After addition of further Et_3N (0.2 ml) and stirring for another 0.5 hour the reaction mixture was added to 30 ml of water, and freeze-dried overnight to afford a black solid residue. The residue was dissolved in DMF/H_2O (1:1) (10 ml) and the solution was analysed by HPLC.

HPLC: The above solution (0.05 ml) was loaded onto a micro μBondapak C_{18} reverse phase column (Solvent I: Flow rate 1 ml/minute, a linear gradient from 45% to 52% of solvent B over 30 minutes). A wavelength of 405 nm and sensitivity of 2.0 were set up for the detection. The retention times for all the compounds were as follows: protoporphyrin IX (starting material) **216**, 9 minutes, 9.1% yield; mono-conjugate of protoporphyrin IX-phenylalanine **220**, 14 minutes, 71% yield; two double-conjugates of protophyrin IX-phenylalanine **221a**, 20 minutes, 10% yield and **221b**, 22.5 minutes, 9.5% yield (Figure 45a). The analytical sample was obtained by trapping the different peaks from isocratic reverse phase HPLC on a μBondapak C_{18} column (Solvent I: 55% of solvent B, 0.1 ml x 20 times) and the purity of the separated products was confirmed by HPLC analysis.
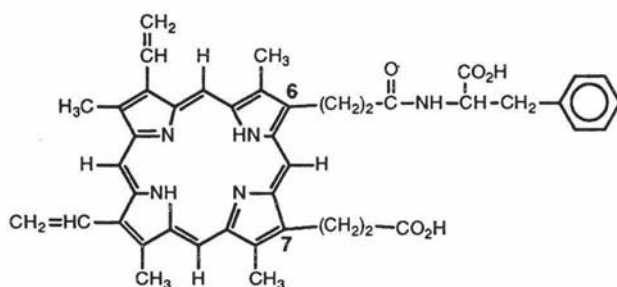
220 (mixture of 6 and 7 mono-conjugates)

The mono-conjugation of protoporphyrin IX **216** or hemin IX **227** always produced an equal mixture of two isomeric (6, 7) protoporphyrin IX or hemin mono-conjugates. In this thesis, the structures of 6-mono-conjugated porphyrin or hemin products are used to represent the mixture (50 : 50) of these two isomers.

For compound **220**: Electronic spectrum (λ_{max}, chloroform): 408 nm, 506 nm, 542 nm, 578 nm, 630 nm; FABMS: m/z, 710 (MH)$^+$; δ_H (DMSO-d$_6$) -3.94(s, 2H, 2NH), 6.23(d, J = 11.36 Hz, 2H, CH$_2$=), 6.46(d, J = 18.33 Hz, 2H, CH$_2$=), 6.82(m, 5H, 1 phenyl), 8.32-8.58(m, 3H, 2 =CH and CONH), 10.22-10.31(m, 4H, 5,10,15, and 20-H) (Figure 45d).

For compound **221a**: Electronic spectrum (λ_{max}, chloroform): 408 nm, 506 nm, 542 nm, 578 nm, 630 nm; FABMS: m/z, 857 (MH)$^+$; δ_H (DMSO-d$_6$) -3.90(s, 2H, 2NH), 6.23(d, J = 12.09 Hz, 2H, CH$_2$=), 6.46(d, J = 17.95 Hz, 2H, CH$_2$=), 6.68(m, 10H, 2 phenyl), 8.26(d, 2H, 2 CONH), 8.52(m, 2H, 2 =CH), 10.28(m, 4H, 5,10,15, and 20-H) (Figure 45e).
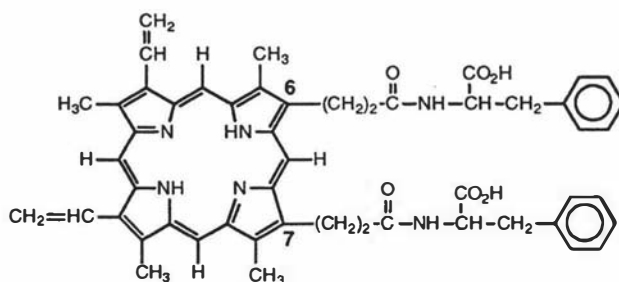
221a, 221b (double-conjugates)

For compound **221b**: Electronic spectrum (λ_{max}, chloroform): 408 nm, 506 nm, 542 nm, 576 nm, 630 nm; FABMS: m/z, 857.5 (MH)$^+$; δ_H (DMSO-d$_6$) -3.86(s, 2H, 2NH), 6.24(d, J = 11.35 Hz, 2H, CH$_2$=), 6.53(d, J = 17.58 Hz, 2H, CH$_2$=), 6.67(m, 10H, 2 phenyl), 8.30(d, 2H, 2 CONH), 8.54(m, 2H, 2 =CH), 10.29(m, 4H, 5,10,15, and 20-H) (Figure 45f).

The stereochemistry of the above two double-conjugates of protoporphyrin IX-phenylalanine (**221a** and **221b**) will be discussed in section 4.3 (Results and Discussion).

Protoporphyrin IX-phenylalanine conjugates **220**, **221a** and **221b** were also prepared from the protophyrin IX N-hydroxysuccinimide ester **219** (Scheme 40) according to the same procedure as above except that N-hydroxysuccinimide (10.5 mg, 0.09 mmol) was used to react with compound **216** instead of *p*-nitrophenol as starting material. After the reaction, the HPLC (same solvents and gradient as above) trace showed different yields of products compared to the products prepared by the di-*p*-nitrophenyl active ester **218**. For compound **216** (starting material); 18.5%; Compound **220**: 53.7%; Compound **221a**: 9.1%; Compound **221b**: 9.8%; impurity: 8.9% (Figure 45b).

L-Phenylalanine was also used in the reaction according to the same procedure as using the di-*p*-nitrophenyl active ester of protoporphyrin IX **218**. The reaction gave similar results except that only one double coupling product **221a** was formed for L-phenylalanine instead of two conjugates **221a** and **221b** when DL-phenylalanine was used as starting material (Figure 45c).
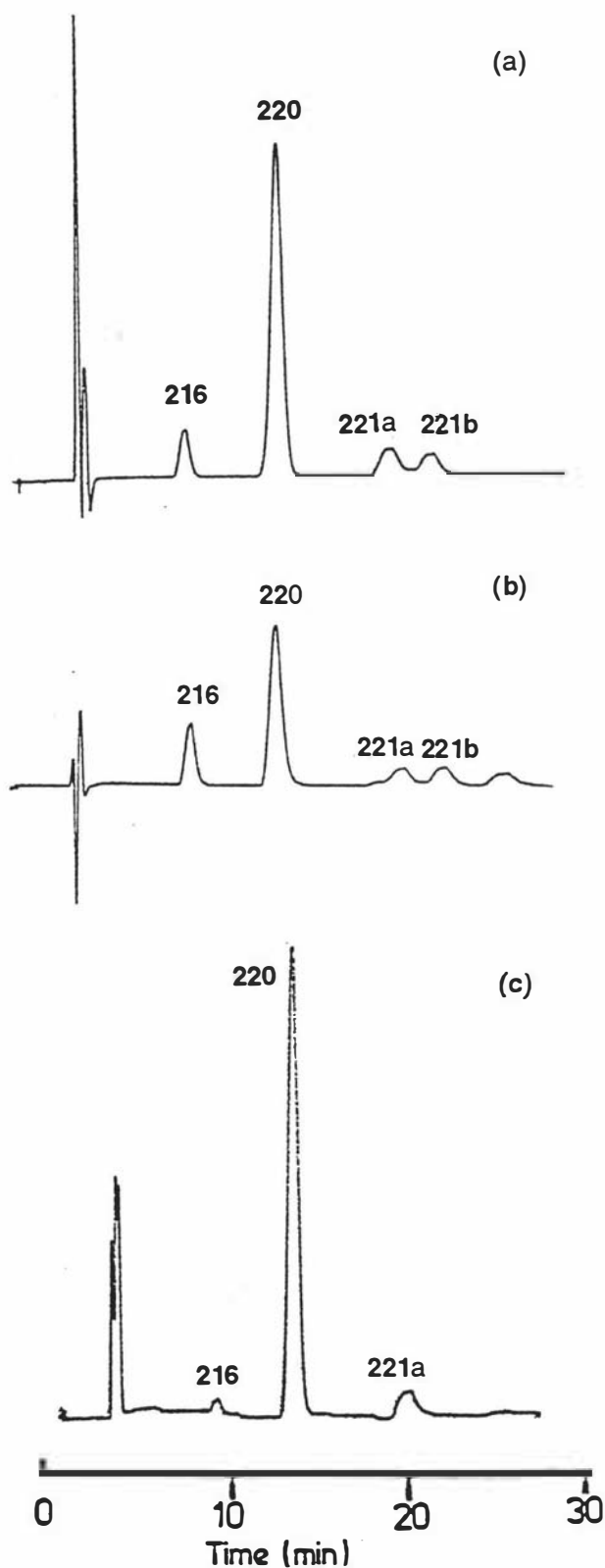
Figure 45. (a) HPLC analysis of the reaction mixture of protoporphyrin I X di-*p*-nitrophenyl active ester **218** with DL-phenylalanine showing the high yield of mono-conjugates **220** and two double-conjugates **221a** and **221b** present; (b) HPLC analysis of the reaction mixture of protoporphyrin IX N-hydroxysuccinimide active ester **219** with DL-phenylalanine; (c) HPLC analysis of the reaction mixture of protoporphyrin IX di-*p*-nitrophenyl active ester **218** with L-phenylalanine showing the high yield of mono-conjugates **220** and only one double-conjugate **221a** present.
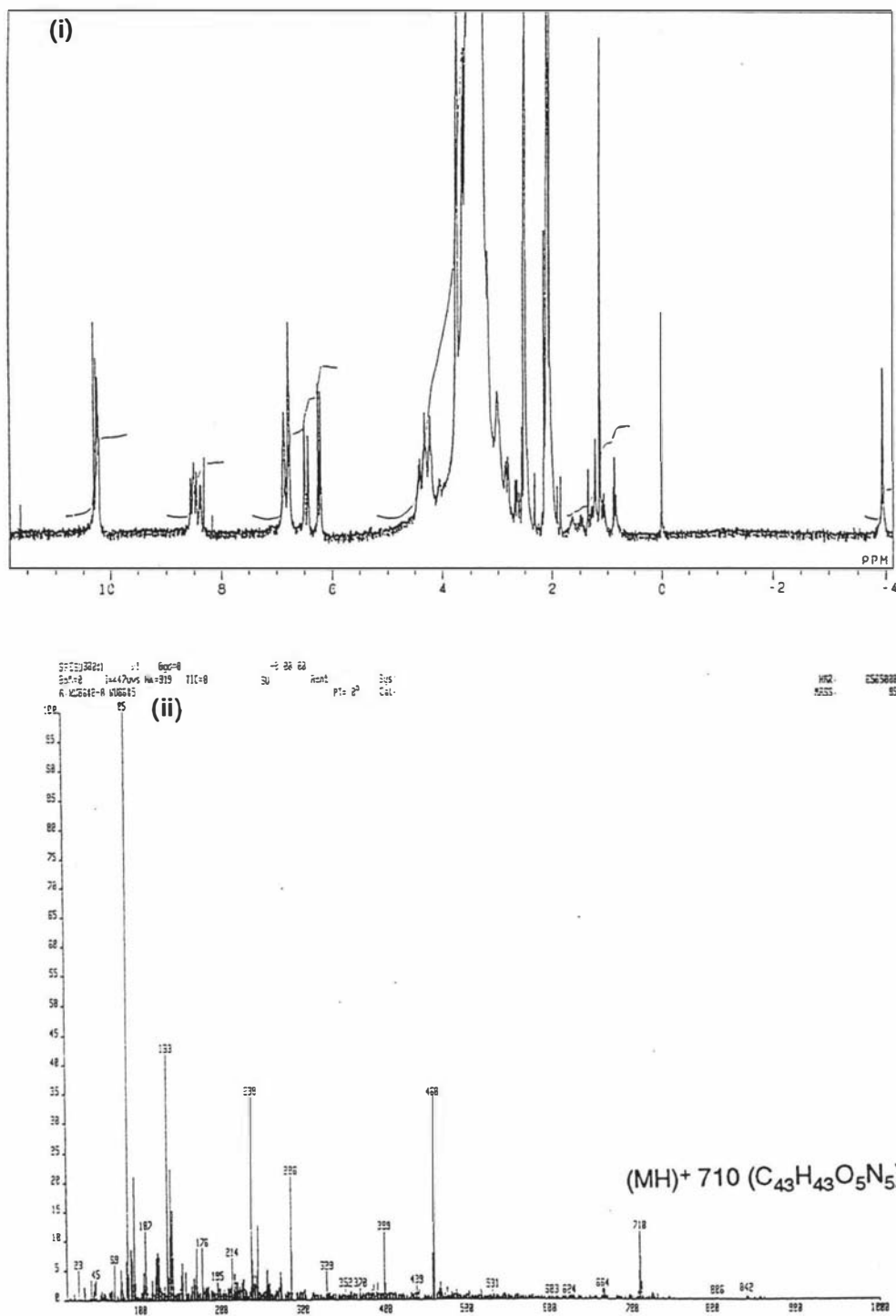
Figure 45d (i). ¹H NMR spectrum of compound **220** showing the mono-conjugate structure of protoporphyrin IX with DL-phenylalanine. i.e. δ = -3.94 (2NH), 6.23 and 6.46(2CH$_2$=), 8.32-8.58(2=CH and CONH), 10.22-10.31(4H) from 1protoporphyrin IX ring; while δ=6.82(5H, 1 phenyl) from 1 DL-phenylalanine. (ii). FAB mass spectrum of compound **220** showing the mono-conjugate structure (MH)⁺ 710 (C$_{43}$H$_{43}$O$_5$N$_5$).
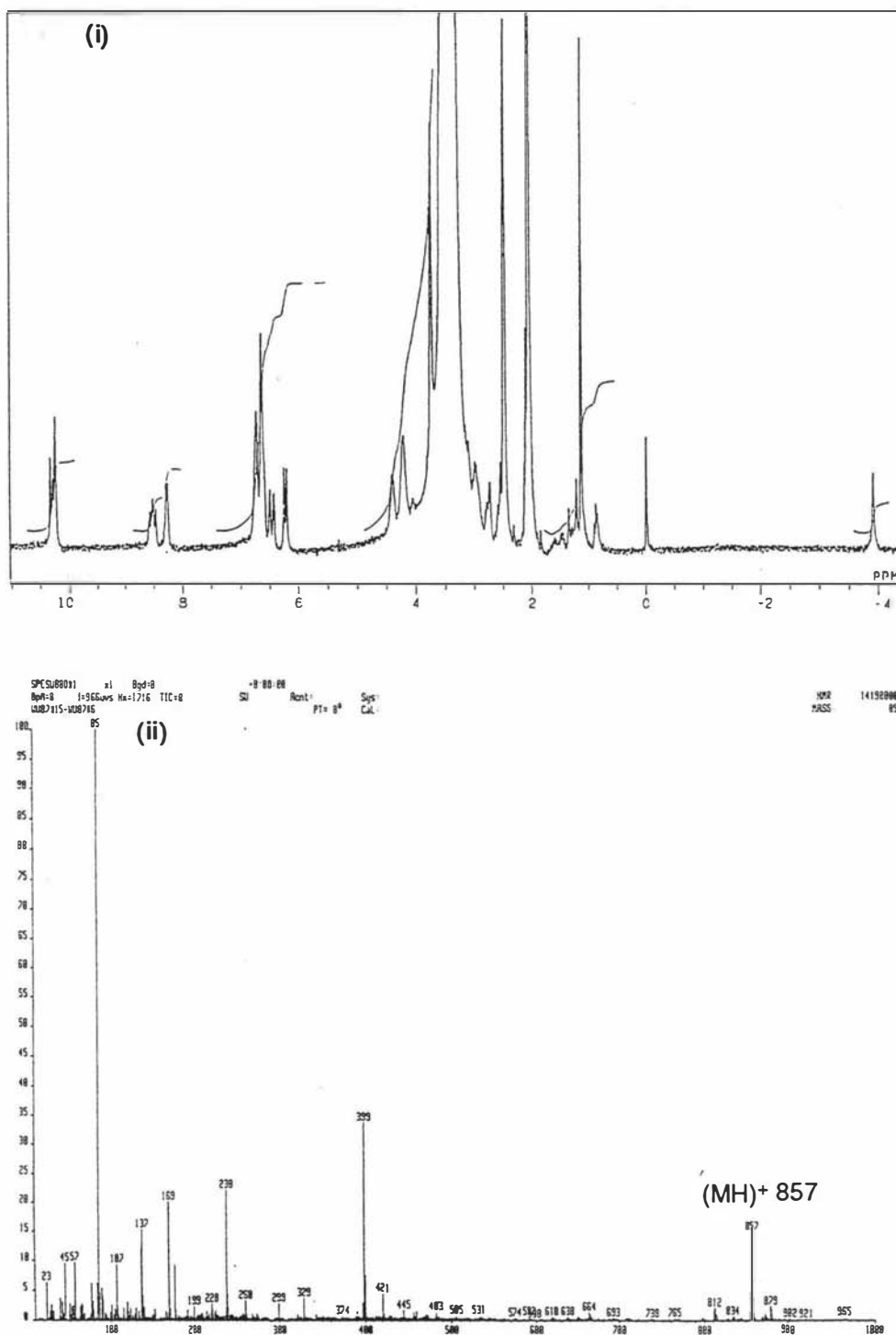
Figure 45e (i)^{1}H NMR spectrum of compound **221a** showing the double-conjugate structure of protoporphyrin IX with DL-phenylalanine. i.e.δ = -3.90(2NH), 6.23 and 6.46(2CH$_2$=), 8.52(2=CH), 10.28(4H) from 1 protoporphyrin IX ring; while δ = 6.68 (10H, 2 phenyl) from 2 DL-phenylalanines. (ii) FAB mass spectrum of compound **221a** showing the double-conjugate structure (MH)$^+$ 857 (C$_{52}$H$_{52}$O$_6$N$_6$).

Figure 45f (i) ^{1}H NMR spectrum of compound **221b** showing the double-conjugate structure of protoporphyrin IX with DL-phenylalanine. i.e. δ = -3.86 (2NH), 6.24 and 6.53(2CH$_2$=), 8.54(2=CH), 10.29(4H) from 1 protoporphyrin IX ring; while δ = 6.67 (10H, 2 phenyl) from 2 DL-phenylalanines. (ii) FAB mass spectrum of compound **221b** showing the double-conjugate structure (MH)$^+$ 857.5 (C$_{52}$H$_{52}$O$_6$N$_6$).

4.2.3.4 *Protoporphyrin IX-tryptophan (L) conjugates 222, 223*

The preparation of the title compounds was performed by a procedure similar to that used in the preparation of **220**. L-Tryptophan (2.6 mg, 0.0127 mmol) and protoporphyrin IX di-*p*-nitrophenyl active ester **218** (0.01 mmol) were used in the reaction. HPLC (same solvents and gradient as above) analysis showed the following results: For compound **216** (starting material); retention time: 9 minutes, 9% yield; mono-conjugates of protoporphyrin IX-tryptophan (L) **222**; retention time: 10.3 minutes, 65% yield (Figure 46a); FABMS: m/z, 750 (MH)$^+$ (C$_{45}$H$_{45}$O$_5$N$_6$); δ_H (DMSO-d$_6$) -3.81(s, 2H, 2NH), 6.24(d, J = 10.99 Hz, 2H, CH$_2$=), 6.48(d, J = 17.95 Hz, 2H, CH$_2$=), 6.80-7.38(m, 4H, phenyl), 8.48-8.62(m, 3H, 2=CH and CONH), 10.29-10.38(m, 4H, 5,10,15, and 20-H), 10.62(s, 2H, $^+$NH$_2$) (Figure 46b); double-conjugate of protoporphyrin IX-tryptophan (L) **223**; retention time: 15.5 minutes, 18% yield; impurity: retention time: 23 minutes, 8% yield.

222 (mixture of 6, 7 mono-conjugates)
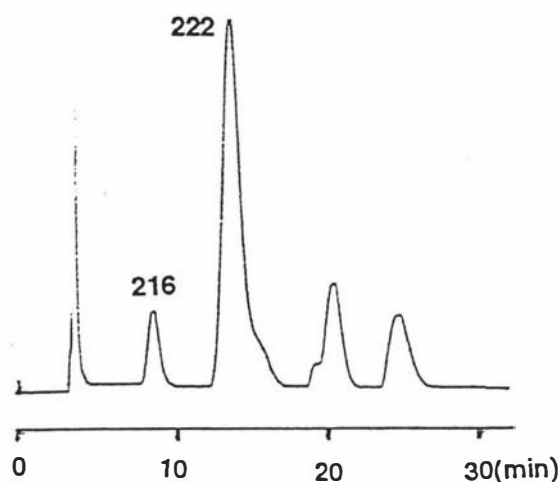

Figure 46a HPLC analysis of the reaction mixture of protoporphyrin IX di-*p*-nitrophenyl active ester **218** with L-tryptophan showing mono-conjugates **222** (retention time: 14.5 minutes, 65% yield).
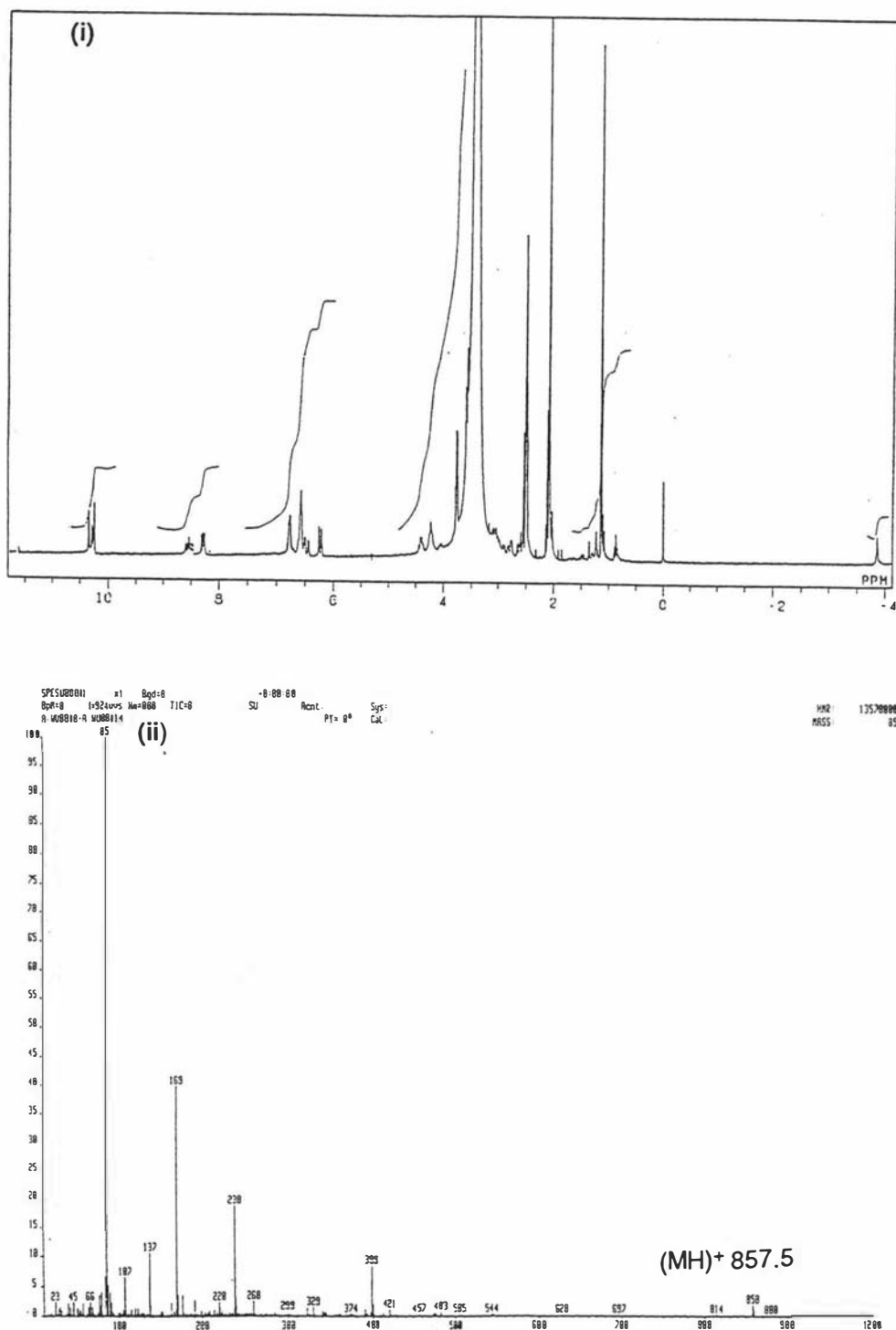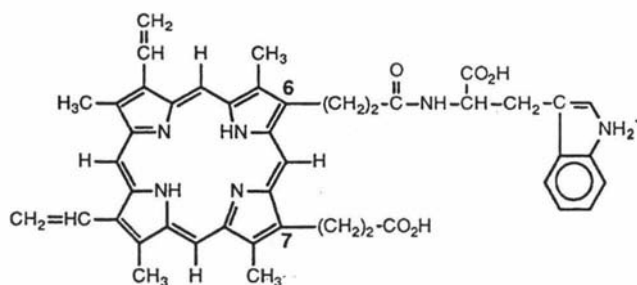
Figure 46b (i). ^{1}H NMR spectrum of compound **222** showing the mono-conjugate structure of protoporphyrin IX with L-tryptophan. i.e. δ = -3.81(2NH), 6.23 and 6.46 (2CH$_2$=), 8.32-8.58 (2=CH and CONH), 10.22-10.31 (4H) from 1protoporphyrin IX ring; while δ = 7.09 (4H, phenyl) from 1 L-tryptophan. (ii). FAB mass spectrum of compound **222** showing the mono-conjugate structure (MH)$^+$ 750 (C$_{45}$H$_{45}$O$_5$N$_6$).

4.2.3.5 *Protoporphyrin IX-arginine (L) conjugates 224*

The preparation of the title compounds was performed by a procedure similar to that used in the preparation of **220**. From the reaction of arginine (2.7 mg, 0.013 mmol) and 0.01 mmol of active ester **218**, the HPLC (same solvents and gradient as above) traces showed the following results: compound **216** (starting material); retention time: 9 minutes, 17% yield; mono-conjugate of protoporphyrin IX-arginine (L) **224**; retention time: 15 minutes, 73% yield; double-conjugate and impurity; 10% (Figure 47).

224 (mixture of 6, 7 mono-conjugates)

Figure 47. HPLC analysis of the reaction mixture of protoporphyrin IX di-*p*-nitrophenyl active ester **218** with L-arginine showing the mono-conjugates **224** (retention time: 17 minutes, 73% yield).
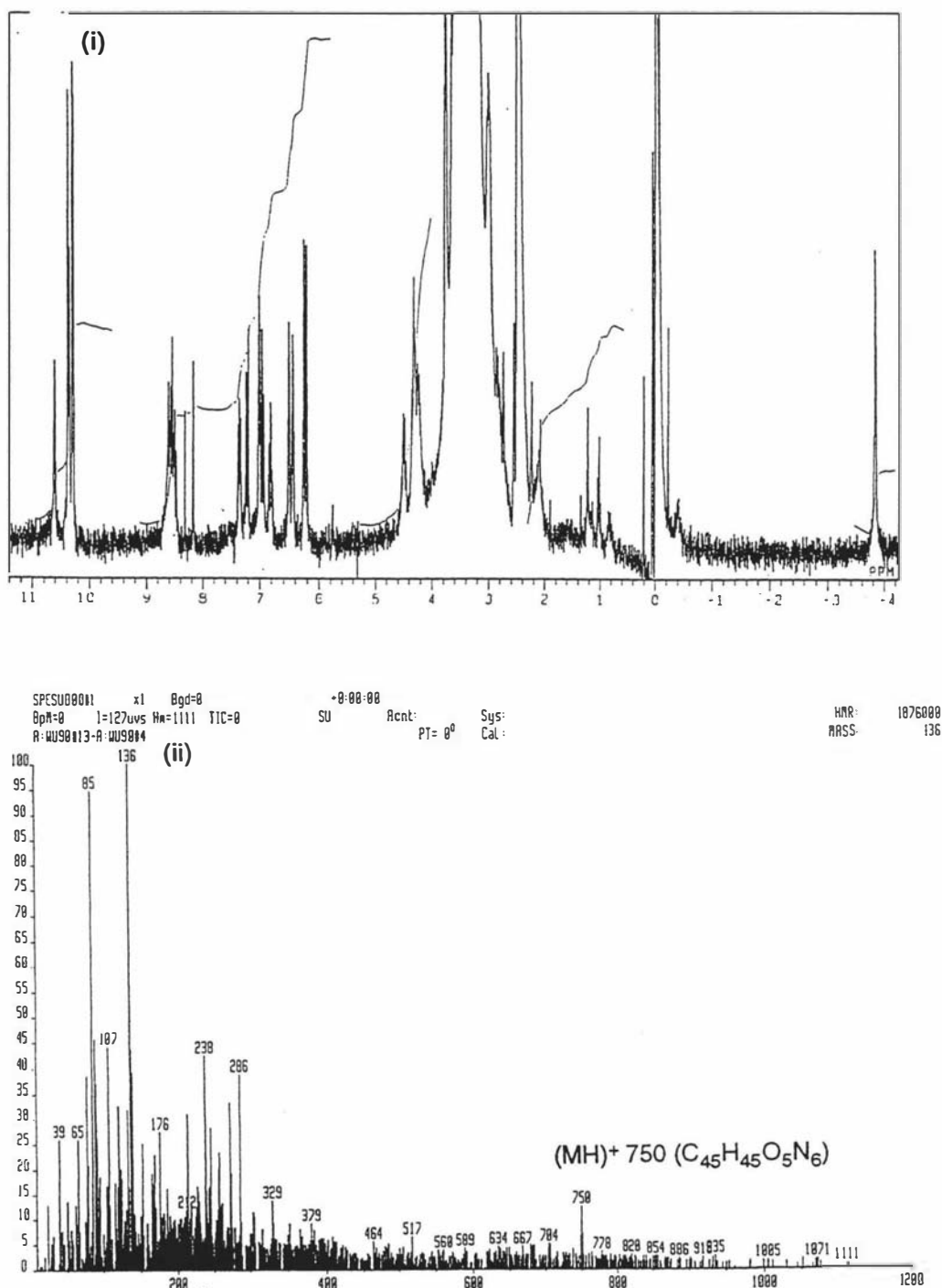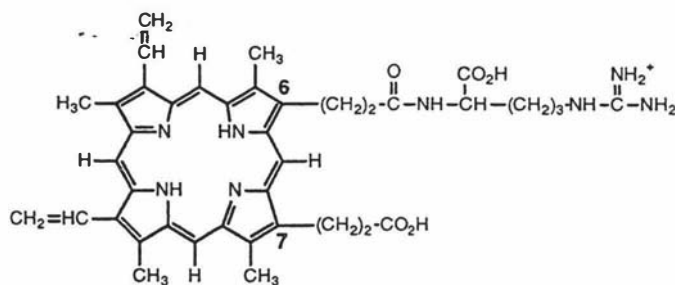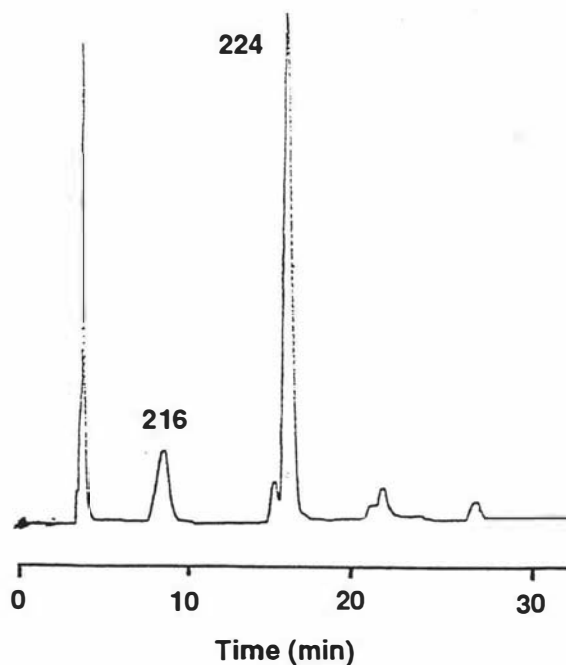
4.2.3.6 *Protoporphyrin IX-estrone glucuronide mono-conjugates 225*

The preparation of the title compound **225** was performed by a procedure similar to that used in the preparation of **220**. Two different HPLC solvent systems were used for the analysis (Solvent I: flow rate: 1 ml/minute, 0 to 5 minutes: 40% of solvent B; 5 to 35 minutes: a linear gradient of solvent B from 40% to 100%, retention times: protoporphyrin IX **216**, 12.3 minutes; protoporphyrin IX-estrone glucuronide mono-conjugates **225**, 13.8 minutes) (Figure 48a); Solvent II: flow rate: 1 ml/minute, 0 to 30 minutes: a linear gradient of solvent B from 0% to 100%, retention times: protoporphyrin IX **216**, 13 minutes; protoporphyrin IX-estrone glucuronide conjugate **225**, 16 minutes) (Figure 48b). The difference of the above two HPLC solvent systems for the isolation of compound **225** from the starting material **216** will be discussed in section 4.3 (Results and Discussion).

From the reaction of N-17-oxo-1,3,5(10)estratriene-3-yl-β-D-glucopyrano-siduronyl-L-lysine **214** (6.3 mg, 0.011 mmol) and 0.01 mmol of di-*p*-nitrophenyl active ester **218**, the HPLC analysis showed the following results: protoporphyrin IX **216**; 45% yield; protophyrin IX-estrone glucuronide mono-conjugate **225**; 45% yield; by-product; 10% yield. The separation of product **225** from the protoporphyrin IX **216** by isocratic reverse phase HPLC on a μBondapak C_{18} column (Solvent I: 45% of solvent B, twice) showed that the product **225** was contaminated by a very small amount of unsubstituted protoporphyrin IX **216** (Figure 48c).

A gel fitration column (Sephadex G-15, 150 mm x 18 mm) and an LKB Bromma automatic fraction collector were connected to the FPLC system for the further separation of product **225** from protoporphyrin IX **216** (solvent: 50% aqueous DMF; flow rate: 0.5 ml/minute; system pressure: 1 MPa). Thirty five 1.5 ml fractions were collected and the purity of the fractions was examined by UV spectrophotometry at 404 nm (Figure 48d). Combining fractions number 7 to 13 showed one peak (product **225**) and numbers 19 to 25 showed a second peak (a mixture of protoporphyrin IX **216** and *p*-nitrophenol). The results of the separation of the products by gel filtration was confirmed by HPLC analysis (Solvent I as above) (Figure 48e).
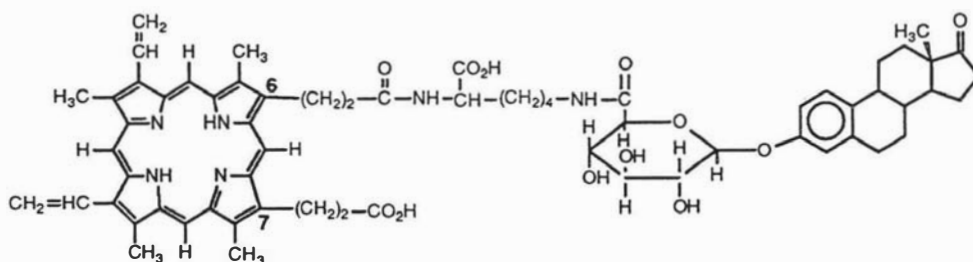
225 (mixture of 6, 7 mono-conjugates)

For compound **225**: Electronic spectrum (λ_{max}, methanol): 404 nm, 504 nm, 540 nm, 574 nm, 630 nm; High Resolution FABMS: m/z, 1119.5458 (MH)$^+$ (calculated for $C_{64}H_{75}N_6O_{12}$, 1119.5443, 1.3 ppm difference) (Figure 48f).

δ_H (DMSO-d$_6$) -3.86 (s, 2H, 2NH from protoporphyrin IX), 0.61(s, 3H, 18-CH$_3$ from steroid), 6.24(d, J = 11.72 Hz, 2H, CH$_2$= from protoporphyrin IX), 6.42-6.51(m, 2H, CH$_2$= from protoporphyrin IX), 6.60(s, 1H, aromatic 4'-H from steroid), 6.68-6.95(m, 2H, aromatic 1' and 2'-H from steroid), 7.79(m, 1H, CONH), 8.50-9.61(m, 2H, 2 =CH from protoporphyrin IX), 10.25-10.37(m, 4H, 5, 10, 15, and 20-H from protoporphyrin IX) (Figure 48g).
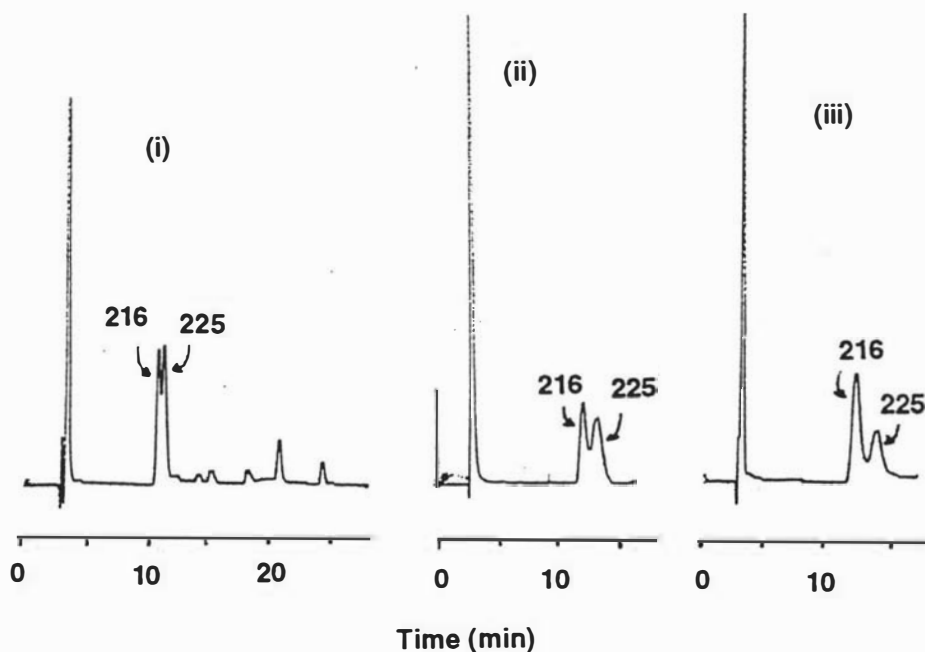
Figure 48a. HPLC analysis of product **225** (Solvent I) **(i):** A linear gradient of solvent B from 40 to 100% over 30 minutes; **(ii):** Isocratic 40% over 5 minutes, then running the same gradient as condition (i) and the result showed that condition (ii) gave better resolution than (i); **(iii):** Same gradient as condition (ii) for the mixture (1:1) of **216** and product **225**. Intensity of the first peak increased showing second peak is product (conjugate) **225**.
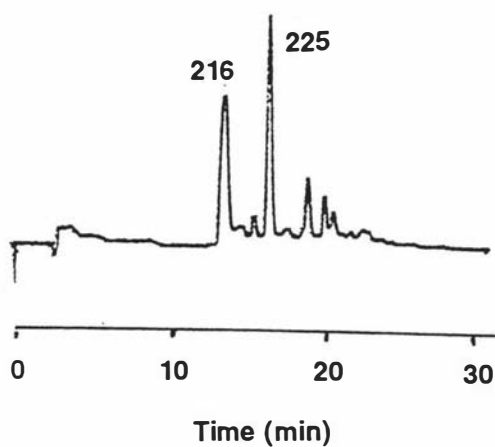
Figure 48b. HPLC (Solvent II) showing the better resolution achieved for product **225** when using solvent II.
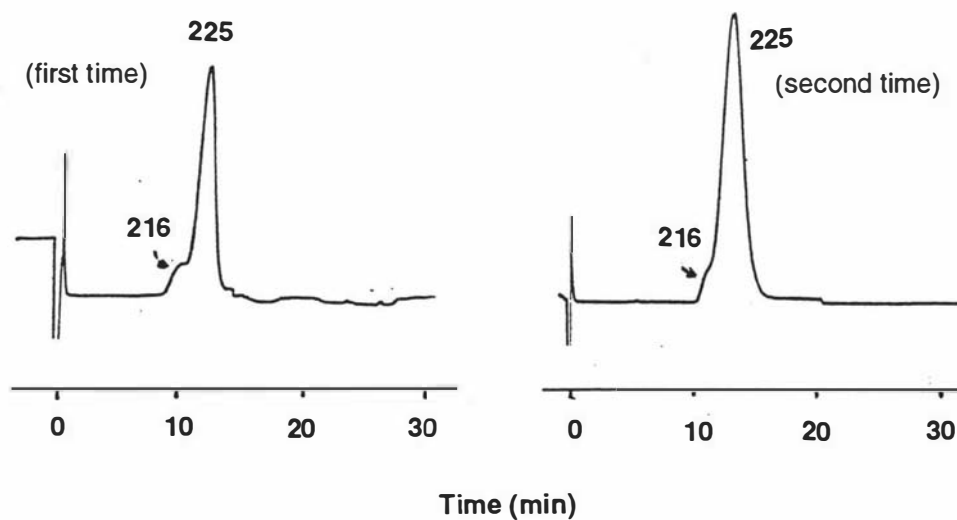
Figure 48c Two HPLC (Solvent I) analyses showing product **225** was contaminated by small amount of protoporphyrin IX **216** after isolation by HPLC (twice).
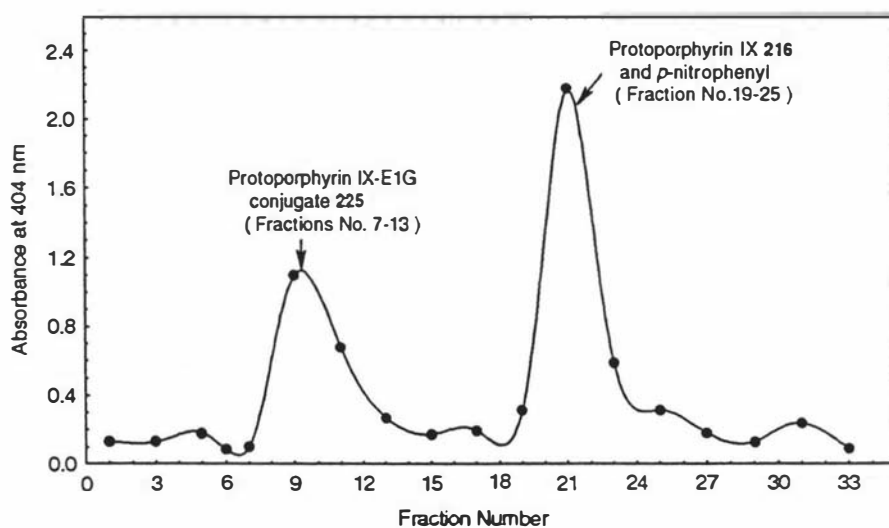
Figure 48d. Gel filtration analysis (50% aqueous DMF) showing excellent separation between the conjugate product **225** and protoporphyrin IX **216**.
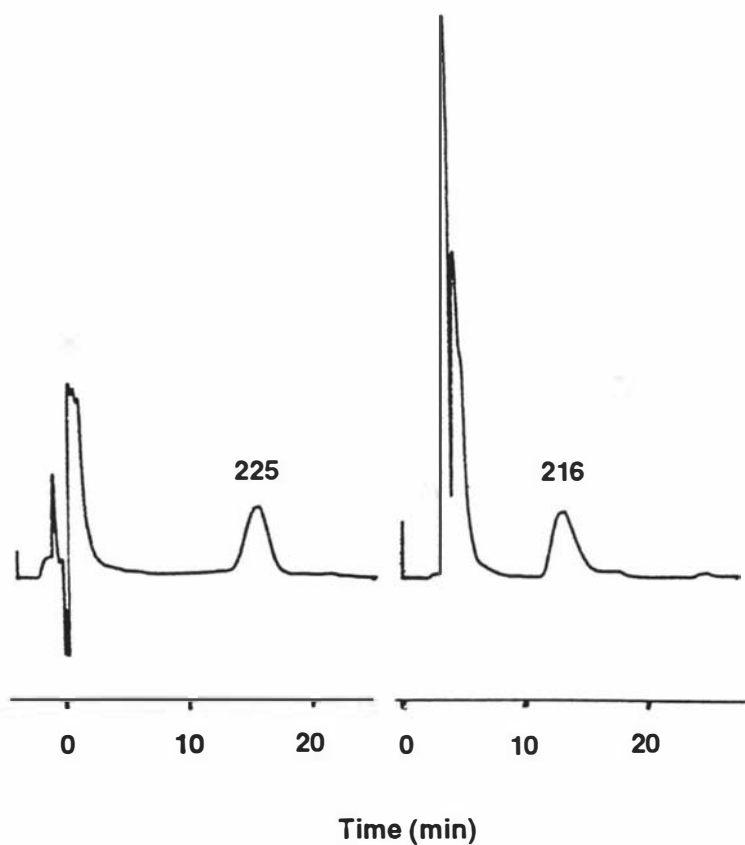
Figure 48e. HPLC (Solvent I) analysis further confirmed the effectiveness of the gel filtration isolation and the high purity of the product **225**.
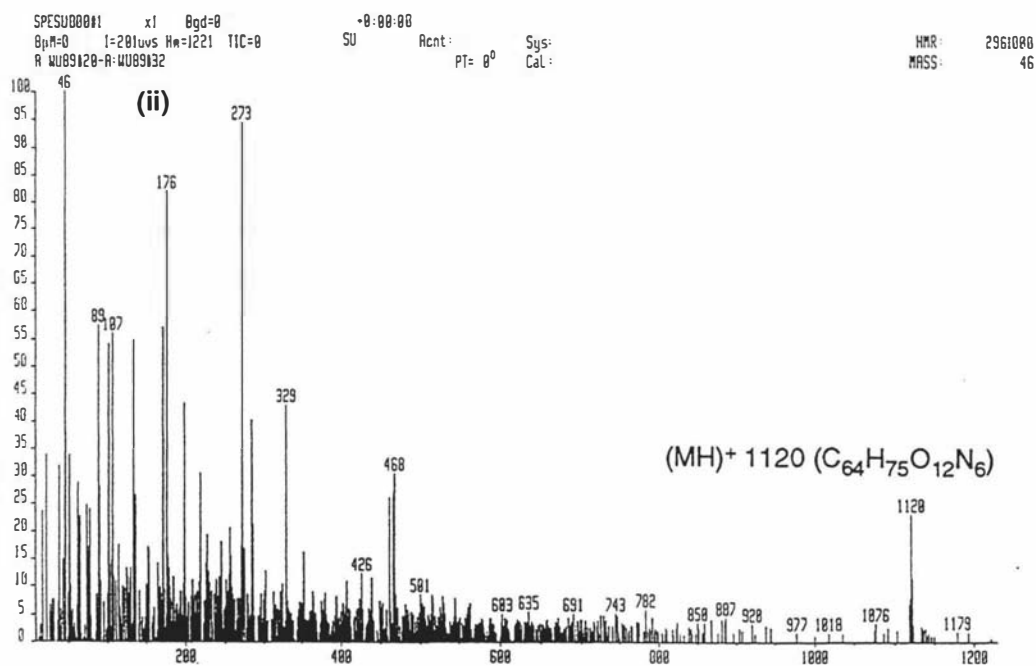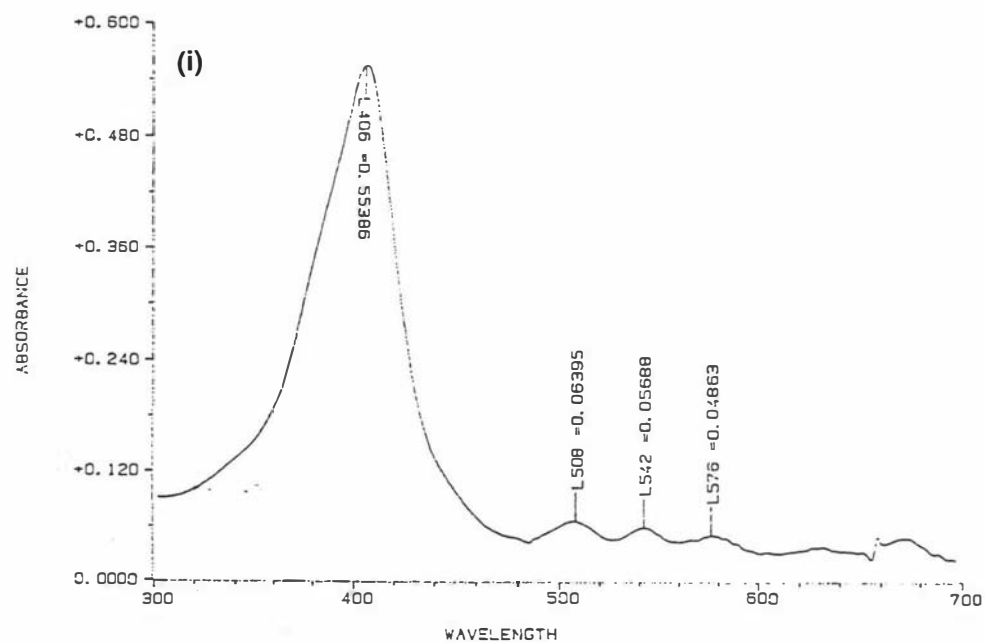
Figure 48f. (i): Electronic spectrum of conjugate product **225** showing its typical porphyrin structure. (ii). FAB mass spectrum of conjugate **225** showing the mono-conjugate structure (MH)$^+$ 1120 ($C_{64}H_{75}O_{12}N_6$).

Figure 48g
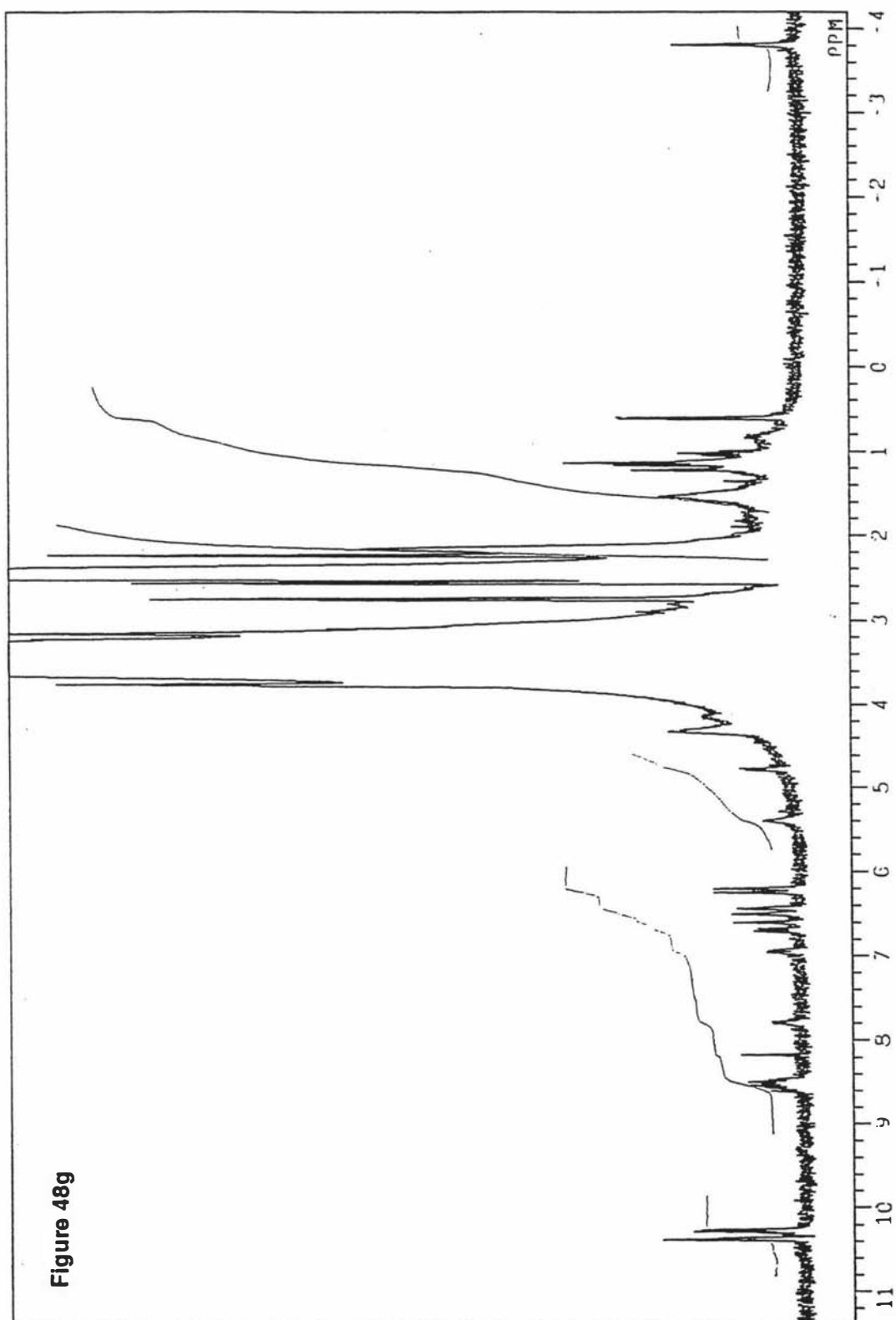
4.2.3.7 *Protoporphyrin IX-pregnanediol glucuronide mono-conjugate 226*

The preparation of the title compound **226** was performed by a procedure similar to that used in the preparation of **220**. The same solvent system and conditions were used for the analysis of compound **226** as described for compound **225** (Solvent I: retention times: protoporphyrin IX **216**, 12.3 minutes, protoporphyrin IX-pregnanediol glucuronide conjugate **226**, 24 minutes) (Figure 49a).

From the reaction of N-20α-hydroxy-5β-pregnane-3α-yl-β-D-glucopyrano-siduronyl-L-lysine **215** (6.9 mg, 0.011 mmol) and 0.01 mmol of di-*p*-nitrophenol active ester **218**, the HPLC analysis showed the following results: protoporphyrin IX **216**, 43% yield; protoporphyrin IX-pregnanediol glucuronide mono-conjugate **226**, 45% yield; by-product: 12% yield. The separation of product **226** from the reaction mixture was achieved by isocratic reverse phase HPLC on a μBoudapak C_{18} column (Solvent I: 55% of solvent B).
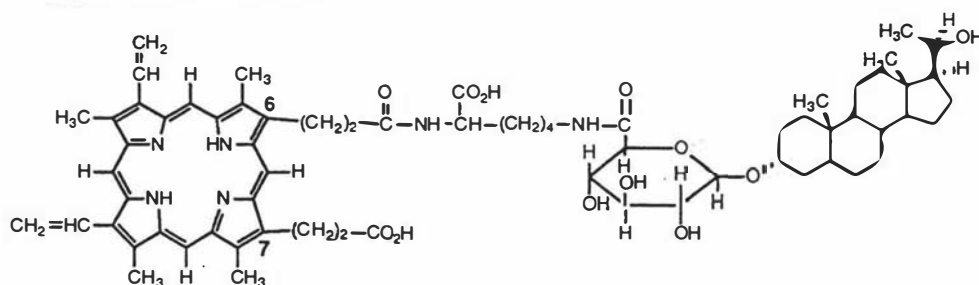
226 (mixture of 6, 7 mono-conjugates)

For the mono-conjugate of protoporphyrin IX-pregnanediol glucuronide **226**: Electronic spectrum (λ_{max}, methanol): 404 nm, 504 nm, 540 nm, 576 nm, 630 nm; FABMS: m/z, 1170 (MH)$^+$ ($C_{67}H_{89}N_6O_{12}$) (Figure 49b).
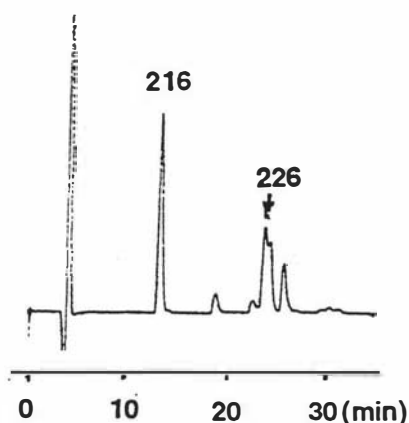
Figure 49a. HPLC (Solvent I) analysis of conjugate compound **226** (retention time: 24 minutes, 45% yield).
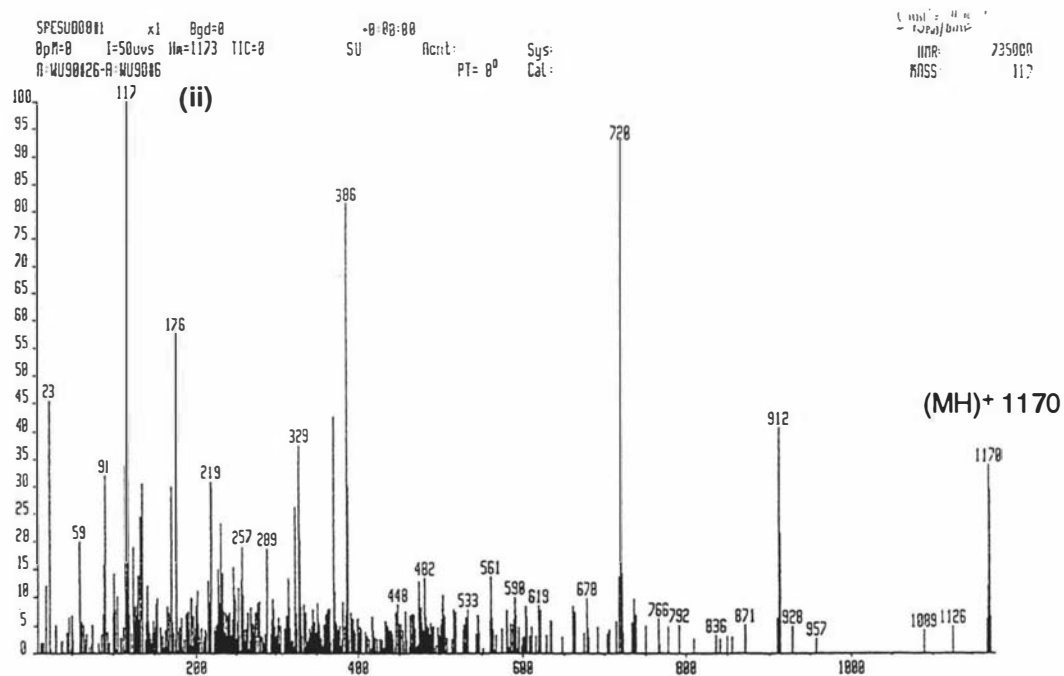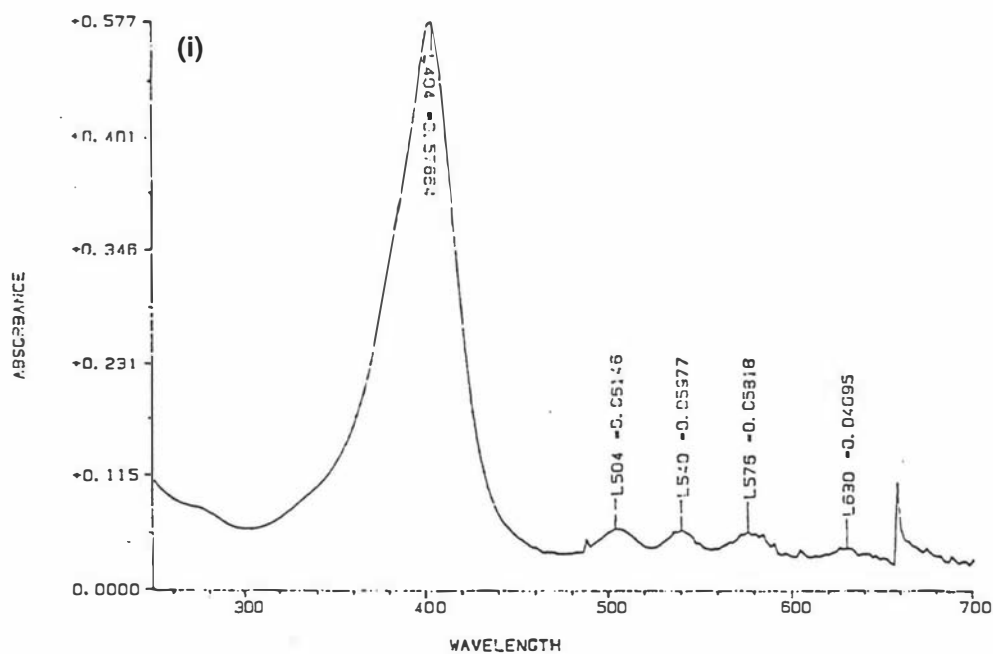
Figure 49b (i): Electronic spectrum of conjugate product **226** showing its typical porphyrin structure. (ii). FAB mass spectrum of conjugate **226** showing the mono-conjugate structure $(MH)^+$ 1170 $(C_{67}H_{89}O_{12}N_6)$.

4.2.4. Synthesis of hemin conjugates of amino acids and steroid glucuronides.

Hemin conjugates can be prepared either by insertion of Fe^{2+} ions into the related protoporphyrin IX conjugates or by direct conjugation from hemin chloride **227** through its active ester (Schemes 39 and 40).

4.2.4.1 *Di-p-nitrophenyl Hemin active ester 228*

Hemin chloride **227** (100 mg, 0.153 mmol), *p*-nitrophenol (85 mg, 0.61 mmol) and dicyclohexylcarbodiimide (63 mg, 0.31 mmol) were dissolved in 4 ml of dry pyridine. The reaction mixture was stirred at room temperature overnight (15 hours) and then filtered to remove N, N-dicyclohexylurea and washed with 2 ml of pyridine. The filtrate and washings were combined and the solvent was removed under reduced pressure. The residue was further dried under high vacuum for 0.5 hour and redissolved in 50 ml of CH_2Cl_2. The solution was then passed through a short column of silica gel and the product eluted using CH_2Cl_2/CH_3COCH_3 (1:1). TLC ($CHCl_3/CH_3OH$, 9:1) showed pure product **228** (R_F = 0.6). After removal of the solvent, product **228** was obtained as a black solid (120 mg, 84%).
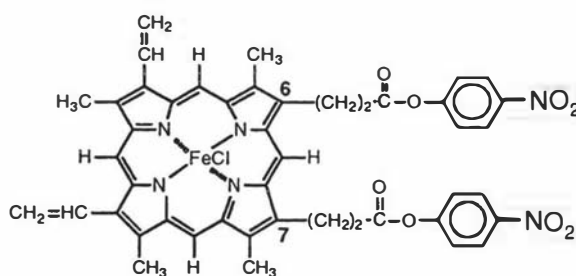
228 (di-*p*-nitrophenyl hemin active ester)

Electronic spectrum (λ_{max}, $CHCl_3$) 270 nm (NO_2), 396 nm; IR ν_{max} ($CHCl_3$) 3393 cm^{-1} (NH), 3020 cm^{-1} (unsaturated C-H), 1755 cm^{-1} (C=O, di-*p*-nitrophenyl ester), 1519 cm^{-1} (asymmetric $ArNO_2$), 1343 cm^{-1} (symmetric $ArNO_2$); High resolution FABMS, m/z, 858.2101 (M-Cl)$^+$ (calculated for $C_{46}H_{38}N_6O_8Fe$, 858.2098).

4.2.4.2 *Hemin mono-conjugate with phenylalanine 230*

To a solution of pure protoporphyrin IX mono-conjugate of phenylalanine **220** (3mg, 4.2 mmol) in dry DMF/CH$_3$CN (1:1) (10 ml) was added excess FeCl$_2$ (100 mg). The reaction mixture was refluxed under argon for 1 hour and protected from the light. The reaction was monitored by reverse phase HPLC analysis on a micro µBondapak C$_{18}$ reverse phase column (Solvent II: flow rate 1 ml/minute, a linear gradient from 0% to 100% of solvent B over 45 minutes, retention times: hemin-conjugate **230**, 12.5 minutes, protoporphyrin IX-conjugate **220**, 32 minutes) (Figure 50a). After 0.5 hour the reaction was cooled down to room temperature and the solvent was removed under reduced pressure. The residue was redissolved in DMF/H$_2$O (1:1) (5 ml) and the resulting solution was separated by reverse phase HPLC separation. The product **230** (2.73 mg, 85% yield) was obtained from the reaction mixture by isocratic reverse HPLC separation (Solvent II: 65% of solvent B, flow rate: 1 ml/minute, injection: 0.2 ml x 10 times). The purity of product **230** was confirmed by reverse phase HPLC analysis. For compound **230**: Electronic spectrum λ_{max}, methanol: 396 nm; FABMS: m/z, 764 (MH-Cl)$^+$ (C$_{43}$H$_{41}$N$_5$O$_5$Fe) (Figure 50d).
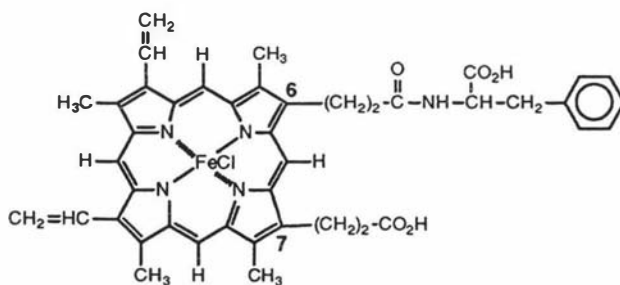
230 (mixture of 6, 7 mono-conjugates)

Hemin conjugates with phenylalanine (**230**, **231**) were also prepared from the conjugation of di-*p*-nitrophenyl hemin active ester **228** with L-phenylalanine as described below:

To a solution of freshly prepared di-*p*-nitrophenyl hemin active ester **228** (9 mg, 0.01 mmol) in dry DMF (1 ml) were added L-phenylalanine (2 mg, 0.012 mmol) and Et$_3$N (0.025 ml). The reaction mixture was stirred at room temperature overnight. After adding further Et$_3$N (0.1 ml) and stirring for another 0.5 hour the reaction

mixture was added to 20 ml of water, and freeze dried overnight to afford a black solid (12 mg). The residue was redissolved by adding a few drops of Et_3N and 5 ml of MeOH. TLC (EtOAc/MeOH/CHCl$_3$/HCOOH, 10:2:2:1) on silica gel showed no difference in R_F value (R_F = 0.73) between hemin **227** and its phenylalanine conjugate (**230, 231**). Hence the solution was analysed by reverse phase HPLC.

HPLC: The above solution (0.05 ml) was loaded onto a micro µBondapak C_{18} reverse phase column (Solvent III: flow rate 1 ml/minute, 30% of solvent B, isocratic). A wavelength of 405 nm and a sensitivity of 2.0 were used for detection. Hemin IX **227**: retention time: 10 minutes, 10% yield; hemin conjugates of phenylalanine (mono- and di-conjugates) (**230, 231**): retention time: 18 minutes, 90% yield; There was no separation between the mono- and double-conjugates (Figure 50b). FABMS m/z, for monoconjugate **230**: 764 (M)$^+$, 786 (M+Na)$^+$; for di-conjugate **231**: 910 (M)$^+$, 932 (M+Na)$^+$.

Hemin conjugates with phenylalanine (**230, 231**) were also prepared by direct coupling using the DCC/NHS method from the hemin mono-hydroxysuccinimide active ester **229** (Scheme 40), according to a literature procedure[164] as described below:

To a solution of hemin IX **227** (23 mg, 0.0356 mmol) in dry DMF (0.5 ml) N-hydroxysuccinimide (8 mg) was added, the solution was cooled to 0 ^{0}C, and a solution of dicyclohexylcarbodiimide (10 mg) in DMF (0.5 ml) was added dropwise by syringe with stirring over 45 minutes. The reaction was then kept at 0 ^{0}C (ice bath in cold room) overnight with stirring. The solution containing the mono-N-hydroxysuccinimidyl ester **229** was directly used for the next step without further purification. The solution of L-phenylalanine (6 mg, 0.036 mmol) and Et_3N (0.25 ml) in DMF (0.5 ml) was added next day, and the reaction mixture was stirred for 24 hours at room temperature. After adding cold water (50 ml) to the reaction mixture, the solution was titrated to pH = 3.5 until a red precipitate formed. The fine red precipitate was separated from the reaction mixture by centrifugation, and further dried under high vacuum. The black solid (25 mg) was prepared for HPLC analysis. The HPLC (Solvent III: flow rate 1 ml/minute, 30% of solvent B, isocratic) trace showed a low yield of products: hemin IX **227** (starting material); 70% yield; mono- and di-conjugate (**230, 231**): 30% yield (Figure 50c).

Figure 50b. HPLC analysis showing the high yield of products (**230, 231**), but no separation between the mono-conjugate **230** and the double-conjugate **231**.

Figure 50a. (i). HPLC analysis showing the protoporphyrin IX-conjugate **220** before the insertion of FeCl₂;(ii).HPLC analysis showing the mixture of hemin product **230** and the starting material **220** after 15 minutes; (iii). HPLC analysis showing the pure product **230** after 30 minutes.
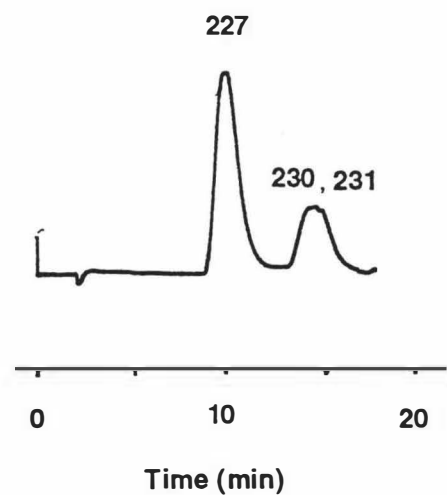
Figure 50c. HPLC analysis showing the poor yield of conjugates (**230, 231**) with the direct DCC method.
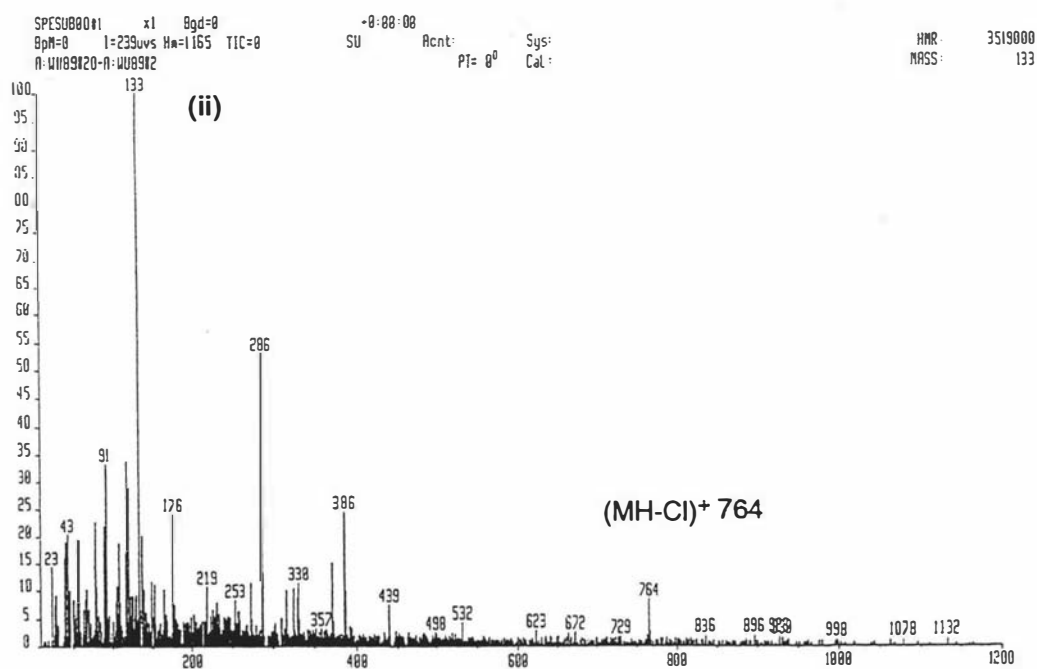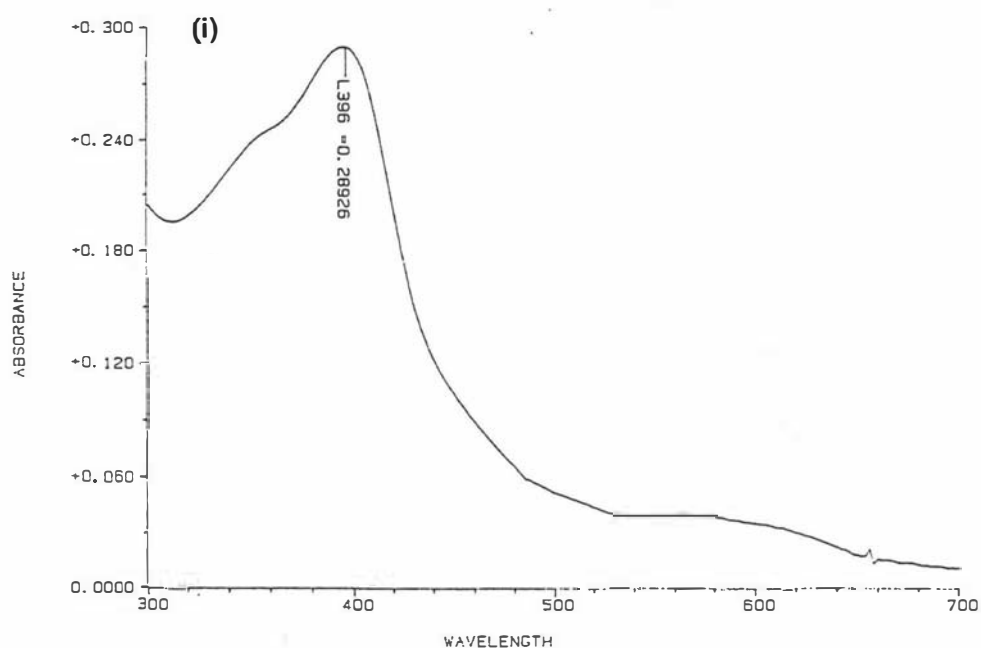
Figure 50d (i): Electronic spectrum of conjugate product **230** showing its typical heme structure;(ii).FAB mass spectrum of conjugate **230** showing the hemin mono-conjugate structure (MH-Cl)$^+$ 764 ($C_{43}H_{41}N_6O_5Fe$).

4.2.4.3 *Hemin mono-conjugate of estrone glucuronide 232*

The preparation of the title compound **232** was performed by an Fe^{2+} insertion procedure similar to that used in the preparation of **225** and the reaction was also monitored using the same reverse phase HPLC analysis as used for compound **230**. After the reaction and evaporation of the solvent, the residue was added to 30 ml of citrate buffer (pH = 5.3, 0.1M) and the solution was passed through 2 Sep-Pak columns in series. The column assembly was washed with citrate buffer (30 ml) and deionized water (30 ml) until the filtrate became colourless, and the product **232** was eluted with pure MeOH (20 ml). After evaporating the MeOH, the hemin mono-conjugate of estrone glucuronide **232** (0.11 mg, 8.85 x 10^{-5} mmol, 75% yield) was obtained from the protoporphyrin IX-conjugate **225** (0.13 mg, 1.18 x 10^{-4} mmol). The purity of the product was confirmed by reverse phase HPLC analysis (Solvent III: flow rate 1 ml/minute, 70% of solvent B, isocratic, retention times: hemin mono-conjugate of estrone glucuronide **232**, 6 minutes; protoporphyrin IX-estrone glucuronide mono-conjugate **225**: 13.5 minutes) (Figure 51a). For compound **232**: Electronic spectrum (λ_{max} methanol): 402 nm; High resolution FABMS: m/z, 1172.4487 $(M-Cl)^+$ (calculated for $C_{64}H_{72}N_6O_{12}Fe$, 1172.4558, -6.0 ppm difference) (Figure 51e). The structure of the hemin mono-conjugate of estrone glucuronide **232** is shown in Figure 40 (section 4.1.2 Introduction).

The hemin-estrone glucuronide conjugate **232** was also prepared from the reaction of di-*p*-nitrophenyl hemin active ester **228** (0.01 mmol) with N-17-oxo-1,3,5-(10)estratriene-3-yl-β-D-glucopyranosiduronyl-L-lysine **214** (6.2 mg, 0.011 mmol) in the same procedure as used for the preparation of compound **230**. The HPLC (Solvent III: 30% of solvent B, isocratic) analysis showed the following results: hemin IX **227**: retention time: 10 minutes, 45% yield; hemin mono-conjugate of estrone glucuronide **232**: retention time: 15.5 minutes, 55% yield (Figure 51b); FABMS: m/z, 1172 (M-Cl)$^+$.

The conjugate **232** was also prepared by the direct DCC/NHS coupling procedure[164] as described for the preparation of hemin-phenylalanine conjugates. From the reaction of hemin IX **227** (29 mg, 0.044 mmol) and N-17-oxo-1,3,5-(10)estratriene-3-yl-β-D-glucopyranosiduronyl-L-lysine **214** (6.2 mg, 0.011 mmol), it was shown by HPLC (Solvent III: 30% of solvent B, isocratic) analysis that 11% of the hemin conjugate **232** and 89% of hemin IX **227** were present in the reaction products (Figure 51c).
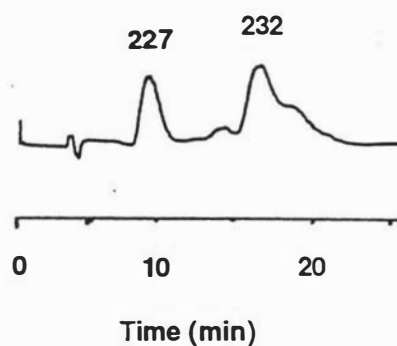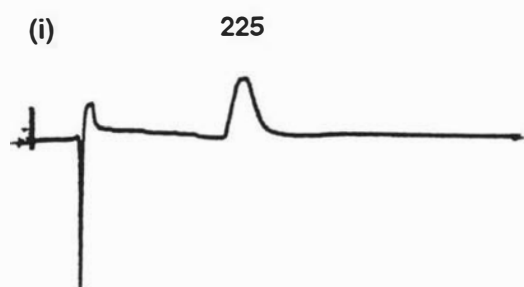
Figure 51b. HPLC analysis showing the mixture of products **232** and the starting material **225** prepared with the hemin di-*p*-nitrophenyl active ester method.
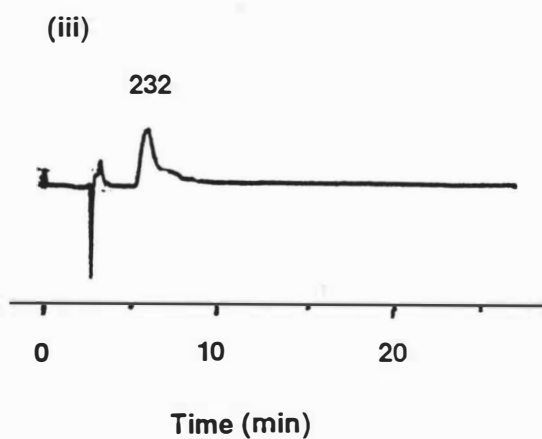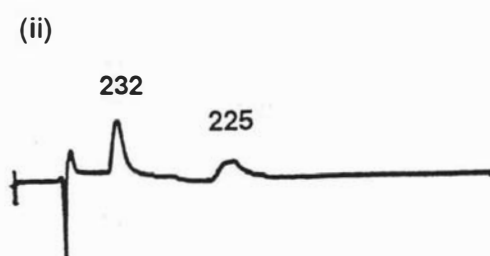
Figure 51a. (i). HPLC analysis showing the protoporphyrin IX-E1G conjugate **225** before the insertion of FeCl$_2$; (ii). HPLC analysis showing the mixture of hemin product **232** and the starting material **225** after 20 minutes; (iii). HPLC analysis showing the pure product **232** after 30 minutes.
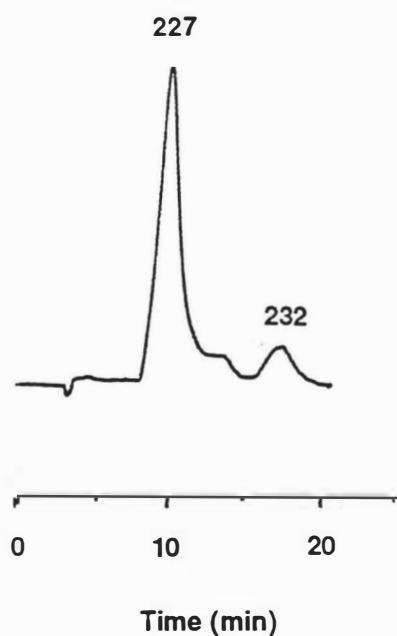
Figure 51c. HPLC analysis showing the very poor yield of product **232** with the direct DCC method.

A Further separation of hemin mono-conjugates of estrone glucuronide **232** from hemin IX **227** was successfully achieved with an alternative reverse phase HPLC system (Column Type: VYDAC, 218TP54 Protein & Peptide C18; <u>Solvent V:</u> 50% of solvent A, 25% of solvent B, 25% of C, isocratic) (Figures 51d and 51e). HPLC (Figure 51d) clearly showed that the mixture of two hemin (6, 7) mono-conjugates of estrone glucuronide **232** and hemin IX **227** were well separated. For the purified hemin mono-conjugates of estrone glucuronide **232**, FAB mass spectrum showed that only the mono-conjugates [(M-Cl)⁻, 1172] were present. The HPLC analysis (Figure 51e) also proved that the conjugates **232** had no contamination by unsubstituted hemin IX **227** after HPLC isolation to remove compound **227**.

Figure 51d. HPLC of mixture of hemin **227** and hemin-E1G conjugates **225**
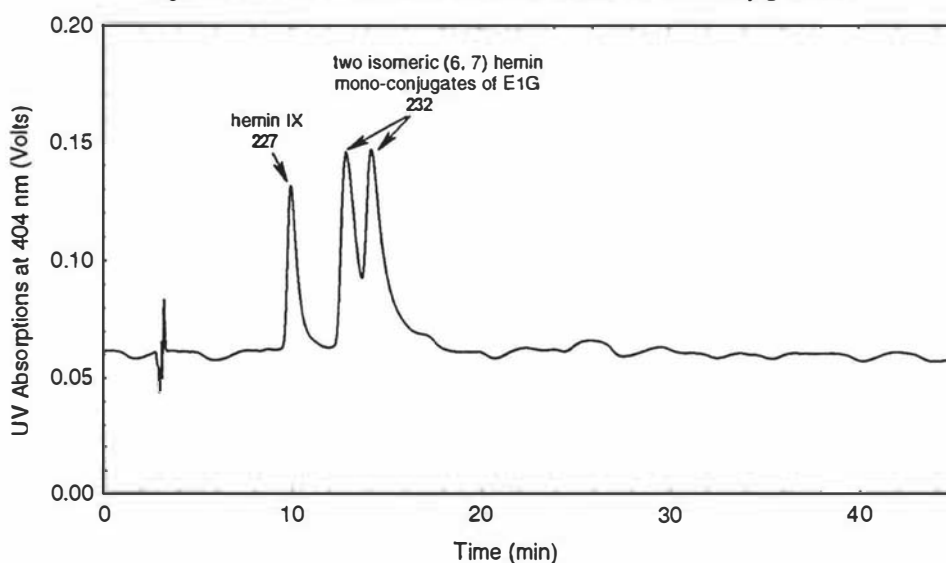
Figure 51e HPLC of purified mono-conjugates **232** separated from hemin 227
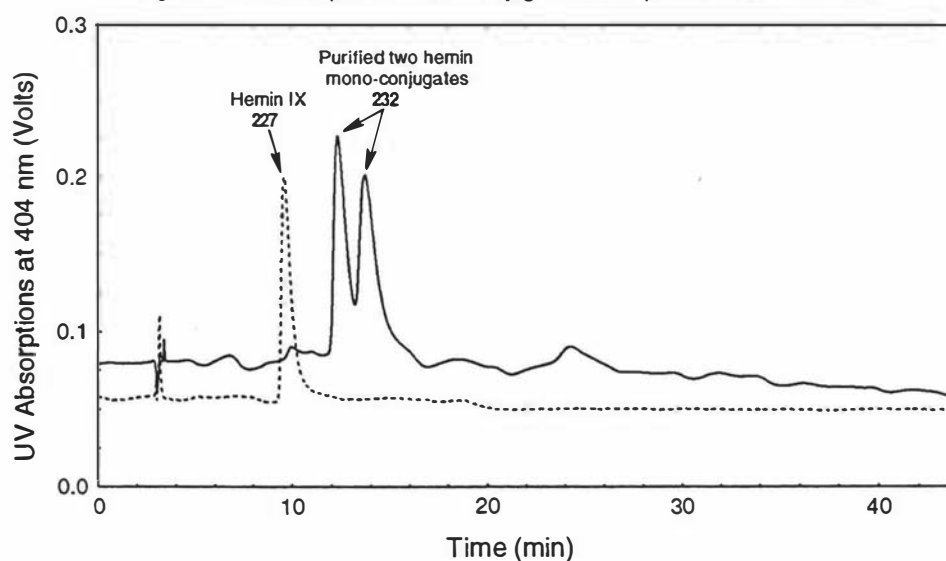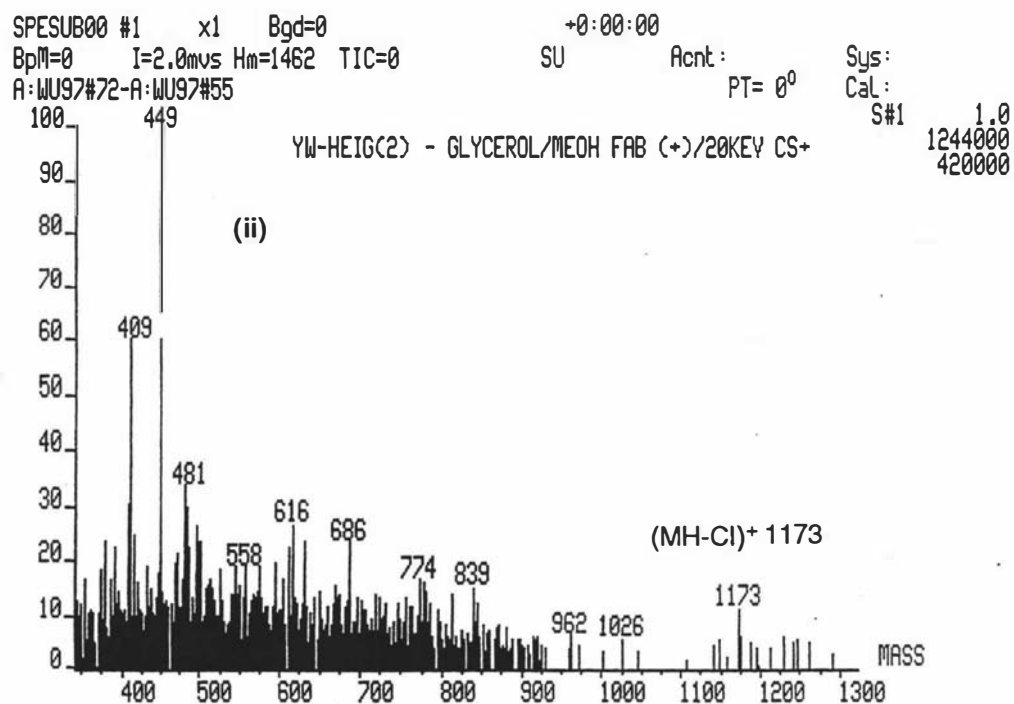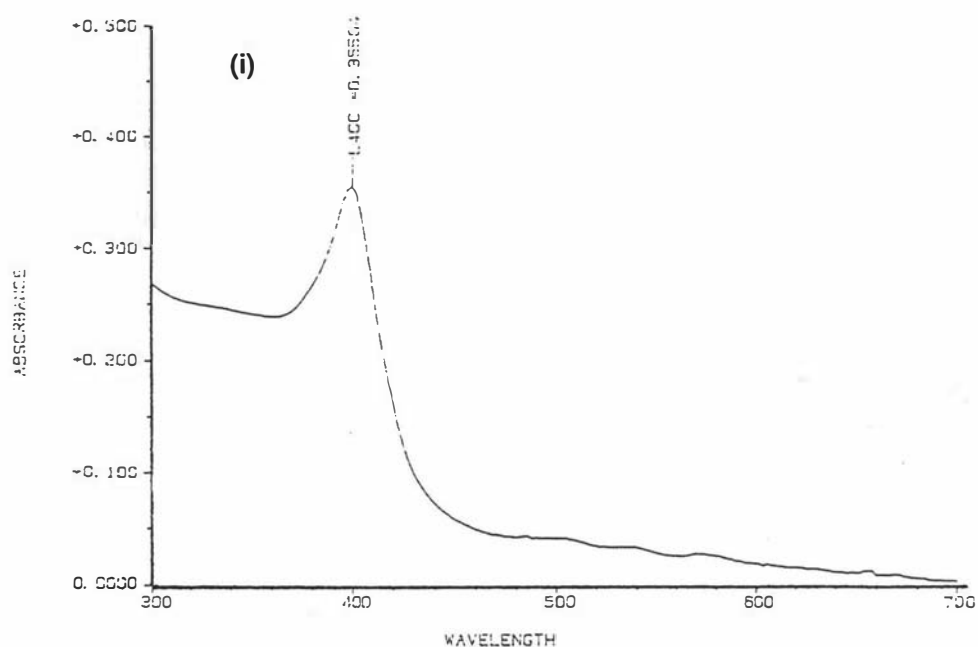
Figure 51f (i): Electronic spectrum of conjugate product **232** showing its typical heme structure;(ii).FAB mass spectrum of conjugate **232** showing the hemin mono-conjugate structure (MH-Cl)$^+$ 1173 ($C_{64}H_{72}N_6O_{12}Fe$).

4.2.4.4 *Hemin mono-conjugate with pregnanediol glucuronide 233*

The preparation of the title compound **233** was performed by a procedure similar to that used in the preparation of **232**. Reaction of protoporphyrin IX mono-conjugate of pregnanediol glucuronide **226** (0.10 mg, 8.65 x 10^{-5} mmol) and $FeCl_2$ (100 mg) afforded the product **233** (0.08 mg, 6.06 x 10^{-5} mmol, 70% yield). The purity of the product **233** was also confirmed by reverse phase HPLC analysis (Solvent III: 70% of solvent B, isocratic, retention times; hemin-pregnanediol glucuronide conjugate **233**: 6 minutes; protoporphyrin IX-pregnanediol glucuronide conjugate **226**: 12.5 minutes) (Figure 52a). For compound **233**: Electronic spectrum (λ_{max}, methanol): 400 nm (Figure 52b). FABMS: m/z, 1224 (MH-Cl)$^+$ ($C_{67}H_{86}N_6O_{12}Fe$).


233 (mixture of 6, 7 mono-conjugates)
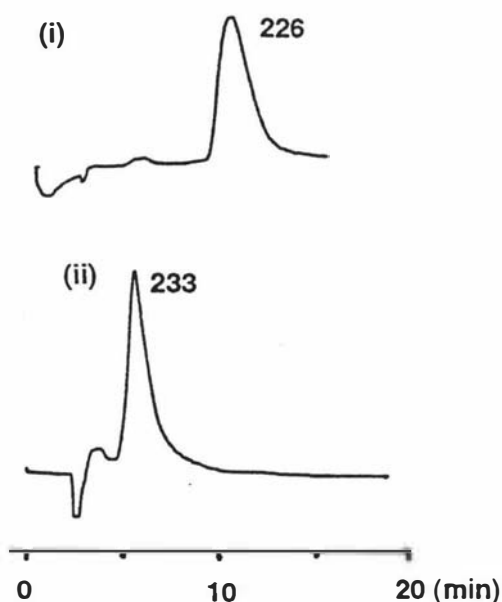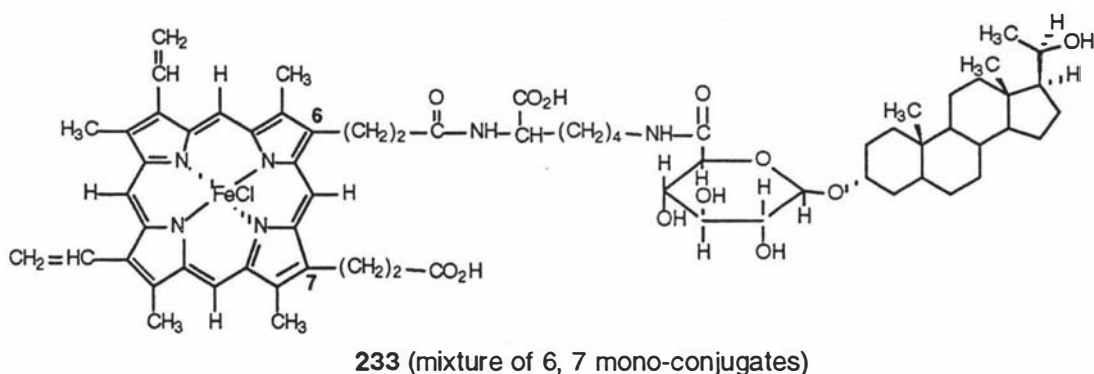
Figure 52a. (i). HPLC analysis showing the protoporphyrin IX-PdG conjugate **226** before the insertion of $FeCl_2$;(ii).HPLC analysis showing the pure hemin-conjugate product **233** after 30 minutes of the insertion reaction with $FeCl_2$.
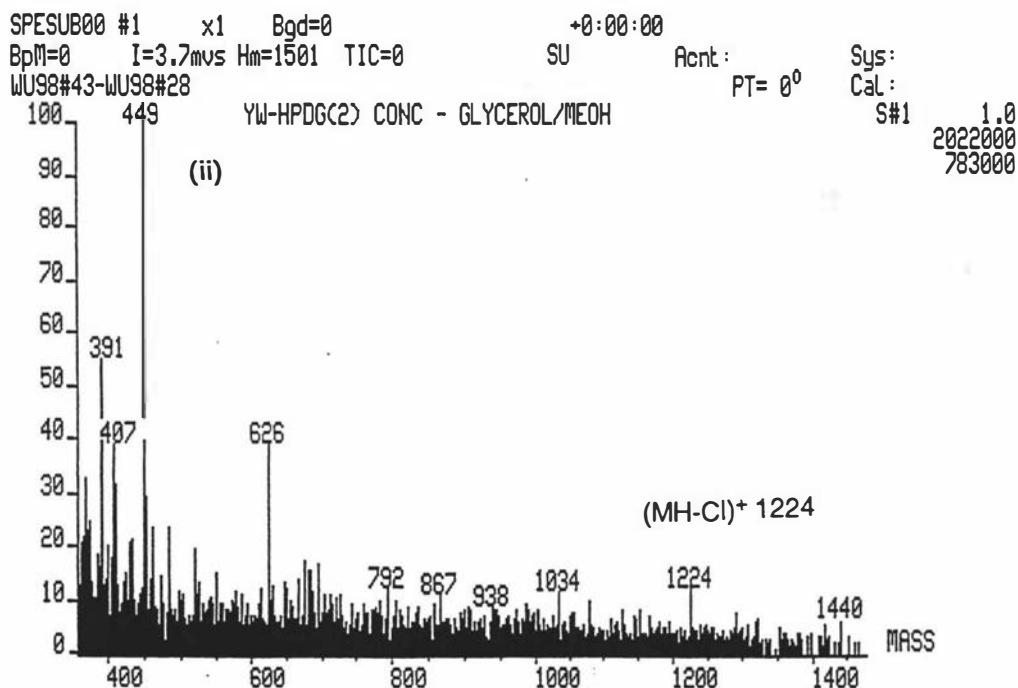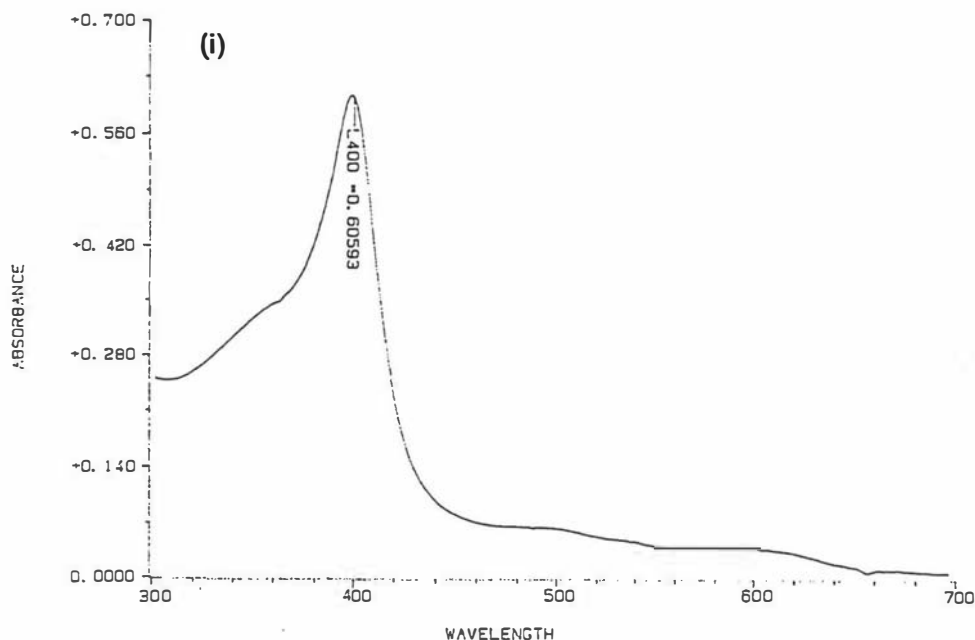
Figure 52b (i): Electronic spectrum of conjugate product **233** showing its typical heme structure;(ii).FAB mass spectrum of conjugate **233** showing the hemin mono-conjugate structure $(MH-Cl)^+$ 1224 $(C_{67}H_{86}N_6O_{12}Fe)$.

4.3 Results and Discussion

4.3.1 Preparation of estrone glucuronide and pregnanediol glucuronide-L-lysine conjugates

In the present work, a simple procedure for the preparation of the key steroid glucuronide-L-lysine conjugates (**214, 215**), required for development of new assays for definition of the fertile period, has been developed and the results described. The free amino group of the bis-copper-L-lysine chelate **184** was easily coupled to the carboxylic acid group of the steroid glucuronides by a standard peptide-forming reaction at room temperature. Without any isolation or purification, the resulting product was directly removed from the copper in the presence of Chelex 100 resin to give the required steroid glucuronide-L-lysine conjugates in moderate yields (Scheme 39) and good purity.

The E1G-L-lysine and PdG-L-lysine conjugates (**214, 215**) were well distinguished from the starting materials (E1G **12** or PdG **16**) as shown by HPLC analysis. The HPLC (Figure 43a) clearly showed significant differences in retention times between the conjugate **214** (10.25 minutes) and the starting material **12** (15.07 minutes). The same was also true for the conjugate **215** (7.72 minutes) and its starting material **16** (1.89 minutes) (Figure 44a). The purity of both conjugates **214** and **215** was demonstrated by HPLC, where it was shown that only trace amounts of starting materials were present. The FAB mass spectroscopy (Figures 43b and 44b) of E1G- and PdG-L-lysine conjugates **214** and **215** showed a molecular ion peak m/e at 575 or 625, respectively, which was consistent with the assigned structures of both conjugates.

Since steroid glucuronides contain acid-sensitive glycosidic bonds, the present procedure provided neutral reaction conditions for the removal of copper by using Chelex resin, which is much more suitable than a reported literature procedure[149] using EDTA/HCl. This simple, one-pot reaction procedure also provided an opportunity for employing different side chain lengths or types of amino acids as molecular linkers for conjugation with other compounds.

4.3.2 Acylation reactions of unprotected amino acid derivatives

As discussed in the introduction of this chapter (section 4.1.4), for the synthesis of the hemin-steroid glucuronide conjugates, it is the strategy in this thesis to introduce an extra carboxyl group into a position similar to that of the hemin propionic acid position by the molecular linker. The new enzymes arising from the reconstitution of these hemin conjugates with apo-proteins are expected therefore to maintain higher enzymatic activities. Obviously, this structural requirement needs both carboxyl and amino groups at the same end of the molecular linkers such as with L-lysine **183** and other α-amino acids. The amino group can be used in the second stage for the linkage with the hemin IX propionic acid, while the carboxyl group can be preserved for supporting the successful reconstitution of hemin conjugates with apo-proteins.

The coupling reaction of the α-amino group of L-lysine **183** with one of the two hemin propionic acid groups can be performed starting with the α-amino acid ester or the unprotected α-amino acid directly. If the reaction commenced with the α-amino acid ester, both selective protection of the carboxyl group before the coupling and the deprotection after the coupling reaction are required. These two extra steps would be very inconvenient for the synthesis and purification of such complicated hemin-steroid glucuronide conjugates. Therefore, direct acylation of the unprotected α-amino acid derivatives was investigated and provided a simple and useful approach for the synthesis of hemin-E1G and hemin-PdG conjugates in this thesis (Scheme 39).

The acylation of a carboxyl group by conversion to the corresponding N-hydroxysuccinimide (HOSu) or *p*-nitrophenyl (HONp) active ester, followed by reaction with amino acids or esters under very mild conditions is known to be a useful and simple method for amide synthesis. However, the choice of suitable reaction conditions is always important in determining the chemical yields and structures of the reaction products. The acylation of α-amino acids by HOSu or HONp active ester derivatives is normally performed in a mixture of water and organic solvents.[154,155] There have been several reports in the literature on the formation of various side-products arising during peptide synthesis where the acylation of the carboxyl group is promoted by N-hydroxysuccinimide (HOSu). For example, in the presence of a basic aqueous system, the acylation reaction gives rise to a mixed succinohydroxamic anhydride **234** from the succinimidyl ester of fatty acids (scheme 41)[165] due to hydrolysis of the succinimide ring.

Scheme 41

$R = C_9H_{19}, C_{11}H_{23}, C_{15}H_{31}$
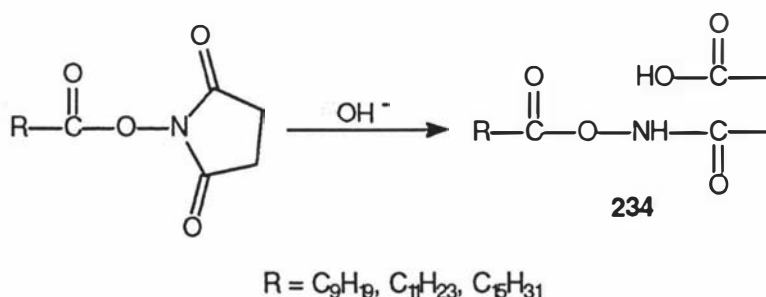
The reason for this side-product is that the long chain of the fatty acid sterically hinders the active ester group and gives rise to a greater chance for the OH⁻ ions to attack the succinimide carbonyl group by basic hydrolysis. When the acylation reaction was carried out under anhydrous conditions, only a very small amount of the above side-product, hydroxamic acid derivatives **234**, could be detected.[165]

Recently, research also showed that many carbohydrate compounds, which normally have polyhydric alcohol structures, can accelerate the hydrolysis of active esters, such as *p*-nitrophenyl esters, in aqueous solution.[166] Since the pKa values of hydroxyl groups in most carbohydrates and polyhydric alcohols are approximately 12 to 13,[166] the ionisation of the hydroxyl groups in these carbohydrate compounds or polyhydric alcohol often results in the formation of small amounts of the anion (RO⁻), which can display nucleophilic reactivity with active esters in neutral to alkaline aqueous solutions. Hence, careful consideration should be given to this fact when acylation with active esters is performed by an amine component having a carbohydrate moiety or polyhydric alcohol structure attached. For the synthesis of estrone glucuronide and pregnanediol glucuronide conjugates with protoporphyrin IX or hemin IX as in this thesis, it is obvious that aqueous reaction conditions should be avoided for the acylation step since the steroid glucuronides contain a polyhydric alcohol structure (the glucuronide ring). In general, anhydrous reaction conditions are more favourable than aqueous systems for the acylation of α-amino acids. Aqueous hydrolysis of active esters always produces either the free acids (by hydrolysis) or the above side-products, which compete with the desired aminolysis reaction and thus decrease the chemical yields.

The kinetics of acylation by *p*-nitrophenyl esters (ONp) **201** (scheme 37) indicates that the rate-limiting step for the aminolysis reaction is the addition of the

amino acid to generate the tetrahedral intermediate **203**.[154] Hence, (i) the choice of a polar solvent to provide the higher demand for solvation as a result of the ionic character of the tetrahedral intermediate **203**; and (ii) keeping the reaction conditions anhydrous to avoid hydrolysis of the active ester are the main criteria for successful acylation reactions. A simple procedure described in this thesis (scheme 40) provided a useful method for the selective acylation of α-amino acid derivatives with protoporphyrin IX or hemin compounds. The methodology satisfied the above requirements by directly using isolated succinimidyl (ONSu) **200** or p-nitrophenyl (ONp) **201** active esters of protoporphyrin IX or hemin IX in dry DMF solution and the solid form of the amino acids or their derivatives in the presence of Et_3N. The acylation reactions gave mainly the mono-coupled products despite the fact that the protoporphyrin IX **216** or hemin IX **227** active esters (**200, 201**) have very strong steric hindrance to the amino acids or steroid glucuronide derivatives.

There are several ways to prepare succinimidyl esters (ONSu) **200** for the acylation reactions. In the present work, it was found that the isolated, or pure, active esters gave much higher chemical yields of acylation products than those impure active esters **200** (crude mixture contaminated with other reagents) obtained by the direct DCC method[164] (see Figures 50b, 50c, 51b and 51c). Several side products were found in all cases and complete removal of the N, N-dicyclohexylurea (DCU) was not always possible. Hence, the prepared impure ONSu esters by the DCC method were usually used directly in acylation reactions without any separation or purification step. Therefore, a low yield of products was expected in the acylation reactions, especially in cases where both sterically hindered protoporphyrin IX or hemin acids and steroid glucuronide compounds are present.

We have found that use of isolated, pure ONp or ONSu esters of protoporphyrin IX or hemin, which were prepared from the corresponding acid chlorides with p-nitrophenol or N-hydroxysuccinimide, are superior to the direct DCC method for the acylation reactions, providing a simple method and good yield for the synthesis of monoacylated porphyrin or hemin derivatives. Similar superiority and convenience was also obtained by use of the thallium salt of N-hydroxysuccinimide with the corresponding acid chloride for the preparation of pure ONSu esters.[167] Recently, a new method for the preparation of pure succinimidyl esters (ONSu) **200** has been reported in a literature.[168]

Scheme 42
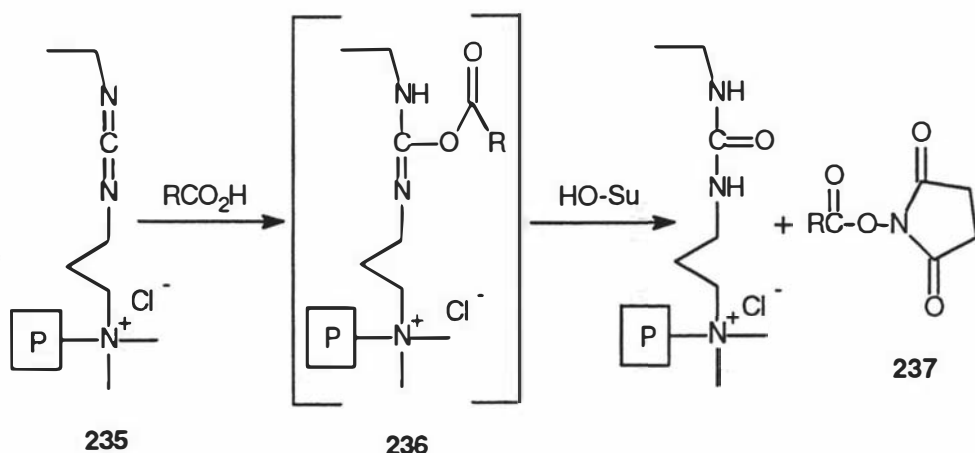
A variety of carboxylic acids were activated and linked to the polymer supported EDAC **235** to form the active intermediate **236**, which reacted with N-hydroxysuccinimide (HOSu) to produce the N-hydroxysuccinimidyl active ester **237** in good to excellent yield (scheme 42). Since urea as a by-product is always linked to the polymer backbone, complete removal of urea from the active ester **237** was achieved by simple filtration. Therefore, the polymer-supported reagents also provided another useful approach for the preparation of pure active succinimidyl esters (ONSu) **200**.

During the course of writing this thesis, a synthesis of peptide-sandwiched mesoheme **239c** (Figure 53) was reported.[169] In the presence of DMSO as solvent and diisopropylethylamine as a base, two identical 13 residue peptides (**238**) have been covalently linked to iron (III) mesoporphyrin IX *via* the bis-*p*-nitrophenyl ester of iron(III) mesoporphyrin IX resulting in amide formation between the heme propionyl groups and the ε-amine group of the lysine side chains. A small amount of monopeptide adduct (**239a**, **239b**) was also obtained from the reaction. The reaction conditions are similar to the conditions used in the present work. The bis-*p*-nitrophenyl ester is the same activated ester and both DME and DMSO as polar solvents were used in both situations. However, these researchers used mesoheme, instead of the more commonly encountered hemin IX **227**, to avoid side reactions of the vinyl groups such as hydration. In the present work, the good yield of mono-conjugation of hemin IX **227** with amino acids or their derivatives (Figures 45, 46a, 47, 48b, 50b and 51b) clearly indicated that no side reactions of the vinyl groups of the protoporphyrin IX **216** or hemin IX **227** occurred under the present non-aqueous reaction conditions.

Ac-A-K-E-A-A-H-A-E-A-A-E-A-A-NH₂   Ac-A-K-E-A-A-H-A-E-A-A-E-A-A-NH₂

Ac-A-K-E-A-A-H-A-E-A-A-E-A-A-NH₂   **239a:** R¹ = CH₃; R² = CH₃CH₂
239c   **239b:** R¹ = CH₃CH₂; R² = CH₃

238 (peptide):   Ac-A-K-E-A-A-H-A-E-A-A-E-A-A-NH₂
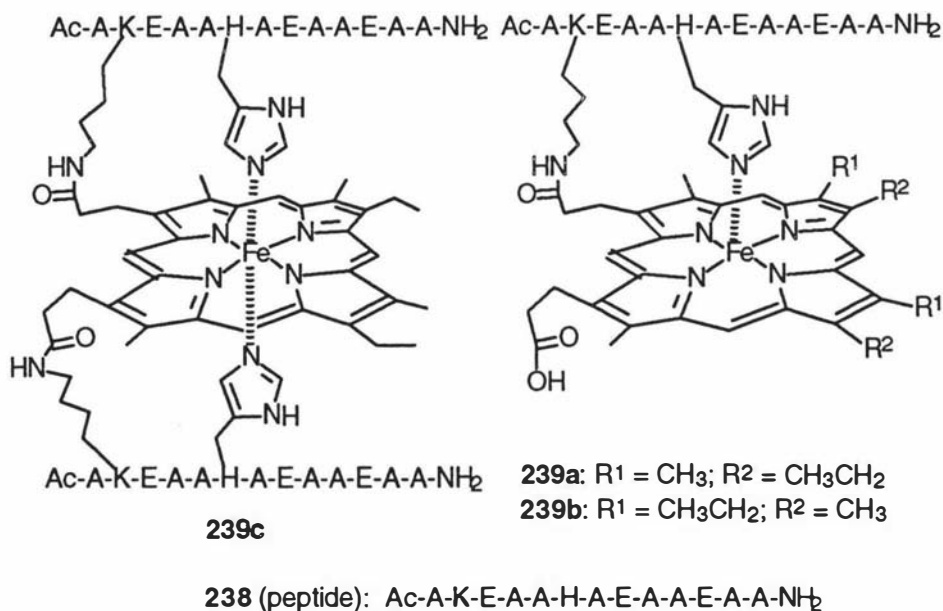
Figure 53. The structures of peptide-sandwiched mesohemes

4.3.3 Porphyrin derivatives and modified hemins

For many years, porphyrins have proven to be excellent substrates for testing important physical, chemical, biological, and medical hypotheses and principles. This has been aided by the unique properties exhibited by porphyrin macrocycles, particularly with regard to chelation of chemically interesting metal ions, which constitute the active, usually catalytic, centre of the chemical system. Hence, there have been many substituent manipulations of the side chains in commercially available protoporphyrin IX and its metal complex (hemin) reported in the literature.[170] Since the propionic acid side chains at the 6- and 7-positions in many porphyrins or metal-porphyrins are comparatively easy to modify by other compounds using amide or ester linkages, there have been many applications of side chain manipulations.

4.3.3.1 *Porphyrin derivatives as photodiagnostic and phototherapeutic agents*

In recent years, porphyrin derivatives exhibiting photosensitising activity and affinity for cancer cells when employed in conjunction with irradiation by laser light, have increasingly produced excellent results in the diagnosis and treatment of cancer. These properties and procedures of porphyrin derivatives are called "photodiagnosis"

and "phototherapy". As a general requirement, the compounds intended for phototherapy ideally should have the following properties:

(i) be non-toxic at normal therapeutic dosages unless and until activated by light;

(ii) selectively photoactive;

(iii) when light rays or electromagnetic waves are applied, they should emit characteristic and detectable fluorescence;

(iv) when irradiated with light rays or electromagnetic waves, they should be activated to an extent sufficient to exert a cell killing effect against the tumour;

(v) be easily metabolised or excreted after treatment.

Porphyrin derivatives are ideal compounds which meet the above general requirements. At present, hematoporphyrin derivatives (HpD) are the most clinically used porphyrins but these have many disadvantages since they are usually prepared as a complex mixture of monomers and oligomers with variable composition. This renders it quite difficult to secure a compound of invariable composition and consequently constitutes a great difficulty in conducting tests on efficacy, toxicity and the like. In order to solve such problems, it is important to synthesise and biologically evaluate pure, characterised, monomeric porphyrin compounds for photodiagnosis and phototherapy.

A series of pure porphyrin derivatives were synthesised through the amidation of the carboxyl groups with different amine compounds either *via* the acid chlorides or by using 1,1'-carbonyldiimidazole as the coupling reagents.[163,171] These porphyrin derivatives having two amides in the side chains were found to be photosensitising substances useful in the diagnosis or treatment of cancer.

There is another serious problem which is associated with hematoporphyrin derivatives (HpD). These substances are accumulated not only in cancer tissues but also in normal tissues, particularly the liver and the skin in large quantities, which constitutes a great obstacle in the clinical application of these substances.

Comparing the hematoporphyrin derivatives or pure, monomeric porphyrin dicarboxamide compounds, it was found that porphyrin derivatives having one amide structure in the side chains were less accumulative in the body since these compounds were easily excreted after treatment, thus causing less side effects.[172,173] Mono-

amide conjugates of porphyrins also possess greater fluorescence in tumours than do the corresponding basic tetrapyrroles, providing the best contrast in tumours compared with normal tissue around the tumour.[173] Therefore, the porphyrin mono-amide derivatives, especially the mono-amino acid conjugates of the porphyrin have attracted great attention for use in the photodiagnosis and phototherapy of cancer.

Mari *et al*[172] have prepared the porphyrin mono-amide conjugates **243** and **245** from porphyrin mono-acid ester **240** *via* the corresponding acid anhydride **241** as the active intermediate as shown in Scheme 43.

Scheme 43
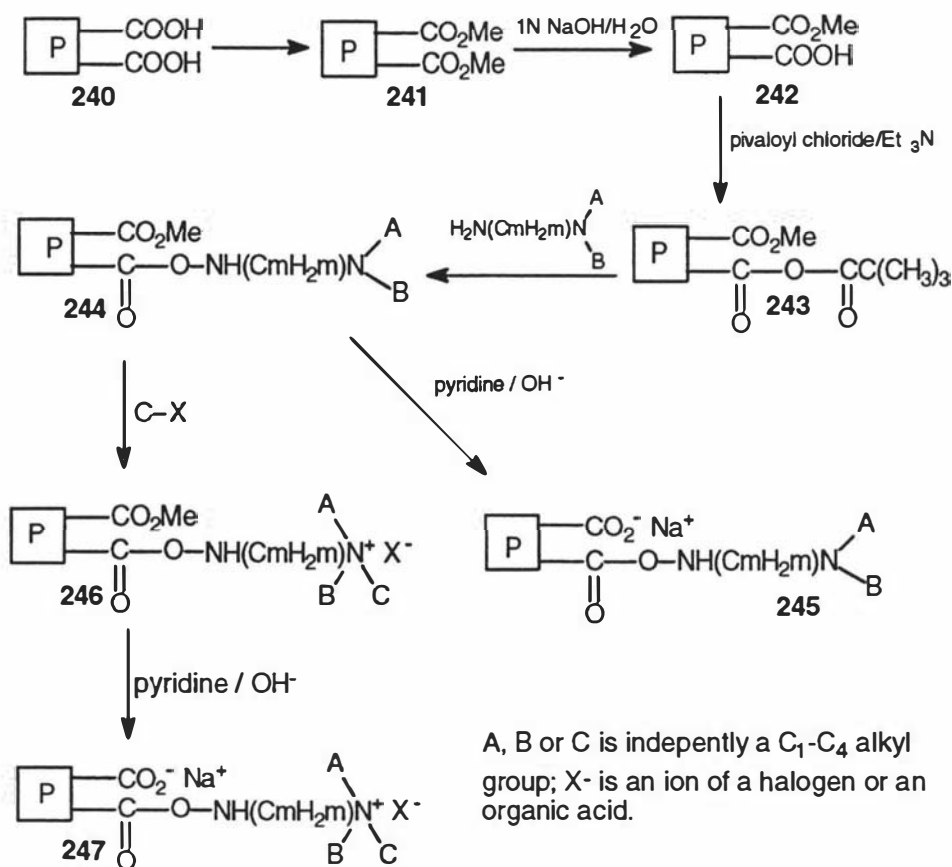
The partial hydrolysis of the porphyrin diester **241** under dilute basic conditions provided the porphyrin mono-acid ester **242**, which was then converted to the corresponding acid anhydride **243** by pivaloyl chloride in the presence of triethylamine. Reaction with different amine compounds afforded the porphyrin mono-amide conjugates **244**. Compound **244** can be directly hydrolysed either to the porphyrin mono-acid amide product **245**, or further reacted with an alkyl halide followed by basic hydrolysis to give another type of porphyrin mono-acid amide

conjugate **247**. The whole synthesis took several steps and resulted in a low yield of products.

In the literature,[174] there is also described an amino monocarboxylic acid adduct of the pigment bonellin obtained by extraction of the body wall of the marine echuroid B.Viridis. The structure of these adducts **248** is presumed to be an amide formed through the reaction of either of the free carboxyl groups of bonellin with the amino acid (Figure 54).
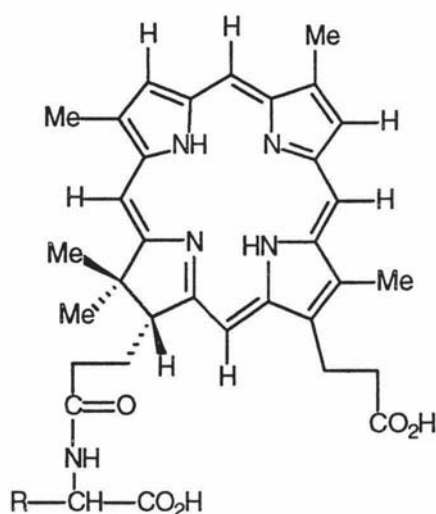
Figure 54. Mono-peptide conjugates of bonellin **248**

Hydrolysis of the adduct **248** yielded a mixture of valine, isoleucine, leucine and alloisoleucine.
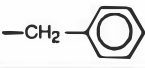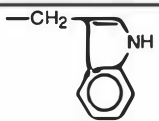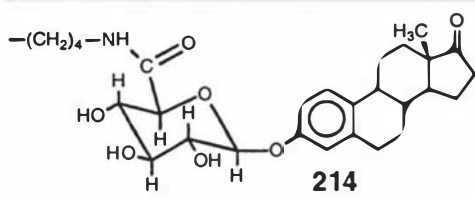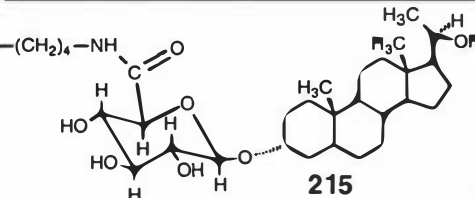
Scheme 44
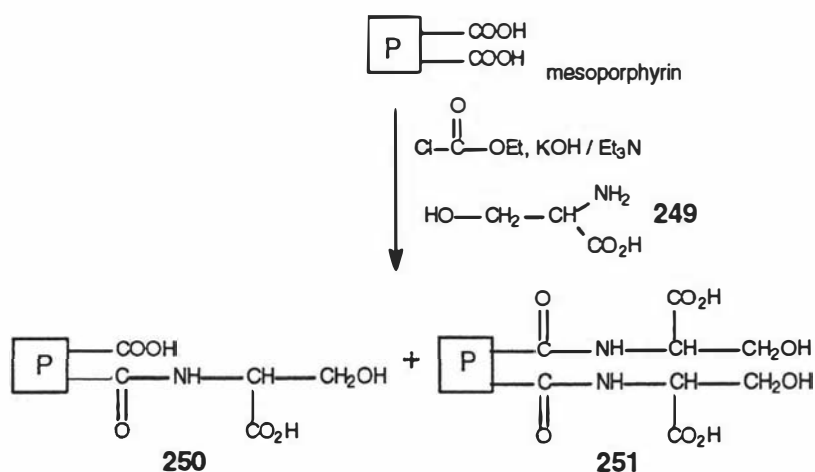
Inspired by the above results, direct amidation of the porphyrin acids to make porphyrin mono-peptide conjugates and investigation of their use for photodiagnosis and phototherapy of cancer was also reported in a few patents.[173,175] The reaction of mesoporphyrin with DL-serine **249** activated by $ClCO_2Et$ in the presence of Et_3N and KOH gave a mixture of mono-DL-serylmesoporphyrin **250** and di-DL-serylmesoporphyrin **251** (Scheme 44).[175] The reaction gave a low yield of mono-peptide conjugates of mesoporphyrin.

A series of mono-amino acid conjugates of porphyrins was also synthesised from the reaction of porphyrins with different amino acids by using 1-ethyl-3-(3-dimethylaminopropyl)carbodiimide as the coupling reagent.[173] The reaction not only gave a low yield of the mono-peptide conjugates of the porphyrins, but also there were some special requirements for the conjugation reactions. When a primary amino-acid was used, it had to contain at least one sulfonic acid group. Hence, so far there has been no general and satisfactory coupling method for the synthesis of mono-peptide conjugates of porphyrins, starting from the porphyrin acids and unprotected amino acids or their derivatives.

Table 9. Monoacylations of Protoporphyrin IX active esters **218** or **219** with amino acids or steroid glucuronide derivatives

Amino acid derivatives R $\left(-CH{<}^{NH_2}_{CO_2H}\right)$	Porphyrins (yield)[*]	Mass	Heme products (yield)	Mass
—CH₂—⟨○⟩ DL or L-phenylalanine	**220** (71%) **220'** (54%)	710 (MH)+	**230** (85%)	764 (MH-Cl)+
—CH₂ indole L-tryptophan	**222** (65%)	750 (MH)+		
steroid glucuronide **214**	**225** (45%)	1120 (MH)+	**232** (75%)	1172 (MH-Cl)+
steroid glucuronide **215**	**226** (45%)	1170 (MH)+	**233** (70%)	1224 (MH-Cl)+

[*] The porphyrin products were prepared from the protoporphyrin IX di-p-nitrophenyl active ester **218** except that **220'** was made from the protoporphyrin IX di-N-hydroxysuccinimide active ester **219**.

The selective mono-coupling procedure described in this thesis provides a simple method for the synthesis of these monoacylated porphyrin derivatives. Table 9 outlines the results of the mono-coupling reactions.

Protoporphyrin IX di-*p*-nitrophenyl active ester **218** or its di-N-hydroxysuccinimide ester **219** underwent monoacylation on the propionic side chains with 1.2 equivalents of the amino acid derivatives in dry DMF/Et$_3$N overnight affording monoacylated protoporphyrins with isomeric mixtures in moderate yield. This non-aqueous procedure is especially useful for acylation reactions when amino acids containing carbohydrates such as compounds **214** and **215** were used as nucleophiles, which cause the hydrolysis of the active ester **218** in aqueous solution as discussed above.[166]

Conversion of the monoacylated protoporphyrins into the relevant hemin derivatives in good yields was achieved simply by refluxing the monoacylated protoporphyrins with excess FeCl$_2$ in DMF/CH$_3$CN (1:1) for 1 hour. Alternatively, the hemin mono-acylated products could be also prepared directly from the reaction of di-*p*-nitrophenyl hemin active ester **228** with amino acids (Figure 50b) or their derivatives (Figure 51b). Compared with previous methods for the synthesis of mono-acylated porphyrins, this new procedure can start the monoacylation from the porphyrin or hemin propionic acids and unprotected α-amino acids or their derivatives directly without the need of mono-protection before the coupling and deprotection after the coupling reaction. This offers greater overall yields and ease of reaction.

4.3.3.2 *Modified metal-porphyrins as heme models of proteins*

The mono-coupling procedure described in Table 9 is not only useful for the preparation of porphyrin derivatives as photodiagnostic and phototherapeutic agents, but it also can be used for the synthesis of different metal-porphyrins as heme models of proteins, which are important in biological research.

In studies of myoglobin (Mb) and haemoglobin (Hb), the replacement of the neutral iron porphyrin prosthetic group with different modified metal-porphyrins has proved to be a useful technique. As synthetic models for oxygen binding proteins, five-coordinated heme compounds in solution usually have been prepared by three approaches:

(i) Steric protection of one side of the heme, such as in "cyclophane" metalloporphyrins **252**,[176] "capped" porphyrin iron complexes **253**,[177] "strapped" porphyrins **254**,[178] "bridged" porphyrins **255**,[179] "crowned" porphyrins **256**[180] and "picket fence porphyrins **257**[181] (Figure 55).
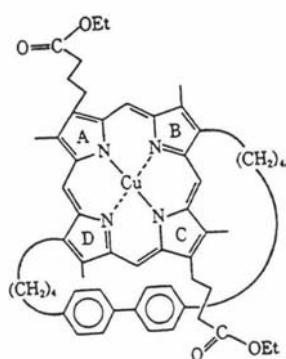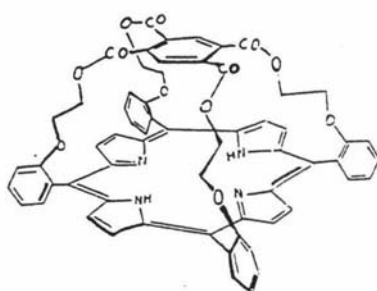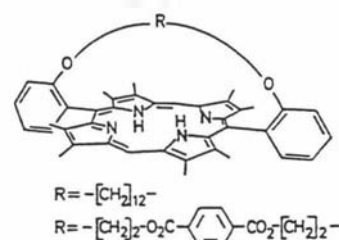
252 253 254
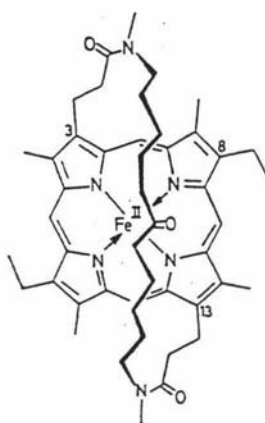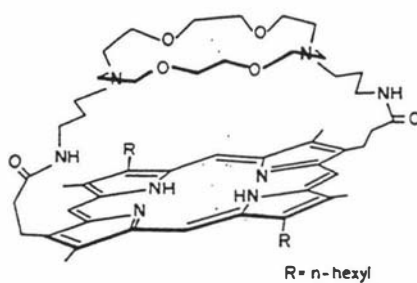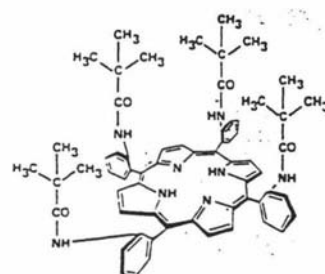
255 256 257

Figure 55. Different structures of one-side protected porphyrin compounds.

All of these modified elegant porphyrins have been developed for provision of steric hindrance above the porphyrin plane, which can successfully prevent the second imidazole from complexing with the heme in some cases.[180,181] However, although these model compounds are very elegant they require many steps to synthesise.

(ii) Use of 2-methylimidazole as a sterically hindered base: (Scheme 45)[182]

Scheme 45
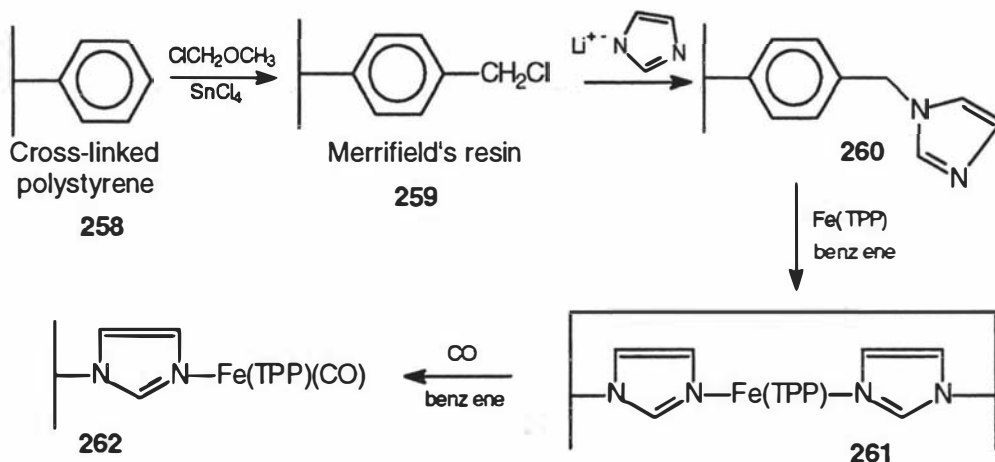
Cross-linked polystyrene **258** was converted to Merrifield's resin **259** by chloromethylation, which further reacted with the lithium salt of imidazole to provide resin-bonded imidazole **260**. Preparation of a model for oxygenated myoglobin by treating 5,10,15,20-tetraphenyl-21H,23H-porphine iron chloride Fe(TPP) with resin-bonded imidazole **260** afforded **261**. Treatment of **261** with CO yielded the diamagnetic carbonyl **262**. Since the 2-methylimidazole moiety has greater steric hindrance than 1-methylimidazole and can effectively prevent the binding of a second 2-methylimidazole to form the six-coordinated heme, this method was found to result in almost exclusive formation of five-coordinated heme. However, the greater steric hindrance from the 2-methylimidazole moiety also reduced the affinity of carbon monoxide to the heme compared to the 1-methylimidazole, which the result that these compounds were poor five-coodinated heme models for oxygen binding proteins.

(iii) Covalent attachment of a proximal base to the heme:[157,164,183,184] This method has none of the drawbacks of using external bases as proximal ligands due to the neighbouring group or chelation effect that maintains a very high local concentration of the base. Both the mono- and di-imidazole compounds, prepared by an amidation reaction of imidazole with porphyrin acids, exist in solvents as five-coordinated hemes. In hemin diimidazole compounds, one imidazole was coordinated

to the iron atom, while the second imidazole did not seriously interfere with dioxygen or carbon monooxide binding. However, the mono-imidazole compound bound dioxygen or carbon monoxide faster than did the diimidazole compounds.[184] Hence, the heme mono-amide derivatives are more useful and have been preferred as the model compounds for oxygen-binding research.

The preparation of hemin mono-amide derivatives in scheme 38 involved several steps including mono-esterification of porphyrin acid sodium salts in the presence of phosphorous pentachloride and ethanol resulting in a low yield (30%).[157] The direct amidation of hemin, which was activated by pivaloyl chloride and without the isolation or purification of the active intermediate-anhydride **263**, also resulted in a low yield of the mono-amide **264** (30%), compared with the present procedure (Table 9), and a mixture of hemin diacid and diamide as the main by-products (Scheme 46).

Scheme 46

242   263   264

+ diacid and diamide
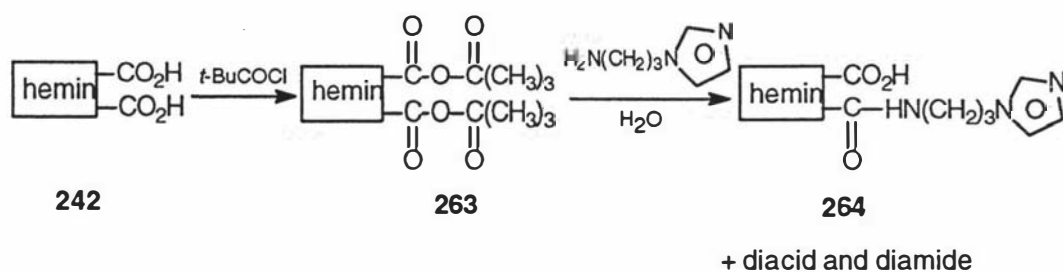
The importance of monoacylated hemin derivatives is also shown in other areas. The hemin-acridine **265** (Figure 56)[185] has been prepared and used as a glycopeptide antibiotic bleomycin model. Its function as a DNA intercalating cleavage agent involved in intercalative binding to DNA and subsequent oxidative scission.
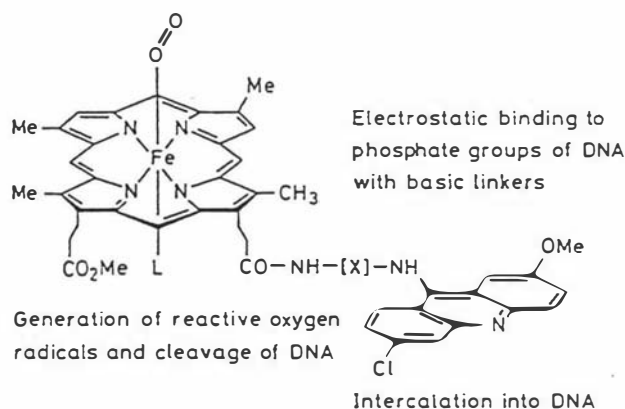
Figure 56. Structure of a mono-acylated hemin-acridine conjugate **265**.

Studies on substituted hemins as probes for structure-function relationships in horseradish peroxidase (HRP) also revealed that mono-substitution at the hemin acid side chains is important for binding to the apo-peroxidase protein. Generation of an active substituted enzyme,[151] which is related to this thesis, will be discussed further in Chapter 5.

Recently, mono-substituted hemin derivative **266** has been successfully used for the designing and synthesis of membrane-bound proteins. (Scheme 47).[186,187]

Scheme 47
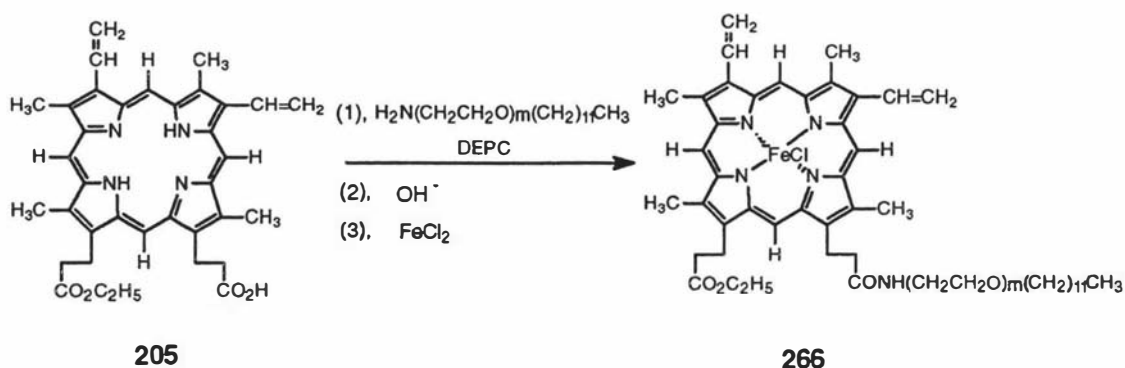
The presence of an alkyl chain as an anchor, which was incorporated into the hemin by mono-acylation in 60% yield in the presence of diethyl cyanophosphate, was crucial not only for enhanced membrane affinity of the water-soluble protein but also for controlled orientation on the bilayer membrane. However, like other syntheses of mono-substituted hemin or porphyrin derivatives, they had to use porphyrin monoethyl ester as the starting material. The whole synthesis required prior mono-protection of the porphyrin acids before the coupling and deprotection reactions after the conjugation, which took extra steps and usually resulted in a low overall yield.

The selective mono-coupling procedure described in this thesis (Scheme 39) provides a general method for the synthesis of these mono-acylated conjugates of porphyrin or metal-porphyrin compounds, and allows both amino acids or their derivatives and porphyrin or hemin acids to be used directly without any prior protection, giving good yields of the mono-acylated products. The whole reaction procedure is very simple, and should be the preferred method for the general syntheses of monoacylated porphyrin or hemin derivatives in future.

4.3.4 Separations and purification of porphyrin or hemin derivatives

The isolation and purification of porphyrins or metal-porphyrins is one of the more interesting and important areas of separation in chemistry and related disciplines. The complexity of porphyrins has prompted the development of various chromatographic techniques for the separation and analysis of synthetic and naturally occurring porphyrins. Carboxylated porphyrins are one of the more common porphyrin compounds since they are found widely distributed in biological materials. They are characterised by the number of carboxyl groups and their substituted positions. Numerous improved methods have been developed for the separation of porphyrins and metalloporphyrins, which include normal-phase chromatography using an aminopropyl-bonded silica stationary phase,[188] reversed-phase chromatography,[189-193] thin-layer chromatography[194,195] and gel permeation chromatography.[196,197] More recently, the separation of individual carboxylic acid porphyrins on a cyclodextrin-bonded phase[198] and the micellar electrokinetic chromatographic separation of some porphyrin free acids and their metal complexes[199] have also been reported. In most studies on the separation of porphyrins and/or metalloporphyrins, reversed-phase HPLC mode has been employed successfully.

4.3.4.1 *The effects of mobile phase on the isolation of porphyrin or hemin derivatives*

For the isolation and purification of the porphyrin- or hemin-steroid glucuronide conjugates in this thesis, the complexity of the molecules containing both porphyrins or hemins and steroid glucuronide moieties made the separations more difficult than those of simple porphyrin and hemin compounds. Since the R_F values showed no difference on a normal phase silica gel TLC plate between the porphyrin or hemin and their estrone glucuronide or pregnanediol glucuronide conjugates, it was necessary to use reversed-phase HPLC for the separation of these compounds.

The mobile phase design for separating the porphyrin or hemin-steroid glucuronide conjugates depends on the stability and solubility of the substituted porphyrins and hemins, which are the major concerns in developing a chromatographic method. The use of different acids[188,189,193,195,198] to dissolve the porphyrin or hemin compounds for HPLC analysis is a common method for sample pre-treatment. Considering the lack of stability of some porphyrins or metalloporphyrins in acidic conditions, several modifications have been made by

using DMF,[191] pyridine[192] or phosphate buffer[190] as the dissolving solvents to avoid using acids. Since the hemin-steroid glucuronide conjugates contain an acid-sensitive glycosidic bond, the use of a non-acid solvent such as DMF would seem to be the obvious choice. The choice of a μ-Bondapak C_{18} reversed-phase column as a stationary phase, which has been commonly used in reversed-phase HPLC mode, and three different solvent systems as the mobile phases were examined in this thesis. Later, an alternative reversed-phase column (VYDAC, 218TP54 Protein and Peptide C18) was also used for the further isolation of two isomeric mixtures of hemin (6, 7) mono-conjugate of estrone glucuronide **232** from hemin IX **227** and gave a superior performance.

Generally, there are three variables, including pH, elution strength and ionic strength of buffers, which characterise the mobile phase composition. The results of earlier studies indicated that a pH of 5.3 was necessary for the complete separation of porphyrin acids by liquid chromatography.[189] Increasing the pH of the mobile phase from 3 to 7 resulted in a gradual decrease of resolution and there was incomplete separation of all porphyrins at or near neutral pH.[189] However, the isolation of protoporphyrin IX-amino acid conjugates from unreacted protoporphyrin IX **216** in phosphate buffer (Solvent I: pH = 6.85) gave very good separations of porphyrin mono-conjugates, double-conjugates and protoporphyrin IX itself. The efficiency of this HPLC system was demonstrated by the HPLC traces (Figures 45a, 45b, 45c, 46a and 47; experimental section 4.2.3) and the structures of the mono-conjugates were confirmed by ^{1}H NMR analysis (Figures 45d and 46b).

The choice of a near neutral pH (6.85) buffer in the present work was used for convenience in the hope that the separated hemin-E1G and hemin-PdG conjugates could then be recombined directly with the apo-horseradish peroxidase which requires neutral conditions. The reason for the good separations under high pH buffer conditions is due to the fact that THF was introduced into the mobile phase as an important organic modifier to increase the solubility of the porphyrin-amino acid conjugates as well as to improve the mobile phase selectivity.[200] Another organic modifier, pyridine, also showed similar functions and is reported in the literature.[198] Furthermore, the elution strength of the mobile phase was much stronger as a result of the addition of THF than the simple phosphate buffer alone. Ionic strength did not seem to significantly influence the resolution of the porphyrins,[189] which could therefore be kept as low as 0.01 M phosphate buffer in the solvent I.

When solvent I (phosphate buffer, pH = 6.85) was applied for the isolation of the protoporphyrin IX-estrone glucuronide conjugate **225** from unreacted protoporphyrin IX **216**, a poor separation was observed (Figure 48a). However, a better separation was achieved by using solvent II, which had a lower pH value and much stronger elution strength by introducing n-butanol into the mobile phase (Figure 48b). Unfortunately, the solubility of porphyrin-estrone glucuronide **225** in solvent II was much lower than that in solvent I. The reason is probably that THF functions as a better organic modifier in solvent I than n-butanol in solvent II. Hence, for preparative scale separation, solvent II was not suitable for the isolation of protoporphyrin IX-estrone glucuronide conjugate **225**. After two isocratic isolation runs with solvent I, the separated protoporphyrin IX-estrone glucuronide conjugate **225** was still contaminated by a very small amount of the unsubsited protoporphyrin IX **216** (Figure 48c). Since both conjugate **225** and the unsubstituted porphyrin **216** had very close retention times (12.3 and 13.8 minutes) in HPLC analysis they were very difficult to completely isolate by solvent I.

A gel filtration column was used to improve the purity of the protoporphyrin IX-estrone glucuronide conjugate **225** from unreacted protoporphyrin IX **216**. Previously, Sephadex LH-20 was used for the purification of chlorophyll,[201] chloroplast pigment[202] and hematoporphyrin derivatives (HPD).[197] A polystyrene-divinylbenzene copolymer was also used for the separation of hemin-μ-oxo-dimers from monomeric hemins or free porphyrins.[196] For the particles of Sephadex LH-20, the adsorptive characteristics of the gel, such as the specific affinity towards compounds having a carboxylic group, played a major role in the resolution of fatty acids, phospholipids and chloroplast pigments. However, the elution of the fatty acids in order of decreasing molecular weight from Sephadex LH-20 suggests that molecular sieving also contributed to the fractionation. Unlike Sephadex LH-20, the retention behaviour of porphyrin derivatives in polystyrene-divinylbenzene copolymer column is based on a pure steric exclusion mechanism.[196] The isolation of protoporphyrin IX-estrone glucuronide conjugate **225** from unreacted protoporphyrin IX **216** by utilising Sephadex G-15 was successfully achieved in this thesis (Figure 48d). Since a large amount of DMF (50% in volume) was used as solvent, there was no solubility problem for the protoporphyrin IX-estrone glucuronide conjugate **225** during the gel filtration isolation on a preparative scale. The presence of two fractions (numbers 7-13 and numbers 19-25), represented by two peaks, clearly demonstrated that the conjugate **225** was well separated from the unsubstituted protoporphyrin IX **216**. The purity of the conjugate **225** was further confirmed by HPLC analysis (Figure 48e), which showed no contamination by compound **216** in the purified conjugate **225**

after isolation. The result clearly indicated that purification of the conjugate **225** by gel filtration column was much better than the separation by reversed-phase HPLC.

Since unreacted protoporphyrin IX and *p*-nitrophenol were not separated on the column although there is a reasonable difference in molecular weight between them, the separation mechanism probably involved mainly the different adsorptive characteristics of the porphyrin compounds. In particular the carbohydrate moiety of the protoporphyrin IX conjugate may play an important role in the gel filtration separation by interacting with the carbohydrate matrix of the Sephadex G-15. The structure of the purified protoporphyrin IX-estrone glucuronide conjugate **225** was confirmed by high resolution mass spectrum (1119.5458 for $C_{64}H_{75}N_6O_{12}$) and ^1H NMR analytical data (see experimental section 4.2.3.6) (Figures 48f and 48g).

Because there was a large difference in the retention times between the pregnanediol glucuronide conjugates **226** and unreacted protoporphyrin IX **216**, the protoporphyrin IX-pregnanediol glucuronide conjugate **226** was comparatively easy to purify by reversed phase HPLC (Figure 49a).

Unfortunately the hemin derivatives were more polar than the related protoporphyrins, and the difference in polarity between the acylated hemins and unreacted hemin was much smaller than that of the porphyrin conjugates and unreacted porphyrin. Hence, it was found that separation of the hemin derivatives was more difficult than the separation of the porphyrin compounds during HPLC analysis. When solvent I (pH = 6.85) was used, good separations were seen for the mixture of porphyrin-phenylalanine mono-conjugate **220**, porphyrin-phenylalanine double-conjugate (**221a, 221b**) and unreacted protoporphyrin IX **216** (Figures 45a, 45b and 45c). However, for the hemin-phenylalanine conjugates (**230, 231**), made from the conjugation of di-*p*-nitrophenyl hemin active ester **228** with L-phenylalanine, there was no separation between the hemin-phenylalanine conjugates and unreacted hemin **227**. Even using solvent III, which had a lower pH value (pH = 5.50) for the mobile phase compared with solvent I, separation was only achieved between the sum of the hemin-phenylalanine conjugates (**230, 231**) and unreacted hemin **227**, not between the hemin mono-conjugate **230** and its double-conjugate **231** (Figures 50b and 50c).

For the isolation of hemin-estrone glucuronide conjugates **232** from the unsubstituted hemin IX **227**, the very low solubility of conjugate **232** in solvent III was a serious problem when a μ-Bondapak C_{18} reversed-phase column was used in the HPLC isolation. Large amounts of THF (Solvent IV) were required to be added to

the HPLC solvent system to improve the solubility of the conjugate **232**. However, all the hemin compounds, including conjugate **232** and the unsubstituted hemin **227**, eluted immediately in solvent IV with no separation at all.

An alternative reverse phase column (VYDAC, 218TP54 protein and peptide C_{18}) and solvent IV (isocratic, experimental section 4.2.4.4) was successfully used for the isolation of the hemin-estrone glucuronide conjugate **232** from the unsubstituted hemin IX **227** (Figure 51d and 51e). The HPLC analysis clearly showed that the two hemin (6, 7) mono-conjugates of estrone glucuronide were well separated from unreacted hemin **227** (Figure 51d), and the purified conjugates **232** had no contamination by hemin **227** after HPLC isolation (Figure 51e). Their mono-conjugated structure was also confirmed by mass spectrum [FABMS(-), m/z 1172 (M-Cl)$^{-}$]. This is very important since any contamination by hemin IX **227** in the conjugate **232** will confuse the result of enzymatic activity after reconstitution of the conjugate **232** with apo-horseradish peroxidase. The enzymatic activity of the reconstituted HRP from the conjugate **232** would be incorrect since some activities would result from reconstitution of unreacted hemin IX **227** if the conjugates **232** were contaminated by **227**. The new HPLC system (VYDAC reverse column and solvent IV) not only can efficiently isolate conjugate **232** from unreacted hemin IX **227** on a preparative scale without solubility problems. It can also separate the two mono-conjugate isomers, which is very surprising and will be discussed in section 4.3.4.2 of this chapter. Obviously, the VYDAC reverse phase column is more suitable than the μ-Bondapak C_{18} reversed-phase column for the HPLC purification of the hemin-estrone glucuronide conjugates since the VYDAC reverse phase column allowed a large amount of THF to be used as an organic modifier to increase the solubility of the conjugates **232** during the HPLC isolation without destroying the resolution.

From the results of this thesis and the above discussion, it can be concluded that hemin IX **227** is a better starting material than protoporphyrin IX **216** for the synthesis of hemin-steroid glucuronide conjugates. Since hemin IX **227** is cheaper and more stable than protoporphyrin IX **231**, and can be efficiently separated and purified from the unsubstituted hemin IX by the above reverse phase HPLC system (without the need of the iron ion insertion step), it is preferable to use hemin IX as a starting material.

4.3.4.2 *Isolation of regio- and stereo-isomers of acylated porphyrin or hemin derivatives*

Since the two propionic acid chains in protoporphyrin IX **216** or in hemin IX **227** are unsymmetrically situated, and the coupling reactions should not discriminate between the two propionic acid groups, an equal mixture of the two isomeric (6, 7) protoporphyrin IX or hemin mono-conjugates would be expected. However, the separation of this isomeric mixture of two mono-conjugates has been very difficult, since even with very careful HPLC techniques, no separation has so far been achieved.[203] Some researchers transformed the two isomers of protoporphyrin IX monomethyl esters into the corresponding acetylprotoporphyrin IX derivatives and separated them on TLC silica gel plates. The whole process took many reaction steps,[203] and it would be not suitable for the separation of the complex porphyrin- or hemin-steroid glucuronide conjugates.

Recently, a small amount of mesoheme monopeptide adduct has been observed[169] by HPLC (VYDAC C4 peptide/protein column). However, this isomeric mixture of two monopeptide conjugates was eluted as two broad, poorly resolved peaks (no HPLC traces were reported in the literature[169]), and was thus only isolated as a mixture of the two isomers (**239a**, **239b**) (Figure 53, section 4.3.2). In the present work, two isomers of hemin mono-conjugates of estrone glucuronide **232** were successfully separated by a new reverse phase HPLC system (VYDAC column and solvent IV) (Figures 51d and 51e, section 4.2.4.3). FAB mass spectrum of this purified product showed that only the mono-conjugates [(M-Cl)⁻, 1172] were present. It is not intended to attempt to isolate these two isomers of protoporphyrin IX or hemin mono-conjugates in this thesis since the apo-horseradish peroxidase can selectively recognise and bind with the correct isomer to form the active enzyme-conjugate. However, these two isomers (two sharp and well separated peaks) can be completely isolated in the present HPLC system, which provides a useful approach to identify the relative importance of the hemin 6- or 7-propionic acid groups towards the reconstitution with apo-horseradish peroxidase in future work.

It is interesting to note that there were two different double conjugates of protoporphyrin IX-phenylalanine (**221a**, **221b**) formed when DL-phenylalanine was used for the conjugation, while for L-phenylalanine as a staring material only one double conjugate **221a** was obtained. The two different double conjugates probably represented two different conformational isomers (*cis* and *trans*) (Figure 57).
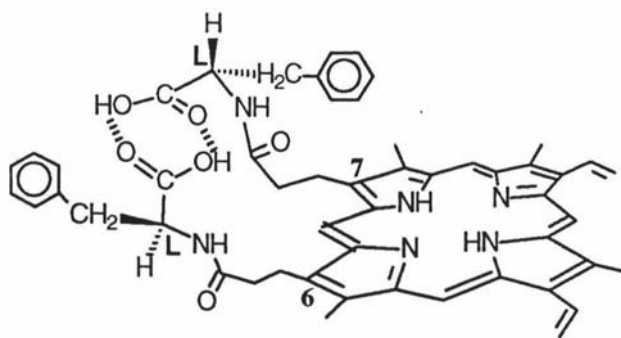
221a (*trans*-configuration, L-L or D-D isomer)
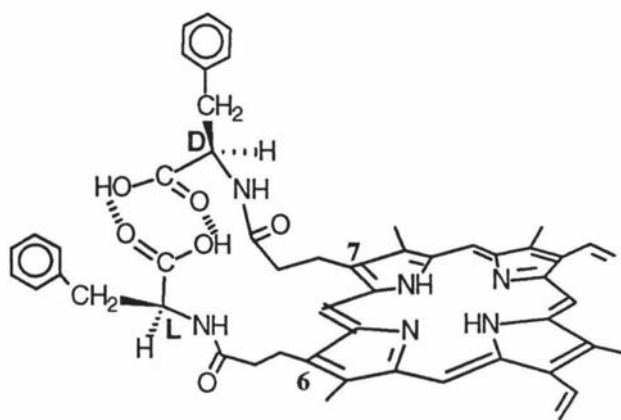
221b (*cis*-configuration, L-D or D-L isomer)

Figure 57. Possible conformations of two stereoisomers of **221a** and **221b**

When DL-phenylalanine was used for the conjugation, the double conjugates at the two propionic acid chains (6 and 7) can be formed in four different ways by intermolecular hydrogen bonding from the two acid groups; i.e DL, LD, DD and LL. The DD or LL isomers allowed one phenylalanine chain to be situated above the protoporphyrin IX plane, while the other phenylalanine chain is below the porphyrin plane (**221a**, *trans*-configuration). However, for the DL or LD isomers, the two phenylalanine chains are situated on the same side of the porphyrin plane (**221b**, *cis*-confugration). These two double conjugate isomers were clearly shown to be present in equal amounts by the HPLC traces (Figures 45a and 45b) and the structures were confirmed by mass spectroscopy and ^1H NMR analysis (Figures 45e and 45f). Consistent with this explanation when L-phenylalanine was used as a starting material, only one double conjugate (**221a**, LL, *trans*-confugration) could be formed. Hence, the HPLC analysis showed only one double conjugate peak (Figure 45c).

4.3.4.3 *Insertion of Fe^{2+} ions into the protoporphyrin IX ring*

The insertion of the divalent metal salts, such as Fe^{2+}, into porphyrin rings using DMF as a solvent is a general method for the preparation of various types of metalloporphyrins.[204] The advantages of using DMF as a reaction medium stems from its good solubility for many different porphyrin materials and high boiling point. Hence, the insertion reactions could be performed in DMF under high temperatures to facilitate and complete the reactions. The products are easily obtained by addition of an equal volume of water to the completed reaction, which frequently quantitatively precipitates the product for ready filtration or enables ready extraction into a low boiling organic solvent for crystallisation.

However, for the very small quantities of water-soluble products, such as hemin-estrone glucuronide conjugate **232** (0.11 mg, 8.92 x 10^{-5} mol) obtained in this thesis, the isolation and purification of the product was very difficult to achieve by the above method. A large excess of $FeCl_2$ (100 mg) had to be used for facilitating a rapid insertion reaction and driving the reaction to stoichiometric completion. Hence, it was very difficult to remove the excess Fe^{2+} from the reaction mixture by simple filtration or extraction after addition of water, which was ineffective due to the very small quantities of water-soluble conjugate **232**. A reversed phase HPLC system was reported previously for the analysis of heme, protoporphyrin and iron.[205] However, for isolation on a preparative scale, this HPLC method was too time-consuming involving multiple injections of the sample.

A simple procedure was developed in this thesis for separating the hemin-estrone glucuronide conjugate **232** from excess Fe^{2+} ions by using two reversed phase SEP-PAK C_{18} cartridges in series. It was found that the hemin-estrone glucuronide conjugate **232** was quantitatively adsorbed and retained on the cartridges, while the water-soluble Fe^{2+}-citrate complex, which was made by simply adding citrate buffer (pH = 5.3, 0.1 M) to the reaction mixture, was passed through the cartridges. The hemin-estrone glucuronide conjugate **232** was then eluted from the cartridges with methanol. The purity of the product was confirmed by UV, high resolution mass spectra and by HPLC analysis (Figures 50a and 51f).

There have been some applications of different reversed phase cartridges in the isolation of different porphyrins reported in the literature.[195,206] However, there has been no efficient separation method reported for the purification of very small quantities of water-soluble, hydrophobic metalloporphyrins. It is impossible to extract

these products using organic solvents or precipitate the products when a large excess of $FeCl_2$ is also present in the solution. The technique described in the present work, by transforming free Fe^{2+} to the water-soluble citrate complex and utilising a simple cartridge isolation, provided a useful and simple method for the general isolation or purification of small quantities of water-soluble metalloporphyrins after $FeCl_2$ insertion.

4.3.5 Summary

In summary, the syntheses of hemin-estrone glucuronide mono-conjugate **232** and hemin-pregnanediol glucuronide mono-conjugate **233** have been successfully achieved in this chapter either by selective mono-acylation of protoporphyrin IX, followed by insertion of Fe^{2+} or by direct mono-conjugation of the hemin with steroid derivatives. Good yields and ease of reaction conditions provided in the present work can be useful for the general syntheses of different mono-acylated porphyrins or metal-porphyrins for use as photodiagnostic and phototherapeutic agents or heme models of proteins. Although it is intended to produce all the hemin-monoconjugates with E1G, E3-3G, E3-16G and PdG, E1G was chosen as a model in this thesis to establish the feasibility of the methodology before trying all the other hemin-steroid glucuronide conjugates. The results clearly showed that the mono-conjugation method in the present work is generic, and can be used for synthesis of the hemin monoconjugates with general analytes. The structure and purity of the hemin-phenylalanine mono-conjugate **220**, made from the monocoupling of protoporphyrin IX followed by iron insertion, was confirmed by its ^1H NMR, mass spectrum and HPLC analysis (Figures 45d, 50a and 50d). The purified hemin mono-conjugate with estrone glucuronide **232**, made from direct mono-coupling reaction of the hemin **227** with E1G-L-lysine derivative **214**, also showed its mono-conjugated structure in its mass spectrum and had no contamination by unreacted hemin **227** after HPLC isolation (Figure 51e). Both hemin mono-conjugates **220** and **232** will be used for the reconstitution with apo-HRP to make horseradish peroxidase-conjugates, and will be discussed in the next chapter.

Chapter 5

Reconstitution of apo-Horseradish Peroxidase
with Modified Hemin Derivatives

5.1 Introduction

Before the large amount of work involved in development of new immunoassays for the possible urinary markers of fertility (E1G, E3-3G, E3-16G and PdG) using horseradish peroxidase conjugates is commenced, it is necessary to demonstrate that it is possible to reconstitute apo-horseradish peroxidase (apo-HRP) with a substituted hemin derivative. Clearly, it is essential to establish (i) that a hemin modified at the 6 (7) propionic acid group will bind to apo-horseradish peroxidase, (ii) that the reconstituted HRP still retains an acceptable level of enzymic activity and (iii) the semi-synthetic E1G-HRP binds to an anti-E1G antibody. If point (iii) is not achieved further work is still possible to achieve immune reactivity by adjusting types and length of the molecular linker between the hemin propionic acid group and the steroid glucuronides. But if points (i) and (ii) cannot be achieved further research in this direction is not likely to be productive. This chapter therefore concentrates on points (i) and (ii), and discusses attempts to reconstitute apo-HRP with L-phenylalanine-hemin monoconjugate **230** or estrone glucuronide-hemin mono-conjugate (E1G-hemin) **232** to produce an active semi-synthetic horseradish peroxidase.

5.1.1 Active site of horseradish peroxidase (HRP)

Before discussing attempts to modify the active site region of horseradish peroxidase it is appropriate to review briefly the current state of knowledge. The catalytic properties of heme-dependent peroxidases are governed by the nature of the prosthetic group, the ligands to the iron atom, the catalytic residues provided by the protein, and the general topological and physicochemical properties of the active site.[207] The crystal structure of cytochrome c peroxidase[208,209] indicates that the iron atom is coordinated to a histidine residue and suggests that during catalysis cleavage of the peroxide dioxygen bond to yield the catalytically active ferryl ($Fe^{IV}=O$) species is promoted by distal histidine and arginine residues (see Chapter 1, Figure 15). The distal histidine is thought to function as an acid-base catalyst and the arginine as a polarizing residue that facilitates dissociation of the terminal oxygen as a molecule of water. Hence, these three amino acid residues and the prosthetic group represent the

catalytic core of classical peroxidases. Hydrogen-bonding and other interactions also appear to modulate their detailed catalytic functions. Scheme 48 summarises the basic features of the catalytic mechanism.
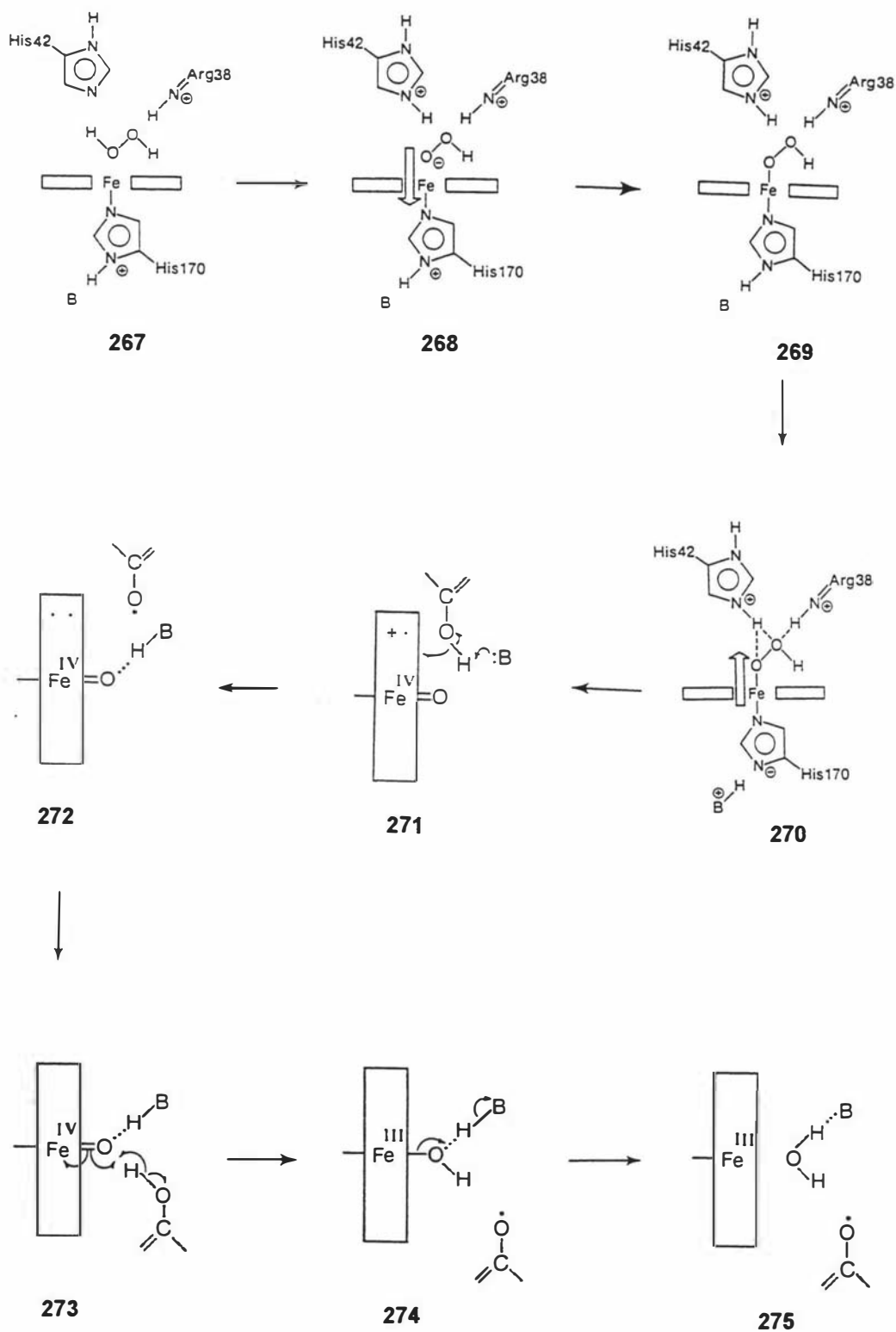
Scheme 48. The electron push-pull catalytic mechanism of horseradish peroxidase.

Spectroscopic and kinetic evidence suggests that the proximal and distal histidines and distal arginine are also part of the catalytic mechanisms of other classical peroxidases.[207] For horseradish peroxidase, an electron push-pull mechanism has been discussed for the heterolytic cleavage of the O-O bond of hydrogen peroxide (Scheme 48).[207] The unionised form of H_2O_2 is the initial reactant **267**; it is converted into a much better nucleophile upon transfer of its proton to the distal basic His42 group **268**. Formation of the iron-peroxide bond is facilitated by positive charge on the proximal His170. The negative charge on His170 and positive charge on His42 and Arg38 facilitate heterolytic cleavage of the O-O bond leading to formation of the ferryl group, Fe = O. One-electron reduction of HRP-I **271** to HRP-II **272** is carried out by a phenol or enol compound. Electron transfer occurs to the porphyrin ring, in the region of the δ-meso carbon and the 8-methyl group of the heme, and the proton transfer occurs to a distal basic His42 group. The protonated distal His42 group, which is hydrogen bonded to the ferryl oxygen atom, is catalytically essential for the one-electron reduction of HRP-II **273** to native HRP **275** by a second phenol or enol to complete the catalytic cycle. Both proton and electron transfer occurs to the ferryl group, simultaneously reducing iron (IV) to iron (III) and forming water as the leaving group (Scheme 48). The aromatic radical then undergoes further reaction (often a coupling reaction) to produce coloured products which may be used to monitor progress of the reaction.

The primary sequence of horseradish peroxidase is known,[210] and alignment of the protein sequences of horseradish peroxidase and cytochrome c peroxidase led Welinder[211] to propose that both structures are made up of two similarly assembled domains. The most important information on the structure of the active site of horseradish peroxidase relevant to this thesis has been provided by Professor Oritiz de Monteliano et al[212-220] on the basis of heme alkylation experiments using aryl- and alkylhydrazines. The reaction of phenylhydrazine with myoglobin,[212-214] hemoglobin,[214-216] catalase,[217] cytochrome P_{450},[218] and metalloporphyrins[216] resulted in the alkylation of the iron or nitrogen atoms of the heme (**276, 277**). In contrast, the same alkylation reaction of phenylhydrazine with horseradish peroxidase resulted partially in attachment of the phenyl group to the δ-meso carbon (**278**) and partially in conversion of the heme to the 8-hydroxylmethyl derivative (**279**) (Scheme 49).[219] However, for the reaction of horseradish peroxidase with alkylhydrazines, the δ-meso-alkylhemes are the only products.[220,221] Hence, individual peroxidases have some important differences in their active sites and catalytic potentials since the hydrogen-bonding and other interactions with the peroxidase to modulate their detailed function are different.[222] The different binding properties of the hemin 6-

and 7-propionates to different apo-proteins also results in some   differences among the hemoproteins, which will be discussed later in this chapter.
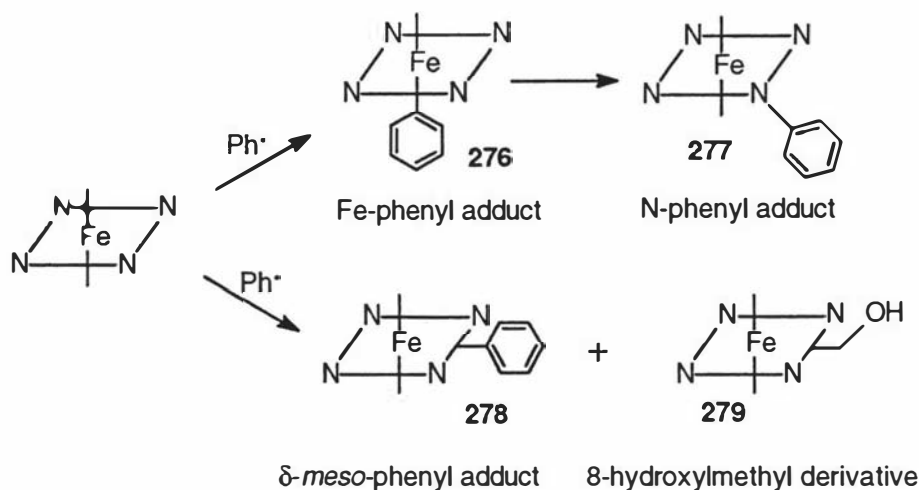
Scheme 49. The reaction of a phenyl radical with the prosthetic heme group. **(i)** Fe-phenyl and N-phenyl adducts obtained with myoglobin and cytochrome P_{450}; **(ii)** δ-*meso*-phenyl adduct and the 8-hydroxylmethyl derivative obtained with horseradish peroxidase.
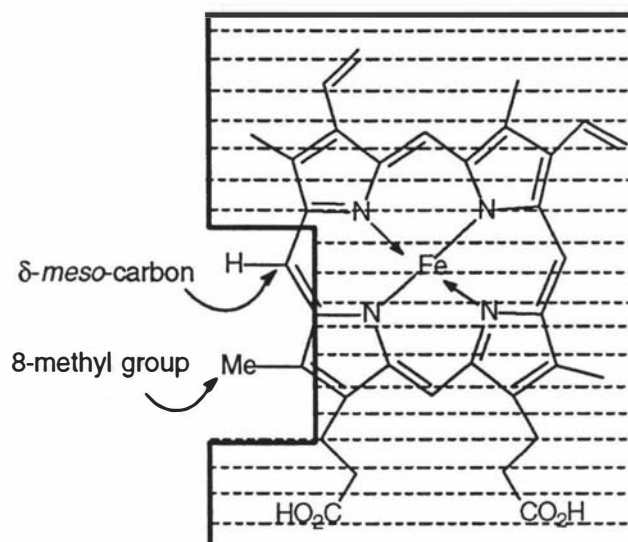
Figure 58 Active site model of horseradish peroxidase predicted by heme alkylation experiments. The shading indicates covering of the heme by the apo-protein tertiary structure.

The above heme alkylation experiments have clearly shown that the iron and pyrrole nitrogens of the heme are not accessible to the phenyl or alkyl radicals for horseradish peroxidase, but these sites are exposed in some other hemoproteins. The

alkylation experiments with horseradish peroxidase also indicated that only one of the four *meso* carbons (the δ-*meso*-carbon) and one of the four methyl groups (the methyl group at the edge of pyrrole ring D) are physically accessible to the substrates. Based on these results, a model for the active site of horseradish peroxidase was proposed by Professor Oritiz de Monteliano *et al*[219] (Figure 58).

Further support from NMR studies also suggested that organic substrates bind to horseradish peroxidase in the vicinity of the 8-methyl group[223] and that the heme group is buried inside the protein.[224] This is consistent with the above active site model structure (Figure 58). A comparison of the active site model of horseradish peroxidase and the crystal structure of cytochrome *c* peroxidase[207] shows that their active sites bear a striking resemblance in that very nearly the same region of the heme is exposed in both enzymes. Since both horseradish peroxidase and cytochrome *c* peroxidase contain two similarly assembled domains[211] and have similar heme active site enviroments,[225] the crystal structure of cytochrome *c* peroxidase is a useful model for assessing the effects of heme structural modification in horseradish peroxidase. Hence, the heme enviroment in the known crystal structure of cytochrome *c* peroxidase has been used for constructing a three dimensional structure of the heme-modified horseradish peroxidase in this thesis. The hemin-estrone glucuronide mono-conjugate **232**, made in this thesis, has also been inserted into the crystal structure of cytochrome *c* peroxidase by computer graphic techniques to replace the native hemin for structural modelling experiments and further active site analysis.

5.1.2 Structural modifications at hemin edge positions of HRP

Heme modification of ferric hemoproteins has been extensively studied by recombination of their apo-proteins with synthetic hemins including ligand binding behavior,[226] spectroscopic properties,[151,227] drug oxidation studies,[228] and their catalytic activities.[151,152] For research of catalytic activities, early studies[151] by extensive heme modification showed that the 2 and 4-substituents of the hemins in horseradish peroxidase all interact with the protein. A variety of 2- and 4-substituted hemins were observed to bind with apo-horseradish peroxidase. However, when the hemin 2 and 4 side chains are made large, the hemin may no longer be able to generate an active substituted peroxidase. Although the polypeptide chain possesses some conformational flexibility in the 2- and 4-substituents area, the large 2- and 4-substituents of hemins can still adversely affect binding since heme 2- and 4-substituents are bound in pockets of limited size and buried in the interior of the enzyme. Hence, it is unlikely that good binding with apo-horseradish peroxidase

would be achieved when a large molecule, such as a steroid glucuronide, was linked to the 2- or 4-possition of hemin IX.

Recently, heme modification was further investigated at other heme edge positions of horseradish peroxidase by Professor Oritiz de Monteliano *et al*[220-222] (Figure 59). Replacement of the prosthetic heme group of horseradish peroxidase with 8-(hydroxylmethyl)heme **280** yielded an enzyme which had similar catalytic properties with the native horseradish peroxidase. In contrast to the 8-(hydroxylmethyl)heme **280**, the 8-formylheme derivative **281** caused large differences between the reconstituted and native enzyme.[222] The result was consistent with previous studies[152] showing that carbonyl substituents at the 2, 4-, and 8-positions of the heme group in horseradish peroxidase strongly destabilize the binding of hemin with apo-horseradish peroxidase. Retention of the catalytic activity of horseradish peroxidase by the δ-meso-methyl group **282**, but not the δ-meso-ethyl analogue **283**, also demonstrates that the δ-meso substituent strongly interferes with substrate oxidation by a steric mechanism rather than by critically altering the conformation or redox properties of the heme group.[220,221]

(280) 8-(hydroxymethyl)heme
($R = HOCH_2$, R' = H)

(281) 8-formylheme
(R = CHO, R' = H)

(282) δ-meso-methyl heme
($R = CH_3$, $R' = CH_3$)

(283) δ-meso-ethyl heme
($R = CH_3$, $R' = CH_2CH_3$)
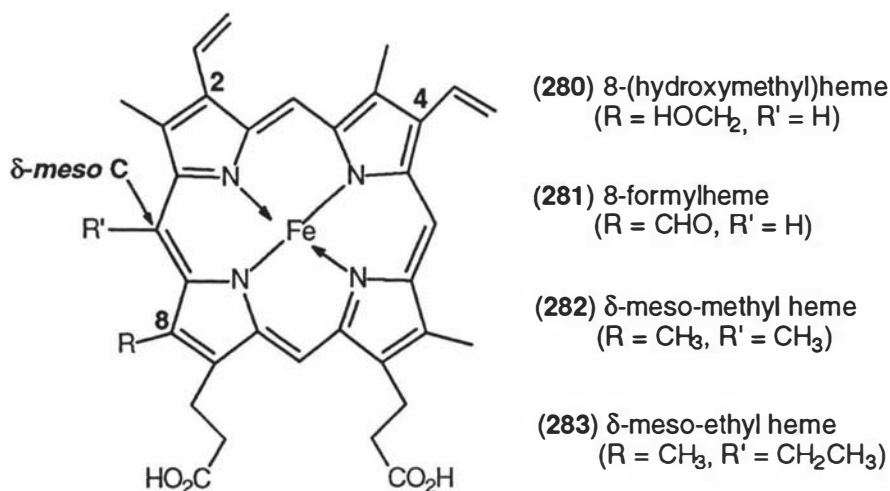
Figure 59. The structures of synthetic hemin derivatives

Clearly, very small size changes in these heme edge positions (2, 4, 8 and δ-meso carbon positions) (Figure 59) have drastic effects on the rate of binding to apo-horseradish peroxidase and the activities of the resulting reconstituted enzymes for steric reasons. Hence, it is very difficult to retain a significant amount of peroxidase activity in the reconstituted enzymes by modifications at these heme edge positions.

In particular it is obviously impossible to retain horseradish peroxidase activity after introduction of a large functional group, such as a steroid glucuronide, in these positions.

5.1.3 Chemical modifications at hemin propionate side chains

For horseradish peroxidase, earlier studies on heme-modification showed that the hemin 6 and 7-propionate side chains are very important for efficient binding to apo-horseradish peroxidase. For example, reconstitution of the hemin monoester with apo-horseradish peroxidase showed only 18% of the enzymatic activity of the native enzyme, and the enzyme containing heme diesters showed no peroxidase activity at all.[152] Later, research has also concluded that in addition to terminal carboxyl groups, the length of the hemin 6- and 7-propionic acid side chains were all important for rapid and efficient binding to apo-horseradish peroxidase to form an active enzyme.[151] The conclusion was based on the experimental results for reconstitution of apo-HRP with a variety of synthetic hemins, such as dibutyric acid hemin, dialcohol hemin and protohemin diamide,   compared with reconstitution of protohemin. These results have discouraged most workers from attempting the synthetic strategy outlined in this thesis.

284

R = CH$_3$ or CH$_2$CH$_3$

Heme diesters

285

R' = CH$_2$CH$_2$CH$_3$

iron-tetrapropylporphycene
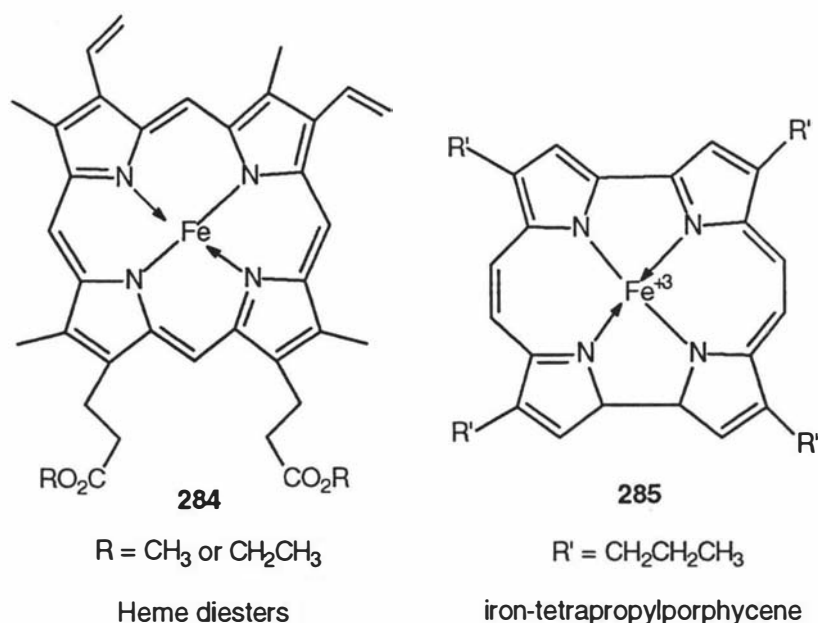
Figure 60. The structures of hemin compounds containing no free carboxyl groups.

Recently, a new investigation on structure/activity relationships of horseradish peroxidase further confirmed that the presence of free hemin carboxyl groups is

essential to the enzymatic activity for both apo-horseradish peroxidase and apo-porphobilinogen oxygenase.[229] All the hemin diesters (methyl or ethyl) did not recombine with these two apoproteins. Reconstitution attempts using a tenfold excess of either the hemin diesters **282** or the apo-proteins were also unsuccessful. The same was also true for iron-tetrapropylporphycene **283**, which contains no free carboxyl group in the structure (Figure 60).

In spite of these studies, there are three aspects relating to the properties of heme 6 and 7 propionates which still remain unclear; (i) Are the heme 6- and 7-propionates of equal importance for binding with apo-horseradish peroxidase? If they are not, as suggested by the crystal structure of cytochrome *c* peroxidase (Figure 39, Section 4.1.2), is the hemin 7-propionate more important? (ii) Can we selectively modify the less important propionate side chain and keep the other important one untouched to maintain reasonable peroxidase activity? (iii) Can we get more activity by introduction of an extra carboxyl group in a similar position to the original hemin propionate group? Also, what is the maximum amount of peroxidase activity we can get by this type of heme modification? To answer these questions, it is certain that X-ray crystallographic studies of horseradish peroxidase will be very useful. There is no X-ray analysis available for horseradish peroxidase during the course of writing this thesis but a structure for a recombinant HRP is due to appear shortly. Hence, we can only analyse the functions of heme 6- and 7-propionates in horseradish peroxidase with the help of structures of other hemoproteins.

The binding of the heme prosthetic group within its binding site in hemoproteins, is mainly determined by a number of heme-protein interactions. These include the axial imidazole-iron bond, van der Waals interactions between hydrophobic amino acid chains and the polarisable heme π system, and salt bridges or hydrogen bonds to the heme 6- and 7-propionate side chains. The role of the hemin propionate side chains is to stabilise the heme binding pocket by forming "salt bridges" or hydrogen bonds between the hemin carboxylate residues and some specific basic anchoring groups of the amino acid side chains.[230] The relative importance of these salt bridges for heme binding varies for the different hemoproteins. For example, octaethylhemin **286**, as a synthetic hemin which has no propionate side chain in the structure (Figure 61), has been shown to recombine satisfactorily with apo-myoglobin. The reconstituted and native myoglobins have much unexpected functional similarity.[231] In contrast to the behaviour of the myoglobins, hemin IX diesters did not recombine with either apo-horseradish peroxidase[151,152,229] or apo-porphobilinogen oxygenase.[229] Therefore, for

horseradish peroxidase, it is apparently essential to have free carboxylate residues in the hemin compounds for efficient binding and reconstitution of a synthetic hemin with the apo-protein.
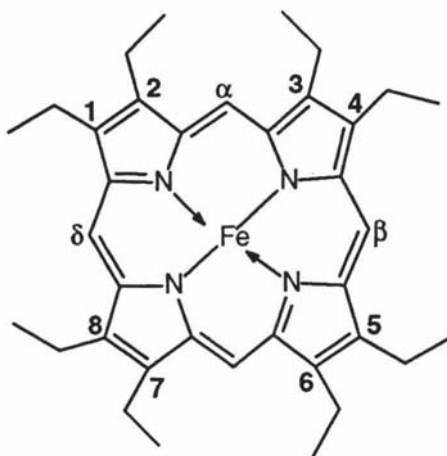
Figure 61. The structure of octaethylheme **286**

. Are the relative importance of the two hemin propionate salt bridges to the protein matrix the same? The answer appears to be no. Since the protein environment for the two propionates is different, the stabilities of these two salt bridges cannot be the same. The recent NMR studies on the heme propionates of myoglobin carried out by Professor La Mar *et al*[232,233] provided some interesting and important results on this question. The two hemin propionates in myoglobin are oriented toward the hydrophilic portion of the heme cavity near the protein surface, where the 6-propionate group forms a salt bridge with surface Arg CD3 and the 7-propionate forms a salt bridge to the interior His FG3. The relative stabilities of the propionate salt bridges depend on the individual hemoproteins. In sperm whale Myoglobin, the 6-propionate salt bridge appears more stable than the 7-propionate link by ~400 cal, while in horse Myoglobin, the 6-propionate link to the protein is ~240 cal less stable than the 7-propionate salt bridge.[232] However, reconstitution of synthetic mono-propionate hemin compounds always have an orientational preference for occupying the crystallographic 7-propionate position which makes a link to the interior His FG3 in both proteins.[232] The same was also true for the reconstitution of cytochrome b_5.[233] The structures of the transient protein complexes after reconstitution reveal that the initial encounter complexes during assembly of the holoprotein from the apoprotein and hemin involves the propionate-protein linkers at the 7-propionate position. These results clearly show that the 7-propionate position of hemin is more

important than the 6-propionate position for the reconstitution of synthetic mono-propionate hemins with both apo-myoglobins and cytochrome b_5.

Could the above results also apply to the horseradish peroxidase or other hemoproteins? Since horseradish peroxidase and cytochrome c peroxidase have similar heme binding pockets,[225] the crystal structure of cytochrome c peroxidase was adopted as a model to analyse the possible positions and functions of heme 6- and 7-propionates in horseradish peroxidase. As part of the crystal structure of cytochrome c peroxidase, Figure 39 (Chapter 4, section 4.1.2) clearly shows that the 7-propionate has many more interactions with the protein matrix than does the 6-propionate group. This is consistent with the previous results with myoglobins. If this is also true for horseradish peroxidase, it is not surprising that it might be possible to modify the 6-propionate group and keep the 7-propionate free for maintaining a certain amount of catalytic activity of the reconstituted horseradish peroxidase. Furthermore, an extra carboxyl group can also be introduced at a similar location as in the native hemin IX by using a suitable molecular linker (Figure 40, Chapter 4, section 4.1.2). The strategy adopted in this thesis of using L-lysine as a linking group introduces an extra carboxyl group to compensate for the loss of the hemin 6-propionic acid group as a result of amide bond formation. Hence, this chapter explores the use of the synthetic hemins made by mono-substitution at the 6- or 7-position of the hemin IX, such as L-phenylalanine-hemin mono-conjugate **230** and estrone glucuronide-hemin mono-conjugate **232**, for reconstitution experiments with apo-horseradish peroxidase.

5.2 Experimental

5.2.1 Materials

General details: see sections 2.2.1 and 3.2.1 Experimental.

Horseradish peroxidase (HRP) type VI, isozymes C, H_2O_2 and o-dianisidine (97%) were all purchased from Sigma Chemical Company. Phenylalanine-hemin monoconjugate **230** was synthesised by inserting an iron atom into the corresponding porporphyrin which was prepared from the monoacylation reaction of protoporphyrin IX **216** with L-phenylalanine. Estrone glucuronide-hemin monoconjugate (E1G-hemin) **232** was directly prepared from hemin IX **227** *via* the mono-conjugation reaction of the di-p-nitrophenyl hemin active ester **228** with estrone glucuronide-L-lysine conjugate **214**. Both synthetic procedures were described in chapter 4 (Schemes 39 and 40).

PD-10 columns (Sephadex G-25M, code No. 17-0851-01) were purchased from the Pharmacia Biotechnology Company and used for the removal of methylethylketone residues in the apo-protein fraction after extraction of the heme from horseradish peroxidase. Quaternary ammonium cellulose beaded resins (Ostsorb Tessek, Praha Czechoslovakia) were obtained from Mr D. Elgar (Department of Chemistry and Biochemistry, Massey University) and DE 52 (Diethylaminoethyl Cellulose) anion exchange resins were purchased from PIERCE Chemical Company, USA. Both materials were used for the removal of excess hemin or modified hemins, not bound at the peroxidase active site, after reconstitution of hemin IX or modified hemins with apo-horseradish peroxidase. Absorption spectra and enzyme assays were performed on a Hewlett-Packard Model 8452A diode-array spectrophotometer.

5.2.2 Preparation of apo-horseradish peroxidase

Apo-horseradish peroxidase was prepared essentially according to a literature method.[234] HRP solution (1.9 ml) in sodium phosphate buffer (0.005 M, pH = 6.5) was cooled down to 0 °C, and the solution was adjusted to pH = 2.4 by dropwise additions of 0.1 M HCl and immediately mixed with 2 ml of ice-cold 2-butanone. The mixture was vigorously shaken for 0.5 minute and allowed to stand at 0 °C for 1 minute until the deeply coloured upper layer of the butanone phase formed. The hemin IX in upper layer was well separated from the colourless lower layer of aqueous phase which contained the apoenzyme. The butanone phase was siphoned

off. The remaining aqueous phase was treated twice more with butanone and then dialysed against one change of $NaHCO_3$ (0.01 M) for 2 hours, followed by two changes of tris-buffer (0.01 M, pH = 8) for 5 hours each. The apo-HRP solution in tris-buffer (3.5 ml) was collected after dialysis. Alteratively, after extraction of the hemin from the acidified HRP solution (1.8 ml, pH = 2.45), the apo-HRP solution (1.8 ml) was directly filtered through a commercial PD-10 column and the purified apo-horseradish peroxidase was collected in a 3.5 ml aliquot. The concentration of the apo-HRP solution was determined spectrophotometrically using an extinction coefficient of 2×10^4 mol^{-1}· cm^{-1} at 278 nm.[152]

5.2.3 Reconstitution of apo-HRP with synthetic hemins (230, 232)

5.2.3.1 Reconstitution of apo-HRP with L-phenylalanine-hemin monoconjugate 230

An aliquot (0.3 ml) of apo-HRP solution (2.16×10^{-5} mmol.mL^{-1} in tris-HCl, 0.1 M, pH = 8 buffer) was combined with 0.7 ml of tris-buffer solution (0.1 M, pH = 8), containing a 1.5 fold excess of the L-phenylalanine modified hemin **230**. Pure hemin IX **227** was used as a reference standard to determine the reconstitution potential of the apo-HRP solution. After standing overnight at 4 °C in a cold room, the samples were passed through a column containing a quaternary ammonium cellulose beaded resin (2 x 0.5 cm), equilibrated in 0.1 M tris-buffer (pH = 8), to remove hemin IX **227** or L-phenylalanine modified hemin **230** not bound at the peroxidase active site. The column was washed with tris-buffer (0.1 M, pH = 8) to get a colourless solution (3 ml) for each sample, which was ready for dilution and the *o*-dianisidine peroxidase assays.

Enzyme assays (*o*-dianisidine peroxidase assays) were carried out using the following procedure:

An aliquot (0.97 ml) of citrate buffer (0.1 M, pH = 5.3), 5 µL of dilute enzyme solution and 5 µl of *o*-dianisidine (a saturated solution in MeOH) were incubated at 25 °C for 5 minutes and then a blank run at 460 nm. After addition of 20 µL of dilute H_2O_2 (0.3% solution in citrate buffer) to the above solution, a time-based scan measurement of the oxidised product of *o*-dianisidine was determined at 460 nm (run time = 60 seconds, cycle time = 1 second, start time = 0 second, integration time = 0.5 second). The results of the assays were expressed as $\Delta Au \cdot min^{-1} \cdot nmol^{-1}$ of enzyme (Specific activity).

5.2.3.2 Reconstitution of apo-HRP with estrone glucuronide-hemin monoconjugate 232

Reconstitutions of the apo-HRP with hemin IX **227** or estrone glucuronide-hemin mono-conjugate (E1G-hemin) **232** were performed by a similar procedure as previously described for the reconstitution of apo-HRP with L-phenylalanine-hemin **230** except for the following differences; (i) reconstitution of apo-HRP with E1G-hemin or hemin IX was monitored by a spectrophotometric titration at room temperature; (ii) the reconstituted hemin-HRP or estrone glucuronide bonded-HRP was purified by filtration through a DE 52 column instead of using a quaternary ammonium cellulose column as for the L-phenylalanine modified-HRP.

In a pre-incubated cuvette (1 ml) at room temperature, a spectrophtometric titration was carried out (pH = 8, tris-buffer, 0.1 M) of the apo-HRP solution (0.3 ml of apo-HRP and 0.7 ml of the same tris-buffer) with excess hemin IX **227** or E1G-hemin monoconjugate **232**, using pure hemin IX **227** or E1G-hemin monoconjugate **232** as a titration control. The reconstituted hemin-HRP solution (0.6 ml) or E1G-HRP solution (0.6 ml) was taken from the cuvette (1 ml), and filtered through a DE 52 column to remove the excess hemin IX **227** or E1G-hemin monoconjugate **232**. After concentration, the purified reconstituted hemin-HRP solution (0.37 ml) or E1G-HRP solution (0.21 ml) was obtained. Both enzymes were diluted for the following enzyme assays.

(a). An aliquot (1.9 ml) of pre-incubated citrate buffer (0.1 M, pH = 5.3) in a water bath (37 ^{0}C) was transfered into a 2 ml plastic cuvette, and left for 5 minutes to reach temperature equilibrium;

(b). o-Dianisidine (20 μL) was added followed by 20 μL of dilute enzyme solution to the cuvette;

(c). The reaction solution was mixed by inversion (using a parafilm cover), and left to incubate for a further 5 minutes and then a blank run at 460 nm. After addition of 20 μl of dilute H_2O_2 to the solution, the enzyme assay was performed as for L-phenylalanine modified HRP.

5.2.4 Model building and fitting experiments

The structure of estrone glucuronide **12** was constructed on the Silicon Graphics 4D 30 workstation and then an energy minimisation was performed by the Macromolecules programme. Because of too much structural randomness for the estrone glucuronide-L-lysine conjugate **214**, the energy minimisation for compound **214** could not be performed on the completed model structure. Hence, the conjugate **214** was built up slowly by repeating the process of increasing the structure by one CH_2 unit followed by energy minimisation, until the whole conjugate **214** was constructed and the total energy was minimised.

The co-ordinates of the energy-minimised estrone glucuronide-L-lysine **214** structure were transferred into an Evans and Sutherland PS 770 Picture display system and chemically bonded to the hemin 6-propionic acid group by forming an amide linkage in the crystal structure of cytochrome *c* peroxidase to perform the model fitting experiments.

5.3 Results and Discussion

5.3.1 Preparation of apo-horseradish peroxidase

To examine the reconstitution potential of modified hemins it is necessary to produce a sample of apo-horseradish peroxidase which has a very small amount of residual peroxidase activity. Otherwise it is difficult to distinguish a small amount of binding by a modified hemin from the background enzymic activity. A separation of the hemin and apo-protein components of horseradish peroxidase has been efficiently achieved by the acid/butanone method of Teale.[234] However, from the results of this thesis, the quality of the apo-horseradish peroxidase prepared from the procedure was strongly affected by the amount of acid used before the extraction proccess. The purity of a sample of horseradish peroxidase is given by its reinheitszahl (RZ) value, or purity number, which is calculated from the ratio of A_{403}/A_{278}. The most pure HRP samples have an RZ value of around 3.0. The more apo-HRP present in the sample the higher will the A_{278} value be and hence the lower the ratio A_{403}/A_{278} or RZ value. When the pH value was 1.5~2 before the extraction process, the RZ value of the acidified horseradish peroxidase was only 1.33, much lower than the RZ value (2.85) of the original native HRP. Most of the peroxidase activity was lost (only 4% left compared with native HRP) under this extreme acidic condition. Also, the reconstitution of apo-HRP from this lower pH extraction procedure with hemin IX **227** was only 42% of the enzymatic activity compared with native HRP.

In contrast, if the pH value was carefully controlled at 2.45 before the extraction, the resulting acidified HRP solution showed an RZ value of 2.15, which although lower than that of the native HRP, is much higher than the RZ value of the HRP obtained from the lower pH condition. Most of the peroxidase activity was still retained (95% of native HRP) under this acidic condition. The resulting apo-HRP from the extraction at pH = 2.45 showed good specific activity (92% of native HRP) when it was recombined with hemin IX **227**. This result was in good agreement with a recent literature value (86% of native HRP).[229] Hence, in order to obtain good quality apo-HRP for reconstitution with synthetic hemin compounds, it was very important to control the pH value before starting the extraction process with butanone.

Removal of the acid/butanone residue from the apo-HRP solution can be performed in two different ways; (i) by dialysis against phosphate buffer[229] or tris-buffer as in this thesis; or (ii) by filtration through a PD-10 column. Both methods

gave good quality apo-protein, which had a very low residual HRP activity (less than 0.3% of native HRP), and high peroxidase activity when recombined with hemin IX **227**, as confirmed by enzyme assays both in the literature[229] and in this thesis. However, the PD-10 column procedure was more rapid and hence was the method of choice.

Apo-HRP is reasonably stable and can be stored below 0 ^0C for certain period of time. However, after 3 months, the enzymatic activity after reconstitution of apo-HRP with hemin was only 15% of that obtained after reconstitution with freshly prepared apo-HRP. Hence, in this thesis all the apo-protein samples were freshly prepared, and used for reconstitution with hemin IX **227** or modified hemins (**230, 232**) on the same day.

The details of the preparation of apo-HRP are in experimental section;
HRP (3.95 mg) was dissolved in sodium phosphate buffer (2 ml, 0.005 M, pH = 6.5) and 0.1 ml of the resulting solution was taken to make up 1 ml of dilute sodium phosphate buffer solution. The concentration of HRP was determined spectrophoto-metrically using an extinction coefficient of 1.077×10^5 mol^{-1}·cm^{-1} at 403 nm[152] (Figure 62). There was one major band at 402 nm with an aborbance of 0.4535 and small shoulders at 500 nm and 278 nm (A = 0.1585). For the stock solution, the RZ value was therefore 2.86 and the concentration of the stock horseradish peroxidase solution was $4.535/1.077 \times 10^5$ or 4.21×10^{-5} mmol.mL^{-1} (42.1 μmol.L^{-1}). Since the molecular weight of HRP is 4.4×10^4 mg.mmol^{-1},[43] the total weight of HRP in the original 2 ml of solution was $4.21 \times 10^{-5} \times 4.4 \times 10^4 \times 2$ or 3.7 mg. The purity of the original HRP solution therefore was $(3.70/3.95) \times 100\%$ or 93.7%.
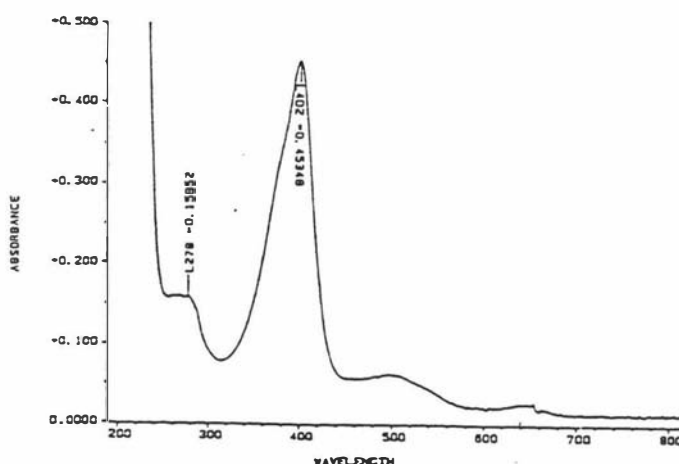
Figure 62 High RZ value (2.86) of native horseradish peroxidase in electronic spectrum showing its high purity.

The original stock HRP solution was then diluted 2000 times, and 5 μl of the diluted HRP solution was taken for the *o*-dianisidine peroxidase assay as described in methods (section 5.2.3). The enzyme activity was 8.14×10^{-3} ΔAu sec^{-1}, which gave an activity for the original HRP sample of $8.14 \times 10^{-3} \times 2000 \times (1/0.005) \times 60$ or 195360 ΔAu min^{-1}.mL^{-1}, giving 195360/42.1 or 4.64×10^3 ΔAu min^{-1}.nmol^{-1}.
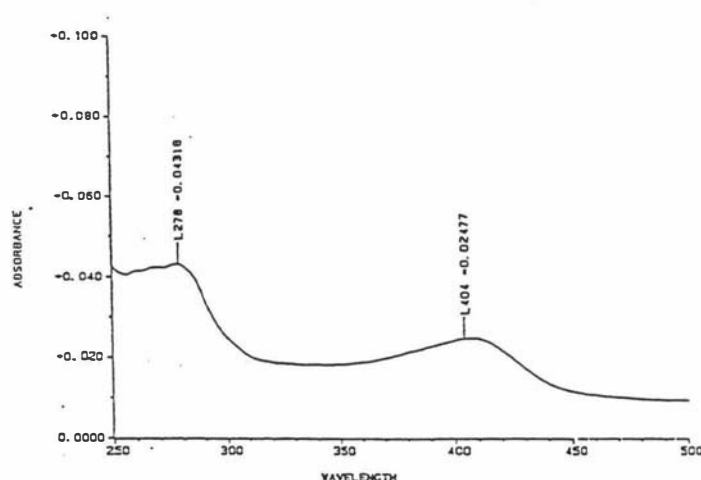
Figure 63 Low RZ value (0.5376) of apo-horseradish peroxidase in the electronic spectrum indicated that most of the hemin IX **227** was removed from the native horseradish peroxidase solution.

For the undiluted apo-HRP solution, prepared in this thesis, the absorbance at 278 nm was 0.4318 and hence the concentration was $0.4318/2 \times 10^4$ or 2.16×10^{-5} mmol.mL^{-1} (21.6 μmol.L^{-1}) with an RZ value of 0.5376 (Figure 63). The total number of nmoles of apo-HRP (3.5 ml) was 21.6×3.5 or 75.6 nmoles and the number of nmoles of original HRP solution (1.9 ml) was 42.1×1.9 or 80 nmoles. Hence, the chemical yield of apo-HRP was 75.6/80 or 95%. Comparing Figure 63 with Figure 62, the major absorbance at 402 nm, which is proportional to the concentration of active HRP, was substantially reduced; while the absorbance at 278 nm, which corresponded to the concentration of the apo-protein, was increased. The overall result indicated that most of the hemin IX **227** was removed from HRP and the native HRP was transformed into the apo-protein.

The apo-HRP solution was diluted by 20 times, and 5 μL of the diluted sample was taken for the o-dianisidine peroxidase assay. The activity was 1.44×10^{-3} ΔAu sec^{-1}, giving an activity for the original apo-HRP solution of $[1.44 \times 10^{-3} \times 20 \times (1/0.005) \times 60]/21.6$, or 16 ΔAu min^{-1}.nmol^{-1}. Hence, the residual HRP activity of the apo-HRP solution was $16/4.64 \times 10^{3}$, or 0.3%. A low residual activity for the apo-HRP solution is vital since it is possible to have low activities for the binding and reconstitution of the modified hemins with apo-HRP. It is therefore necessary to be sure that a low reconstitution activity is not due to residual enzymic activity of the apo-HRP. From the above result, the apo-HRP prepared in this thesis has high purity (low RZ value, 0.5376) and low residual activity (0.3% of native HRP).

5.3.2 Reconstitution of apo-HRP with L-phenylalanine mono-conjugate 230

In order to establish the procedures for a successful reconstitution of a modified hemin the first attempts were carried out with L-phenylalanine-hemin mono-conjugate **230** with apo-HRP. The spectrum of the reconstituted HRP from the pure hemin IX **227** with apo-HRP is shown in Figure 64 and a single main peak was shown at 402 nm, which is identical with the position of the major absorbance band (402 nm) in native HRP (Figure 62). The aborbances at 278 nm (A = 0.0462) and 402 nm (A = 0.1387) (see Figure 64) gave an RZ value of 3.0, and a value for the concentration of reconstituted HRP of $0.1387/1.077 \times 10^{5}$, or 1.29×10^{-6} mmol/mL (1.29 μmol.L^{-1}). Since the number of nmoles of apo-HRP (0.3 ml) for reconstitution was 21.6×0.3 or 6.48 nmoles and the number of nmoles of reconstituted HRP solution (3 ml) was 1.29×3 or 3.87 nmoles, the yield of the reconstituted HRP was $(3.87/6.48) \times 100\%$, or 60%.
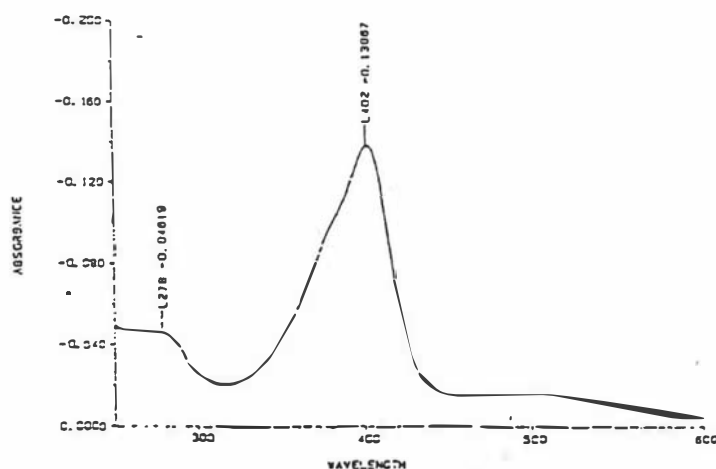
Figure 64 High RZ value (3.0) in the electronic spectrum showing good reconstitution between the hemin IX **227** and apo-horseradish peroxidase.

The reconstituted HRP solution was diluted by 66.7 times, and 5 μL of the diluted HRP solution was taken for the o-dianisidine peroxidase assay to give an activity of 6.16×10^{-3} $\Delta Au \cdot sec^{-1}$. This corresponds to an activity for the reconstituted HRP of $[6.16 \times 10^{-3} \times (1/0.005) \times 66.7 \times 60]/1.29$, or 3.82×10^3 $\Delta Au.min^{-1}.nmol^{-1}$. Thus, the recovery of enzymatic activity was $(3.82 \times 10^3/4.64 \times 10^3)$ - 0.3%, or 82% of the original HRP solution.
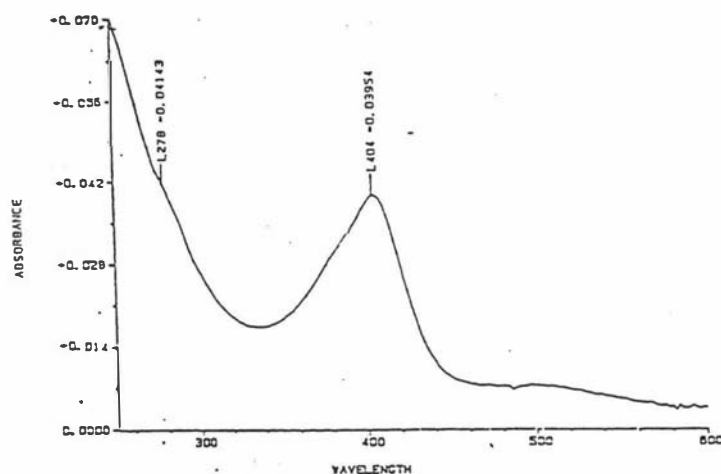
Figure 65 Low RZ value (0.95) of phenylalanine-HRP in electronic spectrum showing poor reconstitution between the hemin-phenylalanine mono-conjugate **230** and apo-horseradish peroxidase.

For the L-phenylalanine-hemin mono-conjugate, the spectrum of L-phenylalanine-HRP gave a low RZ value (0.95) (Figure 65), which shows poor reconstitution between the L-phenylalanine-hemin mono-conjugate and apo-HRP. If the extinction coefficient of $\varepsilon_{402} = 1.077 \times 10^5$ for the hemin IX **227** bound in native HRP was taken as applying to the reconstituted HRP with hemin-phenylalanine mono-conjugate **230**, the concentration of the reconstituted HRP-phenylalanine enzyme was $0.03954/1.077 \times 10^{-7}$, or 3.67×10^{-7} mmol.ml^{-1} (0.367 μmol.L^{-1}). The number of nmoles of apo-HRP (0.3 ml) for reconstitution was 21.6×0.3 or 6.48 nmoles and the number of nmoles of reconstituted phenylalanine-HRP solution (3 ml) was 0.367×3 or 1.1 nmoles. Thus, the yield of the **reconstituted** phenylalanine-HRP was $(1.1/6.48) \times 100\%$, or 17%.

The reconstituted phenylalanine-HRP solution was diluted by 66.7 times, and 5 μl of the diluted phenylalanine-HRP solution was taken for the o-dianisidine peroxidase assay. The enzyme activity was 2.52 x 10^{-4} ΔAu·sec^{-1}, thus giving a value for the activity for the reconstituted phenylalanine-HRP of [2.52 x 10^{-4} x 66.7 x (1/0.005) x 60]/0.367 or 550 ΔAu.min^{-1}.nmol^{-1}. The recovery of peroxidase activity for the reconstituted enzyme was (550/4.64 x 10^3) - 0.3% or 12% (relative to native HRP). Alternatively, the activity of phenylalanine-HRP was 12%/82% or 15% (relative to reconstituted hemin-HRP).

The low reconstitution yield (17%) and activity (15%) clearly shows poor reconstitution between the phenylalanine-hemin mono-conjugate **230** with apo-horseradish peroxidase. The reason for the poor binding and low activity of the phenylalanine-hemin mono-conjugate **230** with apo-HRP is probably due to a relatively large steric interaction by the phenylalanine side chain in the heme pocket. This steric disruption strongly destabilises the proper heme-protein interactions, possibly including axial imidazole-iron bond and van der Waals interactions between amino acid chains and the heme π system, and prevents the higher binding of the apoprotein with the hemin compound **230**.

The reconstitution of hemin IX **227** or L-phenylalanine-hemin mono-conjugate **230** with apo-HRP and their enzyme assays are summarised in scheme 50.

Scheme 50. Enzyme Assay of L-phenylalanine-HRP
(hemin IX227 control)

Original HRP
(3.95 mg in 2 ml phosphate buffer)
RZ=2.86, **42.1** μ**mol.L^{-1}**
1.9 ml left

→ dil. 2000 times
0.1 ml

Assay (**5** μ**L**): 8.14 x 10^{-3} ΔAu·sec^{-1}
Activity:
x 60 x (1/ 0.005) x 2000 / 42.1
= 4.64 x 10^3 ΔAu·min^{-1}·nmol.L^{-1}

remove hemin and
purified by dialysis

Apo-HRP (**3.5 ml**)
RZ = 0.0432, **21.6** μ**mol.L^{-1}**
Chemical yield:
(21.6 x 3.5)/(42.1 x 1.9)
= 95%

→ dil. 20 times

Assay (**5** μ**L**): 1.44 x 10^{-3} ΔAu·sec^{-1}
Activity:
x 60 x 20 x (1/ 0.005) / 21.6
= 16 ΔAu·min^{-1}·nmol.L^{-1}
Activity residue: 16/4.64 x 10^3 **= 0.3%**

apo-HRP
(**0.3 ml**)

apo-HRP
(**0.3 ml**)

Reconstituted HRP (**3 ml**)
RZ = 3.0, **1.29** μ**mol.L^{-1}**
Reconstitution yield:
(1.29 x 3)/(21.6 x 0.3)
= 60%

Reconstituted phenylalanine-HRP (**3 ml**)
RZ = 0.95, **0.367** μ**mol.L^{-1}**
Reconstitution yield:
(0.367 x 3)/(21.6 x 0.3)
= 17%

dil. 66.7 times

dil. 66.7 times

Assay (**5** μ**L**): 6.16 x 10^{-3} ΔAu·sec^{-1}
Total activity:
x 60 x 66.7 x (1/0.005) / 1.29
= 3.82 x 10^3 ΔAu·min^{-1}·nmol.L^{-1}
The recovery of activity:
= [(3.82 x 10^3) / (4.64 x 10^3)] - 0.3%
= 82% (relative to native HRP)

Assay (**5** μ**L**): 2.52 x 10^{-4} ΔAu·sec^{-1}
Total activity:
x 60 x 66.7 x (1/0.005) / 0.367
= 550 ΔAu·min^{-1}·nmol.L^{-1}
The recovery of activity:
= [550 / (4.64 x 10^3)] - 0.3%
= 12% (relative to native HRP)
or 12% / 82%
= 15% (relative to reconstituted-HRP)

5.3.3   Reconstitution of apo-HRP with E1G-hemin mono-conjugate 232

The reconstitution of apo-HRP with E1G-hemin mono-conjugate **232** was performed in a similar procedure as for reconstitution of apo-HRP with L-phenylalanine-hemin mono-conjugate **230** except that a spectrophotometric titration at room temperature was used to monitor the reconstitution process of the apo-HRP with E1G-hemin mono-conjugate **232** using pure hemin IX **227** as a titration control.

For the original HRP solution ($1.80 \, mg.mL^{-1}$, 3.60 mg HRP in 2 ml phosphate buffer, 0.005 M, pH = 6.5), the absorbance at 280 nm ($A_{280} = 1.2746$) and 403 nm ($A_{403} = 3.7790$) gave an RZ value of 2.96. The concentration of HRP was $3.78/1.077 \times 10^5$ or 3.51×10^{-5} $mmol.mL^{-1}$ (35.1 $\mu mol.L^{-1}$). The HRP solution was then diluted 2000 times, and 20 μl of the final diluted HRP solution was taken for the *o*-dianisidine peroxidase assay. The enzymic activity was 1.15×10^{-2} $\Delta Au \, sec^{-1}$, which corresponded to the specific activity for the original HRP solution of [$1.15 \times 10^{-2} \times 2000 \times (2/0.02) \times 60$] / 35.1, or 3.93×10^3 $\Delta Au \, min^{-1}.nmol^{-1}$.

For the acidified HRP solution prior to extraction of the hemin (pH = 2.45), the A_{280} and A_{403} values gave an RZ value of $3.2884/1.5217$ or 2.15. The concentration of HRP was $3.2884/1.007 \times 10^5$ or 3.05×10^{-5} $mmol.mL^{-1}$ (30.5 $\mu mol.L^{-1}$). Thus, active HRP remaining was 30.5/35.1 or 87%. The above acidified HRP solution (pH = 2.45) was diluted 1000 times, and 20 μl of the final diluted HRP solution was taken for the *o*-dianisidine peroxidase assay to give an enzymic activity of 1.89×10^{-2} $\Delta Au \, sec^{-1}$ (20 μl). The activity of the acidified HRP was therefore [$1.89 \times 10^{-2} \times 1000 \times (2/0.02) \times 60$] / 30.5 or 3.72×10^3 $\Delta Au \, min^{-1}.nmol^{-1}$. The remaining activity was ($3.72 \times 10^3/3.93 \times 10^3$) $\times 100\%$ or 95% (relative to native HRP).

The preparation of apo-HRP was performed by a similar procedure as previously described except that the apo-HRP was filtered through a PD-10 column to remove the butanone instead of using dialysis against water. After extraction of the hemin from the acidified HRP solution (1.8 ml, pH = 2.45), the apo-HRP (1.8 ml) was directly filtered through a commercial PD-10 column and the purified apo-HRP was collected in a 3.5 ml aliquot. Since the apo-HRP solution contained very small amount of residual butanone, the concentration of apo-HRP solution can not be obtained by calculation from its A_{278} value. Hence, the concentration of apo-HRP solution (protein concentration) was determined by Coomassie Blue method instead.

The value of 0.690 mg.mL^{-1}, provided by Ms Delwyn Cooke, corresponded to 0.690/ 4.4 x 10^4 or 15.68 mmol.mL^{-1} (15.68 μmol.L^{-1}). Therefore, the chemical yield of apo-HRP was (15.68 x 3.5)/(35.1 x 1.8) or 87%. The apo-HRP solution (20 μl) was directly taken for the o-dianisidine peroxidase assay and the result was 7.76 x 10^{-3} ΔAu sec^{-1}. Hence, the residual activity for apo-HRP was [7.76 x 10^{-3} x (2/0.02) x 60]/15.68 or 3 ΔAu.min^{-1}.nmol^{-1}, giving a residual peroxidase activity of 3/3.93 x 10^3 or 0.08% of the original HRP solution.

In a pre-incubated cuvette (1 mL) at room temperature, spectrophotometric titrations (pH = 8, tris-buffer, 0.1 M) of the apo-HRP solution (0.3 ml of apo-HRP and 0.7 ml of the same tris-buffer) with aliquots of excess hemin IX **227** or E1G-hemin **232**, using pure hemin IX or E1G-hemin as a titration control, were carried out and the results are shown in Figure 66 and Figure 67, respectively.

When hemin IX **227** binds to apo-HRP there is an increase in the extinction coefficient at 404 nm and thus the binding is observed as a hyperbolic increase (Figure 66). Once the available apo-HRP binding sites are saturated, the increase in A$_{404}$ with the increase in concentration of hemin IX **227** become parallel to the control line and the maximum difference corresponds to the concentration of reconstituted enzyme.

Figure 66. Titration of Hemin IX **227** with or without Apo-HRP
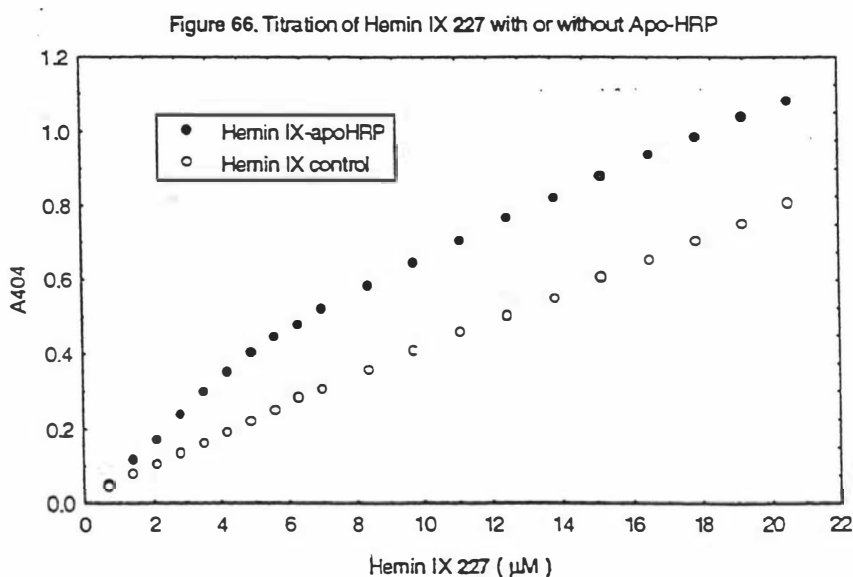
Similar results were obtained with the E1G-hemin monoconjugate **232** (Figure 67), indicating a much greater degree of binding to the apo-HRP than found for L-phenylalanine-hemin mono-conjugate **230**.

Figure 67. Titration of Hemin-E1G 232 with or without Apo-HRP
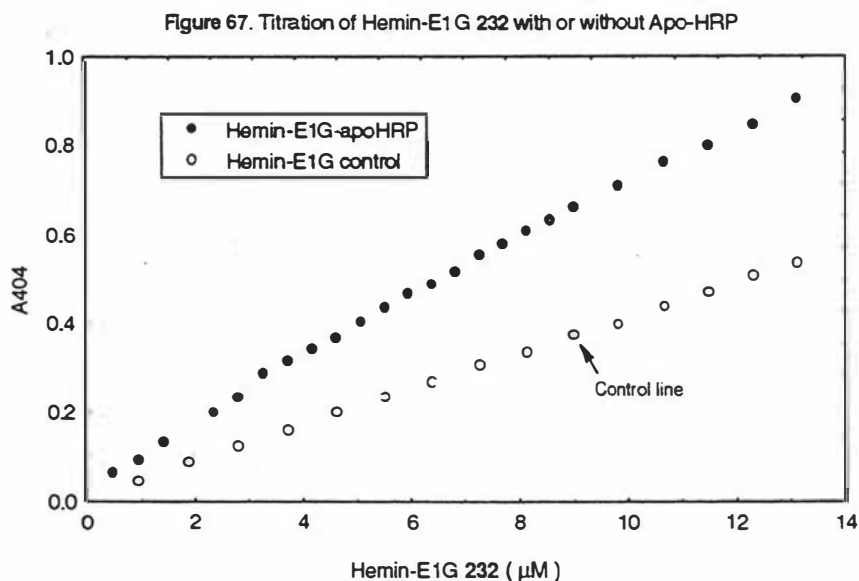
On titration of all the apo-protein in solution, the concentration of occupied binding sites reaches a maximum, equivalent to the total heme binding site concentration. Thus, a plot of ΔA_{404} against the total hemin concentration should be a hyperbola. Difference plots of this kind curve are shown for the hemin IX **227** and E1G-hemin **232** titrations (Figures 68 and 69). These can be fitted by non-linear regression to give Bmax (proportional to the maximum amount binding) and K_D (the enzyme dissociation constant) parameters, which can be carried out conveniently by the non-linear curve fitting package of the program Graphpad Prism (San Diego, CA).

The concentration of the hemin IX **227** was determined spectrophotometrically using an extinction coefficient of 58.4 mmol·cm^{-1} at 385 nm.[235] The same extinction coefficient of 58.4 mmol·cm^{-1} was also taken as applying for determination of the concentration of E1G-hemin mono-conjugate **232**. Since an isomeric mixture of 6- and 7-monosubstituted E1G-hemin was used for the spectrophotometric titration with apo-HRP and only one isomer (most likely 6-substituted isomer) can bind with apo-HRP, the X values in Figure 68 were taken as half the formal concentration. Therefore, the Bmax values and the enzyme dissociation constants (K_D) for the two reconstituted enzymes (hemin-HRP and E1G-HRP) were obtained from these two binding curves (Figures 68 and 69); for hemin-HRP: Bmax 0.3900, K_D 6.435 µM; for E1G-hemin: Bmax 0.4118, K_D 8.465 µM.
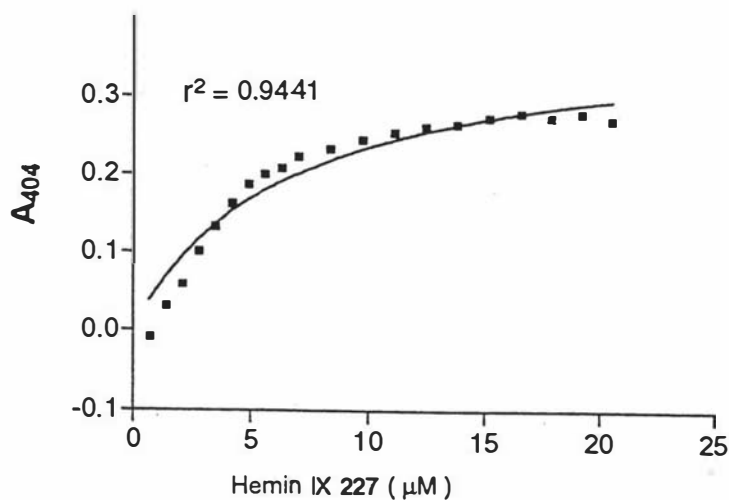
Figure 68 Binding curve for hemin IX-apo-HRP with baseline subtraction.
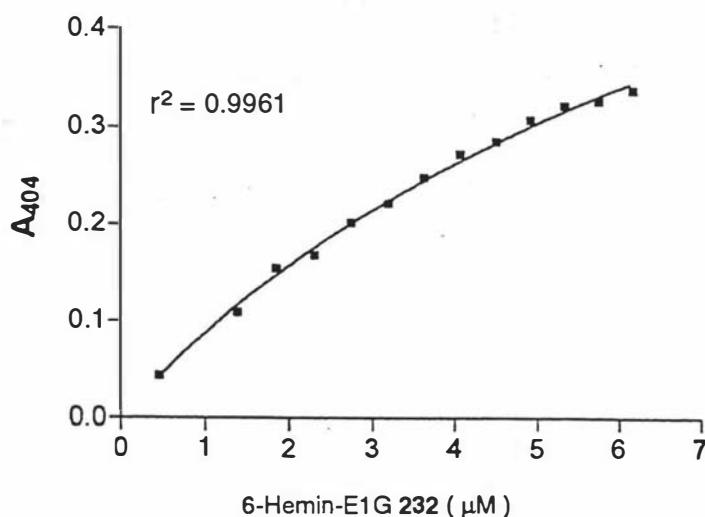
Figure 69 Binding curve for E1G-hemin-apo-HRP with baseline subtraction.

The similarity of the K_D values and the Bmax values for both reconstituted enzymes shows that the E1G-hemin mono-conjugate **232** binds to apo-horseradish peroxidase almost as well as does hemin IX **227**. Some hydrogen-bonding interactions between the carbohydrate moiety of the steroid glucuronide and the protein matrix,[236] together with the hydrophobic effect of the non-polar steroid, possibly helps to stabilise the enzyme structure despite the bulky nature of the estrone glucuronide moiety.

The reconstituted hemin-HRP or E1G-HRP solution (0.6 ml each) was taken from the titration cuvette (1 ml), and filtered through a DE 52 column to remove excess hemin **227** or E1G-hemin **232**. After concentration, purified reconstituted hemin-HRP (0.37 ml) or E1G-HRP (0.21 ml) was obtained. The purified reconstituted hemin-HRP solution was diluted 6.67 times, and the concentration of reconstituted hemin-HRP was determined spectrophotometrically. The absorbance at 403 nm was 0.07021 (Figure 70). The purified reconstituted E1G-HRP solution was diluted 20 times, and its concentration was also determined spectrophotometrically. The absorbance at 403 nm was 0.03656 (Figure 70). Hence in the titration solution (1 ml) the concentration of reconstituted HRP was $[(0.070 \times 6.67)/1.077 \times 10^5] \times (0.37/0.6)$ or 2.67×10^6 mmol.mL^{-1} (2.67 μmol.L^{-1}) and the concentration of E1G-HRP was $[(0.037 \times 20)/1.077 \times 10^5] \times (0.21/0.6)$ or 2.4×10^6 mmol.mL^{-1} (2.4 μmol.L^{-1}). Since the concentration of apo-HRP in the same titration solution was 15.68×0.3 or 4.7 μmol.L^{-1}, ignoring losses of the enzymes on the DE column, the reconstitution yields were 2.67/4.7 or 57% for hemin IX-HRP and 2.40/4.7 or 51% for E1G-HRP.
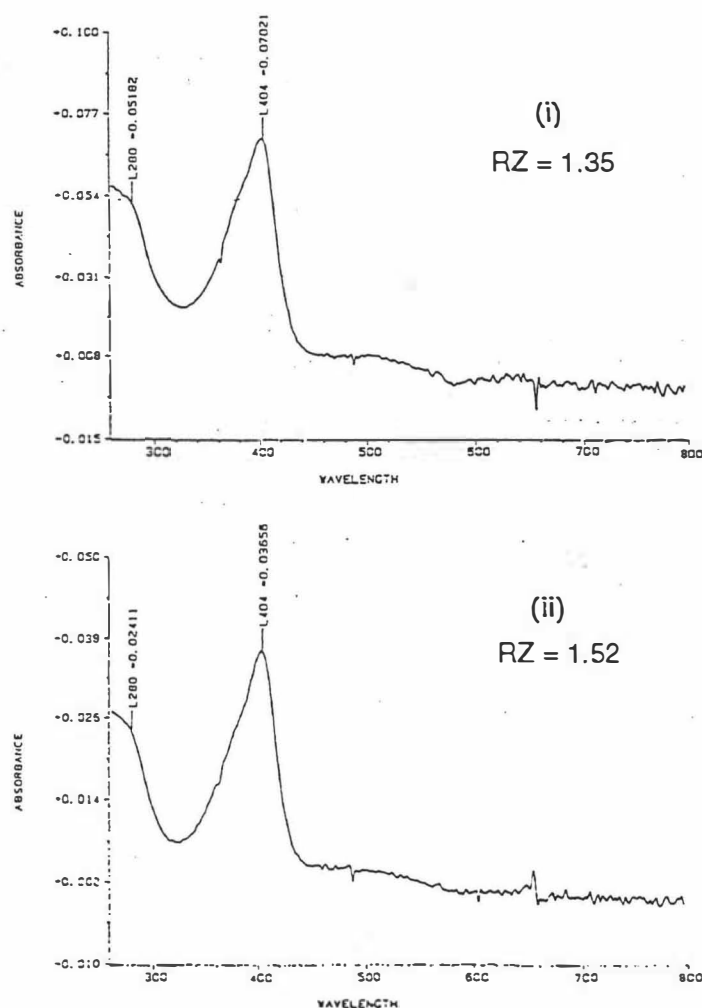
Figure 70. Both reconstituted hemin IX-HRP (i) and E1G-HRP (ii) enzymes showing the similar electronic spectra and RZ values.

The concentrated reconstituted hemin-HRP solution was diluted 500 times, and 20 μl of the final diluted HRP solution was taken for the o-dianisidine peroxidase assay. The enzymic activity was 5.23×10^{-3} ΔAu·sec^{-1} (20 μl), which gave the overall enzyme activity for concentrated hemin-HRP of $[5.23 \times 10^{-3} \times 500 \times (2/0.02) \times 60] / 2.67 \times (0.6/0.37)$ or 3.62×10^3 ΔAu.min^{-1}.nmol^{-1}. The overall recovery of activity was $(3.62 \times 10^3/3.93 \times 10^3) - 0.08\%$ or 92% (relative to native HRP).

The reconstituted E1G-HRP solution was also diluted 500 times, and 20 μl of the final diluted E1G-HRP solution was taken for the *o*-dianisidine peroxidase assay. The enzymic activity was 6.29×10^{-3} ΔAu sec^{-1} (20 μl), which corresponded to a total enzymic activity for E1G-HRP of $[6.29 \times 10^{-3} \times 500 \times (2/0.02) \times 60] / 2.4 \times (0.6/0.21)$ or 2.75×10^3 ΔAu.min^{-1}.nmol^{-1}. The overall recovery of activity was $(2.75 \times 10^3/3.93 \times 10^3) - 0.08\%$ or 70% (relative to native HRP). Alternatively, the activity of E1G-HRP was $(70\%/92\%) \times 100\%$ or 76% (relative to the activity of the reconstituted hemin-HRP).

From the above results, it is clearly shown that estrone glucuronide modified horseradish peroxidase has been successfully obtained by reconstitution of estrone glucuronide-hemin **232** with apo-HRP. The reconstituted E1G-HRP retains significant peroxidase activity (76%), which can be used in immunoassays without any doubt. The new enzyme (E1G-HRP) has a similar spectrum (Figure 70) and K_D value to those of the reconstituted hemin-HRP enzyme. The results indicate that the E1G-HRP has good binding with apo-HRP and good stability.

The reconstitution of hemin IX **227** or estrone glucuronide-hemin mono-conjugate **232** with apo-HRP and their enzyme assays are summarised in scheme 51.

Figure 51. Enzyme assay of E1G-HRP (hemin IX227 control)
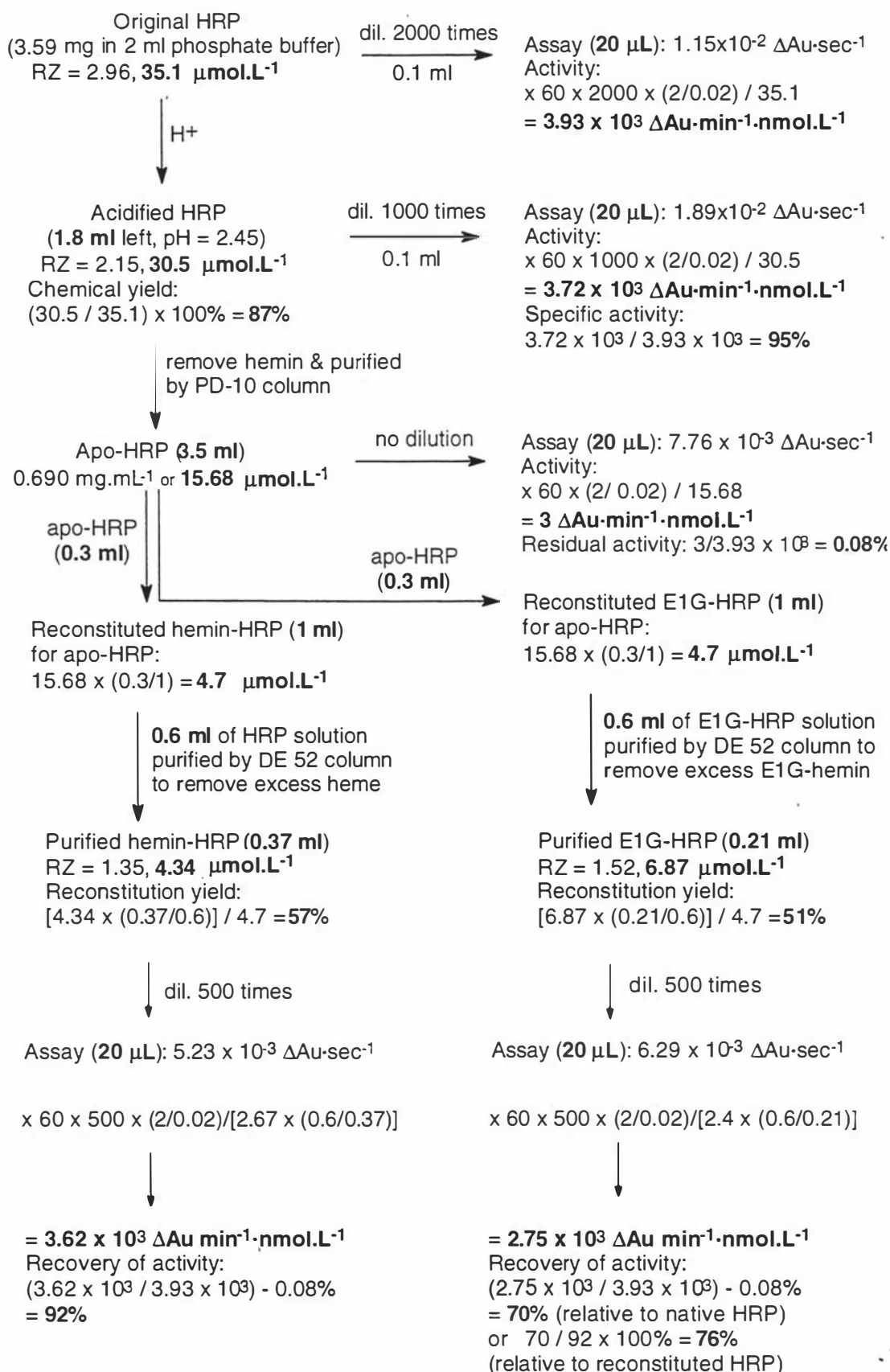
5.3.4 Peroxidase activities of reconstituted HRP from synthetic hemins

For a long time, extensive theoretical research on heme modification of hemoproteins, including horseradish peroxidase (HRP), has been concentrated on the structure and activity relationship of heme pockets, but usually only small functional group transformations have been investigated and very low peroxidase activities have been achieved. For the first time, in this thesis, a very large biological compound - estrone glucuronide (E1G) **12** has been introduced into the heme pocket of horseradish peroxidase, and still gives good peroxidase activity (76% of reconstituted HRP), which is much higher than all the literature values from the other synthetic hemin compounds (Table 10).[151-152,229] Comparing the structures of E1G-hemin mono-conjugate **232** and L-phenylalanine-hemin mono-conjugate **230** in this thesis with a variety of other synthetic hemin compounds for the reconstitution with apo-HRP (Table 10), we can now discuss some new and important issues relating to the studies of heme modification:

(i). Very small size changes in the hemin 2- and 4-position cause a dramatic loss of peroxidase activities of HRP. [from the hemin IX **227** (100%) to diacetyldeuterohemin **292** (17%)], compared with changes of the hemin 6- and 7-positions [from hemin IX **227** (100%) to E1G-hemin monoconjugate **232** (76%) or to dibutyric acid hemin **287** (32%)]. Hence, it has been confirmed that heme modification at 6- and 7-propionate side chains is far better tolerated by the protein tertiary structure than at the hemin 2- and 4-positions.

(ii). One free carboxyl group of the hemin compounds (more likely the 7-propionate) is crucial for the genaration of an active enzyme. The number of free carboxyl groups also seems to be important, such as activities of E1G-hemin monoconjugate **232** (76%), dibutyric acid hemin **287** (32%) and hemin I **293** (23%) all having two carboxyl groups in their structures are higher than those of hemin monoester **290** (18%) and hemin diester (0%), which contains only one or no carboxyl group. But the relative positions of the carboxyl groups appear to be of far more importance than their number. For example, the activity of E1G-hemin monoconjugate **232** (76%), although containing a very large substituent, is much higher than that of the much smaller dibutyric acid hemin **287** (32%) and also the hemin I **293** (23%). The results suggest that the extra carboxyl group, introduced by the L-lysine linker in this thesis, has a beneficial effect being better than the carboxyl groups in hemin compounds **287** and **293**.

Table 10. Reconstitution yields and peroxidase activities of reconstituted HRP from synthetic hemins

Hemin	Reconstitution yield (%)	Peroxidase activity(%)	Ref
native (227)		116	229
	100 a	109	thesis
hemin IX (227)	57-60	100 b	thesis
hemin-E1G (232)	51	76	thesis
hemin-phenylalanine (230)	17	15	thesis
dibutyric acid hemin (287)		32	151
dialcohol hemin (288)		7	151
hemin diamide (289)		7	151
hemin monoester (290)		18	152
deuterohemin (291)		33	229
diacetyl-deuterohemin (292)		17	229
hemin I (293)		23	229

a, native HRP was taken as 100% reconstitution yield for all synthetic hemins;
b, Specific activity of reconstitution of hemin IX227 with apo-HRP was taken as 100% peroxidase activity for other synthetic hemins
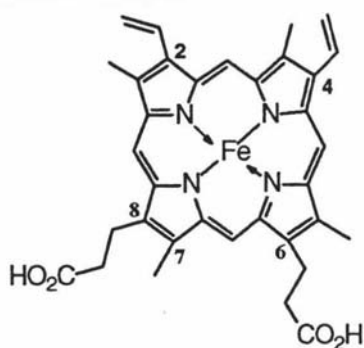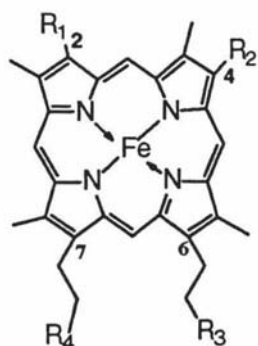
227 $R_1 = R_2 = $ -CH=CH$_2$, $R_3 = R_4 = $ -COOH;
287 $R_1 = R_2 = $ -CH=CH$_2$, $R_3 = R_4 = $ -CH$_2$COOH;
288 $R_1 = R_2 = $ -CH=CH$_2$, $R_3 = R_4 = $ -CH$_2$OH;
289 $R_1 = R_2 = $ -CH=CH$_2$, $R_3 = R_4 = $ -CONH$_2$;
290 $R_1 = R_2 = $ -CH=CH$_2$, $R_3 = $ CO$_2$Me, $R_4 = $ CO$_2$H
　　　　　　　or $R_3 = $ CO$_2$H, $R_4 = $ CO$_2$Me;
291 $R_1 = R_2 = $ H; $R_3 = R_4 = $ -COOH;
292 $R_1 = R_2 = $ COCH$_3$, $R_3 = R_4 = $ -COOH;

293

(iii). The length of the less important propionate side chain (more likely the 6-propionate) is clearly not a serious obstacle for the reconstitution of the apo-protein with hemin derivatives, such as the E1G-hemin mono-conjugate **232**, (76% activity recovery), despite the fact that a long chain and a large steroid glucuronide molecule (E1G) is linked into the heme pocket. The earlier conclusion[151] that the length of both hemin 6- and 7-side chains is important has been shown to be incorrect by the present work.

Based on the experimental results and theoretical analysis, a model building experiment carried out by linking the estrone glucuronide-L-lysine **214** to the hemin 6-propionate side chain of cytochrome c peroxidase is shown in Figure 71. The hemin-steroid glucuronide fits well in this modelling picture. The substrate channel is clearly shown by the 8-methyl group and the δ-meso carbon, and estrone glucuronide (E1G) moiety emerges from the protein possibly through the peroxide channel[219] *via* the L-lysine side chain and fits well just outside the protein surface (Figure 71).
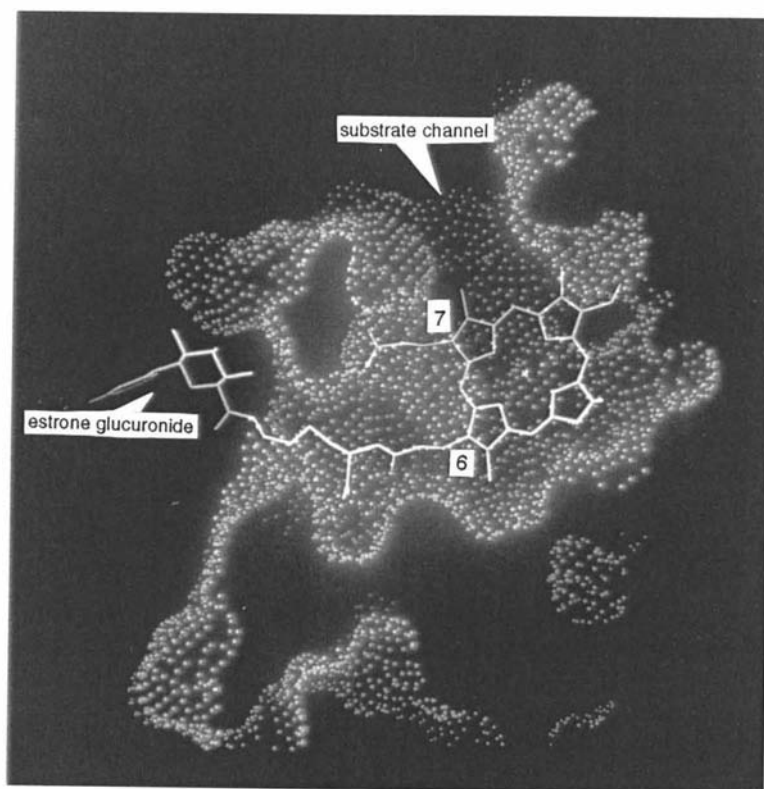
Figure 71. An estrone glucuronide-HRP mono-conjugate model produced by linking estrone glucuronide-L-lysine **214** to the hemin 6-propionic acid group of cytochrome c peroxidase. The model generated a water accessible surface to show the possible channels within the cytochrome c peroxidase structure.

From Figure 71, it is clearly shown that the use of a suitable molecular linker is crucial for the reconstitution of hemin compounds with the apoprotein. Phenylalanine-hemin monoconjugate **230** has a poor reconstitution with the apo-HRP due to the absence of a molecular linker. A relatively larger phenylalanine side chain has to be accommodated inside the protein and results in strong steric interactions with the amino acid residues of the protein to destabilise the efficient heme-protein binding. In contrast, E1G-HRP has much higher activity (76%) than phenylalanine-HRP (15%) since L-lysine is a suitable linker, which is long enough to enable the steroid glucuronide (E1G) to fit outside the protein. The experimental results in this thesis are in good agreement with the above theoretical hypothesis and model building analysis.

During the time of writing this thesis, studies on a structural model for horseradish peroxidase have been reported.[237] Since both lignin peroxidase (LiP) and horseradish peroxidase (HRP) have in the active site a distal and a proximal phenylalanine, which is tryptophan in cytochrome c peroxidase (CcP), and both have a larger molecular weight than CcP, the amino acid sequence of LiP in the region of the active site is even more closely related to HRP than is CcP. Therefore, these researchers have built a starting structural model of HRP on the basis of molecular dynamic (MD) simulations from the X-ray structure of LiP, which has become available only recently.[238] In their studies on the active site structure, an extensive hydrogen bonded network was found. A water molecule is hydrogen-bonded to the guanidinum group of arginine 48 and two oxygen atoms, one of the 6-propionate and one of the 7-propionate. However, only the carboxylate of the 7-propionate, which is hydrogen-bonded to a histidine residue in CcP and to an aspartic acid residue in LiP, interacts directly with the side chain amide of an asparagine (Asn 175) residue. Since only the 7-propionate is hydrogen-bonded directly to the protein matrix in this HRP model, similar to the 7-propionate in both CcP and LiP, the 7-propionate is clearly more likely to be important than the 6-propionate for the binding of hemin with the apoprotein, which is in good agreement with the experimental results in this thesis.

5.3.5 Further work

Further work is now needed to be developed on the basis of the results of this thesis in the following areas:

(i) To separate the two different isomers of hemin 6- and 7-monoconjugates with estrone glucuronide **232** on the basis of HPLC analysis (Figures 51d and 51e, chapter 4, section 4.2.4.3); to characterise the two isomers separately with different NMR techniques and identify them; to reconstitute each isomer with apo-HRP separately to confirm that one isomer is more important than the other one by checking their different peroxidase activities.

(ii) To perform further model building experiments by linking estrone glucuronide-L-lysine **214** to the hemin 6-propionate side chain of horseradish peroxidase isomer C (co-ordinates to be available shortly) and see how well it fits with an anti-estrone glucuronide antibody (available in this laboratory already); to achieve immune reactivity of the new enzyme (E1G-HRP) and inhibition by the anti-estrone glucuronide antibody experimentally by adjusting the length of different molecular linkers between the estrone glucuronide and the hemin propionic acid under the guidance of the model fitting experiment.

(iii) To extend the methodology in preparation of estrone glucuronide-hemin conjugate **232** and its reconstitution with apo-HRP to the synthesis of general HRP-conjugates with other steroid glucuronides (E3-3G, E3-16G and PdG) and some other interesting analytes such as pesticide residues and expand more areas for the application of this useful methodology.

(iv) To develop different colour test strips or dipstick type kits (to be validated against the authentic Ovarian Monitor assay) on the basis of above results; to achieve a simple, economical and accurate method in home assays for fertility, or site and field testing for product quality control or for environmental pollution monitoring.

5.3.6 Summary

In summary, it has been demonstrated that estrone glucuronide-hemin mono-conjugate **232** can been successfully reconstituted with apo-horseradish peroxidase to form a new enzyme. Compared with the reconstituted HRP from pure hemin IX **227**, the new enzyme (E1G-HRP) retains good peroxidase activity (76% relative to reconstituted HRP), which is sufficient for exploitation in immunoassays. Both the new enzyme (E1G-HRP) and the reconstituted HRP from pure hemin IX have very similar electronic spectra. The maximum binding amount (Bmax) and the enzyme dissociation constant (K_D) of the new enzyme (E1G-HRP) also show close values to those of the reconstituted HRP from pure hemin IX. It is also shown in this chapter that a suitable molecular linker such as L-lysine between the hemin propionate side chain and the estrone glucuronide moiety is very important for retaining good peroxidase activity. Without a molecular linker, reconstituted L-phenylalanine-HRP shows a very poor reconstitution yield and activity. The extra carboxyl group, introduced by the molecular linker - L-lysine, probably makes a contribution in retaining a high peroxidase activity of the new enzyme (E1G-HRP).

This thesis exploits a new methodology in the preparation of horseradish peroxidase-hapten conjugates *via* hemin-modification. The synthesised HRP-conjugates are homogeneous, without any unconjugated horseradish peroxidase present and therefore there is no contamination and interference from free HRP in enzyme immunoassay systems. The ratio (1:1) of the hapten with the enzyme and the exact position of the hapten on the enzyme surface are all well known by this conjugation method. The orientation of the hapten, the recognition of the antigen by an antibody, and the antibody inhibition of the enzyme can also be controlled by choosing different types of molecular linkers with variable length between the hemin propionate side chains and the analytes. Since the new methodology used in this thesis for the preparation of estrone glucuronide-HRP conjugates is very general, it can be extended to the synthesis of horseradish peroxidase-conjugates with other steroid compounds of interest as markers of fertility (E3-3G, E3-16G and PdG) or many other different analytes, such as pesticide residues or any other environmental pollutants. It will be very useful for enzyme immunoassays in many areas such as food, agriculture, medicine and other biological fields. Therefore, the wide commercial applications for this new technology are expected in the near future.

References

(1)   Wilcox AJ, Weinberg CR and Baird DD (1995) Timing of Sexual Intercourse in Relation to Ovulation. *New England Journal of Medicine* **333**:1517-1521.

(2)   World Health Organization Task Force on Methods for the Determination of the Fertile Period (1983). Temporal relationships between indices of the fertile period. *Fertil Steril* **39**:647-655.

(3)   Odeblad E (1994). Discovery of different types of cervical and the the Billings ovulation method. *Bulletin of the Ovulation Method Research and Reference Centre of Australia* **21**:No 3.

(4)   Brown JB (unpublished results).

(5)   Doody MC, Gibbons WE, Zamah NM (1987). Linear regression analysis of ultrasound follicular growth series: statistical relationship of growth rate and calculated date of growth onset to total growth period. *Fertility and Sterility* **47**:436-440.

(6)   McNatty KP (1981). Hormonal correlates of follicular development in the human ovary. *Aust J Biol Sci* **34**:249-268.

(7)   Blackwell LF (unpublished results).

(8)   Hoff JD, Quigley ME, Yen SSC (1983). Hormonal dynamics at midcycle: a reevaluation. *J Clin Endocrinol Metab* **57**:792-796.

(9)   Stryer L (1981). Biochemistry. W. H. Freeman and Company, New York, P. 474-477.

(10)   Hall PF (1986). Cytochromes P-450 and the regulation of steroid synthesis. *Steroids* **48**:131-196.

(11)   Fishman J (1982). Biochemical mechanism of aromatization. *Cancer Research Suppl* **42**:3277s-3280s.

(12)   Baird DT (1977). Synthesis and secretion of steroid hormones. Academic Press, New York. P. 305.

(13)   Bolt HM (1979). *Metabolism of estrogens-natural and synthetic.* Pharmaceutical Therapeutics, Pergamon Press, Great Britain. **4**:19

(14)   Musey PI, Green RN, Hobkirk R (1972). The role of an enterohepatic system in the metabolism of 17β-E2-17G in the human female. *J Clin Endocrin Metab* **35**:448-457.

(15)   Baker TS, Jennison K, Kellie AE (1980). A possible method for the detection of ovulation and the determination of the duration of the fertile period. *J Steroid Biochem* **12**:411-415.

(16)   Serra GB (Ed) (1983). *Comprehensive Endocrinology-The Ovary.* Raven Press, New York. P. 432.

(17). Blackwell LF, Brown JB (1992). Application of time-series analysis for the recognition of increases in urinary estrogens as markers for the beginning of the potentially fertile period. *Steroids* **57**:554-562.

(18)   Brown JB, Blackwell LF, Holmes JM, Smith K (1989). New assays for identifying the fertile period. *Int J Gynecol Obstet Suppl* **1**:111-122.

(19)   Marrian CF (1930). The chemistry of estrine. 4) The chemical nature of crystalline preparations. *Biochem J* **24**:1021-1030.

(20)   Astwood FB (1938). A six-hour assay for the quantitative determination of estrogen. *Endocrinology* **23**:25-31.

(21)   Kober S (1938). The colorimetric estimation of the oestrogenic hormones: oestrone. *Biochem J* **32**:357-365.

(22)   Brown JB (1955). A chemical method for the determination of oestriol, oestrone and oestradiol in human urine. *Biochem J* **60**:185-193.

(23)   Price CP, Newman DJ (Ed) (1991). Principles and practice of immunoassay. Stockton press, New York, P. 246

(24) Kellie AE (1975). The radioimmunoassay of steroid conjugates. *J Steroid Biochemistry* **6**:277-281.

(25) Baker TS, Jennison KM, Kellie AE (1979). The direct radioimmunoassay of estrogen glucuronides in human female urine. *Biochem J* **177**:729-738.

(26) Samarajerwa P, Cooley G, Kellie AE (1979). The radioimmunoassay of pregnanediol-3α-glucuronide. *J Steroid Biochem* **11**:1165-1171.

(27) Stanczyk FZ, Miyakawa I, Goebelsmann U (1980). Direct radioimmunoassay of urinary estrogen and pregnanediol glucuronides during the menstrual cycle. *Am J Obstet Gynecol* **137**:443-450.

(28) Brown JB, Blackwell LF, Cox RI, Holmes JM, Smith MA (1988). Chemical and homogeneous enzyme immunoassay methods for the measurement of estrogens and pregnanediol and their glucuronides in urine. *Prog Clin Biol Res* **285**:119-138.

(29) Chatterton RT (1982). Ovulation detection and an indicator strip for this use. Eur Pat Appl EP 75,193 (*Chem Abstr* **99**:17314x).

(30) Lewis JG, Clifford JK, Elder PA (1990). Monoclonal antibodies to pregnanediol-3-glucuronide: application to a direct enzyme-linked immunoasorbent assay of urine. *Steroids* **55**:314-318.

(31) Kohen F, Kim JB, Barnard G, Lindner HR (1980). An assay for urinary estriol-16α-glucuronide based on antibody-enhanced chemiluminescence *Steroids* **36**:405-419.

(32) Eshhar Z, Kim JB, Barnard G, Collins WP (1981). Use of monoclonal antibodies to pregnanediol-3α-glucuronide for the development of a solid phase chemiluminescence immunoassay. *Steroids* **38**:89-109.

(33) Burd JF, Wong RC, Feeney JE, Carrico RJ, Boguslaski RC (1977). Homogeneous reactant-labelled fluorescent immunoassay for therapeutic drugs exemplified by gentamicin determination in human serum. *Clin Chem* **23**:1402-1408.

(34) Rubenstein KE, Schneider RS, Ullman EF (1972). Homogeneous enzyme immunoassay. New immunochemical technique. *Biochem Biophys Res Commun* **47:**846-851.

(35) Blackwell LF (personal database).

(36) Blake C, Gould BJ (1984). Use of enzymes in immunoassay techniques. A Review. *Analyst* **109:**533-547.

(37) Morris DL, Ellis PB, Carrico RJ, Yeager FM, Schroeder HR, Albarella JP, Boguslaski RC, Hornby WE, Rawson D (1981). Flavin adenine dinucleotide as a label in homogeneous colorimetric immunoassays. *Anal Chem* **53:**658-665.

(38) Carrico RJ, Christner JE, Boguslaski RC, Yeung KK (1976). A method for monitoring specific binding reactions with cofactor labelled ligands. *Anal Biochem* **72:**271-283.

(39) Burd JF, Carrico RJ, Fetter MC, Buckler RT, Johnson RD, Boguslaski RC, Christner JE (1977). Specific protein-binding reactions monitored by enzymatic hydrolysis of ligand-fluorescent dye conjugates. *Anal Biochem* **77:**56-67.

(40) Finley PR, Williams RJ and Lichti DA (1980). Evaluation of a new homogeneous enzyme inhibitor immunoassay of serum thyroxine with use of a bichromatic analyser. *Clin. Chem* **26:**1723-1726.

(41) Zappelli P, Pappa R, Rossodivita A, Re L (1978). Carboxylic and polyethylenimine-bounded FAD derivatives. synthesis, coenzymic properties, conformational and enzyme-coenzyme interaction studies. *Eur J Biochem* **89:**491-499.

(42) Tyhach RJ, Rupchock PA, Pendergrass JH, Skjold AC, Smith PJ, Johnson RD, Albarella JP, Profitt JA (1981). Adaptation of prosthetic-group-label homogeneous immunoassay to reagent-strip format. *Clin. Chem* **27:**1499.

(43)   Ryan O, Smith MR, Fagain CO (1994). Horseradish peroxidase: the analyst's friend. *Essays in biochemistry* **28**:129-146.

(44)   The structure of HRP isomer C has been solved in two crystal forms: with and without the substrate benzene hydroxamine acid bound in the active site. A detailed analysis of the two structures will be presented in the following paper: Gajhede M, Schuller DJ, Henriksen A, Smith AT, Poulos TL. Horseradish peroxidase C: crystal structure with and without the substrate: benzene hydroxamine acid (BHA) bound in the active site. (in preparation).

(45)   Part of the crystal structure of cytochrome *c* peroxidase was taken from the Cambridge Crystallographic Data Centre.

(46)   Rajkowski KM, Cittanova N (1981). The efficiency of different coupling procedures for the linkage of oestriol-16α-glucuronide, oestrone-3-glucuronide and pregnanediol-3α-glucuronide to four different enzymes. *J Steroid Biochem* **14**:861-866.

(47)   March SC, Shlpchandler MT (1984). Alkaline phosphatase labelled steroid hormone glucuronides. Eur Pat Appl EP 114,615 A2.

(48)   Smales CM, Cooke D, Blackwell LF (1994). Use of ion-exchange and hydrophobic-interaction chromatography for the rapid purification of lysozyme-estrone glucuronide conjugates. *J Chromator. B* **662**:3-14.

(49)   Stabenfeldt GH, Daels PF, Munro CJ, Kindahl H, Hughes JP (1991). An oestrogen conjugate enzyme immunoassay for monitoring pregnancy in the mare: limitations of the assay between days 40 and 70 of gestation. *J Reprod Fert Suppl* **44**:37-44.

(50)   Sauer MJ, Foulkers JA, Cookson AD (1981). Direct enzyme immunoassay of progesterone in bovine milk. *Steroids* **38**:45-53.

(51)   Exley D, Abuknesha R (1977). The preparation and purification of a β-D-galactosidase-17β-estradiol conjugate for enzyme immunoassay. *FEBS Lett* **79**:301-304.

(52)   Exley D, Abuknesha R (1978). A highly sensitive and specific enzyme-immunoassay method for oestradiol-17β. *FEBS Lett* **91**:162-165.

(53)   Van Weenman BK, Schuurs AHWM (1975). The influence of heterologous combinations of antiserum and enzyme-labelled estrone on the characteristics of estrone enzyme-immunoassays. *Immunochemistry* **12**:667-670.

(54)   Sauer Mj, Foulkers JA, O'Neill PM (1989). A comparison of alkaline phosphatase, β-galactosidase, penicillinase and peroxidase used as labels for progesterone determination in milk by heterologous microlitre plate enzyme-immunoassay. *J Steroid Biochem* **33**:423-431.

(55)   Bernstein S, Solomon S (1970). Chemical and biological aspects of steroid conjugation. Springer-Verlag, New York Inc. P. 3-5.

(56)   Elce JS, Carpenter JGD, Kellie AE (1967). The synthesis of estrogen monoglucuronides. *J. Chem. Soc (C)* 542-550.

(57)   Nambara T, Imai K (1967). Synthesis of estriol monoglucuronides. *Chem Pharm Bull* **15**:1232-1238.

(58)   Joseph JP, Dusza JP, Cantrall EW, Bernstein S (1969). Steroid conjugates. V. The synthesis of a sulfoglucuronide derivative of estriol. *Steroids* **14**:591-601.

(59)   Nambara T, Kawarada Y, Shibata K, Abe T (1972). Studies on steroid conjugates. IX. New synthesis of estriol 16- and 17-monoglucuronides. *Chem Pharm Bull* **20**:1968-1992.

(60)   Conrow RB, Bernstein S (1971). Steroid conjugates. VI. An improved Koenigs-Knorr synthesis of aryl glucuronides using cadmium carbonate, a new and effective catalyst. *J. Org. Chem.* **36**:863-870.

(61)   Numazawa M, Nagaoka M, Tsuji M (1983). Novel and efficient synthesis of estriol and its 16-glucuronide *via* 2,4,16α-tribromoestrone. *J Chem Soc Perkin Trans I* 121-125.

(62)   Ohkubo T, Wakasawa T, Nambara T (1990). Synthesis of 2-hydroxyestriol monoglucuronides and monosulfates. *Steroids* **55:**128-132.

(63)   Shimada K, Kaji H, Kuwabara K (1993). Determination of estriol monoglucuronide derivatives in the Koenigs-Knorr reaction by high-performance liquid chromatography. *J Chromatogr Sci* **31:**363-365.

(64)   Koenigs W, Knorr E (1901). *Chem Ber* **34:**957

(65)   Lemieux RU, Hayami JI (1965). The mechanism of the anomerization of the tetra-O-acetyl-D-glucopyranosyl chlorides. *Can J Chem* **43:**2162-2173.

(66)   Paulsen H, Lockhoff O (1981). Building units for oligosaccharides. XXX. new effective β-glycoside synthesis of mannose glycosides. syntheses of mannose containing oligosaccharides. *Chem Ber* **114:**3102-3114.

(67)   Garegg PJ, Konradsson P, Kvarnstrom I, Norberg T, Svensson SCT, Wigilius B (1985). Studies on Koenigs-Knorr glycosidations. *Acta Chemica Scandinavica B* **39:**569-577.

(68)   Wallace JE, Schroeder LR (1977). Koenigs-Knorr reactions. part 3. Mechanistic study of Mercury(II) cyanide promoted reactions of 2-O-acetyl-3,4,6-tri-O-methyl-α-D-glycopyranosyl bromide with cyclohexanol in benzene-nitromethane. *J Chem Soc Perkin Trans II* 795-802.

(69)   Garegg PJ, Norberg T (1979). Observation on silver trifluoromethane sulfonate-promoted syntheses of 1,2-*trans*-glycosides from acylated glycosyl bromides. *Acta Chemica Scandinavica B* **33:**116-118.

(70)   Burt RA, Chambers CA, Chiang Y, Hillock CS, Kresge AJ, Larsen JW (1984). Heats of formation of 1,3-dioxolenium ions from ortho ester precusors in sulfuric acid solution: methyl vs. phenyl substitution at the pro-acyl carbon atom. *J Org Chem* **49:**2622-2624.

(71)   Lubineau A, Malleron A (1985). Stannous triflated glycosidation. A stereoselective synthesis of β-D-glucosides. *Tetrahedron Lett.,* **26:**1713-1716.

(72)   Dess D, Kleine HP, Weinberg DV, Kaufman RJ (1981). Phase-transfer catalyzed synthesis of acetylated aryl β-D-glucopyranosides and aryl β-D-galactopyranosides. *Synthesis* 883-885.

(73)   Nishizawa M, Shimomoto W, Momii F, Yamada H (1992). Stereoselective thermal glycosylation of 2-deoxy-2-acetoamino-3,4,6-tri-O-acetyl-α-D-glucopyranosyl chloride. *Tetrahedron Lett.,* **33**:1907-1908.

(74)   Mukaiyama T, Murai Y, Shoda S (1981). An efficient method for glucosylation of hydroxy compounds using glucopyranosyl fluoride. *Chem Lett* 431-432.

(75)   Matsumoto T, Maeta H, Suzuki K, Tsuchihashi LG (1988). First total synthesis of mycinamicin IV and VII. successful application of new glycosidation reaction. *Tetrahedron Lett* **29**:3575-3578.

(76)   Lonn H (1985). Synthesis of a tri- and a hepta-saccharide which contain α-L-flucopyranosyl groups and are part of the complex type of carbohydrate moiety of glycoprotein. *Carbohydrate Res* **139**:105-113.

(77)   Sato S, Mori M, Ito Y, Ogawa T (1986). A efficient approach to O-glycosides through $CuBr_2$-Bu_4NBr mediated activation of glycosides. *Carbohydrate Res* **155**:C6-C10.

(78)   Pozsgay V, Jennings HJ (1987). A new method for the synthesis of O-glycosides from S-glycosides. *J Org Chem* **52**:4635-4637.

(79)   Ito Y, Ogawa T (1990). Benzenselenenyl triflate as an activator of thioglycoside for glycosylation reactions. *Carbohydrate Res* **202**:165-175.

(80)   Veeneman CH, Van leeuwen SH, Van Boom JH (1990). Iodonium promoted reactions at the anomeric centre. II An efficient thioglycoside mediated approach toward the formation of 1,2-*trans*-linked glycosides and glycosidic ester. *Tetrahedron lett* **31**:1331-1334.

(81)   Sasaki M, Tachibana K (1991). An efficient and stereocontrolled synthesis of the nephritogenoside core structure. *Tetrahedron lett* **32**:6873-6876.

(82) Kihlberg JO, Leigh DA, Bundle DR (1990). The in *situ* activation of thioglycosides with bromine: an improved glycosylation method. *J Org Chem* **55**:2860-2863.

(83) Fukase K, Hasuoka A, Kinoshita I, Aoki Y, Kusumoto S (1995). A stereoselective glycosidation using thioglycosides, activation by combination of N-bromosuccinimide and strong acid salts. *Tetrahedron* **51**:4923-4932.

(84) Ferrier RJ, Furneaux RH (1976). Synthesis of 1,2-*trans*-related 1-thioglycoside esters. *Carbohydrate Res* **52**:63-68.

(85) Tropper FD, Andersson FO, Roy CCR (1991). Stereospecific synthesis of 1,2-*trans*-1-phenylthio-β-D-disaccharides under phase transfer catalysis. *Synthesis* 734-736.

(86) Sinay P (1978). Recent advances in glycosylation reactions. *Pure Appl Chem* **50**:1437-1452.

(87) Fugedi P, Garegg PJ, Oscarson S, Rosen G, Silwanis BA (1991). Glycosyl 1-piperidinecarbodithioates in the synthesis of glycosides. *Carbohydrate Res* **211**:157-162.

(88) Kahne D, Walker S, Chen Y, Engen DV (1989). Glycosylation of unreactive substrate. *J Am Chem Soc* **111**:6881-6882.

(89) Zhang H, Wang Y, Voelter W (1995). A new strategy for the synthesis of the nephritogenoside trisaccharide unit using phenylsulfenyl donors. *Tetrahedron lett* **36**:1243-1246.

(90) Hashimoto S, Honda T, Ikegami S (1989). A rapid and efficient synthesis of 1,2-*trans*-β-linked glycosides *via* benzyl- or benzoyl-protected glycopyranosyl phosphates. *J Chem Soc (C)* 685-687.

(91) Hashimoto S, Honda T, Ikegami S (1990). A mild and rapid 1,2-*trans*-glycosidation method *via* benzoyl-protected glycopyranosyl P,P-diphenyl-N-(P-toluenesulfonyl)phosphinimidates. *Heterocycles* **30**:775-778.

(92)   Hashimoto S, Yanagiya Y, Honda T, Ikegami S (1992). An efficient construction of 1,2-*trans*-β-glycosidic linkages capitalizing on glycopyranosyl N,N,N',N'-tetramethylphosphoroamides as shelf-stable glycosyl donors. *Tetrahedron lett* **33**:3523-3526.

(93)   Hashimoto S, Honda T, Ikegami S (1991). A new and general glycosidation method for podophyllum lignan glycosides. *Tetrahedron lett* **32:**1653-1654.

(94)   Sabesan S, Neira S (1992). Synthesis of glycosyl phosphates and azides. *Carbohydrate Res* **223:**169-185.

(95)   Roy R, Tropper FD, Maiter CC (1991). Synthesis of glycosyl phosphates by phase transfer catalysis. *Can J Chem* **69:**1462-1467.

(96)   Hashimoto S, Umeo K, Sano A, Watanabe N, Nakajima M, Ikegami S (1995). An extremely mild and stereocontrolled construction of 1,2-*trans*-β-glycosidic linkages capitalizing on benzyl-protected glycopyranosyl diethyl phosphites as glycosyl donors. *Tetrahedron lett* **36:**2251-2254.

(97)   Kochetkov NK, Khorlin AJ, Bochkov AF (1967). A New Method of Glycosylation. *Tetrahedron* **23:**693-707.

(98)   Kunz H, Pfrengle W (1986). Effective 1,2-*trans*-glycosylation of complex alcohols and phenols using the oximate orthoester of O-pivaloyl glycopyranose. *J Chem Soc (C)* 713-714.

(99)   Schmidt RR, Michel J (1985). O-(α-D-Glucopyranosyl)trichloroacetimidate as a glycosyl donor. *J Carbohydr Chem* **4:**141-169.

(100) Urban FJ, Moore BS, Breitenbach R (1990). Synthesis of Tigogenyl β-O-Cellobioside Heptaacetate and Glycoside Tetraacetate *via* Schemid's Trichloroacetimidate Method; Some New Observations. *Tetrahedron lett* **31:**4421-4424.

(101) Koide K, Ohno M, Kobayashi S (1991). A new glycosylation reaction based on a "remote activation concept": glycosyl 2-pyridinecarboxylate as a novel glycosyl donor. *Tetrahedron lett* **32:**7065-7068.

(102) Charette AB, Marcoux JF, Cote B (1991). Carbohydrates as chiral auxiliaries: synthesis of 2-hydroxy-β-D-glucopyranosides. *Tetrahedron lett* **32**:7215-7218.

(103) Hashimoto S, Hayashi M, Noyori R (1984). Glycosylation using glucopyranosyl fluorides and silicon-based catalysis. solvent dependency of the stereoselection. *Tetrahedron lett* **25**:1379-1382.

(104) Ito Y, Ogawa Y (1987). Sulfenate esters as glycosyl acceptors: a novel approach to O-glycosides from thioglycosides and sulfenate esters. *Tetrahedron lett* **28**:4701-4704.

(105) Hashimoto S, Honda T, Ikegami S (1990). An efficient construction of 1,2-*trans*-β-glycosidic linkages *via* benzyl-protected glycopyranosyl P, P-diphenyl-N-(P-toluenesulfonyl)phosphinimidates. *Chem Pharm Bull* **38**:2323-2325.

(106) Schmidt RR, Behrendt M, Toepfer A (1990). Nitriles as Solvents in Glycosylation Reactions: Highly Selective β-Glycoside Synthesis. *Synlett* 694-696.

(107) Kanie O, Kiso M, Hasegawa A (1988). Glycosylation using methylthioglycosides of N-acetylneuraminic acid and dimethyl(methylthio)-sulfonium triflate. *J Carbohydrate Chem.*, **7**:501-506.

(108) Toshima K, Nozaki Y, Tatsuta K (1991). Highly Stereoselective Glycosylation by Conformational Assistance of Glycosyl Donor. *Tetrahedron lett* **32**:6887-6890.

(109) Spijker NM, van Boeckel CAA (1991). Double Stereodifferentiation in Carbohydrate Coupling Reactions: The Mismatched Interaction of Donor and Acceptor as an Unprecedented Factor Governing the α/β Ratio of Glycoside Formation. *Angew Chem Int Ed Engl* **30**:180-183.

(110) (a) Goebel WF, Babers FH (1934). Derivatives of glucuronic acid. IV. The synthesis of α- and β-tetraacetylglucuronic acid methyl ester and of 1-chlorotriacetylglucuronic acid methyl ester. *J Biol Chem* **106**:63-69.
(b) Goebel WF, Babers FH (1935). Derivatives of glucuronic acid. VI. Preparation of α-chloro- and α-bromotriacetylglucuronic acid methyl esters, and the synthesis of β-glucuronides. *J Biol Chem* **111**:347-353.

(111) Lugemwa FN, Esko JD (1993). Synthesis of β-estradiol-β-D-xylopyranoside, primers of heparan sulfate in Chinese hamster ovary cell. *Carbohydr Res*. **239**:285-290.

(112) Bollenback GN, Long JW, Benjamin DG, Lindquist JA (1955). The synthesis of aryl-D-glucopyranosiduronic acids. *J Am Chem Soc* **77**:3310-3315.

(113) Ernst B, Winkler T (1989). Preparation of glycosyl halides under neutral conditions. *Tetrahedron lett* **30**:3081-3084.

(114) Smales CM (1992). Preparation and Charaterization of conjugates in the urinary assay of estrogen and pregnanediol. Thesis, Massey university.

(115) Nagao Y, Fujita E, Kohno T, Yagi M (1981). An efficient method for selective acetylation of alcoholic hydroxyl groups. *Chem Pharm Bull* **29**:3202-3207.

(116) Perrin DD, Perrin DR, Amarego WLF (1966). Purification of laboratory chemicals. Pergamon Press Ltd. Oxford.

(117) Wu Y, Blackwell LF (1993). Synthesis of estriol 16- and 17-monoglucuronides from estriol. *Steroid* **58**:452-455.

(118) Neeman M, Hashimoto Y (1962). The structure of esatriol monoglucosiduronic acid from human pregnancy urine. *J Am Chem Soc* **84**:2972-2978.

(119) Horiuchi CK, Haga A, Satoh JY (1986). Novel regioselective iodination of estradiol 17β-acetate. *Bull Chem Soc Jpn* **59**:2459-2462.

(120) Laurent H, Bittler D, Beier S, Elger W (1985). Estriol esters. Eur Pat Appl EP 163,596 (*Chem Abstr* **105**:P134239e).

(121) Corey EJ, Venkateswarlu A (1972). Protection of hydroxyl groups as *tert*-butyldimethylsilyl derivatives. *J Am Chem Soc* **94:**6190-6191.

(122) Cooke D (1993). Studies relating to the Ovarian Monitor. Thesis, Massey University, New Zealand. P. 176.

(123) Kunz H (1987). Synthesis of glycopeptides, partial structures of biological recongnition components. *Angew Chem Int Ed Engl* **26:**294-308.

(124) Dodd GH, Golding BI, Ioannou PV (1975). Limitation of *t*-butyldimethylsilyl as a protecting group for hydroxy-functions. *J Chem Soc (C)* 249-250.

(125) Brown DS, Ley SV, Vile S, Thompson M (1991). Use of 2-phenylsulfonyl cyclic ethers in the preparation of the tetrahydropyran and tetrahydrofuran acetals and in some glycosidation reactions. *Tetrahedron* **47:**1329-1342.

(126) Whitfield DM, Shah RN, Carver JP, Krepinsky J (1985). Insoluble promoters of O-glycosylation reaction: thallium, cobalt, and cadmium zeolites 4Å and 13X. *Synth Commun* **15:**737-747.

(127) Hadd HE, Jr Slikker W, Miller DW, Helton ED, Duax WL, Strong PD, Swenson DC (1983). Synthesis and characterization of the anomeric pair of 17β-glucuronides of ethynylestradiol. *J Steroid Biochem* **18:**81-87.

(128) MolEN, (1990). An interactive structure solution procedure, Enraf-Nonius, Delft, The Netherland.

(129) Sheldrick GM, (1976). SHELXS-76 program for crystal structure determination, University of Cambridge.

(130) Sheldrick GM, (1986). SHELXS-86 program for crystal structure determination, University of Cambridge.

(131) Lemieux RU, Kullnig RK, Bernstein HJ, Schneider WG (1958). Configurational effects on the proton magnetic resonance spectra of six-membered ring compounds. *J Am Chem Soc* **80:**6089-6105.

(132) Wittstruck TA, Willams KIH (1973). Carbon-13 magnetic resonance spectroscopy of steroids, estra-1,3,5(10)-trienes. *J Org Chem* **38:**1542-1548.

(133) Wu Y, Waters JM, Blackwell LF (1996). X-Ray crystal structure analysis and ^{13}C NMR investigation of estriol 16- and 17-monoglucuronide derivatives. *J Chem Soc Perkin Trans II* (7) 1449-1453.

(134) Boucheau V, Renaud M, de Ravel MR, Mappus E, Guilleron CY (1990). Proton and carbon-13 nuclear magnetic resonance spectroscopy of diastereoisomeric 3- and 17β-tetrahydropyranyl ether derivatives of estrone and estradiol. *Steroids,* **55:**209-221.

(135) Zsolnai L (1994). ZORTEP Graphics program, University of Heidelberg.

(136) Cooper A, Norton DA, Hauptman H (1969). Estrogenic steroids. III. The crystal and molecular structure of estriol. *Acta Crystallogr Sect B* **25:**814-828.

(137) Precigoux G, Marsau P, Leroy F, Busetta B (1980). 17β-Hydroxymethyl-1,3,5(10)-estratrien-3-ol monohydrate. *Acta Crystallogr Sect B* **36:**749-751.

(138) GO K, Kartha G, Neeman M (1982). Structure of 4-fluoro-1,3,5(10)-estratrien-3,17β-diol-hemimethanol. *Acta Crystallogr Sect B* **38:**3142-3144.

(139) Altona C, Giese HJ, Romers C (1968). Conformation of nonaromatic ring compounds. XXV. Geometry and conformation of ring D in some steroids from X-ray structure determinations. *Tetrahedron,* **24:**13-32.

(140) Thomas SA (1982). On the conformation of five-membered D-ring in sterotds. *Journal of Crystallographic and Spectroscopic Research* **12:**171-189.

(141) Lee RT, Wong TC, Lee R, Yue L, Lee YC (1989). Efficient coupling of glycopeptides to proteins with a heterobifunctional reagent. *Biochemistry* **28:**1856-1861.

(142) Roy R, Tropper FD, Morrison T, Boratynski J (1991). Syntheses and transformations of glycohydrolase substrates into protein conjugates based on michael additions. *J Chem Soc Chem Commun* 536-538.

(143)   Magnnsson G, Ahlfors S, Dahmen J, Jansson K, Nilsson U, Noori G, Stenvall K, Tjornebo A (1990). Prespacer glycosides in glycoconjugate chemistry. dibromoisobutyl glycosides for the synthesis of neoglycolipids, neogglycoproteins, neoglycoparticles, and soluble glycosides. *J Org Chem* **55**:3932-3946.

(144)   Bhatia SK, Lake LCS, Prior KJ, Georger JH, Calvert JM, Bredehorst R, Ligler FS (1989). Use of thiol-terminal silane and heterobifunctional crosslinkers for immobilization of antibodies on silica surfuces. *Analytical Biochemistry* **178**:408-413.

(145)   Janda KD, Ashley JA, Jones TM, Mcleod DA, Schloeder DM, Weinhouse MI (1990). Immobilized catalytic antibodies in aqueous and organic solvents. *J Am Chem Soc* **112**:8886-8888.

(146)   Bartsch RA, Cason CV, Czech BP (1989). Phase-transfer-catalyzed synthesis of oligoethylene glycols and derivatives. *J Org Chem* **54**:857-860.

(147)   Santana VF, Albernas JRM, Bencomo VV, Martinez CSP (1989). Glycoside of monoallyl diethylene glycol. a new type of spacer group for synthetic oligosaccharides. *J Carbohydr Chem* **18**:531-537.

(148)   Bertozzi CR, Bednarski MD (1991). The synthesis of heterobifunctional linkers for the conjugation of ligands to molecular probes. *J Org Chem* **56**:4326-4329.

(149)   Pleurdeau A, Rabadeux JC, Gueniffey H, Lenuz EC (1981). Syntheses de polymers a proprietes pharmacologiques introduction de sequence peptidique en chaine laterale. *Eupean Polymer Journal* **17**:801-805.

(150)   Wang GT, Matayoski E, Huffaker HJ, Krafft GA (1990). Design and synthesis of new fluorogenic HIV protease substrates based on resonance energy transfer. *Tetrahedron Lett* **31**:6493-6496.

(151)   DiNello RK, Dolphing DH (1981). Substituted hemins as probes for structure-function relationships in horseradish peroxidase. *The Journal of Biological Chemistry* **256**:6903-6912.

(152) Tamura M, Asakura T, Yonetani T (1972). Heme-modification studies on horseradish peroxidase. *Biochim Biophys Acta* **268:**292-304.

(153) (a) Veliky IA, Cross J V (1990). Acylation of amines and amino acids. PCT Int Appl WO 91 12,229 (*Chem Abstr* **115:**280559g).
(b) Itsushiki K, Masamoto T, Makino K, Akikaze Y, Yamamoto M (1991). Preparation of N-(long-chain acyl)-sustituted acidic amino acids. Jpn Kokai Koho Jp 03,278,354 (*Chem Abstr* **116:**194879a).

(154) Barra M, de Rossi RH (1991). Catalysis by cyclodextrin in the reaction of *p*-nitrophenyl acetate with α-amino acids. *Can J Chem* **69:**1124-1130.

(155) Paquet A (1976). Succinimidyl esters of fatty acids for amino acid acylations. *Can J Chem* **54:**733-737.

(156) Shenbagamurthi P, Kundu B, Becker JM, Naider F (1985). Synthesis and biological activity of N-acyl derivatives of a saccharomyces cerevisiae mating pheromone. *Int J Pept Protein Res* **25:**187-196. (*Chem Abstr* **103:**105286w).

(157) Tsuchida E, Nishide H, Sato Y, Kaneda M (1982). The preparation of protoheme mono-N-[5-(2-methyl-1-imidazolyl)pentyl]amide and its oxyhenation. *Bull Chem Soc Jpn* **55:**1890-1895.

(158) Kouge K, Koizumi T, Okai H, Kato T (1987). Peptide synthesis in aqueous solution. I. application of *p*-dialkylsulfoniophenol as a water-soluble coupling reagents. *Bull Chem Soc Jpn* **60:**2409-2418.

(159) Katsushige T (1987 & 1989). (4-Alkylanoyloxyphenyl)dimethylsulfonium methylsulfates as acylating agents. Jpn Kokai Tokkyo Koho JP 01 83,029 (*Chem Abstr* **111:**114847x); Jpn Kokai Tokkyo Koho JP 01 83,060 (*Chem Abstr* **111:**13376f).

(160) Nasho Y, Seki T, Kondo M, Ohfuji T, Tamura M, Okai H (1990). Molecular design of inverted-aspartame-type sweeteners. *J Agric Food Chem* **38:**1368-1373.

(161) Fujitaki JM, Steiner AW, Nichols SE, Helander ER, Lin YC, Smith RA (1980). A simple preparation of N-phosphorylated lysine and arginine. *Preparative Biochemistry* **10**:205-213.

(162) Scott JW, Parker D, Parrish DR (1981). Improved synthesis of N$^\varepsilon$-*tert*-butyl-oxycarbonyl-L-lysine and N$^\alpha$-benzyloxycarbonyl-N$^\varepsilon$-*tert*-butylcarbonyl-L-lysine. *Synthetic Communications* **11**:303-314.

(163) Yozo F, Takuzo O, Haruo Y, Michikazu S, Katsuo A, Mari U, Michito K (1987). Porphyrin derivatives. Eur Pat Appl EP 233,701 (*Chem Abstr*).

(164) Radyukhin VA, Filippovich EI, Evstigneeva RP (1980). Synthesis of mono-C-aminoacyl peptide derivatives of protohemin IX. Translated from *Zhurnal Obschei Khimii* **50**:673-679.

(165) Paquet A, Bergeron M (1982). Formation of unusual side-products from succinimidyl esters of fatty acids during the acylation of amino acids. *Can J Chem* **60**:1806-1808.

(166) Killion RB, Stella VJ (1990). The nucleophilicity of dextrose, sucrose, sorbitol, and mannitol with p-nitrophenyl ester in aqueous solution. *International J Pharmaceutics* **66**:149-155.

(167) Paquet A (1979). Further studies on the use of the thallium salt of N-hydroxysuccinimide for the preparation of succinimidyl esters. *Can J Chem* **57**:2775-2778.

(168) ADamczyk M, Fishpaugh JR, Mattingly PG (1995). An easy preparation of hapten active esters *via* solid supported EDAC. *Tetrahedron lett* **36**:8345-8346.

(169) Benson DR, Hart BR, Zhu X, Doughty MB (1995). Design, synthesis, and circular dichroism investigation of a peptide-sandwiched mesoheme. *J Am Chem Soc* **117**:8502-8510.

(170) Smith KM, Cavaleiro JAS (1987). Protoporphyrin IX: some useful substituent manipulations. *Heterocycles* **26**:1947-1963.

(171)   Woodburn KW, Bellinger GCA, Phillips DR, Reiss JA (1992). Synthesis of porphyrins derived from the amidation of protoporphyrin IX for use as potential chemotherapeutic agents. *Aust J Chem* **45:**1745-1751.

(172)   Mari U, Michito S, Hirofumi K, Takuzo O, Katsuo A (1989). Porphyrin derivatives for the photodynamic diagnosis and treatment of cancer. Eur Pat Appl EP 355,539 (*Chem Abstr* **112:**216560m).

(173)   Bommer JC, Burnham BF (1989). Preparation of tetrapyrrolecarboxamide for use in tumor phototherapy. Eur Pat Appl EP 322,795 (*Chem Abstr* **112:**98293b).

(174)   Pelter A, Abela MA, Ballantine JA, Ferrito V, Ford S, Jaccarini V, Psaila AF (1978). The structures of amino-acid conjugates of bonellin derivated from the marine echuroid Bonellia Viridis. *Tetrahedron lett* 2017-2020.

(175)   Nippon Petrochemicals Co Ltd (1987). Fluorescent porphyrin derivatives of amino acids and pharmaceutical compositions containing them for photochemotherapy and diagnosis of tumors. Jpn Kokai Tokkyo Koho JP 62 05,924 (*Chem Abatr* **107:**134134n).

(176)   Diekmann H, Chang CK, Traylor TG (1971). Cyclophane Porphyrin. *J Am Chem Soc* **93:**4068-4070.

(177)   Almog J, Baldwin JE, Huff J (1975). Reversible Oxygenation and Autoxidation of a "Capped" Porphyrin Iron (II) Complex. *J Am Chem Soc* **97:**227-228.

(178)   Baldwin JE, Klose T, Peters M (1976). Syntheses of "Strapped" Porphyrins and the Oxygenation of their Iron (II) Complex. *J Chem Soc Chem Commun* 881-883.

(179)   Battersby AR, Buckley DG, Hartley SG, Turnbull MD (1976). Synthetic Studies Related to Myoglobin: Syntheses of Bridged Porphyrin Systems. *J Chem Soc Chem Commun* 879-881.

(180)   Chang CK (1977). Stacked Double-Macrocyclic Ligands.1.Synthesis of a "Crowed" Porphyrin. *J Am Chem Soc* **99:**2819-2822.

(181) Collman JP, Gagne RR, Christopher AR, Halbert TR, Lang G, Robinson WT (1975). "Picket Fence Porphyrins." Synthetic Models for Oxygen Binding Hemoproteins. *J Am Chem Soc* **97**:1427-1439.

(182) Collman JP, Christopher AR (1973). Syntheses of Ferrous-Porphyrin Complex. A Hypothetical Model for Deoxymyoglobin. *J Am Chem Soc* **95**:2048-2049.

(183) Chang CK, Traylor TG (1973). Synthesis of the Myoglobin Active Site. *Proc Nat Acad Sci USA* **70**:2647-2650.

(184) Traylor TG, Chang CK, Geibel J, Brezinis A, MinceyT, Cannon J (1979). Syntheses and NMR Characterization of Chelated Heme Models of Hemoproteins. *J Am Chem Soc* **101**:6716-6731.

(185) Lown JW, Joshua AV (1982). Bleomycin Models. Haemin-Acridines which bind to DNA and cause Oxygen-dependent Scission. *J Chem Soc Chem Commun* 1298-1230.

(186) Hamachi I, Nakamura K, Fujita A, Kunitake T (1993). Anisotropic Incorporation of Lipid-Anchored Myoglobin into a Phospholipid Bilayer Membrane. *J Am Chem Soc* **115**:4966-4970.

(187) Hamachi I, Higuchi S, Nakamura K, Fujimura H, Kunitake T (1993). Lipid Anchored Myoglobin 2. Effect of the Anchor Structure on Membrane Binding. *Chem Lett* 1175-1178.

(188) Kotal P, Porsch B, Jirsa M, Kordac V (1985). Rapid isocratic high-performance liquid chromatography of porphyrin esters on aminopropyl-bonded silica. *J Chromatogr* **333**:141-151.

(189) HO J, Guthrie R, Tieckelmann H (1986). Detection of δ-aminolevulinic acid, porphobilinogen and porphyrins related to heme biosynthesis by high-performance liquid chromatography. *J Chromatogr* **375**:57-63.

(190) Meyer HD, Vogt W, Jacob K (1984). Improved separation and detection of free porphyrins by high-performance liquid chromatography. *J Chromatogr* **290**:207-213.

(191) Bailey GG, Needham LL (1986). Simultaneous quantification of erythrocyte zinc protoporphyrin and protoporphyrin IX by liquid chromatography. *Clin Chem* **32:**2137-2142.

(192) Culbreth P, Walter G, Carter R, Burtis C (1979). Separation of protoporphyrins and related compounds by reversed-phase liquid chromatography. *Clin Chem* **25:**605-610.

(193) Ho JW (1989). High-performance liquid chromatographic determination of zinc protoporphyrin and porphyrin carboxylic acids in urine. *Anal Biochem* **183:**134-138.

(194) Petryka ZJ, Watson CJ (1979). Separation and spectrodensitometric quantitation of porphyrin esters on thin-layer chromatograms. *J Chromatogr* **179:**143-149.

(195) Friedmann HC, Baldwin ET (1984). Reversed-phase purification and silica gel thin-layer chromatography of porphyrin carboxylic acids. *Anal Biochem* **137:**473-480.

(196) Friley BK, Phelps JB, Kincaid JR (1983). Gel permeation chromatography of porphyrins and hemins. *J Chromatogr* **258:**310-313.

(197) Kessel D, Thmpson P (1987). Purification and analysis of hematoporphyrin and hematoporphyrin derivative by gel exclusion and reverse-phase chromatography. *Photochem Photobiol* **46:**1023-1025.

(198) Ho JW (1990). Separation of porphyrins on cyclodextrin-bonded phase with a novel mobile phase. *J Chromatogr* **508:**375-381.

(199) Kiyohara C, Saitoh K, Suzuki N (1993). Micellar electrokinetic capillary chromatography of haematoporphyrin, protoporphyrin and their copper and zinc complexes. *J Chromatogr* **646:**397-403.

(200) Ho JW (1989). Effects of mobile phase pH, ionic strength and buffer compositions on HPLC. *LC-GC* **7:**348, 351-352.

(201) Iriyama K, Yoshiura M (1979). Separation of chlorophyll *a* and *b* by column chromatography with sephadex LH-20 or powdered sugar. *J Chromatogr* **177:**154-156.

(202) Shimizu S (1971). Separation of chloroplast pigments on sephadex LH-20. *J Chromatogr* **59:**440-443.

(203) Shiau FY, White BJ, Castelfranco PA, SmithKM (1991). Partial syntheses of the isomerically pure magnesium (II) protoporphyrin IX monomethyl esters, and their identification. *J Chem Soc Perkin Trans 1* 1781-1785.

(204) Adler AD, Longo FR, Kampas F, Kim J (1970). On the preparation of metalloporphyrins. *J Inorg Nucl Chem* **32:**2443-2445.

(205) Houston T, Fitzsimons EJ, Moore MR (1988). A simple reversed phase high performance liquid chromatographic method for the separation of haem, protoporphyrin and iron. *Biochem Soc Trans* **16:**831-832.

(206) Sanitrak J, Krijt J (1987). Determination of porphyrins in tissue: pre-adsorption followed by high-performance liquid chromatography. *J Chromatogr* **415:**129-135.

(207) Dunford HB (1991) "Horseradish peroxidase: structure and kinetic properties" in *Peroxidases in Chemistry and Biology* (Everse J, Everse KE & Grisham MB, Eds.) CRC Press, Boca Raton FL. **2:**1-24.

(208) Poulos TL, Freer ST, Alden RA, Edwards SL, Skogland U, Takio K, Eriksson B, Xuong N, Yonetani T, Kraut J (1980). The crystal structure of cytochrome *c* peroxidase. *J Biol Chem* **255:**575-580.

(209) Poulos TL, Kraut J (1980) The stereochemistry of peroxidase catalysis. *J Biol Chem* **255:**8199-8205.

(210) Welinder KG (1979). Amino acid sequence studies of horseradish peroxidase. amino and carboxyl termini, cyanogen bromide and tryptic fragments, the complete sequence, and some structural characteristics of horseradish peroxidase C. *Eur J Biochem* **96:**483-502.

(211) Welinder KG (1985). Plant peroxidase. their primary, secondary and tertiary structures, and relation to cytochrome *c* peroxidase. *Eur J Biochem* **151**:497-504.

(212) Ringe D, Petsko GA, Kerr DE, Ortiz de Montellano PR (1984). Reaction of myoglobin with phenylhydrazine: a molecular doorstop. *Biochemistry* **23**:2-4.

(213) Ortiz de Montellano PR, Kerr DE (1985). Inactivation of myoglobin by ortho-substituted arylhydrazines. formation of prosthetic heme aryl-iron but N-aryl adducts. *Biochemistry* **24**:1147-1152.

(214) Saito S, Itano HA (1981). β-meso-Phenylbiliverdin IXα and *N*-phenylprotoporphyrin IX, products of the reaction of phenylhydrazine with oxyhemoproteins. *Proc Natl Acad Sci USA* **78**:5508-5512.

(215) Augusto O, Kunze KL, Ortiz de Montellano PR (1982). N-Phenylprotoporphyrin IX formation in the hemoglobin-phenylhydrazine reaction. evidence for a protein-stabilized iron-phenyl intermediate. *J Biol Chem* **257**:6231-6241.

(216) Ortiz de Montellano PR, Kunze KL (1981). Formationof *N*-phenylheme in the hemolytic reaction of phenylhydrazine with hemoglobin. *J Am Chem Soc* **103**:6534-6536.

(217) Ortiz de Montellano PR, Kerr DE (1983). Inactivation of catalase by phenylhydrazine. formation of a stable aryl-iron heme complex. *J Biol Chem* **258**:10558-10563.

(218) Jonen HG, Werringloer J, Prough RA, Estabrook RW (1982). The reaction of phenylhydrazine with microsomal cytochrome P-450. catalysis of heme modification. *J Biol Chem* **257**:4404-4411.

(219) Ator MA, Ortiz de Montellano PR (1987). Protein control of prosthetic heme reactivity. *J Biol Chem* **262**:1542-1551.

(220) Ator MA, David SK, Ortiz de Montellano PR (1987). Structure and catalytic mechanism of horseradish peroxidase. regiospecific meso alkylation of the prosthetic heme group by alkylhydrazines. *J Biol Chem* **262**:14954-14960.

(221) Ator MA, David SK, Ortiz de Montellano PR (1989). Stabilized isoporphyrin intermediates in the inactivation of horseradish peroxidase by alkylhydrazines. *J Biol Chem* **264:**9250-9257.

(222) Harris RZ, Liddell PA, Smith KM, Ortiz de Montellano PR (1993). Catalytic properties of horseradish peroxidase reconstituted with the 8-(hydroxymethyl)- and 8-formylheme derivatives. *Biochemistry* **32:**3658-3663.

(223) Sakurada J, Takahashi S, Hosoya T (1986). Nuclear magnetic resonance studies on the spatial relationship of aromatic donor molecules to the heme iron of horseradish peroxidase. *J Biol Chem* **261:**9657-9662.

(224) La Mar GN, de Ropp JS, Smith KM, Langry KC (1980). Proton nuclear magnetic resonance study of the eletronic and molecular structure of the heme crevice in horseradish peroxidase. *J Biol Chem* **255:**6646-6652.

(225) Ortiz de Montellano PR (1987). Control of the catalytic activity of prosthetic heme by the structure of hemoproteins. *Acc Chem Res* **20:**289-294.

(226) Seybert DW, Moffat K, Gibson QH, Chang CK (1977). Electronic and steric factors affecting ligand binding: horse hemogloobins containing 2,4-dimethyldeuteroheme and 2,4-dibromodeuteroheme. *J Biol Chem* **252:**4225-4231.

(227) Hauksson JB, La Mar GN, Pandey RK, Rezzano IN, Smith K (1990). NMR study of heme pocket polarity/hydrophobicity of myoglobin using polypropionate-substituted hemins. *J Am Chem Soc* **112:**8315-8323.

(228) Shinohara A, Kamataki T, Iizuka T, Ishimura Y, Ogoshi H, Okuda K, Kato R (1987). Drug oxidation activities of horseradish peroxidase, myoglobulin and cytochrome P-450cam reconstituted with synthetic hemes. *Jpn J Pharmacol* **45:**107-114.

(229) Fernandez M, Frydman RB, Hurst J, Buldain G (1993). Structure/activity relationships in porphobilinogen oxygenase and horseradish peroxidase. An analysis using synthetic hemins. *Eur J Biochem* **218:**251-259.

(230) Kuriyan J, Wilz S, Karplus M, Petsko GA (1986). X-ray structure and refinement of carbon-monoxy (Fe II)-myoglobin at 1.5 A resolution. *J Mol Biol* **192:**133-154.

(231) Saburo N, Noriaki F, Kiyohiro I (1988). Structure and function of the myoglobin containing octaethylhemin as a prosthetic group. *J Biol Chem* **263:**8810-8815.

(232) Hauksson JB, La Mar GN, Pandey RK, Rezzano IN, Smith K (1990). ^{1}H NMR study of the role of individual heme propionates in modulating structural and dynamic properties of the heme pocket in myoglobin. *J Am Chem Soc* **112:**6198-6205.

(233) Lee K, La Mar GN, Pandey RK, Rezzano IN, Mansfield KE, Smith KM (1991). ^{1}H NMR study of the role of heme carboxylate side chains in modulating heme pocket structure and the mechanism of reconstitution of cytochrome b_5. *Biochemistry* **30:**1878-1887.

(234) Teale FWJ (1959). Cleavage of the haem-protein link by acid methylethylketone. *Biochem Biophys Acta* **35:**543-548.

(235) Beaven GH, Chen SH, D'Albis A, Gratzer WB (1974). A spectroscopic study of the haemin-human-serum-albumin system. *Eur J Biochem* **41:**539-546.

(236) Hamachi I, Kimura O, Takeshita H, Shinkai S (1995). Peroxidase activity of cytochrome c generated by phenylboronic acid modification. *Chem Lett* 529-530.

(237) Banci L, Carloni P, Savellini GG (1994). Molecular dynamics studies on peroxidases: a structural model for horseradish peroxidase and a substrate adduct. *Biochemistry* **33:**12356-12366.

(238) Piontek K, Glumoff T, Winterhalter K (1993). Low pH crystal structure of glycosylated lignin peroxidase from phanerochaete chrysosporium at 2.5Å resolution. *FEBS Lett* **315:**119-124.